Investigation of actions of Parathyroid hormone-related protein (PTHrP) independent of PTH1R

Yao Sun

Submitted in total fulfilment of the requirement of the degree of Doctor of Philosophy to the University of Melbourne

June 2020

Bone Cell Biology and Disease Unit

St. Vincent's Institute of Medical Research

Department of Medicine (St Vincent's Hospital)

Faculty of Medicine, Dentistry and Health Sciences

University of Melbourne

Abstract

Parathyroid hormone-related protein (PTHrP; gene name *PTHLH/Pthlh*) acts as a paracrine/autocrine factor to produce a range of effects, including contributing to skeletal development and determining trabecular bone mass. By activating the receptor (PTH1R) that PTHrP shares with parathyroid hormone (PTH), it transduces cascades coupled with the stimulation of cyclic adenosine monophosphate (cAMP) - protein kinase A (PKA) and CREB responses. However, in addition to its amino-terminal region that mediates similar actions to PTH, PTHrP has structural features that allow it to exert distinct activities independent of PTH1R. Relatively little is known about the signalling pathways that guide these actions but the novel specific functional regions that exist in PTHrP allow us to ask how PTHrP acts independently and uses non-canonical pathways. The major aim in my thesis is to unveil the PTHrP functions that act through non-canonical pathways associated with regions of the molecule other than PTH1R binding region.

Recently, it has been demonstrated that PTHrP overexpression drives dormant human MCF7 breast cancer cells in mice to colonise the bone marrow and induces osteolytic damages. However, I found that although MCF7 cells activate cAMP in response to prostaglandin E_2 (PGE_2) and calcitonin, the cells do not respond to PTHrP or PTH. This suggests PTH1R in those cells is not functionally linked to adenylyl cyclase. My analysis suggests MCF7 cells express PTH1R mRNA and proteins but such PTH1R does not bind sufficient exogenous PTHrP to activate cAMP. RNA-Seq analysis identified many genes induced by PTHrP overexpression in MCF7 cells, indicating responsiveness to PTHrP, although a shift in cell differentiation because of clonal drift cannot be ruled out. Several potential alternative signalling pathways were identified, notably those related to calcium signalling. These data suggest that the effect of PTHrP overexpression on MCF7 cell dormancy may occur through PTH1R-independent actions of PTHrP.

PTHrP is also essential for bone formation, as indicated by mouse models with genetic depletion of PTHrP, both globally and within the osteoblast lineage. It has been established that *Dmp1Cre.Pthlh*$^{f/f}$ mice have significantly lowered levels of PTHrP in osteocytes resulting in reduced bone mass and strength. This differs strikingly from *Dmp1Cre.Pth1r*$^{f/f}$ mice with a deficiency of PTH1R in osteocytes which exhibit high bone mass. This implies that PTHrP signalling in osteocytes that promotes bone formation occurs through a non-PTH1R-mediated pathway. To identify alternative signalling pathways of PTHrP, RNA-Seq was conducted on OCY454 osteocytes overexpressing secreted PTHrP (OCY454 *PTHrP*^{FL}) and mutant forms of PTHrP lacking both the nuclear localisation sequence (NLS) and C-terminus (OCY454 *PTHrP*$^{\Delta NLS\Delta C}$), the nuclear localisation sequence (OCY454 *PTHrP*$^{\Delta NLS}$), or lacking the signalling peptide required for secretion (OCY454 *PTHrP*$^{\Delta Sec}$). In these cells, expression of PTHrP-activated genes is significantly higher when the PTHrP NLS and C-terminus domains are absent. This shows that the NLS and/or the C-terminus of PTHrP may have a negative impact on genes regulated through PTH1R. However, unlike deletion of the NLS and C-terminus, deletion of NLS alone did not change the number of genes regulated by PTHrP nor the magnitude change. This difference indicates that the C-terminus, but not the NLS, may limit gene expression in response to PTH/PTHrP signalling in OCY454 cells. Importantly, there was no change in cAMP response, CREB responsive gene alterations, or CREB phosphorylation in response to exogenous PTHrP in cells overexpressing the C-terminus, nor was there any difference in the effects of exogenously supplied C-terminus PTHrP compared to full-length PTHrP. This suggests the inhibitory action of the PTHrP C-terminus is intracrine, with regulation taking place beyond CREB activation.

I next performed studies to determine whether the PTHrP C-terminus reduces PTH1R-mediated signalling using qPCR on UMR106.01 overexpressing the C-terminus, focusing on the marked down-regulation of osteocalcin (protein name: BGLAP, bone

gamma carboxyglutamate protein; gene name: *Bglap1/2*) expression, as an example, targeted by PTH/PTHrP signalling. The induction of *Bglap1/2* expression by PTH or PTHrP was significantly lower in osteoblastic-like osteosarcoma UMR106.01 cells overexpressing the PTHrP C-terminus. Subsequent analysis suggests this C-terminus gene suppression effect is cytosolic, but is not dependent on modifying cAMP/PKA signalling. My preliminary data suggests modification of Wnt signalling pathway may be required for this C-terminus effect.

The RNAseq data from OCY454 $PTHrP^{FL}$ cells revealed that osteocyte-derived PTHrP may regulate mineralisation due to significant regulation of mineralisation genes in the gene profile, compared to vector control cells. Since bones from 12-week-old *Dmp1Cre.Pthlh*$^{f/f}$ mice were previously reported to have impaired bone material strength, I next sought to understand how osteocyte-derived PTHrP modifies mineralisation *in vivo*. I used high resolution synchrotron-based Fourier Transform Infrared (FTIR) microspectroscopy to determine the bone composition of 12-week-old *Dmp1Cre.Pthlh*$^{f/f}$ mice and *Dmp1Cre* controls. Male *Dmp1Cre.Pthlh*$^{f/f}$ mice showed significantly higher amide I:II ratio (i.e. less compacted collagen) and lower mineral:matrix ratio compared with controls. This suggests a requirement of PTHrP for both collagen organisation and mineral formation. Surprisingly, preliminary *in vitro* results showed that both PTHrP knocked-down cells and overexpression cells had a low mineralised deposit phenotype. My preliminary data suggests that PTHrP is likely to contribute to bone strength via proper mineral deposition and compaction of collagen, and by modifying osteocyte differentiation.

In conclusion, my thesis describes three major findings. Firstly, although PTHrP promotes breast tumour MCF7 cells aggressively growing in bone, this is not dependent on PTH1R/cAMP/PKA activation. Secondly, in osteocytes, which express PTHR1, the

PTHrP C-terminus appears to inhibit *Bglap1/2* transcription induced by PTH/PTHrP and this occurs through intracellular pathways independent of PTH1R/cAMP/PKA. Moreover, PTHrP is essential for normal bone composition. It is likely that PTHrP contributes to the promotion of mineralisation, thereby contributing to bone strength via collagen compaction, and by modifying osteocyte differentiation. Deciphering these actions above and their crosstalk with non-PTH1R-mediated processes will increase our understanding of how PTHrP manipulates breast cancer metastasis and bone composition.

Declaration

This is to certify that:

i) This thesis comprises only my original work towards the degree Doctor of Philosophy except where indicated in the Preface.

ii) Due acknowledgement has been made in the text to all other material used,

iii) The thesis is fewer than 100,000 words in length, exclusive of tables and bibliography.

Yao Sun

Preface

Pursuant to the regulations governing the degree of Doctor of Philosophy at the University of Melbourne, I hereby submit that:

I. This thesis contains no material that has been accepted for the award of any other degree or diploma in any university.

II. To the best of my knowledge and belief, this thesis contains no material previously published or written by another person, except where due reference has been made.

Chapter 3 contains findings and text that formed a part of a published peer-reviewed article. The following Figures and Tables were included in Johnson R W, Sun Y, Ho P W M, *et al.* Parathyroid hormone-related protein negatively regulates tumour cell dormancy genes in a PTH1R/cyclic AMP-independent manner. Frontiers in endocrinology, 2018, 9. I was the second author of this publication; I contributed the data for Figure 3.2 with the help of Ms Patricia Ho; for Figure 3.3 but not the part of CREB genes list and for Figure 3.4. Figure 3.1 and Figure 3.8 were not part of the paper. I have contributed part of the writing of the manuscript. This manuscript is included in the Appendix.

I would like to acknowledge the help of people in contributing to the work presented in this thesis:

Ms Patricia Ho helped me to perform cAMP assay in MCF7 cells (Chapter 3).

Ms Patricia Ho performed the CRE-luciferase assay in MCF7 cells (Chapter 3).

Dr. Rachelle Johnson analysed the 32 CREB responsive genes by RNA-Seq, and the *BDKRB1* and *CALML3* qPCR transcription analysis (Chapter 3).

Dr. Audrey Chan performed the confocal analysis of PTH1R binding in MCF7 and UMR106.01 cells (Chapter 3).

Ms Patricia Ho helped me with the establishment of MCF7 cell lines (Chapter 3).

Ms Blessing Crimeen-Irwin performed the confocal analysis of PTHrP localisation in OCY454 cell lines (Chapter 4).

Ms Patricia Ho helped me to perform exogenous treatment of hPTHrP(1-141) and hPTHrP(1-84) on the expression of *Bglap* gene expression at 1, 6 and 24 hours in OCY454 osteocytes (Chapter 5).

Ms Patricia Ho performed the cAMP assay in Fig. 5.8 (Chapter 5).

I did the UMR cell lines treatment and Ms Patricia Ho helped to analyse the CREB genes in Fig. 5.10 and Wnt signalling target genes in Fig. 5.13 (Chapter 5).

Ms Ingrid Poulton helped me with the plastic section preparation, tissue cuttings and taught me the silver staining in Chapter 6.

Ms Emma Walker taught me genotyping, tissue collection and assessment of bone mRNA by qPCR.

Publication

The following publication and prepared manuscripts are a result of work generated for this thesis:

Publication

Johnson R W, Sun Y, Ho P W M, *et al.* Parathyroid hormone-related protein negatively regulates tumour cell dormancy genes in a PTH1R/cyclic AMP-independent manner. Endocrinology. Frontiers in endocrinology, 2018, 9.

In preparation

Yao Sun, Ho P W M, Johnson R W *et al*. Identification of PTHrP receptor-independent domain functions using RNA-Seq

Yao Sun, Ho P W M, Johnson R W *et al*. Activation by PTHrP in the osteocyte is profoundly inhibited by the PTHrP C-terminal domain.

Yao Sun, Ho P W M, Johnson R W *et al*. Conditional deletion of PTHrP in late osteoblasts and osteocytes compromise bone matrix mineral composition or maturation

Acknowledgments

Undertaking this PhD has been a truly life-changing experience for me and it would not have been possible to do without the support and guidance that I received from many people.

I would like to first say a very big thank you to my supervisor Prof. Natalie Sims and Prof. Jack Martin, for the continuous support of my PhD study and related research, for the patience, and tremendous knowledge, during both the long months I spent undertaking my field work in St. Vincent Institute. Without their guidance and constant feedback my PhD would not have been achievable. I am especially grateful to them for believing in my research and for the support I received through the ANZBMS and ASBMR conferences to undertake the journey to know about research ideas in other groups. I am also very grateful to them because they were always so helpful and provided me with their assistance throughout my thesis writing and final talk.

Thanks all the members in bone group for all the help and encouragement and always bring me laugh. My research would have been impossible without the aid and kind support of the members of the Bone Biology and Disease Unit. I am grateful to Martha Blank, Emma McGowan, Blessing Crimeen-Irwin, Ingrid Poulton, Narelle McGregor, Tsuyoshi Isojima, Jonathan Gooi, Niloufar Ansari, Christina Vrahnas, Kim Truong, Ling Yeong Chia and Thaisa Lima for teaching me new techniques and supporting me throughout my PhD. I would like to have a special thank you for Pat Ho, the for the powerful supports of the motivation and continuous assistance for the experiments.

I greatly appreciate the support received through the collaborative work undertaken with the Dr. Rachelle Johnson, Vanderbilt University, during the first phase of my field work. My thanks also go out to the support I received from the collaborative work I undertook with Dr. Audrey Chan, The University of Western Australia, for participating the work of confocal and always so helpful and provided me with assistance.

I would like to thank my other friends at SVI, Winnie Tan, Wilson Castillo, Jane Xu, Diannita Kwang, Clea Grace, Tingting Ge, Dingyi Yu, Rui Liu, Evan Pappas, Lenny Straszkowski, Vanessa Tsui, Landing Li, Xining Li, William Stanley, Julienne O'Rourke, Jasmina Markulić, Scott Taylor, Ankita Goradia, Mannu Walia, Monique Smeets, Jacki Heraud-Farlow, Alistair Chalk, Kelli Schleibs, and Gavin Tjin. My sincere thanks to my committee members Dr. Andrew Deans, Dr. Jörg Heierhors and Amanda Edgley, who provided me useful tips for PhD life and useful supports for the PhD research.

I gratefully acknowledge the funding received towards my PhD from the MIRS, MIFRS scholarship from University of Melbourne and SVI top-up scholarship.

Finally, my deep and heartfelt thanks go to my family and my friends for their love and encouragement. Thank you for everything!

Abbreviations

αMEM	Minimum Essential Medium Eagle-Alpha Modification
Ab	Antibody
AC	Adenylyl cyclase
ALP	Alkaline phosphatase
AQP3	Aquaporin 3
AREG	Amphiregulin
BCA	Bicinchoninic acid
Bcl-2	B-cell lymphoma 2
BP	Biological process
BSA	Bovine serum albumin
BV	Bone volume
CaHA	Calcium hydroxyapatite
cAMP	Cyclic Adenosine Monophosphate
CEBPD	CEBP-dela
CK2	Casein kinase II
CaSR	Calcium-sensing receptor
COLI:	Collagen I
CRE	cAMP response elements
CREB	cAMP response element binding protein
CRE-luc	CRE-luciferase
CRTC1/2	CREB-regulated transcriptional coactivators 1/2
C terminus	Carboxyterminal domain beginning residue 107
DEGs	Differentially expressed genes
DEPC	Diethylpyrocarbonate
DMP1	Dentin matrix acidic phosphoprotein 1
ER	Endoplasmic reticulum
ERK	Extracellular signal-regulated kinase
ES	Embryonic stem
FBS	Foetal bovine serum

Fsk	Forskolin
FTIR	Fourier transform infrared
gDNA	Genomic DNA
GFP	Green fluorescent protein
GO	Gene ontology
KEGG	Kyoto encyclopedia of genes and genomes
IBMX	Isobutylmethylxanthine
IHH	Indian Hedgehog
IL-6	Interleukin 6
IP3	1,4,5-inositol trisphosphate
MAPK	Mitogen activated protein kinase
MF	Molecular function
MMA	Methylmethacrylate
NLS	Nuclear localization sequence
Nrp1	Neuropilin-1
OCN	Osteocalcin
OCY	Osteocyte
OPG	Osteoprotegerin
OSX	Osterix
P1NP	Procollagen type 1 N propeptide
PBS	Phosphate buffered saline
PHEX	Phosphate regulating endopeptidase homolog, X-linked
PFA	Paraformaldehyde
PGE_2	Prostaglandin E2
PKA	Protein kinase A
PKC	Protein kinase C
PLC	Phospholipase C
PLSD	Projected least significant difference
PPAR-γ	Peroxisome proliferator-activated receptor gamma
P/S	Penicillin/Streptomycin
Ps. Pm	Periosteal perimeter
PSA	Penicillin-Streptomycin-Amphotericin B
PTH	Parathyroid hormone
PTHR1	Parathyroid hormone/parathyroid-hormone related protein receptor 1
PTHrP	Parathyroid hormone-related protein

PTH^{TMR}	Tetramethylrhodamine-labeled PTH
qPCR	Quantitative polymerase chain reaction
RANKL	Receptor activator of nuclear factor kappa-B ligand
RIA	Radioimmunoassay
ROI	Regions of interest
RT	Room temperature
RUNX2	Runt-related transcription factor 2
S*	Serine
sCT	Calcitonin
SEM	Scanning electron microscopy
SIK2	Salt-inducible kinase 2
sIL-6R	Soluble Interleukin-6 receptor
sL.S	Single-labeled mineralising surface
T*	Threonine
Tb. N	Trabecular number
Tb. Sp	Trabecular separation
Tb. Th	Trabecular Thickness
TGF-b1	Transforming growth factor beta 1
TMB	Tetramethylbenzidine
TMD	Tissue mineral density
TNB buffer	Tris-NaCl-blocking buffer
TNF-α	Tumour necrosis factor-alpha
TRAP	Tartrate-resistant acid phosphatase
TRP	Transient receptor potential
TV	Tissue volume
VDAC2	Voltage-dependent anion-selective channel protein 2
VEGFR2	Vascular endothelial growth factor receptor 2
VPS35	Vacuolar protein sorting

Table of contents

List of figures

List of tables

Chapter 1: Introduction, critical literature review, aims and hypothesis

1.1 PTHrP background and discovery

The discovery of PTHrP came from studies of the syndrome of humoral hypercalcemia of malignancy, in which the biochemical features parallel closely those of parathyroid hormone (PTH) excess. For many years the syndrome had been considered to be due to "ectopic" PTH production by those cancers (Plimpton and Gellhorn 1956). Doubts about this emerged in the 1970s, when immunological methods began to reveal that the cancer-derived activity, although it mimicked PTH actions, differed from PTH immunochemically and therefore in structure (Blair Jr, Hawker *et al.* 1973).

Three clinical studies provided an excellent explanation of the biochemical similarity between primary hyperparathyroidism and this syndrome of humoral hypercalcemia of malignancy (Kukreja, Shemerdiak *et al.* 1980, Stewart, Horst *et al*. 1980, Minkin, Fredericks *et al*. 1981). They showed that in both syndromes the patients had hypercalcemia, hypophosphatemia and increased urinary cyclic AMP. In other words the cancer patients produced some factor that very closely mimicked the action of PTH. By that time, assays sensitive to PTH activity had been developed that measured cAMP production in cells derived from kidney or osteosarcoma. Tumour extracts and culture supernatants of hypercalcemic animal and human tumours were found to contain PTH-like adenylate cyclase responses in osteoblast and kidney targets (Rodan *et al*. 1983, Stewart *et al*. 1983, Strewler *et al.* 1983). This paved the way for purification of PTHrP from a human lung cancer cell line (Moseley *et al*. 1987), with sufficient sequence obtained to lead to cloning of its cDNA (Suva *et al*. 1987). This reveals that eight of the first 13 residues of PTHrP are identical to those in PTH, and any remaining identities are no more than expected by chance. The structural requirements for full biological activity

of PTHrP was contained within the first 34 amino acids (Kemp, Moseley *et al.* 1987), as was known to be the case with PTH. PTHrP was also purified from a breast cancer (Burtis *et al.* 1987) and a renal cancer cell line (Strewler, Stern *et al*. 1987), and further successful cloning was achieved by Broadus *et al*. (1988).

PTHrP was revealed as a protein likely related in evolution to PTH, while preserving sufficient structural similarity to PTH to share action upon the common receptor (Suva, Winslow *et al.* 1987, Juppner, Abou-Samra *et al.* 1991). In the human PTHrP molecule beyond the amino-terminal domain there are no more identities between PTH and PTHrP than would be expected by chance. Biological activities have been ascribed to those regions, that include a functional nuclear localising sequence (NLS; Henderson, Amizuka *et al*. 1995) a mid-terminal domain that mediates placental calcium transport (Kovacs, Lanske *et al*. 1996), and a carboxyterminal domain beginning of residue 107 (C-terminus; Fig. 1.1A). Many effects have been reported for this carboxy-terminal sequence in pharmacological experiments *in vitro* and *in vivo* (Lozano, Fernández‐de‐Castro *et al.* 2011), although no receptors have been identified. It is therefore not possible at present to be sure of any physiological role of the C-terminus domain.

The amino-terminal sequence similarities between PTH and PTHrP (Fig. 1.1B) are such that PTH(1–34) and PTHrP(1–34) bind and activate fully the G protein-coupled receptor, Parathyroid Hormone 1 Receptor (PTH1R) that they share (Juppner, Abou-Samra *et al.* 1991, Mannstadt, Juppner *et al.* 1999, Gardella and Jüppner 2001). Structure-activity requirements within the amino-terminal region of PTHrP (Kemp, Moseley *et al.* 1987) were found to resemble closely those already known for PTH (Tregear, Rietschoten *et al.* 1973). X-ray crystallography by Pioszak *et al*. confirmed the interaction between PTH1R and PTHrP (Pioszak, Parker *et al.* 2009). It has been thus recognised that PTHrP is an

intimate relative of PTH, and that by utilising the PTH1R-binding region both PTH and PTHrP exert actions on target cells (Minagawa, Yasuda *et al.* 2002).

Given the alternative splicing of messenger RNA (mRNA) that occurs, human PTHrP can be expressed as mature protein products of length 139, 141 and 173 amino acids (Brandt, Wachsman *et al*. 1994, Burton, Brandt *et al*. 1994, Nikitovic, Kavasi *et al*. 2016) whereas in mice, there is only a single gene product of 139 amino acids (Mangin, Ikeda *et al*. 1990). Apart from these differences in C terminal sequences, most of the amino acid sequences within PTHrP are highly conserved between human and mice, including the totally conserved sequence of the PTH1R binding region.

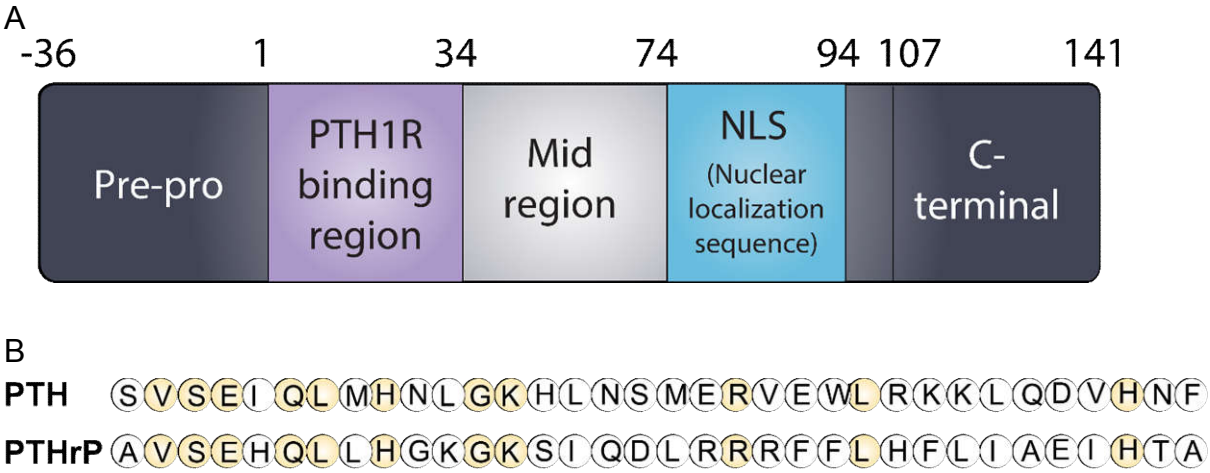

Figure 1.1. PTHrP domains and sequences of PTH, PTHrP with first 34 amino acids. (A) Diagram of PTHrP structure showing the Pre-pro region (amino acid -36–1), PTH1R binding region (amino acid 1–34) that activates the cAMP/CREB pathway and PTH1R receptor-independent regions (Mid region: amino acid 34–74; nuclear localisation sequence (NLS): amino acid 74–94; C-terminus: amino acid 107–141). (B) Sequences of the first 34 amino acids of PTH and PTHrP sequence (human and murine) are shown with residues that are identical with yellow fill.

1.2 Actions through the type 1 PTHrP receptor (PTH1R)

The PTH-like activity of PTHrP is contained in its N-terminal sequence, which allows PTHrP to act upon the common receptor, PTH1R (Suva, Winslow *et al*. 1987). This interaction of PTH1R and PTHrP has been evidenced by X-ray crystallography (Pioszak, Parker *et al*. 2009). It has been thus recognised that PTHrP is an intimate relative of PTH, and that both PTH and PTHrP exert actions on target cells by utilising the N-terminal PTH1R-binding region (Juppner, Abou-Samra *et al*. 1991).

The main actions of PTHrP on osteoblasts, osteocytes, and related cells (e.g. UMR106 osteogenic sarcoma cells) occur primarily through PTH1R and the cyclic AMP (cAMP)- protein kinase A (PKA) signalling cascade (Kondo, Guo *et al*. 2002, Kawane, Mimura *et al*. 2003, Kitase, Barragan *et al*. 2010) mediated by the G-protein alpha s subunit (Gαs; Yavropoulou, Michopoulos *et al*. 2017) followed by cAMP-response element binding protein (CREB) activation that signals from the cytoplasm to the nucleus (Fig. 1.2; Walia, Ho *et al*. 2016). Schwindinger *et al*. (1998) suggest PTH(1–34) increased the incorporation of GTP-AA into Gαs rather than the other two isoforms of Gαq or Gαi, which is correlated with the PTH1R/cAMP/PKA pathway (Schwindinger, Fredericks *et al*. 1998). The subsequent evidence that PTH1R signalling, at least in chondrocytes, requires Gαs activation and is required for endochondral ossification comes from studies showing that embryonic stem (ES) cells homozygous for Gαs ablation stopped proliferating prematurely and closely resembled chondrocytes lacking PTH1R in chimeric mice (Kronenberg 2006).

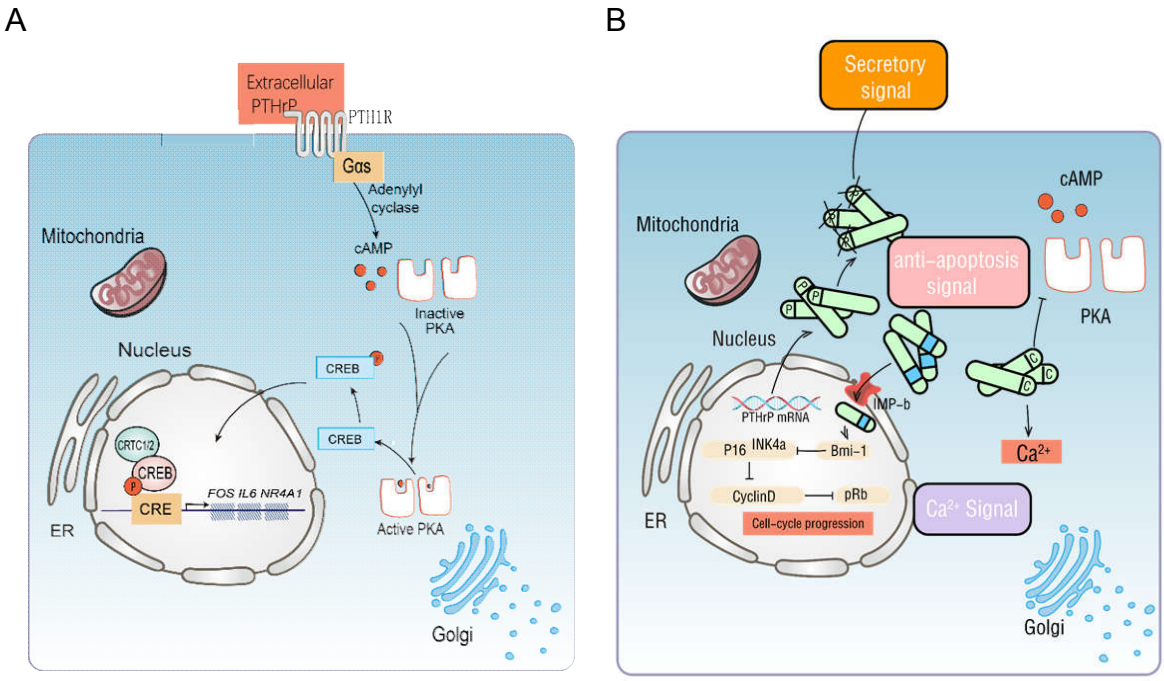

Figure 1.2. PTH1R receptor-mediated and receptor independent signalling by PTHrP. (A) PTH1R receptor-mediated signalling by PTHrP Schematic representation showing the canonical signalling targeted by extracellular PTHrP after engagement with PTH1R mediated by Gαs proteins. After cAMP has been released by adenylyl cyclase, PKA is activated followed by phosphorylation of cAMP response element binding protein (CREB) and increased recruitment of CREB-regulated transcriptional coactivators 1/2 (CRTC1/2) which bind to cAMP response elements (CRE) upstream of the promoter in target genes. This results in PKA-CREB response and transcription of CREB target genes (*FOS*, *IL6*, and *NR4A1*). (B) Secretion of PTHrP and PTH1R receptor-independent signalling. During secretion, the Prepro region (denoted with a P in the PTHrP molecule) includes a 36 amino acid sequence which functions as a signal peptide, directing PTHrP to the secretory pathway (Bhatia, Saini et al. 2009), and is cleaved secreted following secretion cleavage. The PTHrP NLS (shown in blue) drives an anti-apoptosis signal through an intracellular mechanism. After internalisation PTHrP-NLS binds importin-β (IMP-b), activating Bmi-1 in the cytoplasm-nucleus, leading to inhibition of $p16^{INK4a}$ and suppression of CyclinD and pRB. PTHrP(107-–139) C terminus (denoted with a C in the PTHrP molecule) has also been reported to induce Ca^{2+} signalling in rat osteoblastic osteosarcoma UMR106 cells, but inhibits, inhibiting the PKA activities induced by PTH(1–36).

Gαs activation is coupled with stimulation of cyclic adenosine monophosphate (cAMP)-protein kinase A (PKA) via adenylyl cyclase (AC) activation (Kemp, Moseley *et al*. 1987). Following activation of PKA, the cAMP response element binding protein (CREB) is phosphorylated at site S133 (Altarejos and Montminy 2011). This is followed by increased nuclear localisation of CREB-regulated transcriptional coactivators 1/2 (CRTC1/2; Ogawa, Kozhemyakina *et al*. 2014) which bind to an upstream cAMP response element (CRE) to promote expression of CREB responsive genes such as *c-fos* (*Fos*; Ionescu, Schwarz *et al*. 2001), *interleukin 6* (*Il6*; Chen, Koh *et al*. 2004), and *Nr4a1* (Walia, Ho *et al*. 2016).

1.3 Actions of PTHrP that are PTH1R-independent

Although PTHrP acts through PTH1R, the ability of PTHrP to have receptor independent actions was highlighted when PTHrP deficient mice had an impaired placental Ca^{2+} transport system with lower blood calcium and a reduced fetal-maternal Ca^{2+} gradient, whereas this phenomenon was not observed in PTH1R-deleted mice (Kovacs, Lanske *et al*. 1996). Therefore, this study of PTH1R deletion was not sufficient to fully explain the phenotype of PTHrP knockout mice (Kovacs, Lanske *et al*. 1996), raising the possibility that the PTH1R-activating domain does not mediate all PTHrP cellular actions. Some actions of PTHrP beyond the N-terminal domain are established. Care *et al.* (1990) suggested three mid-region PTHrP molecules, namely PTHrP(67–86), PTHrP(75–84), and PTHrP(75–86), stimulated the placental transport of calcium when the peptides were injected into the two umbilical arteries (Care, Abbas *et al*. 1990). This was subsequently supported by (Care, Abbas *et al*. 1990, Wu, Vasavada *et al*. 1996) in the finding that the mid-region helps placental calcium transport from mother to foetus. In these studies, the

placenta was perfused with PTHrP preparations lacking the amino-terminal domain and therefore unable to activate PTH1R.

Further evidence for the biological importance of PTH1R-independent activities of PTHrP come from the contrasting phenotypes of diminished trabecular bone volume and low bone strength in mice, which have less PTHrP in osteocytes (Ansari, Ho *et al*. 2018), but high bone mass in mice with PTH1R gene deletion in osteocytes (Bellido, Saini *et al*. 2013, Delgado‐Calle, Tu *et al*. 2017). This emphasises an important difference between intracrine/autocrine actions of PTHrP and PTH1R-dependent actions through extracellular PTHrP, suggesting that PTHrP can exert actions on the osteocyte independent of using PTH1R. Elucidating the functional regions responsible for non PTH1R-mediated actions of PTHrP may provide a new way to understand the biological influences of PTHrP. There is evidence that multiple regions of the protein have distinct biological activities.

1.3.1 C-terminus region peptide functions

The PTHrP C-terminus region (107–139; Fig. 1.3) has been proposed to exist as a separate circulating peptide that is cleaved by the prohormone thiol protease in lung cancer cells (Hook, Burton *et al*. 2001). Studies of the effects of the C-terminus PTHrP on cell functions have been carried out using pharmacological experiments, in which peptides have been used to treat cells *in vitro*, or in some cases, animals *in vivo*.

Fenton *et al.* (1991) were the first to suggest that the native C-terminus of PTHrP may be important in bone because it exogenously inhibits osteoclast-mediated bone resorption by directly interacting with osteoclasts. Since osteoclasts do not express PTH1R, this indicates that the C-terminus produces this effect through a receptor other than PTH1R. They identified the osteoclast-inhibitory activity within the five residues from T107-W111 and called this peptide “osteostatin”.

The C-terminus of PTHrP(107–139) was also shown to induce Ca^{2+} signalling via a voltage-sensitive Ca^{2+} channel in rat osteoblastic osteosarcoma UMR106 cells, more strongly than PTHrP(1–36; ValÍn, Guillén *et al*. 2001). Although PTHrP(107–139) had stronger activity than PTHrP(1–36) on intracellular Ca^{2+}, the PKA activity induced by PTHrP(1–36) was attenuated when cells were preincubated with PTHrP(107–139; ValÍn, Guillén *et al*. 2001). In addition to this, even though PTHrP(107–139) induced *Il6* and *Fos* messenger RNA, the two gene mRNA levels had not been affected when cells were treated with PKA inhibitor. This suggests that stimulation of intracellular Ca^{2+} on induction of *Il6* and *Fos* by this C-terminus fragment is not through PTH1R, but might be through another pathway (ValÍn, Guillén *et al*. 2001). Understanding any relationship between exogenously supplied PTHrP(107–139) and intracellular Ca^{2+} will require identification of candidate receptors or alternative internalisation mechanisms.

PTHrP(107–139) was suggested to promote human osteoblastic (HOB) cell survival by stimulating Vascular Endothelial Growth Factor Receptor 2 (VEGFR2; Alonso, De Gortazar *et al*. 2008). The protective effect of PTHrP(107–139) on cell survival was abrogated in MG-63 cells with knocked down VEGFR, indicating an association PTHrP(107–139) with VEGFR2. Although PTHrP(107–139) increased the level of phosphorylation of VEGFR2, ERK, and AKT, there was no evidence that this resulted from direct binding. Importantly, because VEGFR2 tyrosine kinase inhibitor abolished the effect of PTHrP(107–139) but not that of PTHrP(1–36), this effect might be beyond the PTHrP(1–36)/PTH1R activation. García-Martín *et al.* (2013) later showed by Western blot, using antibody targeting VEGFR2 Tyr-1059 phosphorylation in cells treated with a maximum dose of PTHrP(107–139), that the C-terminus causes sustained activation of pro-survival extracellular signal-regulated kinase (ERK) and Akt. This suggests the C-terminus promotes VEGFR2 phosphorylation, both in rat UMR106 osteosarcoma and MC3T3-E1 cells for survival (García‐Martín, Acitores *et al*. 2013). This would imply

that PTHrP(107–139) acts through control of VEGFR2 phosphorylation to stimulate osteoblastic cell survival. If correct, it would be suggestive of anabolic action of PTHrP(107–139) in bone. However, these pharmacological studies with high peptide doses *in vitro* do not exclude effects on other signalling pathways and cellular mechanisms.

In vivo approaches have also been employed to identify PTHrP C-terminus functions. For example, treatment with PTHrP(107–139) promoted bone healing after marrow ablation in mice with diabetes (Lozano, Fernández‐de‐Castro *et al*. 2011). A finding that is particularly difficult to explain is that systemic administration of PTHrP(1–34), and PTHrP(107–139) which does not use PTH1R, were found to have comparable effects on restoring bone loss after ovariectomy in mice (De Castro, Lozano *et al*. 2012). This surprising finding would suggest that these two peptides have the same effect on bone formation even though they use different PTHrP signalling pathways. It remains to be determined how C-terminus PTHrP can act as a promoter of bone formation since no receptor has yet been identified that might mediate the effects. It is important that new approaches are used to identify other receptors utilised by PTHrP C-terminus and establish whether it provides a physiologically relevant pathway of action.

It has also been suggested that the C-terminus is associated with cell growth. Using NCI-H520 non-small cell lung cancer cells transfected with a genetic polymorphism located in the PTHrP(107–141) encoding region, Manenti *et al*. (2000) showed that cells transfected to produce the variant $PTHrP^{Pro}$ resulted in increased tumour growth in nude mice relative to non-transfected cells, whereas cells transfected to produce $PTHrP^{Thr}$ resulted in decreased tumour growth. This suggests a role of the C-terminus in regulating cancer proliferation (Manenti *et al*. 2000). Yeast two-hybrid screening with expression of PTHrP(122–141) as a bait, and co-transfection of β-arrestin, has demonstrated that the

C-terminus interacts with β-arrestin, suggesting a role for PTHrP in the β-arrestin/MAPK pathway, perhaps in the modulation of the cellular response to extracellular proliferative signals (Conlan, Martin *et al*. 2002). One study of potential relevance is that by De Miguel, *et al*. (2001), who used vascular smooth muscle cells and mutant PTHrP constructs to explore the mechanism of action through which PTHrP drives proliferation after nuclear entry. They demonstrated that deletion of the NLS region prevents nuclear entry and slows proliferation, but no such effects were observed in cells overexpressing PTHrP with the N-terminus deleted. In this study, absence of the C-terminus dramatically reduced proliferation without affecting nuclear translocation activities, suggesting a role of the C-terminus in promoting cell proliferation. However, no further functional characterisation has been performed to determine the mechanism of how cell growth is mediated by the C-terminus.

As shown above, the exogenous PTHrP C-terminus is likely to have actions that are not mediated by PTH1R. It is still not clear, despite extensive studies of exogenously administered C terminal PTHrP, that this domain of the protein is physiologically affecting cell functions.

1.3.2 Pre-pro region and intracellular trafficking of PTHrP after synthesis

PTHrP is a secretory protein, and its signal sequence (prepro region, -36 to 1 aa; Fig. 1.3) allows translocation of the newly synthesised PTHrP into the endoplasmic reticulum (ER) where it can be cleaved for secretion by the secretory pathway (Nguyen, He *et al*. 2001, Amaya, Nakai *et al*. 2015). Alternative initiation of translation within this signal sequence from one the four CUG codons (non-AUG start sites; Nguyen, He *et al*. 2001), termed alternate start sites of PTHrP mRNA has been demonstrated to result in a non-functional phenotype for ER targeting (Nguyen, He *et al*. 2001). Transcription from these alternate start sites in the secretion region, leads to deficient PTHrP protein in the cytoplasm but

improves the trafficking capacity of PTHrP to the nucleus (Amaya, Nakai *et al*. 2015). The biological importance of this intracellular trafficking of proteins with relation to the Prepro region remains to be explained.

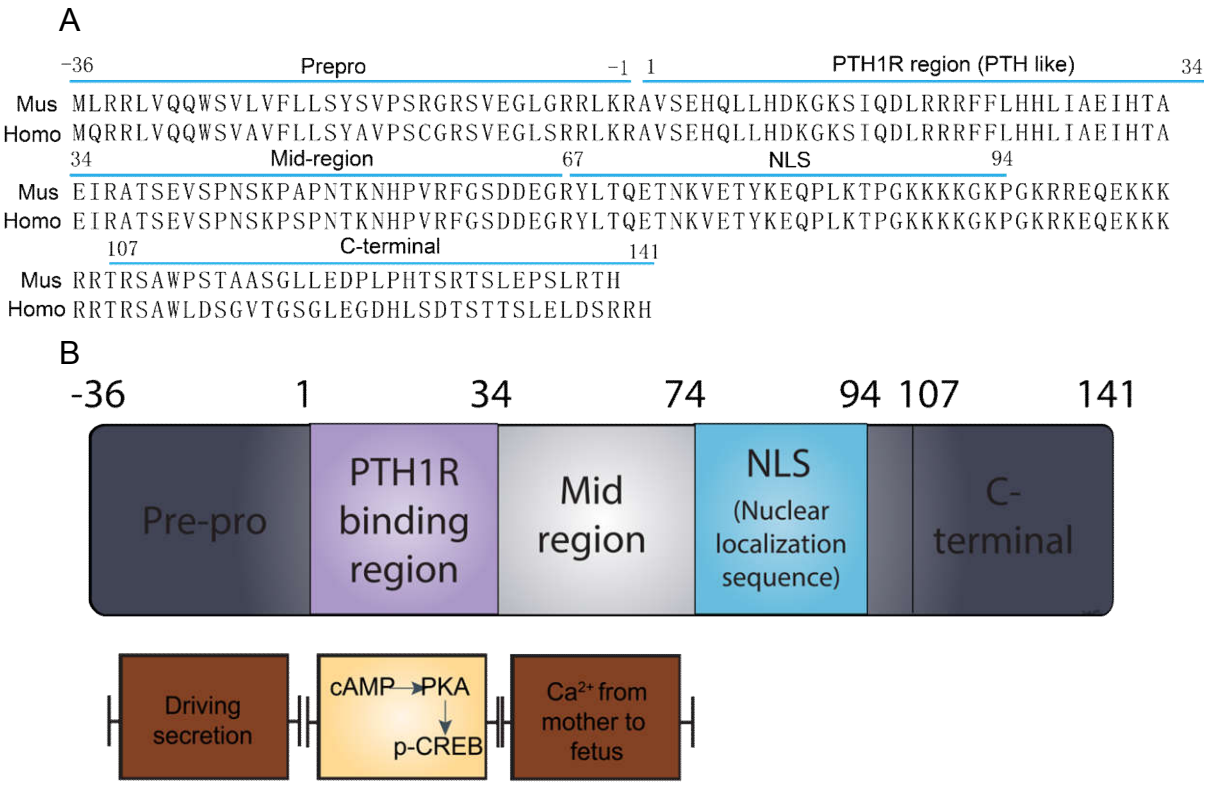

Figure 1.3. (A) PTHrP amino acid sequence. PTHrP protein structure showing the Prepro region required for secretion, the PTH1R-binding region that activates the cAMP/CREB pathway and regions thought to have activity independent of the PTH1R: Mid-region, Nuclear localisation sequence (NLS), C-terminus region. Mus = *Mus musculus* (laboratory mouse), Homo = *Homo sapiens* (human). **(B). Parathyroid hormone-related protein (PTHrP) has several regions with known functions:** a pre-pro signal peptide (-36-1) for endoplasmic reticulum (ER) targeting and secretion after its cleavage; a PTH1R (PTH receptor)-binding region (1-34) that activates cAMP/PKA; a mid-region (34-74), which promotes placental calcium transport from the maternal circulation to the fetal skeleton; an internal nuclear localization sequence (NLS – 74-94), and a C-terminus region (107-141).

1.3.3 Nuclear localisation sequence (NLS) and nuclear activities

The ability of PTHrP to localise to the nucleus was initially observed in chondrocytes by Henderson *et al.* (1995) who found PTHrP promoted enhanced cell survival under serum starvation. The functional NLS domain (Fig. 1.3) was confirmed and defined as contained within residues 67–94 of PTHrP based on its ability to interact with karyophillic importin

proteins (importins) and the nuclear pore complex (Lam, Briggs *et al*. 1999, Lam, Thomas *et al*. 2000) but other residues were suggested by others to contribute to nuclear import (Henderson, Amizuka *et al*. 1995). Cingolani *et al.* (2002) undertook a co-crystallisation of PTHrP with importin-β to identify the fragment that was capable of recognising importin-β, and this resulted in identification of specific PTHrP (67–94) that interacts with importin-β. The PTHrP-NLS binds importin-β directly but not importin-α, which suggests that PTHrP is directly transported into the nucleus in an importin β mediated manner (Lam, Briggs *et al*. 1999, Zhang, Li *et al*. 2019). Further discovery of phosphorylation at the cyclin-dependent kinase residue Thr85 within the NLS revealed decreased PTHrP nuclear translocation, therefore this site of phosphorylation may contribute to some mechanisms in determining the nuclear import process (Lam, Briggs *et al*. 1999). Taken together, these findings confirm that there is an interaction between the NLS region and host cell nuclear transport machinery.

PTHrP may regulate cell proliferation mediated by the NLS-region independently of using PTH1R. One of the functions of PTHrP is to prevent starved cells from undergoing apoptosis (Fig 1.2B), and this has been postulated to occur through a non-PTH1R-dependent process (Tovar Sepulveda *et al*. 2002, Okoumassoun *et al*. 2007). Several studies have ascertained that endogenous PTHrP actively inhibits cell death by altering cell-cycle progression (Aarts *et al*. 2001, Tovar Sepulveda *et al*. 2002). The inhibition of apoptosis of MCF7 breast cancer cells overexpressing full-length PTHrP showed enrichment of G2 +M phase of cell cycle when cells were analysed by flow cytometry to determine the stage of the cell cycle (Tovar Sepulveda *et al*. 2002). However, this was not seen in the MCF7 cells overexpressing an intracrine mutated from of NLS, which are largely in G1 stage, and such cells had abolished the apoptosis-inhibition phenotype. This suggests a role of NLS in inhibiting the inhibition of apoptosis, or in other words, promoting cell survival and thus proliferation. Further to this, Falzon and Du

(2000) suggested that treatment of MCF7 cells with exogenous full-length PTHrP, acting through PTH1R, results in decreased cell proliferation, which is different from the cells overexpressing endogenous PTHrP that increase proliferation. The difference in cell survival between exogenous and endogenous PTHrP indicates that the intracrine PTHrP NLS region may exert functions without requiring PTH1R.

It has been suggested that casein kinase II (CK2) may be a signalling pathway responsible for PTHrP-NLS activities in reducing apoptosis (Lam, House *et al*. 1999). A predicted consensus protein kinase CK2 site was identified in PTHrP-NLS to favour transportation of PTHrP from the nucleus to cytoplasm (Lam, Briggs *et al*. 1999). Mutation of Thr^{85} within this site to Ala^{85} to abolish the phosphorylation resulted in increased nuclear accumulation. In contrast, mutation to Glu^{85} to mimic a phosphorylated residue resulted in localisation of PTHrP to the cytoplasm, suggesting a role of phosphorylation by CK2 is important for decreased PTHrP nuclear accumulation associated with PTHrP in inhibiting apoptosis. However, they did not describe whether this NLS activity was essential for an anti-apoptotic phenotype. The biological importance of this was confirmed when homozygous and heterozygous PTHrP gene deletions in mice lead to increased primary chondrocyte apoptosis, an effect that was attenuated by protein kinase CK2 expression, indicating that CK2 may link the nuclear association with PTHrP-NLS activities (Okoumassoun, Russo *et al*. 2007). Together, these studies only described the role of CK2 in PTHrP's actions that regulate cell survival. It still remains to be determined whether the absence of the NLS region may influence cell death by other mechanisms. It is also important to confirm the role of intracrine NLS region and its association with CK2 signalling and other alternative pathways that may take place.

1.4 PTHrP-induced bone metastasis of breast cancer cells

1.4.1 PTHrP is important for bone metastasis process

PTHrP has a major role in the establishment of breast cancer metastasis in bone. After the finding that PTHrP was commonly expressed in primary breast cancers (Southby, O'Keeffe *et al*. 1995), it was later reported that PTHrP production is enriched in bone metastases as compared to primary tumours and other metastatic sites (Burtis, Brady *et al*. 1990, Southby, Kissin *et al*. 1990, Powell, Southby *et al*. 1991). With that finding it was suggested that the breast cancer cells in bone could establish themselves there by promoting a bone resorption niche through the action of tumour-derived PTHrP (Powell, Southby *et al*. 1991).

PTHrP was shown to be produced by at least 60% of primary breast cancers (Southby, O'Keeffe *et al*. 1995), and its production to be enriched in metastatic breast cancer cells within bone (92%; Grill, Ho et al. 1991, Powell, Southby *et al.* 1991) compared to primary tumours (50%) and other metastatic sites (Burtis, Brady *et al*. 1990, Southby, Kissin *et al*. 1990, Powell, Southby *et al*. 1991).

In vivo studies have demonstrated that PTHrP has the capacity to enhance osteolytic potential of MDA-MB-231 breast cancer cells (Guise, Yin *et al*. 1996, Guise 1997), and that transforming growth factor β (TGF-β), released from the bone environment, stimulates cancer cells to generate PTHrP (Yin, Selander *et al*. 1999). When MDA-MB-231 tumour cells were treated with the TGF-β-neutralising antibody, ID11, this led to attenuated tumour burden-induced bone destruction (Biswas, Nyman *et al*. 2011). Such studies confirmed in a model that tumour-induced PTHrP causes bone destruction in the metastatic process. The combination of these findings in human breast cancer led to the concept that local generation of PTHrP by cancer cells in bone is an important contributor to the bone metastasis process.

The original idea that bone is a favourable site for breast cancer establishment and growth was proposed by Paget (1889), more than a century ago, and a focus of much modern investigation is to determine the mechanisms involved in this. Subsequently, it was established that bone is the soil for tumour cells and subject to invasion, colonisation, and growth of tumours (Berrettoni and Carter 1986; Fig. 1.4A). Invasion refers to the extension and penetration by tumour cells into adjacent tissues, caused by the gradual increase in tumour size and a breach in the boundaries between tissues. Metastatic colonization indicates that the cancer has not only invaded, but has established a clinically relevant metastasis at a secondary site. Breast cancers do not always establish/colonise immediately after spreading to bone but often remain there in a dormant phase which is associated with limited cell proliferation (Aarts, Davidson *et al*. 2001, Weilbaecher, Guise *et al*. 2011).

Dormancy occurs when cancer cells are no longer proliferating, but remain viable. When the majority of a cancer population is in this state, the result is called tumor dormancy. A possible role for PTHrP in the escape of breast cancer cells from the dormancy phase arose from the work of Thomas *et al.* (1999) who demonstrated that MCF7 cells overexpressing PTHrP, injected into the left ventricle of mice, established in bone and caused significantly increased tumour lesion numbers and areas in hind limbs 40 days after inoculation. However, the human breast cancer cells, MCF7, were known to grow minimally or not at all in bone when injected by intracardiac injection in nude mice (Thomas, Guise *et al*. 1999). The MCF7 cells overexpressing PTHrP established in bone was proposed by Thomas *et al.* (1999) that this is due to the increased support of osteoclast formation by PTHrP-expressing breast cancer cells, a finding confirmed by co-culture of breast cancer cells and osteoclast precursors. The mechanism through which PTHrP acts to increase osteolysis was proposed to be through down- and up-regulation of

osteoprotegerin (OPG) and Receptor activator of nuclear factor kappa-B ligand (RANKL) mRNA, respectively; the latter is essential for the process of osteoclastogenesis.

1.4.2 PTHrP promotes breast cancer exit from dormancy in a PTH1R-independent manner

It is well established that bone-derived PTHrP is important factor in the vicious cycle of bone destruction as seen in osteolytic metastases. PTHrP manufactured in tumours has a stimulatory effect on osteoclastic bone resorption, leading to destruction that characterises breast cancer metastases (Guise, Yin *et al*. 2002, Jun, Kim *et al*. 2014, Bendre, Gaddy *et al*. 2003, Croucher, McDonald *et al*. 2016). Berrettoni and Carter (1986) developed the idea that PTHrP is a factor of breast cancer related with osteolytic metastasis, and Mundy (2002) suggested there is communication between tumour cells and osteoclasts.

Recently the novel possibility has been that the human breast cancer cell line MCF7 can been regarded as a tumour dormancy model in bone because of its low cell replication and few osteolytic lesions when injected arterially in nude mice (Johnson, Finger *et al*. 2016). MCF7 cells overexpressing PTHrP overcome this dormancy phenotype, causing them to grow as osteolytic deposits, and have been shown to exhibit significantly lower expression of a panel of genes associated with dormancy (Johnson, Finger *et al*. 2016). The mechanisms by which such a change in MCF7 cell behaviour takes place is of great interest. Since the cells change their phenotypic behaviour with PTHrP overexpression, first thoughts would have been that PTHrP was influencing the cells through a positive cAMP signalling pathway. Actions through PTH1R are predominantly cAMP-dependent, but MCF7 and T47D breast cancer cells have been found in earlier studies to show no PTH1R/ cAMP responsiveness by treatment of PTH, despite being highly responsive in cAMP production to calcitonin and PGE_2 (Findlay, deLuise *et al*. 1980, Martin, Findlay *et al*. 1980). Therefore, I hypothesise that the actions of PTHrP in the overexpressing MCF7 cells result from non-canonical actions that are not linked with cAMP production – i.e.

actions mediated by portions of the PTHrP molecule that are distinct from the amino-terminal domain that interacts with PTH1R/cAMP. Further exploration should be undertaken on the mechanisms of PTHrP involvement in cancer in bone, in particular its possible role on overcoming dormancy via non-canonical PTHrP signalling actions. Understanding of these intracrine pathways could lead to the development of new therapeutic agents.

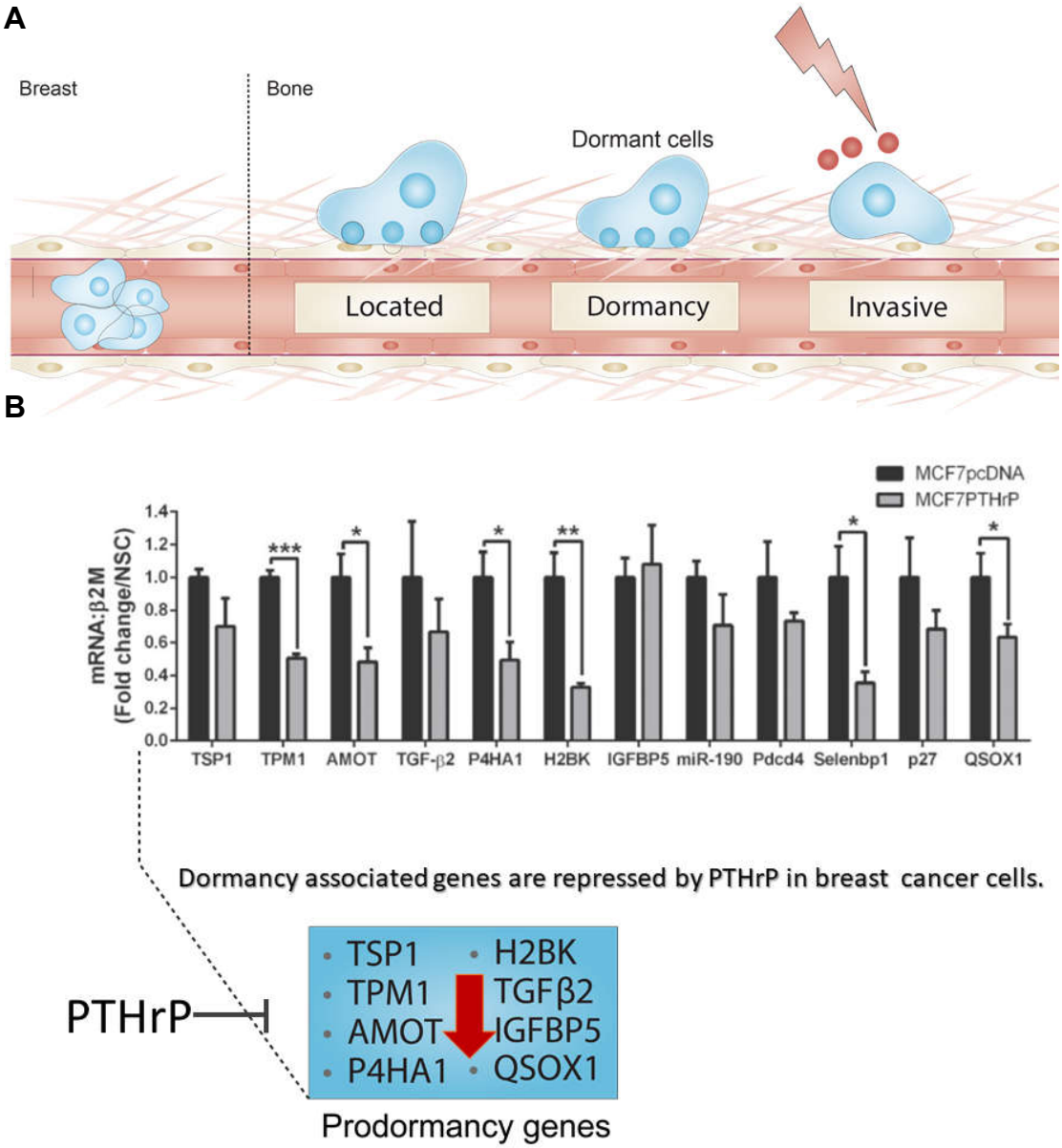

Figure 1.4. PTHrP overexpression drives MCF7 breast cancer cells out of dormancy in the bone microenvironment. (A) Mechanisms involved in tumour dormancy. Bone metastasis development begins when cells from the primary tumour translocate from the breast through the bloodstream to bone marrow, and establish themselves at a second site. After colonisation of the bone marrow, cells may undergo apoptosis, reside in a dormant state, or become an invasive proliferating metastasis. The dormant stage is influenced by a combination of factors and dormancy-associated genes. (B) Elevated Parathyroid hormone-related protein (PTHrP) signalling reduces dormancy-, quiescence- associated genes. mRNA levels of genes associated with dormancy and quiescence (*TSP1*, *TMP1*, *AMOT*, *P4HA1*, *H2BK*, *TGFβ2*, *IGFBP5*, *OSQX1*) in MCF7pcDNA- (control) and MCF7PTHrP-overexpressing cells. Mann–Whitney test. n = 3 biological replicates, one each from three independent experiments. The graph is taken from Johnson *et al*. (2016). To summarise this, as a key regulator of tumour-bone interactions, PTHrP overexpression drives MCF7 breast cancer cells out of dormancy in the bone microenvironment, which promotes the "dormancy" step to the metastatic invasive phase.

1.5 Biological role of PTHrP in bone

1.5.1 Bone development

Although PTHrP was discovered as a tumour-released factor responsible for the hypercalcemia of malignancy in cancer patients (Stewart, Horst *et al*. 1980, Strewler, Stern *et al*. 1987, Suva, Winslow *et al*. 1987, Mangin, Ikeda *et al*. 1988), it was also found to have important biological roles in the skeleton. Karaplis *et al.* (1994) demonstrated that PTHrP is required for normal bone development when PTHrP-null mice died perinatally with extensive premature maturation of chondrocytes and shortened endochondral bones. These mice failed to respire, resulting in hypotonic bodies compared to wild-type (WT) mice of equivalent sizes and masses. Distinct features were also revealed in these mice, showing domed skull and short limbs with anomalous shape. Despite no changes in the mineralisation of the spine and limbs, the costal cartilage tissues contained more mineral contents when mice were stained with Alizarin red. Further investigation revealed that PTHrP delays the production of Indian Hedgehog (IHH) by chondrocytes, an interaction that is required for terminal differentiation of chondrocytes toward the hypertrophic state (Kronenberg 2006).

In addition to this role in endochondral bone formation, PTHrP was found to be produced by osteoblast-like cells when rat osteoblast cells CRP 5/4 were observed to be stained with PTHrP antiserum (Kawane, Mimura *et al*. 2003). Several studies have ascertained that PTHrP mRNA and protein are produced in osteoblast-rich cultures of rat, mouse, and human (Moseley, Hayman *et al*. 1991, Guenther, Hofstetter *et al*. 1995, Tsukazaki, Ohtsuru *et al*. 1995, Suda, Gillespie *et al*. 1996).

This suggests PTHrP is important for adult mice bone as it also produced immunoreactivity in fetal long bones culture (Bergmann, Wolf *et al*. 1990). Another study

identified PTHrP based on its expression in newly formed bone when a defect was introduced into rabbit bone (Kartsogiannis, Moseley *et al*. 1997). An improved understanding of the function of PTHrP in bone development will improve understanding of the mechanisms involved in bone formation overall.

1.5.2 Bone formation

As well as the essential role of PTHrP in chondrocytes that is required for normal bone development, evidence from genetically manipulated mice showed that PTHrP also has a crucial role in bone formation. Although $PTHrP^{-/-}$ mice died around birth (Karaplis, Luz *et al*. 1994), the $PTHrP^{+/-}$ mice that survived were found to have low trabecular bone mass by three months of age (Amizuka, Karaplis *et al*. 1996). This led Miao *et al.* (2005) to knock down PTHrP in the osteoblast lineage using a Collagen Type I alpha1 *(Col1)-Cre* mouse crossed with a PTHrP floxed mouse ($Pthrp^{flox/flox};cre^{ColI}$ mice). Osteopenia, which developed from loss of bone formation or bone resorption, was observed at six weeks of age; a phenotype closely resembling that of $PTHrP^{+/-}$ mice. Since a reduction in osteoblast number and osteoid volume was seen in mutant long bone sections of $PTHrP^{+/-}$ mice, with increased apoptotic osteoblasts/osteocytes, this indicates PTHrP has a role in maintaining osteoblast and osteocyte survival that may make important contributions to bone formation. PTHrP in committed osteoblasts is important; further research into the role of PTHrP signalling in preventing apoptosis in osteoblasts will improve our understanding of pathological bone phenotypes in $PTHrP^{+/-}$ and $Pthrp^{flox/flox};cre^{ColI}$ mice. It is also important to investigate the role of osteocytic PTHrP in bone formation.

1.5.3 Bone mineralisation and material strength

As in osteoblasts, PTHrP is produced in osteocytes as identified by immunostaining and by *in situ* hybridisation (Kartsogiannis, Udagawa *et al*. 1998). Osteocytes have been identified as mechanical sensors of the skeleton that modulate bone remodelling and bone

mineral homeostasis. They comprise 90–95% of all bone cells in the adult skeleton (Aarden, Nijweide *et al*. 1994, Nicolella, Moravits *et al*. 2006). Not only is PTHrP important in osteoblasts, but it also has essential roles in osteocytes. Our laboratory has recently shown that dentin matrix 1 *(Dmp1) Cre.Pthlh*$^{f/f}$ mice with conditional knock-down of *Pthlh* in osteocytes exhibit low trabecular bone mass, impaired bone formation, and reduced bone strength (Ansari, Ho *et al*. 2018). Neither bone size nor bone shape was shown to be the effector to change the bone strength. This suggests there was likely a material defect exerted by PTHrP in the cortical bone matrix that restricts the bone strength, and suggests that PTHrP from osteocytes regulates bone material quality (Ansari, Ho *et al*. 2018). The mRNA of osteocalcin (gene name: *Bglap*), alkaline phosphatase (gene name: *Alpl*), and dentin matrix acidic phosphoprotein 1 (gene name: *Dmp1*), which are well-characterised late markers of mineralisation, were all strongly attenuated in *PTHrP* knock down OCY454 cells differentiated for seven and 14 days (Ansari, Ho *et al*. 2018), indicating that PTHrP is likely to be involved in mineralisation in osteocytes. However, whether this phenotype in *Dmp1Cre.Pthlh*$^{f/f}$ is because of the change in surrounding matrix and/or signalling is not yet well understood. It has also been suggested by Ansari *et al*. (2018) that PTHrP affects cortical strength through a non-receptor-mediated pathway because mice administered PTH through the receptor, did not show compromised bone composition or maturation (Vrahnas *et al*. 2016). Thus, PTHrP is presumably important for bone mineralisation, however, the role of osteocytic PTHrP in regulating bone mineralisation has not yet been examined.

1.6 Hypothesis

Specific actions of PTHrP in osteocytes and breast cancer cells are associated with regions of the molecule other than the N-terminal region that acts through PTH1R.

1.7 Specific aims

1. To determine non-receptor-mediated pathways affected by PTHrP signalling in converting MCF7 breast cancer cells into an invasive phenotype;

2. To identify non-receptor-mediated pathways of PTHrP action in the osteocyte;

3. To establish how the PTHrP C-terminus influences the actions of PTHrP through PTH1R in osteocyte and osteoblastic osteosarcoma cell lines;

4. To assess the role of osteocytic PTHrP in controlling matrix composition *in vitro* and *in vivo*

CHAPTER 2: Materials and methods

2.1 Cell culture

2.1.1 MCF7 breast cancer cells

Human MCF7 breast cancer cells were obtained originally from the American Type Culture Collection (Manassas, United States) and cultured in Dulbecco's Modified Eagle Medium (DMEM; ThermoFisher Scientific, Waltham, United States), supplemented with 10% fetal bovine serum (FBS, Sigma, St. Louis, MO, United States), and Penicillin/Streptomycin (P/S; 5 IU/mL penicillin and 5 μg/mL streptomycin). MCF7 pMSCV and MCF7 cells overexpressing PTHrP cells (MCF7_PTHrP) were established in the host laboratory, St. Vincent's Institute of Medical Research. The cells were engineered to overexpress human PTHrP(-36–141), so that active PTHrP of full length would be secreted, as shown in (Thomas, Guise *et al*. 1999). I confirmed that these cells had maintained high levels of PTHrP production by using PTHrP biological assay, radioimmunoassay (Section 2.4) as well as quantitative polymerase chain reaction (qPCR). I established the following MCF7 cell lines overexpressing full-length and mutant forms of PTHrP, which were kept in identical conditions: $PTHrP^{FL}$ (full-length), $PTHrP^{1\text{-}67}$ (which lacks NLS region and C-terminus), and $PTHrP^{\Delta NLS}$ (which lacks NLS region).

2.1.2 OCY454 cell line

The osteocyte cell line, OCY454 (Spatz, Wein *et al*. 2015) was obtained from Dr. Paola Divieti (Boston University). OCY454 cells were maintained in permissive conditions (33°C), then differentiated at 37°C to reach a stage of osteocytic gene expression after 10–14 days. They were cultured in Minimum Essential Medium Eagle-Alpha Modification (αMEM; Lonza, Basel, Switzerland) supplemented with 10% FBS and 1%

Penicillin-Streptomycin-Amphotericin B (PSA, Life Technologies, Bengaluru, India) and Glutamax (Life Technologies, Carlsbad, CA, USA). Cells were seeded in 6-well plates at 1.6 x 10^6 cells per well or as indicated in specific experiments. Cells were grown at the permissive temperature (33°C) for three days prior to transferring to 37°C for differentiation to osteocytes. Cells were differentiated for up to 14 days or as indicated in individual experiments. The culturing conditions to maintain the OCY454 osteocytic phenotype were twice weekly sub-passaged (1:5) at 33°C for up to 2 months from a frozen stock. The cell line OCY454, which overexpresses full-length and mutant PTHrP (see Chapters 4, 5 and 6), the cell line OCY454 Luc Ctrl, the vector control, and the cell line OCY454, which is PTHrP knocked-down (PTHrP KD; Section 6.6) were cultured and maintained in identical conditions.

2.1.3 UMR 106.01

UMR106.01 cells are a clonal line developed from a rat osteogenic sarcoma (Martin *et al*. 1976; Partridge *et al*. 1983; Forrest *et al*. 1985). Cells were harvested using 0.02% EDT (Sigma) between passages 18 and 24, and subsequently passaged every 3–4 days. Cells were not used beyond passage 35. The cells were maintained in αMEM medium supplemented with 10% fetal bovine serum, 2 mM Glutamax, 100 U/mL penicillin and streptomycin (Life Technologies, Bengaluru, India) antibiotics. This medium was changed every second day. Cells were cultured in a humidified 5% CO_2 atmosphere at 37°C.

2.2 Transient transfection of Cells

The following transient transfections were performed using FuGENE® HD Transfection Reagent (Cat. No. E231, Promega, Australia): MCF7 cells transfected with a cAMP response element (CRE)-luciferase construct (Section 3.3.2), UMR106.01 $PTHrP^{68–141}$, $PTHrP^{107–141}$, and pcDNA stable cell lines transfected with OSE2 reporter plasmids

containing six tandem copies (Section 5.3.2), UMR106.01 $PTHrP^{68–141}$, $PTHrP^{107–141}$, and pcDNA stable cell lines co-transfected with CRE-Luc reporter construct (Section 5.4.2), and UMR106.01 $PTHrP^{68–141}$, $PTHrP^{107–141}$, and pcDNA stable cell lines co-transfected with TOP-flash plasmid DNA and with Renilla Luciferase plasmid DNA (Section 5.5). Cells between 50-80% confluence in a 6-well plate were transfected according to the manufacturer's method. Briefly, for 1 well, 3μL Fugene was diluted in 100μL in a microfuge tube in serum-free DMEM medium or αMEM medium for MCF7 cells or UMR106.01 cells, respectively. 1-2μg of plasmid DNA was then added to the diluted Fugene, gently mixed and incubated for 15 mins at room temperature. The Fugene/plasmid DNA complex mixture was added to the well of cells (1mL media), which were plated the day before, swirled to distribute and the cells returned to the incubator for 24-48 hours.

Monolayer cultures for cells to be transfected and the control cells were passaged in the following manner. The medium was removed and the cells was rinsed in 1x Versene. Enough trypsin to just cover the cells was added to the flask and incubated at 37℃ for 5 mins. The flask was gently tapped to loosen the cells and medium was added to the flask to inhibit any further action by trypsin. The cell suspension was transferred to a 30mL tube and spun at 1,500 rpm for 5 mins. Pelleted cells were resuspended in 10mL of cell culture medium by pipetting before disaggregation to individual cells by syringing the suspension through at 21 G needle. The appropriate volume of cells was added to a fresh flask containing pre-warmed media.

2.3 Stable transfection of cells

The goal of stable transfection is to isolate and propagate individual clones containing transfected DNA. To distinguish non-transfected cells from those that have taken up the exogenous DNA, Zeocin (Cat. No. R25001, Invitrogen, Carlsbad, CA, USA) was used for

selection and establishment of stable lines. Based on zeocin selection experiment to determine the optimal zeocin concentration, Zeocin (20mg/mL) was used for selecting UMR 106.01 and MCF7 cell lines.

2.4 Generating stable cell lines overexpressing *Pthlh* and *Pthlh* gene constructs

2.4.1 Preparation of OCY454 osteocytes overexpressing *Pthlh* mutants

To do this I used the immortalised osteocyte cell line OCY454 (Spatz, J.M., *et al.* 2015). These cells were originally obtained from mice double transgenic for green fluorescent protein (GFP) under the control of 8 kb of the Dmp1 promoter, 8 kb-Dmp1-GFP (Tg(Dmp1- Topaz)^{1Ikal}), and Simian vacuolating virus 40 antigen (SV40 Ag) (Immortomouse Charles River). The cells were obtained from these mice by sequential collagenase digestions followed by Fluorescence activated cell sorting (FACS). The Ocy454 clone was then selected on the basis of their high expression of *Sost* and their responsiveness to the known effects of PTH treatment (Spatz, Wein *et al*. 2015; Fig. 2.1).

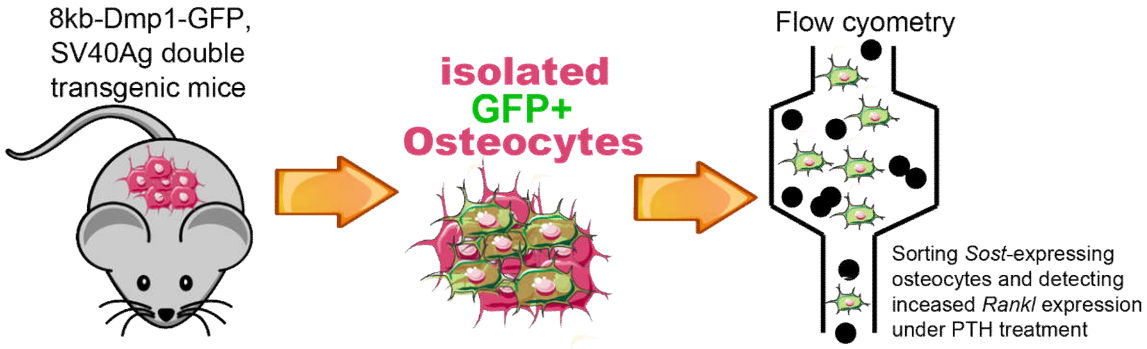

Figure 2.1. Restricted expression of GFP in osteocytes were used to sort osteocytes from 8 kb-Dmp1 promoter Dmp1-GFP mice. FACS-purified GFP+ osteocytes from 6-week old (male and female) were additionally sorted by *Sost*-expressing and dectected with increased *Rankl (Tnfsf11)* expression under PTH treatment.

The approach used was to overexpress constructs of PTHrP that are either (i) the full length secreted molecule (OCY454 $PTHrP^{FL}$), (ii) lacking the NLS (OCY454 $PTHrP^{\Delta NLS}$), (iii) lacking both the NLS and C terminal domain (OCY454 $PTHrP^{\Delta NLS\Delta C}$), or (iv) lacking the secretory apparatus (OCY454 $PTHrP^{\Delta Sec}$) (Fig 2.2). Each construct has a human influenza hemagglutinin (HA) epitope tag at the C terminus. Inclusion of the HA tag at the carboxy-terminus was used so that the synthesised molecules could be tracked by Western blotting and by immunostaining to determine cellular location. Prior to transfection, each of the four constructs were sequenced by the Australian Genome Research Facility. These constructs were overexpressed in OCY454 cells by Patricia Ho, and were published in (Ansari, Ho *et al*. 2018), where the secretion of active PTHrP was analysed and described, and the molecular weights of secreted forms of PTHrP analysed. These clonal cell lines were used to study how the various domains within the PTHrP molecule influence gene expression in osteocytes. Because those engineered cells are so important for the work of this thesis, the method of preparing them is repeated here, although already published in (Ansari, Ho *et al*. 2018).

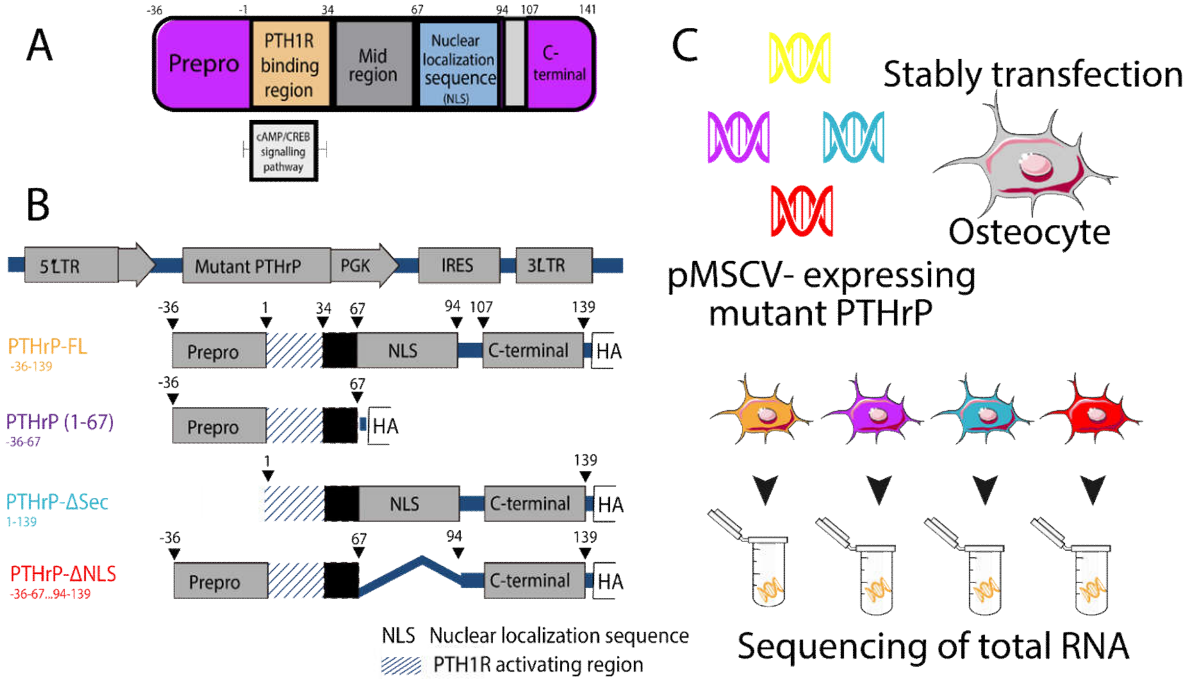

Figure 2.2. Schematic diagram of sequencing analysis of RNA from OCY454 osteocytes expressing mutant PTHrP. (A) Diagram of Prep structure showing PTH1R binding region that sustain cAMP/ CREB pathway and receptor-independent regions. (B) Generation of retroviral pMSCV overexpression constructs for expressing full length (FL) and mutant PTHrP(1-67, ΔSec and Δ NLS). LTR, long terminal repeat; IRES, internal ribosomal entry site; phosphoglycerate kinase (PGK) promoter. (C) OCY454 cells were transduced with constructs schematically illustrated in (B) respectively. Experimental strategy and timeline for cells subjected to RNA-Seq. OCY454 cells were incubated and harvested at day 14.

All four *Pthlh* constructs synthesised by Integrated DNA Technologies (IDT; Coralville, Iowa, USA) were cloned into the plasmid MSCV-zeo using digestion and ligation from Xhol1 / EcoR1 enzymes. Transient transfection of 293T cells (ATCC; mycoplasma-negative according to PCR assay at Victorian Infectious Diseases Reference Laboratory), using the envelope plasmid pCL-Eco (Addgene, Watertown, US), was used to generate retroviruses.

2.4.2 Small Scale Isolation of Plasmid DNA

The purpose of this is the isolation from bacteria of plasmid DNA of $PTHrP^{FL}$, $PTHrP^{\Delta NLS}$, $PTHrP^{\Delta NLS\Delta C}$, $PTHrP^{\Delta Sec}$ used in Chapter 3 (Section 3.5), $PTHrP^{68-141}$ and $PTHrP^{107-141}$ used in Chapter 5 (Section 5.2, 5.3 and 5.4).

(1) **Luria-Bertani medium (LB)** 10g tryptone, 10g NaCl and 5g yeast extract per litre dH_2O. The LB medium was sterilised by autoclaving.

(2) **Solution a** 25mM Tris/HCl (pH 8.0), 50mM EDTA (pH 8.0) and 1% (w/v_ glucose. This solution was autoclaved at 115℃ for 10 mins and stored at 4℃.

(3) **Solution b** 1% (w/v) SDS and 20mM NaOH prepared as required.

(4) **Solution c** To prepare 100mL, add 60mL 5M potassium acetate, 11.5mL glacial acetic acid and 28.5mL dH_2O. This solution was 3M with respect to potassium and 5M with respect to acetate. This solution was autoclaved and stored at 4℃.

5mL of LB medium containing the appropriate antibiotic selection agent was inoculated with single bacterial colony and incubated overnight at 37℃ with aeration. 1.5mL of the overnight culture was microfuged at 13,000 rpm for 2 mins, the supernatant discarded and another 1.5 mL was pelleted in the same tube. The cell pellet was vortexed in 100μL of Solution I then 200μL of Solution b and 150 μL Solution c were added, inverting the tube after each addition. Following a 10-minute incubation on ice, the tube was centrifuged at 13,000 rpm for 10 mins. DNA was then isolated from the supernatant using the Wizard Mini-prep kit according to the manufacturer's instructions. This procedure was used especially for the preparation of DNA sequencing templates. Alternatively, the supernatant was transferred to a fresh 1.5mL tube and treated with DNase free RNase for 5 mins at room temperature. The enzymes were then removed by a phenol: chloroform isoamyl alcohol (1:1) extraction and the aqueous phase precipitated with 0.1 volume 3M sodium acetate and 2 volumes of EtOH on ice for at least 5 mins. The DNA was pelleted at

13,000 rpm for 20 mins, washed in 70% (v/v) ethanol and vacuum dried. The pellet was resuspended in 50μL Water, nuclease-free or TE buffer. The prepared DNA is ready for digestion with restriction enzymes or can be stored at 4℃ until further use.

2.4.3 Transfer clones and assess expression

Following MCF7 and OCY454 cells with the PTHrP constructs shown in Chapter 3 (Section 3.5) and Chapter 4 (Section 4.3) were validated by specific region primers listed in Table 2.1. qPCR was employed to detect the PTHrP secretion region and NLS region deletion, common region, and C-terminal region, demonstrating that *Pthlh* mRNA is produced to approximately the same extent in the separate cell lines. These OCY454 cells were confirmed to overexpress PTHrP, and I have thawed fresh aliquots and checked their expression (results in Chapter 4).

Table 2.1. Mouse primers for assessing expression in OCY454 and MCF7 cells

Genes of interest	Direction	Primer sequence (5' to 3')
Pthlh(Secretion region; Sec region)	Forward	ACATTGCTATGGGAGCCAC
	Reverse	TAGGAATCAGCGCCTCTAAC
Pthlh(Common Region)	Forward	CCAACACCAAAAACCACCCC
	Reverse	GTGTCTTGAGTGGCTGTTCTT
Pthlh(Surrounding NLS)	Forward	CTCAAGACACCCGGGAAGAA
	Reverse	ACCGAGTCCTTCGCTTCTTTT
Pthlh(Within NLS)	Forward	AACAGCCACTCAAGACACCC
	Reverse	GACCGAGTCCTTCGCTTCTT
Pthlh(C terminus)	Forward	GAAGCGAAGGACTCGGTCTG
	Reverse	AATGCGTCCTTAAGCTGGGC

UMR106.01 pcDNA vector control, UMR106.01 $PTHrP^{68\text{-}141}$, and UMR106.01 $PTHrP^{107\text{-}141}$ cell lines mentioned in Chapter 5 (Section 5.3, 5.4 and 5.5) were validated by qPCR using primers in Table 2.2.

Table 2.2. Rat primers for assessing expression in UMR106.01

Genes of interest	Direction	Primer sequence (5' to 3')
Pthlh(C terminus)	Forward	CTCGGTCTGCCTGGCCAGGCACAA
	Reverse	ATGCGTCCTTGAGCTGGGCTCCAG
Pthlh(NLS region)	Forward	CTAACTCAGGAAACCAACAAGG
	Reverse	CTCCTGTTCTCTGCGTTTCCCC

2.4.4 Cryopreserving cultured cells

Cell culture medium was removed and cells were washed in phosphate buffered saline (PBS, Cat. No. D1408, Sigma-Aldrich, USA). Enough Trypsin-EDTA solution (Cat. No. T4049, Sigma-Aldrich, USA) to cover the cells was added and the cells were then incubated for approximately 2 mins in a 37°C in an incubator. Cells were resuspended in cell culture medium and transferred into a 50 mL Falcon tube. Falcon tubes were centrifuged for 5 mins at 1,500 rpm at room temperature. Freezing medium were prepared as 90% FBS plus 10% DMSO. The supernatant was removed and the pellet was gently loosened. Freezing medium was added to 1,000,000 mL. 1 mL was aliquoted into cryovials and the lids were secured. Cryovials were transferred into a room-temperatured CoolCell and put into a -80°C freezer. After approximately 24 hrs the cryovials were removed from the CoolCell and transferred into liquid nitrogen for long term storage. Frozen aliquots of cells were thawed and grown first at the permissive temperature (33°C)

Cells suspended in frozen medium were thawed and then cultured at 33˚C (permissive temperature) for two to three days. Cells were subsequently transfered to 37°C for cell differentiation. The following were conducted for OCY454 cells as in section 2.4: qRT-PCR, cAMP assay, RNA isolation, and PTHrP RIA.

2.4.5 Preparation of MCF7 overexpressing *Pthlh* mutants

The approach used was to use the constructs mentioned in section 2.4.1 combined with stable transfection method (Section 2.3). Validations performed and the results were presented in Chapter 3 section 3.3.

2.4.6 Preparation of UMR106.01 overexpressing *Pthlh* mutants

The approach used was to overexpress constructs of PTHrP that are either PTHrP 68–141 amino acids (UMR106.01 $PTHrP^{68–141}$), PTHrP 107–141 amino acids (UMR106.01

PTHrP$^{107-141}$), and the pcDNA vector. I established UMR106.01 to overexpresses each of these constructs. PTHrP NLS and C-terminus were analysed and confirmed by qPCR. These clonal cell lines were used to study how the C-terminus domain influences gene expression in osteocytes.

2.5 Cell treatment

2.5.1 CREB genes regulation in MCF7 pMSCV vector control and MCF7_PTHrP by treatments of PTHrP

In order to understand how CREB responsive genes are regulated in MCF7 pMSCV vector control and MCF7_PTHrP cells, cells were seeded at 250,000/well in 6-well plates. Confluent cells were treated with the following for 1 hour：

- PBS
- Human PTHrP(1-141) (10 nM)
- Human Calcitonin (sCT; Bachem, Torrance, CA; 10nM)
- PGE_2 (Sigma, St. Louis, MO; 10^{-6}M)

Suppliers of Recombinant human PTHrP(1-141) was prepared as previously described (Hammonds, McKay *et al*. 1989) . After 1 hour, cells were washed with PBS and RNA samples were collected as described in section 2.9. *NR4A1*, *RGS2* and *AREG* mRNA transcription levels were assayed.

2.5.2 *Osteocalcin* gene (OG / *Bglap*) transcription effects in OCY454 osteocytes by exogenous treatments of hPTHrP(1-84) and hPTHrP(1-141)

To study how exogenous C terminus of PTHrP affect *Bglap*, OCY454 osteocytes were allowed to differentiate for 14 days. On the 14th day, cells were starved of serum overnight in αMEM with 1% Glutamax, 1% PSA and 1% FBS. After these cells were treated with

PBS, PTHrP(1–84) (10 nM), PTHrP(1–141) (10 nM) as well as PTH (1–34; Bachem, Bubendorf, Switzerland) for 1, 6, and 24 hours. Cells were collected as described in section 2.9.

2.5.3 Effect of PTHrP C terminus on *Bglap*, CREB responsive genes as well as Wnt targeting genes abundance in UMR106.01 cells

To test the effect of C-terminal PTHrP expression on *Bglap* regulation by PTH/PTHrP, UMR106.01 cells stably overexpressing PTHrP(107-141) (UMR $PTHrP^{107\text{-}141}$) and PTHrP 68-141 (UMR $PTHrP^{68\text{-}141}$) were seeded at 250,000/ well (6-well plate) density and incubated for 3 days until the cells are confluent in the wells. Cells were treated with PBS, 2nM PTH and 2nM PTHrP for 8 hours. Cells were then collected as described in section 2.9.

2.5.4 Exogenous hPTHrP(1-141) and hPTHrP(1-84) effects on CREB genes

To understand whether CREB genes are differently regulated by hPTHrP(1-84) and hPTHrP(1-141), UMR106.01 cells were seeded at 250,000/ well (6-well plate) density initially. Cells were treated with PBS, 10nM hPTHrP(1-84) and 10nM hPTHrP(1-141) for 0, 1, 6 and 24 hours. Cells were then collected as described in section 2.9.

2.6 PTHrP biological assay and radioimmunoassay

2.6.1 PTHrP bioassay (cAMP assay)

Secretions of PTHrP in the medium were biologically assayed as the cAMP produced as a result of treatment of UMR106.01 cells, using a cAMP response induced by PTH(1–34) to serve as the standard curve (Ho, Goradia *et al*. 2015). This assay was further utilised to test the reaction that OCY454 cells exhibit in response to exposure of PTH(1–34), recombinant human PTHrP(1–141), or isoproterenol. Triplicate cell cultures were incubated in 12-well plates containing cell culture medium, supplemented with 1 mM 3-isobutyl-1-methylxanthine (IBMX, Cat. No.15879. Sigma-Aldrich, Australia) added.

After treatment for 12 mins with agonists indicated in each figure legend, Adenosine 3'5'-cyclic Phosphoric Acid, 2'-O-succinyl-[^{125}I]-Iodotyrosine Methyl Ester (cAMP labelled with ^{125}I, PerkinElmer, Boston, MA, USA) was measured by radioimmunoassay after prompt removal of the medium, the addition of acidified ethanol, desiccation, and reconstitution in assay buffer (Ho, Goradia *et al*. 2015).

Reponses of cAMP to different cell preparations were compared. Total protein was calculated from wells treated in the same manner to those in the cAMP assay described above. Cells were washed thrice with PBS and solubilised with 500µL of radioimmunoprecipitation assay buffer (Radio-Immunoprecipitation Assay buffer, RIPA buffer, Sigma, Saint Louis, U.S.).

Extracts of the assay were then centrifuged and the resulting protein supernatants assayed using Pierce bicinchoninic acid (BCA) protein assay buffer (Thermo Fisher, CA, USA). Absorbance was measured at OD562nm using the Polarstar Optima^{+} and a standard curve of bovine serum albumin (BSA).

2.6.2 PTHrP radioimmunoassay

Amino-terminal PTHrP radioimmunoassay (RIA) was conducted as previously described, with a sensitivity of 2 pM, using a single-site assay with a goat antibody against PTHrP(1-34), which detects all N-terminal-containing lengths of PTHrP with similar sensitivity (Grill, Ho *et al*. 1991).

2.7 Luciferase Assay (Reporter assay)

Luciferase assays were performed using the Promega Luciferase Assay System product according to manufacturer's instructions. Briefly, the cells were set up in 96 well culture plates. When the cultures were ready to be assayed, the existing medium was removed and the cells were washed in 100µL of PBS per well. The cells were lysed by the addition of

20 µL of Promega Lysis Buffer (PLB, Promega, NL) 4 volumes of water to 1 volume of 5x lysis reagent). The Luciferase Assay Reagent was prepared by adding Luciferase Assay Buffer to a vial of lyophilised Luciferase Assay Substrate in Luciferase Assay System Kit (Promega, NL). 100µL of Luciferase Assay Reagent was loaded into each well in an automated sequence and luminescence measured by the Fluoro star Optima Luminometer (BMG Labtech, Ortenberg, Germany).

2.8 Mineralisation Assay

OCY454 cells were grown to confluence in 12-well culture plates. When culturing cells, subculture OCY454 cells at a density of 100,000 cells/well in αMEM were supplemented with 10% FBS, 2 mM Glutamax, and 1% PSA, and kept at 33°C. At day three, once the cells were 80% confluent, the media was removed and replaced with mineralisation αMEM medium containing ascorbate (50 µg/mL) and β-glycerophosphate (Cat. No. G5422, Sigma-Aldrich, Australia) at two conditions: 2nM or 5 nM, to efficiently induce strong mineralisation in osteoblast cultures. Half of the medium was replaced every third day with double-concentrated medium. At time points (day 0, day 4 and day 7) specified in each experiment, cells were washed with PBS and fixed in DMSO, then washed with distilled water and incubated in 0.5% Alizarin Red-S (Sigma-Aldrich, Australia) in distilled water for 30 mins, followed by a final water wash. Images of the surfaces were taken using an Epson Perfection V800 Scanner (Epson, Australia). To quantify the Alizarin Red staining, a circular or oval region of minimum size was used as region of interest to omit the edge of well and areas where monolayer cells had become folded using Image J (version 1.52r), limiting measured area. Deposits of calcium and phosphate were quantified and represented as values according to the positive area of pixels over the overall circle pixel area measurements. In image J, the overall area of pixels was calculated when “Limited to threshold” was not selected. The thresholding step used an

experimental colour threshold tool in image J, thus avoiding oversaturation in greyscale images.

2.9 RNA extraction, cDNA synthesis and qPCR

2.9.1 RNA extraction

RNA was extracted using RNA extraction kits with on-column DNase digestion (Qiagen, Limburg, Netherlands; Bioline, London, UK), or TriSure reagent (Bioline, London, UK). Cells were washed twice with PBS before adding TriSure (0.5 mL/well of 6-well plate). Supernatant of the mixture samples were passed through a 21G needle using Luer Lock syringes to shear the RNA.

To extract RNA, 0.1 mL chloroform was added to each 500 mL sample. After shaking for 30 seconds, the samples were settled at room temperature for 15 mins, then centrifuged at 4℃ for 30 mins at a speed of 14000 rpm. The top layers, which contained RNA, were moved to fresh tubes and 250:1 isopropanol was added and mixed evenly. The samples were left at room temperature for another 10 mins, and then spun at 4℃ for 30 mins at a speed of 14000rpm. The supernatant was then discarded and samples were washed with cold ethanol. Pellets were then resuspended in 30 µl of DNase free/RNase free water.

Extracted RNA was DNase treated with Ambion TURBO DNA-free kit (Life Technologies, Carlsbad, CA, USA) and quantified on a NanoDrop ND1000 Spectrophotometer (Thermo Scientific, Wilmington, DE, USA). RNA was quantified on a NanoDrop ND1000 Spectrophotometer (Thermo Scientific, Wilmington, DE, USA). The generally accepted RNA purity ratios for OD260/280 and OD260/230 are approximately 2.0–2.2 and 1.8–2.2, respectively.

2.9.2 cDNA synthesis and qRT-PCR

cDNA was synthesised from total RNA with Tetro cDNA synthesis kits (Table 2.3; Bioline, USA). Vortex solutions and centrifuge briefly before use. Incubate the samples prepared at 45℃ for 30 min. Terminate reaction by incubating at 85℃ for 5 min, chill on ice. The cDNA was diluted (1 in 5) in RNase-free water and stored at -20°C until amplification by qRT-PCR. Gene expression was quantified using Stratagene Mx3000P qPCR system (Agilent) with the master mix including Brilliant II SYBR green qPCR (Table 2.4; Agilent Technologies, Santa Clara, CA, United States) or Multiplex SensiMix II Probe kits (Bioline, London, UK) with primers targeted to replicate the relevant genes (Table 2.7, 2.8, 2.9). The components are listed in Table 2.5 and the reaction conditions are shown in Table 2.6. Expression between the samples was normalised using expression values of *hypoxanthine phosphoribosyltransferase 1 (Hprt1*). Relative expression was calculated via the comparative CT method ($2^{-(\text{Gene Ct} - \text{Normaliser Ct})}$).

Table 2.3. Master mix used for synthesis of first strand cDNA by Tetro cDNA kit. *x* represents the volume of RNA required for each sample, calculated on the basis of its concentration.

Components	µL
Total RNA (up to 5 µg) or mRNA (up to 5 µg)	n
Random Primers (0.1µg/µL)	1
10mM dNTP mix	1
5XRT buffer	4
RiboSafe RNase Inhibitor	1
Tetro reverse transcriptase (200u/ µL)	**1**
DEPC-treated water	**To 20**

Table 2.4. Reaction cycle information needed for cDNA synthesis

Temperature (°C)	Duration (min)
25	5
42	15
95	5

Table 2.5. qPCR reaction

Components	µL (n=1)
H_2O	2
10 µM Forward Primer	0.5
10 µM Reverse Primer	0.5
2X Brilliant II SYBR Green qPCR Master mix solutions	5
cDNA	2
Total	**10**

Table 2.6. SYBR green cycling settings

Cycle	Temperature (°C)	Duration (min)
1	95	10
40	95	0.5
	60	1
1	95	1
	55	0.5
	95	0.5

Table 2.7. Human primers

Genes of interest	Direction	Primer sequence (5' to 3')
PTHR1	Forward	TTCCAGGGATTTTTTGTTGC
	Reverse	AGTCCAATGCCAGTGTCCAG
PTHLH	Forward	GTCTCAGCCGCCGCCTCAA
	Reverse	GGAAGAATCGTCGCCGTAAA
BDKRB1	Forward	AATGCTACGGCCTGTGACAA
	Reverse	TCCCTAGGAGGCCGAAGAAA
RGS2	Forward	GTCCTCAAAAGCAAGGAAAATCTA
	Reverse	CATCAAACTGTACACCCTCTTCTG
AREG	Forward	CACAGGGGACTACGACTACTCAG
	Reverse	TCTTCCTTTTGGGTTTTTCTGTAG
CREB1	Forward	CAAGTCCAAACAGTTCAGATTTCA
	Reverse	TGGTGCATCAGAAGATAAGTCATT
CALML3	Forward	TGGTTGAT TCAGCCCACCTC
	Reverse	TCCGTGTCATTCAGACGAGC

Table 2.8. Mouse primers

Genes of interest	Direction	Primer sequence (5' to 3')
Bglap	Forward	AGCAGACACCATGAGGACCATCTT
	Reverse	GGACATGAAGGCTTTGTCAGAC
Rgs2	Forward	GGAGAAAATGAAGCGGACAC
	Reverse	TGCAGCCAGCCCATATTTAC
Nr4a2	Forward	TGCTGGATATGTTGGGTATCATCT
	Reverse	TCACCTCCGGTGAGTCTGATC
Nr4a1	Forward	CGCCGAAACCGATGTCA
	Reverse	TGTACGCACAACTTCCTTAACCA
Efnb2	Forward	GTGCCAGACAAGAGCCATGAA
	Reverse	GGTGCTAGAACCTGGATTTGG
Btg2	Forward	ACGCACTGACCGATCATTACA
	Reverse	GCTGGCTGAGTCCAATCTG
Ibsp	Forward	CCGAAGCCTATGGGACCAC
	Reverse	ATAAGCTCGGTAAGTGTCGCC
Ifitm5	Forward	CACCACGAGATCACATGCTCT
	Reverse	GGATGTTGTAGCACTTGGCTT
Spns2	Forward	GGCATCTTCTTCTGGTCTGC
	Reverse	AGCATCAATGTGCGTGTGTT
Phospho1	Forward	ACGGAGCAGAAGCACATCATC
	Reverse	TAGGCATCGTAGTCCAACAGC
Enpp1	Forward	GAGTGTCCAGCAGAGTTTGAAT
	Reverse	CACCCCAGGTGTGCAAATACT
Spp1	Forward	TAGCTTGGCTTATGGACTGAGG
	Reverse	AGACTCACCGCTCTTCATGTG
Alpl	Forward	AAACCCAGACACAAGCATTCC
	Reverse	TCCACCAGCAAGAAGAAGCC

Table 2.9. Rat primers

Genes of interest	Direction	Primer sequence (5' to 3')
Bglap	Forward	GACAAGTCCCACACAGCAAC
	Reverse	CCGGAGTCTATTCACCACCT
PTHrP C terminal	Forward	CTCGGTCTGCCTGGCCAGGCACAA
	Reverse	ATGCGTCCTTGAGCTGGGCTCCAG
PTHrP NLS	Forward	CTAACTCAGGAAACCAACAAGG
	Reverse	CTCCTGTTCTCTGCGTTTCCCC
Nr4a2	Forward	CTGGGTTGGACCTGTATGCT
	Reverse	AGATTCCTGGCTTTGCTGAC
Cfos	Forward	TGCAACGCAGACTTCTCATCT
	Reverse	AATCCGAAGGGAACGGAATAAGA
Il6	Forward	TTGCCTTCTTGGGACTGATG
	Reverse	ACTGGTCTGTTGTGGGTGGT
Wnt4	Forward	GCGAGCAACTGGCTGTACC
	Reverse	TCTCGCACGTTTCCTCTTCG
Wisp1	Forward	CCGACCACACATCAAGGCAGG
	Reverse	GGTCGGTAGGTGCGTGTGCTG
Wisp2	Forward	CAAGGGACACGGTGACATGA
	Reverse	GGGCACACACCATTGAGAGA
Lef	Forward	CCCCGAAGAGGAGGGCGACT
	Reverse	TCCGACCACCTCATGCCCGTT
Tnfsf 11	Forward	GGCACCTACCTAAAACAGCAC
	Reverse	TTCCTCACATTCGCACACTC
Dkk1	Forward	CTGTCTGCCTCCGATCATCA
	Reverse	CAGAAATGTCTTGCACAACACA

2.10 Bio-informatic analysis

2.10.1 Sample collection for RNA-sequencing

For each OCY454 line described in section 2.1.1 and 2.2.1, cells were differentiated into osteocytes for 14 days. RNA samples were collected from three separate wells (n=3) per cell line. RNA samples were extracted as above (Section 2.5.1) and made into an mRNA library using the Illumina TruSeq Stranded mRNA Library kit (Illumina, U.S.) according to the manufacturer's instructions. The methods for RNA-Seq samples prepared for MCF7 breast cancer cell lines overexpressing full-length PTHrP and mutant PTHrP were the same.

2.10.2 Processing of sequencing data

RNA samples were frozen at -80°C and shipped to the Vanderbilt Technologies for Advanced Genomics (VANTAGE) core facility (Vanderbilt University Medical Center, Nashville, Tennessee, USA). Samples were analysed for quality on Bioanalyzer Pico chip and confirmed to have RNA integrity >8.0. Library preparation was performed using the Illumina TruSeq total RNA sample prep kit according to the manufacturer's instructions by qualified personnel in the VANTAGE facility. RNA sequencing (RNA-Seq) was performed on an Illumina HiSeq 3000 with 150 bp paired-end reads. In order to identify differentially expressed genes (DEGs) between strains, read counts were normalised and tested for differential expression using pairwise comparisons between the groups by the Vanderbilt Centre for Genomics (VANTAGE, Vanderbilt University, Nashville, Tennessee, USA). Transcript abundance was measured as reads per kilobase of exon per million mapped reads (RPKM; Chepelev, Wei *et al*. 2009) and two transcriptomic analysis methods were used to determine differentially expressed genes: edgeR (Robinson, McCarthy *et al*. 2010) and DESeq2 (Love, Huber *et al*. 2014).

For the MCF7 cells, the library prep and quality analysis were the same, but the samples were sequenced on an Illumina NovaSeq6000, still with 150bp paired-end reads.

To find differentially expressed genes, P-value was determined by DESeq and edgeR. To adjust the p-value for doing a large number of tests, I choose False Discovery Rate (FDR) that produces an adjusted p-value. An FDR adjusted p-value of 0.05 implies that 5% of significant tests will result in false positives.

2.10.3 Sample quality control

The hierarchical cluster of OCY454 and MCF7 cells reads indicates the sample is not cross-contaminated. This was determined at Vanderbilt Technologies for Advanced Genomics (VANTAGE) of Vanderbilt University Medical Center, United States. No samples were excluded from subsequent analysis.

2.10.4 Data analysis

Significant differences identified by VANTAGE (as described in 2.10.2) were provided, and gene regulation profiles were identified using "VLOOKUP" excel formula function (VLOOKUP (lookup, value, table array, col_index_num, [range_lookup]) in Excel software to extract Log_2 fold change data from the normalised results. Heatmaps were made using Graphpad (version 8.0) software.

To determine whether the magnitude of response of genes regulated by PTHrP overexpression is increased when the C terminus is present, I plotted the absolute magnitude of log2 fold change compared to vector-transfected cells in those common genes regulated by both $PTHrP^{FL}$ and $PTHrP^{\Delta NLS\Delta C}$, and subsets of that data in Figure 4.7. The absolute magnitude change (absolute value of a gene log2 Fold change) was compared without denoting positive or negative direction. This is annotated with vertical bars, i.e. a gene with Log2 fold change of -5 has an absolute magnitude change of |Log2

fold change| = 5. Thus, the magnitude regulatory difference of genes were compared between $PTHrP^{FL}$ and $PTHrP^{\Delta NLS\Delta C}$. To determine whether this was due to the absence of the NLS, I also compared between $PTHrP^{FL}$ and $PTHrP^{\Delta NLS}$. Whether these changes were significantly different was determined using Students t-test for each of these comparisons.

The top 50 genes upregulated to a greater extent by the C-terminus deficient construct were determined by calculating the difference in magnitude change of gene expression between the two cell lines possessing ($PTHrP^{FL}$) and lacking the C-terminus ($PTHrP^{\Delta NLS\Delta C}$).

2.10.5 Other analysis

To identify significant pathways that PTHrP overexpression had induced in MCF7_PTHrP, processed RNA-Seq data was down uploaded to STRING: functional protein association networks (Version: 11.0 https://string-db.org/). I used STRING to identify gene symbols known to be PTH1R-related using the 277 differentially expressed genes that were shared by all PTHrP-overexpressing cell lines as input.

Gene ontology (GO) analysis was carried out using DAVID (DAVID Functional Annotation Bioinformatics Microarray Analysis, version 6.8 https://david.ncifcrf.gov/) and Cytoscape (version 3.7.2 https://cytoscape.org/) to generate enrichment datasets. The KEGG means clustering algorithm in Cytoscape was used to generate functional clusters and associations based on the molecular function annotations in DAVID. This was used to identify GO terms on the genes uniquely regulated by $PTHrP^{\Delta Sec}$, to identify KEGG pathways by GO enrichment that are regulated by $PTHrP^{\Delta Sec}$, and to identify GO enrichment within the top 50 upregulated and 50 downregulated genes in which the regulation by $PTHrP^{\Delta NLS\Delta C}$ was greater than that of $PTHrP^{FL}$.

Venn-diagrams were generated using Venny (Oliveros 2007; https://bioinfogp.cnb.csic.es/tools/venny/) to compare number of differentially expressed genes in the four OCY454 cell lines, depict unique and common DE genes, and depict ubiquitination-associated genes regulated by the different constructs.

Circos table viewer (http://mkweb.bcgsc.ca/tableviewer/) was used to generate plots for visualising: (1) CREB regulation genes derived from a previous publication (Walia, Ho *et al*. 2016) and (2) Wnt target genes (described at https://web.stanford.edu/group/nusselab/cgi-bin/wnt/target_genes), regulated by any combination of full-length PTHrP and mutant PTHrP forms from OCY454 overexpression cells.

Genes mapped in proposed ubiquitin proteasome system identified by RNA-Seq are grouped in Fig. 4.13 according to the study that identified that gene's association in the system.

Heat maps were generated in Excel, and used to show whether genes were regulated in similar directions by related constructs, and to show patterns of regulation of CREB-responsive genes among cells overexpressing $PTHrP^{FL}$, $PTHrP^{\Delta NLS\Delta C}$ and $PTHrP^{\Delta NLS}$, the proportion of genes differentially expressed by all cell lines, and Wnt signalling genes shared by cell lines.

Molecular function (MF) and biological process (BP) terms from DAVID analytic data that include “ubiquitination” or “ubiquitin” labels were over-represented in Alluvial Diagram.

Further methods are described in Chapter 4 in the results sections.

2.11 Western blotting

2.11.1 Protein Extraction

Monolayers of cells were washed twice with cold 1x PBS, 1 mL of RIPA lysis buffer was then added and cells were scraped from dish. Cells were disrupted by passing through a 23 G needle attached to a 5mL syringe, and then transferred to microfuge tubes. The lysates were centrifuged at 13,000 rpm for 5 mins and the supernatant transferred to a fresh tube. The pellets were discarded.

2.11.2 Protein Assay

Protein concentrations were determined using a modified assay originally developed by Lowry (Lowry *et al*. 1951). The Bio-Rad DC protein assay kit was used according to the manufacturer's instructions. In brief, a standard curve was created using Bovine Serum Albumin (BSA, Cat. No. A3912, Sigma–Aldrich, Australia) at final concentrations of 0, 0.2, 0.4, 0.8, 1.2, 1.6 and 2mg/mL of protein in a total of 25µL. Samples were used straight or diluted (in 25 µL) and 125µL of solution A, followed by 1mL solution B were added to all tubes. The tubes were vortexed and incubated at room temperature for approximately 30 mins. The solutions were then transferred to disposable plastic cuvettes and the absorbance at 750 nm measured. Protein concentrations were determined by extrapolation from the standard curve and corrected by the appropriate dilution factors.

2.11.3 Protein sample preparation

Extracted total protein samples were transferred to a fresh microfuge tube, to which 4XLDS sample buffer (Cat. No. NP007, Invitrogen, Carlsbad, USA) was added to dilute to 1X with ddiH_2O. Dithiothreitol (DTT, Cat. No. D-1532, Invitrogen, Carlsbad, USA) was added to the samples to give a final concentration of 50mM. The mixture was vortexed and incubated at room temperature for 5 mins, then centrifuged at 13,000 rpm

for 5 mins. The samples were then boiled for 10 mins before being loaded onto the SDS-polyacrylamide gel.

2.11.4 Western blot for PTH1R in MCF7 cells and UMR106.01

5×10^6 MCF7 cells were seeded in 6-well culture plates and cultured with DMEM supplemented with 10% FBS and Penicillin/ Streptomycin (P/S) for 24 hours. To solubilise proteins, methods were used in section 2.11.1. Lysates were cleared by sonicator and resolved by polyacrylamide gel electrophoresis. Ten micrograms of total protein from each lysate was separated by 10% sodium dodecyl sulfate-polyacrylamide gel electrophoresis (SDS-PAGE).

The day before electrophoresis, 700 mL of 1X MES running buffer was prepared from 20X MES running buffer (Cat. No. NP0002, Invitrogen, Carlsbad, USA) 500 µL of 0.5 M DTT was added to 200 mL of MES. For electrophoresis, an iBolt Mini Cell (Invitrogen, Carlsbad, USA) was set up and 15-well 4-12% gradient Bis-Tris NuPAGE gels (Cat. No. NP0032BOX, Invitrogen, Carlsbad, USA) were placed inside. 1X MES running buffer was filled and samples were loaded into the gel along with molecular marker SeeBlue Pre-Stained Standard (Invitrogen, Carlsbad, USA). Gels were electrophorested for 10 mins at 80V and 30 mins at 120V later. Gels were transferred electrophoretically to iBlot Transfer Stack, PVDF, mini (Cat. No. IB401002, Thermo Fisher). PTH1R was determined by Western blotting with an anti PTH1R antibody (Anti-PTH1R Polyclonal, Cat. No. PA3-205, Invitrogen, Carlsbad, USA). The antibody was used at a 1:1000 dilution with an o/n incubation at 4˚C. The blots were subsequently stripped and reprobed with Pan-actin (clone 2A3, Cat. No. MABT1333, Sigma, Australia) to ascertain equal protein loading.

The secondary antibody of the western blot conjugates to the enzyme horseradish peroxidase (HRP). HRP reacts with the HRP substrate luminol. The membranes were visualised using enhanced chemiluminescence (ECL Western blotting detection reagents; Amersham Pharmacia Biotech, Piscataway, NJ, USA). This reaction emits light at 428 nm and thus the emission can be recorded using X-ray film (Fujifilm, Tokyo, Japan).

2.12 Confocal microscopy analysis

2.12.1 PTH1R binding in MCF7 cells and UMR106.01

MCF7 parental, MCF7 pMSCV vector control, MCF7_PTHrP and UMR106.01 cells were cultured on poly-l-lysine-coated glass chamber slides (Merck KGaA, Darmstadt, Germany), for 48h and serum starved for 1h before stimulation with PTH-TMR (100nM), PTH(1-34) labelled with TMR reagent (Chan, Clairfeuille *et al*. 2016). MCF7 parental, MCF7 pMSCV, MCF7_PTHrP as well as UMR106 cells were treated with PTH-TMR for 15 mins. Cells were washed with PBS and replaced with complete medium. Cells were then fixed with 4% paraformaldehyde (PFA, Cat. No. 158127, Sigma-Aldrich, Australia) for 10 min, and permeabilised with 0.1% Triton X-100. The cells were mounted and imaged with a Leica confocal microscope. Fluorescence was detected after subjecting cells to an ice block for 10 mins. The images were integrated by LAS_X_Small (version 3.7.0).

2.13 Mouse breeding and genotyping

2.13.1 Animals

All experimental procedures were approved by St. Vincent's Health Melbourne Animal Ethics Committee, and were conducted in accordance with the Australian Code of Practice for the Care and Use of Animals for Scientific Purposes. *Dmp1Cre* mice (Tg(*Dmp1*-cre)^{1Jqfe}) mice, which express Cre-recombinase under control of the *Dmp1* 10-kb promoter region, were provided by Dr. Bonewald (Indiana University School of

Medicine, Indianapolis, USA; Lu, Xie *et al*. 2007). *Pthlh*-flox (*Pthlh*^{tm1Ack}; name: parathyroid hormone-like peptide; targeted mutation 1, Andrew C Karaplis; MGI ID: 2387462) mice were provided by Dr. Karaplis (McGill University, Montreal; He, Deckelbaum *et al*. 2001). Mice were housed in a specific pathogen free (SPF) facility at St Vincent's BioResources Centre. Animals were kept under conditions of 12-hour light and dark cycle, and *ad lib.* standard food and water.

2.13.2 Breeding

Mice hemizygous at the *Dmp1Cre* locus were crossed with *Pthlh*$^{f/f}$ mice to produce *Dmp1Cre.Pthlh*$^{f/w}$ breeders. *Dmp1Cre.Pthlh*$^{f/w}$ breeders were then mated together to produce progeny that are PTHrP knocked-down (*Dmp1Cre.Pthlh*$^{f/f}$) and *Dmp1Cre.Pthlh*$^{w/w}$ littermates as controls.

2.13.3 Characterisation of *Dmp1Cre.Pthlh$^{f/f}$* mice (genotyping)

The genotype of each mice was determined by qPCR. To do this, toe or tail clips were sampled at weaning for DNA extraction. 600 µL of 50 nM NaOH (Merck Pty. Ltd. Kilsyth, VIC, Australia) was then added to each sample, and left for 20 mins at 95°C for to allow for denaturing. 100 µL of Tris pH 8.0 (Merck KGaA, Darmstadt, Germany) was then added and each sample was gently and evenly mixed.

Each PCR reaction mix consisted of 1 µL forward primer, 1 µl reverse primer (Table 2.10), 2 µL My *Taq* reaction buffer, 0.1 µL *Taq* polymerase (MyTaq HS Red; Bioline, London, UK), 5.9 µl dH_2O, and 1 µL of extracted sample, for a total volume of 10 µL (Table 2.11). This mix was centrifuged, and PCR was performed using a Biometra T3000 Thermocycler (Biometra, GmBH, Germany) according to the cycling conditions described in Table 2.12.

Following PCR amplification, each sample and a standard DNA ladder VI (Roche Pty. Ltd., Melbourne, VIC, Australia) was loaded onto a 2% agarose (Cat. No. BIO-41025, Bioline, Luckenwalde, Germany) gel with 6 µL SYBR Safe (Invitrogen Australia Pty. Limited, Mulgrave, VIC, Australia), and gel electrophoresis was performed in Tris Borate EDTA buffer solution, pH 8 (TBE 1X) at 100V for 30 min. The locations of bands in the gel were then revealed using molecular weight marker HyperLadder TM 100 bp (Cat. No. Bio33029, BIOLINE, London, UK), by fluorescence under ultraviolet (UV) light. The positions of bands in the gel, with respect to the ladder, allowed for the identification of *Dmp1Cre.Pthlh$^{f/f}$* and *Dmp1Cre.Pthlh$^{w/w}$* mice. As a wild-type control, C57 mice were used.

Table 2.10. Genotyping primers sequence for mouse models

.

Genes of interest	Direction	Primer sequence (5' to 3')	Product size (bp)
Dmp1Cre (Lu, Xie *et al*. 2007)	Forward	CCCGCAGAACCTGAAGATG	534
	Reverse	GACCCGGCAAAACAGGTAG	
Pthlh-loxP (Karaplis *et al.* 1994)	Forward	CCCCCTTCCTTCTTCACTTC	172 for *wt* 204-222 for *fl*
	Reverse	GAGGCTAAGCCAGGAGGATT	

Table 2.11. Master mix for mouse genotyping

Component	µl
10 µM primers (forward + reverse)	1
5x My Taq Reaction Buffer	2
Taq Polymerase	0.1
dH_2O	5.9
Tail DNA	1
Final volume	10

Table 2.12. Cycling conditions for genotyping gene of interest

Gene of interest	Temperature (°C)	Time (s)	Number of cycles
Dmp1Cre	94	300	1
	94	30	30
	60	30	
	72	30	
	72	300	1
	15	Pause	
Pthlh-LoxP	94	180	1
	94	30	35
	60	30	
	72	30	
	72	300	1
	15	Pause	

2.14 Tissue collection

Tissue was collected from 12-week-old male and female mice that had been fasted for the previous 16 hrs. Tissue was collected from 12-week-old male and female mice that had been fasted for the previous 16 hrs. Mice were anaesthetised by injection with ketamine/xylazine. After injection, animals were carefully assessed to ensure anaesthesia. Mice were then culled by jugulation. Blood was drained by cardiac puncture. Femora were carefully harvested and detached from muscle by dissection, using forceps and scissors. The femoral distal epiphysis and growth plate were removed, and marrow was flushed from the remaining part of the femur with PBS-filled syringe with a 26 G needle. The femur was flushed until the PBS runs clear. The bone was then snap-frozen in liquid nitrogen, where it remained until ready for RNA preparation (Section 2.9). One tibia of each mouse was placed in methyl-methacrylate and fixed in 4% PFA for FTIR microspectroscopy (Section 2.10).

2.15 Plastic section preparation

2.15.1 Preparation of destabilised methyl methacrylate (dMMA)

To destabilise of MMA (Cat. No. M55909, Sigma-Aldrich, USA), 500 mL was added to a separating funnel with 300 mL of 5% sodium hydroxide (NaOH, Merck, Suprapur), shaken vigorously for 30 s, and then allowed to settle for approximately 10 mins while being held in place by a retort stand. After the solution had settled and separated by weight, the bottom NaOH layer was drained off. The aforementioned process was repeated three more times, and then MMA was rinsed three times, each time by the same procedure using 500 mL of distilled H_2O. The dMMA product was filtered filter through paper containing granular $CaCl_2$, which removed water content. The product was then stored at 4˚C until required, with a small amount of $CaCl_2$ present to absorb excess water.

2.15.2 Dehydration, infiltration and embedding of bone samples

Once bones had been completely cleared of attached muscle tissue, they were dehydrated at 4˚C for at least 1 hour each minimum in scintilation vials (Cat. No. 6000097, PerkinElmer, Boston, MA, USA): each placed in 70% acetone for an hour, 90% acetone for an hour, and 100% acetone for two hours, all kept at 4˚C.

Bone samples were then placed in 4˚C infiltration solution consisting of 90% dMMA, 10% Dibutyl phthalate (DBP, Cat. No. 524980, Sigma-Aldrich, Australia), and 0.05% benzoyl peroxide (BPO, Cat. No. 517909, Sigma-Aldrich, Australia), and left there for three to seven days (Sims, Clément-Lacroix *et al*. 2000) at 4˚C.

In preparation for embedding, polymerised MMA bases were created for each sample using 90% dMMA, 10% DBP, and 4% BPO, each of which was filtered through $CaCl_2$ to remove water. They were polymerised overnight at 37˚C. Once infiltration was complete, samples were embedded atop the prepared bases in 85% dMMA, 15% DBP, and 4% BPO. To soften the base below, 0.5 mL of this solution was placed on polymerised 1 mL bases and left at room temperature for approximately 30 min. When soft, tibiae were submerged in the liquid resin, oriented such that the tibial anterior crest pointed down and the fibula made contact with the base. Fibulae were kept intact. Femora were oriented such that the anterior surface made contacted with the case and the femoral condyles faced upwards. To facilitate polymerisation, vials were placed in a water bath set to 37˚C, where they remained between one night and three days.

A top layer, consisting of 90% dMMA, 10% DBP, and 5% BPO, filtered through granular calcium chloride ($CaCl_2$, Cat. No. 1.02379, Supelco, Bellafonte, PA, USA), was added to tibial samples after they were completely encased in solid plastic. Each vial had approximately 7.5

mL of this solution added, and was allowed to polymerise dry for one to two days at 37˚C. After the top layer had set, a hammer was used to break the glass vials and extract the samples.

2.15.3 Cutting and polishing plastic sections

Embedded tibiae were ground down using a water-cooled Phoenix Beta grinder/polisher (Buehler, Illinois, USA) until the entire sagittal tibial face was showing.

3 μm and 2 μm thick sections, for male and female mice, respectively, were sliced from the methyl methacrylate (MMA) block using a microtome lubricated with 70% ethanol. Sections were placed between glass slides and filter paper, held together by clips.

2.16 Assessment of bone mRNA by qPCR

2.16.1 RNA isolation from bone samples

Prior to RNA extraction, femora were collected (Section 2.13.4) and were homogenised. Homogenisation was performed at 4˚C in 1 mL of QIAzol Lysis Reagent RNeasy Mini Kit (Cat. No./ID: 74104, Sciences, Maryland, USA) using a Polytron PTA 20S homogeniser (Brinkmann Instruments model PT 10/35, Westbury NY) at maximum speed for 30 s, such that bones were broken down into small fragments. Between each specimen, the homogeniser probe was placed in 0.1M NAOH 1% sodium dodecyl sulphate (SDS) for 10 min, washed with purified Elix (de-ionised, pure water, Millipore), and washed with diethylpyrocarbonate (DEPC)-treated water four times. Homogenates were placed on dry ice while other samples were still being homogenised. Once homogenisation was complete all samples were stored at -80˚C.

Next, RNA from homogenates was purified using a Qiagen RNeasy Lipid Tissue Mini Kit (Qiagen Sciences, Maryland, USA), which uses RNeasy spin columns to purify maximum of 100 μg RNA. Homogenates were then separated into aqueous and organic phases via

centrifugation, and the supernatant aqueous phase was isolated. Ethanol was added to this isolated sample and centrifuged in the RNeasy spin column for purification. The spin column's membrane was then eluted with 30–50 µl RNase-free water.

2.16.2 Removal of genomic DNA

To degrade genomic DNA in the eluent, the Turbo DNA-free™ Kit (Cat. No. AM1907, Life Technologies, CA, USA) was added. Reaction mixes consisting of 1 µL 10X Turbo DNase buffer, 1 µL Turbo DNase (2 U/µL), and 10 µL of sample were incubated for 30 mins at 37˚C. Reactions were then inactivated by the addition of 0.1 µL DNase Inactivation Reagent and incubated for 5 mins at room temperature; mixed at least three times during incubation. Finally, tubes were centrifuged at 10,000x g for 1.5 mins at room temperature, and the resulting supernatants were pipetted into new microcentrifuge tubes.

2.17 Bone mineralisation analysis by Fourier Transform Infrared (FTIR) microspectroscopy

FTIR microspectroscopy data were acquired with a Bruker Hyperion 2000 IR (infrared) microscope with a Bruker Hyperion 2000 IR microscope connected to a V80v FTIR spectrometer. This was conducted at the IR beamline of the Australian Synchrotron in Melbourne. The sections prepared in section 2.15 were placed on polished barium fluoride (BaF_2) windows (Crystal Lan Limited, UK) of 0.5 mm x 22 mm for FTIR analysis. IR absorbance spectra were measured in transmission mode and sourced from an intermediate IR region of 750 to 3,850 cm^{-1} at a spectral resolution of 8 cm^{-1} and 128 co-added scan/pixel (Vrahnas, Pearson *et al*. 2016, Vrahnas, Buenzli *et al*. 2018). For each tibial section, spectra were collected across the full width of the tibial cortex on the medial side at 1,500 µm from the base of the hypertrophic zone of the growth plate, as previously described (Vrahnas, Pearson *et al*. 2016, Vrahnas, Buenzli *et al*. 2018). For FTIR measurements, I measured the periosteal

region and progressed across the bone to the endosteal region, taking between five and ten measurements at 10 μm intervals, dependent on the width of the bone. The data was then imported to OPUS version 8.0 (Bruker, Ettlingen, Germany) and was aligned by identification of the periosteal and endosteal regions by the characteristic shapes and heights of their phosphate peaks. Spectra lacking an obvious peak were excluded from the dataset. Spectra were corrected according to baselines, to discount the influence of water and MMA in which the sample was embedded, and to account for differences in beam penetration associated with different wavelengths. OPUS was also used to integrate amide I, amide II, carbonate, and phosphate data.

2.18 Ploton silver stain and microscopy

To aid visualisation under a Nikon bright-field microscope (Nikon, Tokyo, Japan), osteocyte lacuna-canalicular networks were Ploton silver stained (Ploton, Menager *et al*. 1986). This involved dewaxing and rehydration of paraffin-embedded sections (Section 2.18.1) via the use of graded ethanols to distilled deionised water. The solution was produced by dissolving gelatine in 1 g/dL aqueous formic acid to make 2 g/dL. One part of this solution was mixed with two parts of a 50 g/dL aqueous silver nitrate (ACS reagent, ⩾99.0%, Cat. No. 209139, Sigma–Aldrich, Germany) solution to produce the final solution to be used for staining. Bone sections were then immersed in the 50% silver nitrate for 55 mins at room temperature. Sections were then washed with distilled deionised water for 5 mins and dehydrated through graded ethanol to xylene. Microphotographs were viewed with ImageJ.

2.18.1 Preparation for paraffin-embedded sections

Twelve-week-old heterozygous mice tibiae were decalcified by immersion in 15% ethylene-diamine-tetra-acetic acid (EDTA, Cat. No. BIOEB0185, Astral Scientific, Australia) and 0.5% PFA in diethylpyrocarbonate (DEPC)-treated water at pH 8.0 and 4 ˚C for 14 days,

with occasional gentle agitation. Tibiae were subsequently dehydrated, immersed in xylene, and then infiltrated in paraffin wax using a Shandon Excelsior^{TM} ES Tissue Processor (Thermo Fisher Scientific, Waltham, US).

With the use of a Shandon Histocentre-2 embedder (Grale Scientific, Ringwood, Australia), the following protocol was followed: 70% ethanol for 1 hr, 85% ethanol for 1 hr, 90% ethanol for 1 hr, 100% ethanol for 1hr x3, xylene 1hr x3, and finally paraffin wax for 1 hr x3, at 60 ˚C x3.

Embedded samples were then stored at 4 ˚C until sectioning. Dr. Niloufar Ansari assisted with sectioning, whereby samples were sectioned sagittally in 5 µm increments with a Microm HM330 rotary microtome (Microm, Heidelberg, Germany). Sections were incubated overnight at 37 ˚C and stored at 4 ˚C until required for Ploton silver stain and microscopy.

2.19 Statistical analysis

In cases of only one comparison, statistically significant differences were determined by unpaired Student's t-tests. For comparisons of regions between genotypes from FTIR microspectroscopy data (Chapter 6), a two-way ANOVA followed by Fisher's LSD *post hoc* test was used. All data are presented as the mean ± SEM. $P \leq 0.05$ was regarded as statistically significant. All statistical analyses were processed with the software GraphPad Prism 8.

Chapter 3: Parathyroid Hormone-Related Protein Negatively Regulates Tumour Cell Dormancy Genes in a PTHR1/Cyclic AMP-Independent Manner

3.1 Introduction

Bone metastasis development begins with tumour cells translocating from breast to the blood stream, followed by colonisation of a secondary site (Shibue and Weinberg 2011, Valastyan and Weinberg 2011, Ottewell, O'donnell *et al*. 2015). The bone marrow is the most common site where metastatic breast cancer cells tend to travel (Kischel, Bellahcene *et al*. 2012, Scully, Bay *et al*. 2012). Metastatic breast cancer cells in the bone marrow express higher levels of PTHrP than primary tumours and metastatic cells at other sites (Powell, Southby *et al*. 1991). When breast cancer MCF7 cells are injected intracardially into immune deficient mice, they usually grow poorly in the bone (Thomas, Guise *et al*. 1999). This might be in part because the cells lack invasive potential compared with other breast cancer cells (e.g. A375, MDA-MB-231). However, when the cells are engineered to overexpress PTHrP, it can overcome this phenotype, inducing human MCF7 breast cancer cells to colonise bone marrow aggressively and causing osteolysis and bone destruction (Thomas, Guise *et al*. 1999). As suggested by the findings of Thomas *et al*. (1999), PTHrP produced by the cancer cells promotes bone resorption and prepares a niche for tumour establishment and growth. These MCF7 cells had been prepared in my host laboratory (Thomas *et al*.1999), to demonstrate that this overexpression of PTHrP in MCF7 cells was associated with down-regulation of several pro-dormancy genes, and these could contribute to the enhanced bone colonisation (Johnson, Finger *et al*. 2016).

Many years ago it was found that although MCF7 cells exhibited a very sensitive adenylyl cyclase responsiveness to calcitonin and to prostaglandin E (PGE_2), the cells showed no cAMP response to PTH at all (Findlay, deLuise *et al*. 1980). This finding suggests that PTH1R in these cells has no functional association with adenylate cyclase since that data also raised the possibility that PTHrP overexpression effects on tumour dormancy in MCF7 cells may result from actions of PTHrP on the cells that are independent of PTH1R, in other words, non-canonical actions.

In this chapter, I first set out to confirm whether MCF7 cells lack a cAMP response to PTH and determine they are capable of responding to PTHrP though the PTH1R. Additionally, I used multiple assays combined with RNA-Seq analysis to identify the PTH1R/cAMP-independent genes and pathways regulated in MCF7 cells overexpressing PTHrP. In summary, I determined that MCF7 cells do not possess a cAMP PTH response nor they respond to PTHrP via PTH1R. Using multiple assays and RNA-Seq, I identified PTH1R/cAMP-independent genes/ pathways regulated in MCF7 cells overexpressing PTHrP. Several potential alternative pathways, notably those related to calcium signalling and TRP signalling need to be further explored.

3.2 Methods

I first set out to confirm whether MCF7 cells lack a cAMP response to PTH (see methods in Section 2.6.1 and 2.7), and determine they are capable of responding to PTHrP though the PTH1R. Additionally, I used multiple assays (Section 2.5.1, 2.9, 2.11, and 2.12) combined with RNA-Seq analysis (Section 2.10) to identify the PTH1R/cAMP-independent genes and pathways regulated in MCF7 cells overexpressing PTHrP.

3.3 Identifying whether breast cancer cells have functional PTH1R activity

3.3.1 RNA-Seq confirms PTHrP overexpression reduces pro-dormancy genes

Although PTHrP overexpression resulted in a very significant change in MCF7 cells phenotype, I needed to understand how these effects were achieved. Therefore, RNA-Seq was undertaken based on the MCF7 cells overexpressing full-length PTHrP (MCF7_PTHrP) over MCF7_pcDNA vector control. Gene regulatory characteristics were exacted by using the method described in section 2.10. Pro-dormancy genes transcription levels were extracted from DESeq and EdgR (Section 2.4.10). Pro-dormancy genes identified in prior work by (Johnson, Finger *et al*. 2016) were inhibited in the cells overexpressing PTHrP in our RNA-Seq data. Fig.3.1 shows a heat-map of the pro-dormancy genes *AMOT* (Martin 2005), *P4HA1* (Johnson, Finger *et al*. 2016), *HIST1H2BK* (Kim, Avivar-Valderas *et al*. 2012), *SELENBP1* (Johnson, Finger *et al*. 2016), and housekeeping genes *FBXO11* (Sardiello, Palmieri *et al*. 2009), *HPRT1* (Sardiello, Palmieri *et al*. 2009), *KPNA2* (Sardiello, Palmieri *et al*. 2009), *MTX2* (Sardiello, Palmieri *et al*. 2009) identified by RNA-Seq using DESeq and EdgeR analysis tools. The colour code represents relative Log_2 fold changes of each gene in MCF7_PTHrP compared to MCF7_pcDNA vector control.

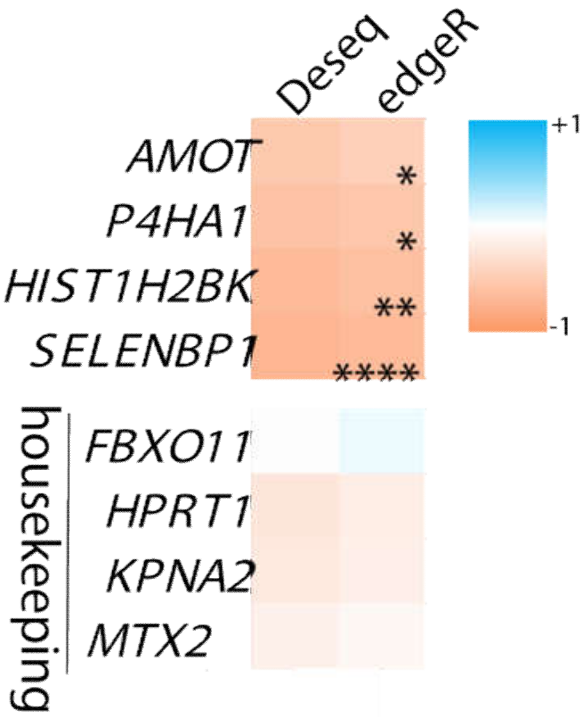

Figure 3.1. Pro-dormancy genes are reduced with PTHrP over-expression in MCF7 cells. Pro-dormancy genes are reduced with PTHrP over-expression in MCF7 cells. MCF7 cells stably overexpressing vector (pcDNA) or full- length secreted PTHrP (MCF7_PTHrP) were subjected to RNA Seq analysis, as described in 2.10. Shown are DESeq and EdgeR analysis showed the differentially expressed pro-dormancy genes and housekeeping genes (control). The colour code represents relative Log2 fold changes of each gene in MCF7_PTHrP compared to MCF7 pcDNA vector control. Scale shown on the left.

3.3.2 Neither PTHrP nor PTH activates cAMP in MCF7 breast cancer cells

Pioneering research has shown that MCF7 cells do not respond to PTH treatment with increased expression of cAMP or activation of cAMP-dependent protein kinase. This finding implies that PTH1R lacks a functional link to adenylyl cyclase in those cells (Findlay, deLuise

et al. 1980). These data indicate that the effect of PTHrP overexpression on tumour dormancy in MCF7 cells may occur through actions that are independent of PTH1R on the PTHrP molecule. I confirmed that MCF7 cells responded in a dose-dependent and sensitive manner to calcitonin and PGE_2, with increased cAMP production, but failed to promote cAMP production to multiple doses of PTH (1–34) or of PTHrP(1–141) in MCF7 cells (Fig 3.2).

In addition, in order to investigate later cellular responses, MCF7 cells were transiently transfected with a cAMP response element (CRE)-luciferase construct (CRE-Luc; as described in Chapter 2; Methods), whereas calcitonin and produced a substantial response there was no effect of PTH, confirming that the MCF7 cells have no functional PTH1R/cAMP/PKA signal, the receptor pathway shared equally by PTH and PTHrP. MCF7 wild-type cells did not exhibit any detectable activities of a CRE-luciferase reporter (Fig. 3.2B CRE-reporter assay by Mrs Ho). This confirmed the lack of cAMP and of CRE-luciferase response in MCF7 cells to full-length PTHrP and PTH in a wide range of doses, whereas the cells still respond to the positive controls, Forskolin, Calcitonin and PGE_2. These findings indicate that MCF7 breast cancer cells have no functional PTH1R receptor linked to adenylate cyclase activation, indicating that the ability of PTHrP to overcome dormancy in these cells must be mediated by some action independent of PTH1R/ cAMP that results in expression of a large number of genes. My interest is in determining which regions of PTHrP are responsible for non-canonical effects of PTHrP and what might be the signalling pathways.

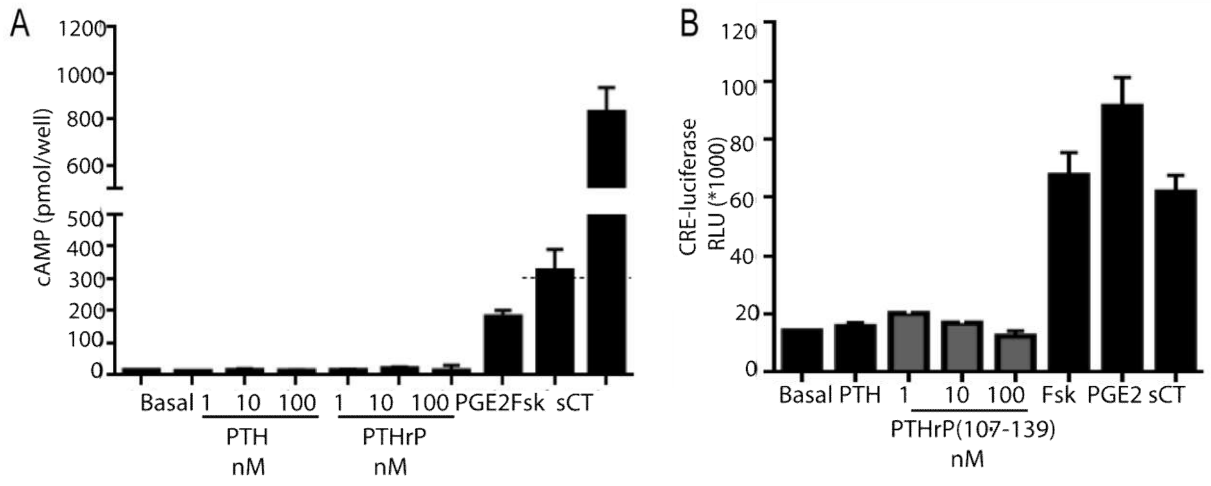

Figure 3.2. PTH and PTHrP do not activate cAMP or CRE-luciferase activity in MCF7 cells. (A)MCF7 cells treated with parathyroid hormone (PTH), PTH-related protein (PTHrP), prostaglandin E_2 (PGE_2) (10^{-6}M), salmon Calcitonin (sCT) (10^{-6}M) or Forskolin (Fsk) (10^{-5}M). PGE_2 and Fsk serve as positive controls for cAMP activation. (B) MCF7 cells transfected with a cAMP luciferase reporter and treated with PTH (10^{-8}M), PTHrP(107-139), PGE_2 (10^{-6}M), sCT (10^{-9}M) or Fsk (10^{-4}M). Data shown in panel B was generated by Patricia Ho.

3.3.3 Lack of cAMP gene response in MCF7 cells

I next sought to determine whether any cAMP-dependent genes responded to PTHrP in MCF7 cells. Using qRT-PCR, it has been confirmed that transfection of pMSCV:PTHrP plasmid resulted in a ~1.8-fold increase in PTHrP gene expression in MCF7 cells (Fig. 3.3A). Although no cAMP- linked PTH1R response took place in MCF7 cells, the possibility still had to be considered that PTH1R is expressed. Therefore, PTH1R was determined by Western blotting with an anti-PTH1R antibody. A 66-kd PTH1R receptor band was detected in MCF7_pcDNA vector control cells and MCF7_PTHrP cells (Fig.3.3B), appreciable fainter than that in the osteosarcoma UMR106 cells that are known to express high levels of functional PTH1R (Kawane, Mimura *et al*. 2003; Fig. 3.3B). The protein expression of PTH1R was not regulated by overexpressing of PTHrP in the MCF7_PTHrP compared with MCF7_pcDNA vector

control (Fig. 3.3B). Fig. 3.3C showed the *PTH1R* mRNA transcription was expressed but not downregulated with PTHrP overexpression by qRT-PCR, which is further evidence for lack of a cAMP/PKA action through PTH1R in these cells, with no functional PTH1R.

Although there was no cAMP production, in response to PTHrP, nor CRE-luciferase activation, it was still necessary to investigate any possible effects on CREB-responsive genes. RNA-Seq was been employed by our collaborator Dr. Johnson to analyse which pathways are activated in response to PTHrP overexpression in MCF7 cells. More than 2,500 genes were differentially regulated with a log2 fold change >1 and $P<0.05$ in MCF7_PTHrP normalised by MCF7 vector control cells (Johnson, Finger *et al*. 2016). Among the more than 2,500 genes regulated in PTHrP-overexpressing MCF7 cells (Fig. 3.3C) there were only two out of 32 candidate CREB-responsive genes (Walia, Ho *et al*. 2016) upregulated (Fig. 3C). The two up-regulation genes were *Amphiregulin (AREG)* and *Neuropilin-1 (NRP1)* and the three down-regulated genes are *FOS*, *Aquaporin 3 (AQP3)* as well as *CEBP-delta (CEBPD)*. The remaining 27 were not altered by PTHrP overexpression. This indicated that although stable overexpression of PTHrP exerted long term effects on MCF7 cells, the majority of CREB responsive genes were not changed.

Subsequently I validated three candidate CREB target genes that are supposed to be up-regulated when cAMP/PKA signalling has been activated (*Nuclear Receptor Subfamily 4 Group A Member 1,NR4A1*; *Nuclear Receptor Subfamily 4 Group A Member 2*, *NR4A2* and *Regulator Of G Protein Signalling 2*, *RGS2*) and two other important CREB responsive genes (*CAMP Responsive Element Binding Protein 1*, *CREB1*; Majumder, Varadharaj *et al*. 2004, Kandel 2012; *Protein Kinase CAMP-Dependent Type I Regulatory Subunit Alpha*, *PRKAR1*; Drozdov, Svejda et al. 2011, Yin, Pringle et al. 2011) that are not in the 33 CREB gene list by PCR. The result was consistent with the RNA-seq data except that the *NR4A1* and *AREG*

messenger RNA showed statistically significant increase in MCF7_PTHrP cells compared with the control (Fig. 3.3C). *RGS2*, *CREB1* and *PRKAR1* were not changed in PTHrP overexpression MCF7 cells. This further indicated that the changes in gene expression seen with PTHrP overexpression in MCF7 cells are the result of actions of PTHrP independent of PTH1R. MCF7 breast cancer cells thus offer a model to investigate non-canonical PTHrP signalling actions, particularly with regard to their exiting dormancy in the bone marrow.

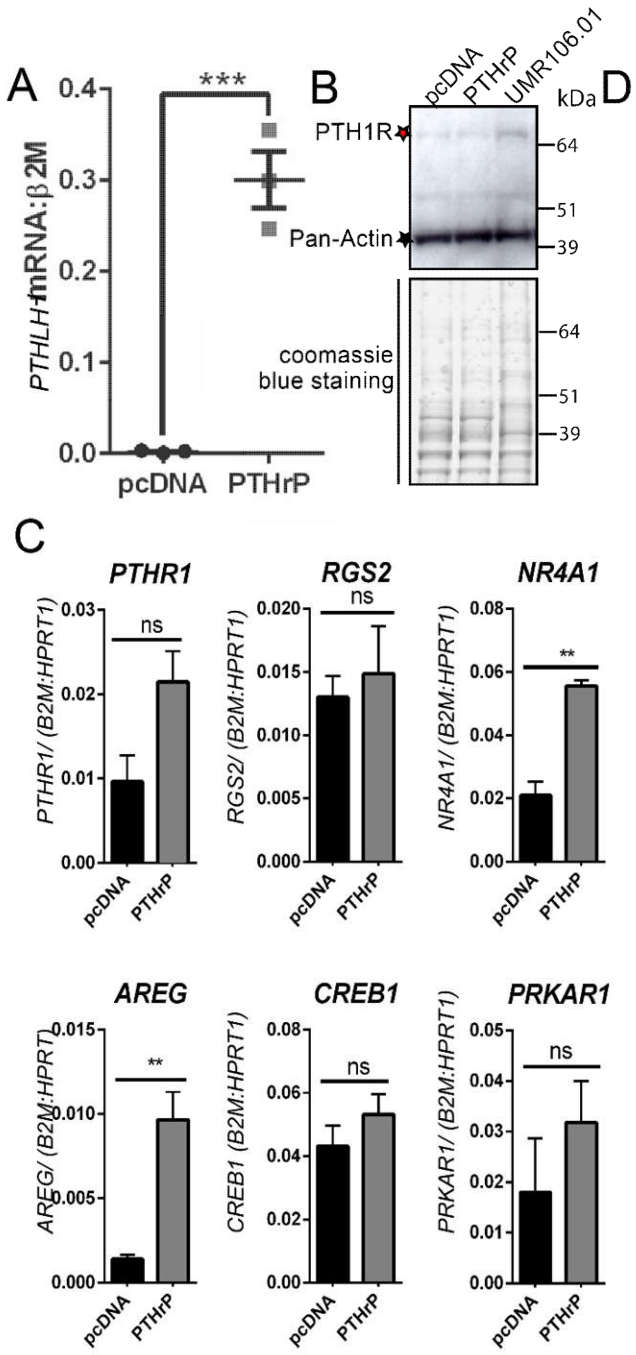

D

Gene name	Log2fold change	p-value	Significant?
SOX9	-0.41	0.41	
NR4A3	-0.07	0.93	
BTG2	-0.29	0.53	
AREG	3.58	1.25E-07	**** UP
UGDH	0.06	0.87	
FOS	-0.74	0.03	* DOWN
DUSP1	-0.12	0.75	
NR4A2	0.14	0.69	
GEM	-0.47	0.66	
RGS2	-0.12	0.93	
TCF7	0.19	0.56	
VEGFA	-0.03	0.96	
NR4A1	0.52	0.53	
AQP3	-1.07	1.14E-03	** DOWN
TEX2	0.04	0.88	
CEBPD	-0.83	0.03	* DOWN
IFNGR1	0.07	0.88	
EFNB2	0.53	0.10	
SIK2	-0.16	0.49	
PLAUR	0.39	0.34	
BMP8A	0.14	0.82	
JUNB	0.15	0.72	
IER3	0.83	0.17	
NRP1	0.75	5.12E-04	*** UP
USP2	-0.38	0.40	
NFIL3	0.02	0.95	
NFKB2	0.08	0.75	
DLEC1	0.25	0.65	
FOXC2	0.67	0.65	
LST1	-0.05	0.97	
KCNE4	0.25	0.56	
IL6	0.60	0.81	

Figure 3.3. Minimal regulation of cAMP/CREB-responsive mRNA levels by RNA-Seq analysis and qRT-PCR in MCF7 cells overexpressing PTHrP. (A) PTHLH mRNA levels in MCF7 pcDNA and MCF7_PTHrP overexpressing cells, normalised to Beta-2 microglobulin, B2M. Graphs = mean + SE. **p < 0.01 by unpaired Student's T-test. (B) Western blot for PTH1R protein in MCF7 pcDNA and MCF7_PTHrP and WT UMR106.01 cells. (C) mRNA levels of cAMP/CREB-target genes detected by qRT-PCR. Graphs = mean + SEM. **p < 0.01 by unpaired Student's T-test. (D) RNA-Seq analysis of MCF7_PTHrP vs MCF7 pcDNA cells. MCF7_pcDNA: MCF7 pcDNA vector control cells; MCF7_PTHrP: MCF7 overexpressing PTHrP; WT UMR106.01: Wild-type UMR106.01 cells. *SOX9*:

SRY-Box Transcription Factor 9; NR4A3: *Nuclear Receptor Subfamily 4 Group A Member 3; BTG2*: *B-Cell Translocation Gene 2; AREG*: *Amphiregulin; UGDH: UDP-glucose 6-dehydrogenase; FOS: Fos Proto-Oncogene, AP-1 Transcription Factor Subunit; DUSP1*: *Dual Specificity Phosphatase 1; NR4A2*: *Nuclear Receptor Subfamily 4 Group A Member 2; GEM: GTP Binding Protein Overexpressed In Skeletal Muscle; RGS2*: *Regulator Of G Protein Signalling 2; TCF7*: *Transcription Factor 7; VEGF-A*: *Vascular endothelial growth factor A; NR4A1*: *Nuclear Receptor Subfamily 4 Group A Member 1; AQP3*: *Aquaporin 3; TEX2*: *Testis Expressed 2; CEBPD*: *CCAAT Enhancer Binding Protein Delta; IFNGR1: Interferon Gamma Receptor 1; SIK2*: *Salt Inducible Kinase 2; PLAUR*: *Plasminogen Activator, Urokinase Receptor; BMP8A: Bone Morphogenetic Protein 8a; JUNB*: *JunB Proto-Oncogene, AP-1 Transcription Factor Subunit; IER3*: *Immediate Early Response 3; NRP1: Neuropilin 1; USP2*: *Ubiquitin Specific Peptidase 2; NFIL3*: *Nuclear Factor, Interleukin 3 Regulated; NFKB2: Nuclear Factor Kappa B Subunit 2; DLEC1*: *Cilia And Flagella Associated Protein; FOXC2*: *Forkhead Box C2; LST1*: *Leukocyte Specific Transcript 1; KCNE4*: *Potassium Voltage-Gated Channel Subfamily E Regulatory Subunit 4; IL6: Interleukin 6*

3.3.4 cAMP gene responses to exogenous PTHrP are absent in MCF7 cells

Because of the evidence that MCF7 cells lack functional PTH1R linked to cAMP/PKA (Findlay, deLuise *et al*. 1980), I studied the effects of exogenous salmon calcitonin (sCT), prostaglandin E2 (PGE_2) as well as PTHrP treatments on transcript levels of genes that are expected to be CREB-responsive in MCF7 cells. Treatment with positive controls PGE_2 and sCT induced significantly greater mRNA levels of CREB-responsive genes *AREG*, *NR4A1*, or *RGS2*, but qPCR analysis clearly showed no *NR4A1* or *RGS2* response to PTHrP treatment and an attenuated *AREG* response compared with the PGE_2 or sCT in MCF7 cells (Fig. 3.4B). This confirms that gene transcription downstream of cAMP response to exogenous PTHrP is largely absent in MCF7 cells.

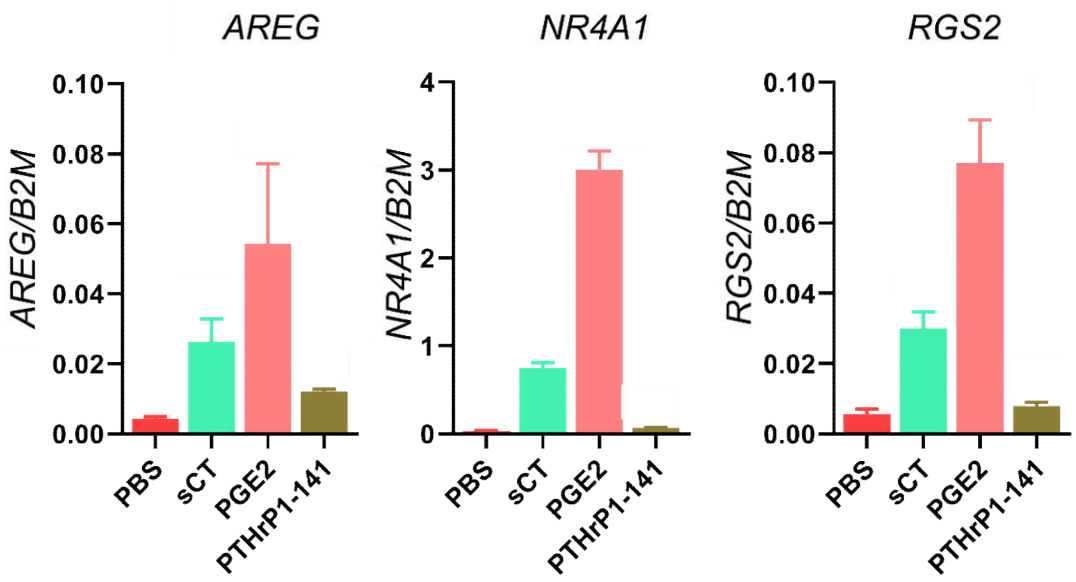

Figure 3.3. Both calcitonin and PGE2 activate downstream PKA responses in MCF7 cells, but not PTH nor PTHrP. qRT-PCR analysis of three different PKA/CREB target genes in MCF7 pcDNA treated with with PTHrP(1–141) or positive controls prostaglandin E_2 (PGE_2) or salmon calcitonin (sCT). Graphs = mean + SEM. n = 3 replicates from three independent experiments. *$p < 0.05$, **$p < 0.01$, ***$p < 0.001$ vs no treatment by one-way ANOVA with multiple comparisons.

3.3.5 PTH is not binding the receptor and is not functional in MCF7 cells

To determine whether PTH1R is expressed on the cell surface of MCF7 cells, I examined Tetramethylrhodamine-labeled PTH (PTH^{TMR}) binding (Guo, Song *et al*. 2012, Yu, Zhao *et al*. 2012), carried out by Dr Chan. PTH^{TMR} binds to PTH1R and has been demonstrated to be consistently internalised into vacuolar protein sorting-associated protein (VPS35; Seaman, Marcusson *et al*. 1997, Linhart, Wong *et al*. 2014)-positive endosomes (typically within 10–30 min; Chan, Clairfeuille *et al*. 2016). It has been demonstrated as a useful tool to monitor

binding by interacting with the partner PTH1R and the internalisation of amino-terminal PTH (Chan, Clairfeuille *et al*. 2016).

Following agonist stimulation (when this maximises ligand binding to the surface receptor, and subsequent internalisation of the receptor-ligand complex into endosomes), UMR106 cells typically retained $PTH1R^{TMR}$, as prominently marked by the distinct localisation toward the perinuclear (Golgi) region of the cell (Vilardaga 2010; Fig. 3.5j). This means the PTH1R binds PTH^{TMR} in these cells. The encapsulated ligand-receptor complexes in early endosomes were visualised, as determined by its co-localisation with VPS35 (Fig. 3.5k, l). However, MCF7 parental, vector-transfected, or PTHrP-transfected cells showed no co-localisation of PTH^{TMR} internalisation (Fig. 3.5a, d, g). At the same time, co-localisation with VPS35 were not detected in these cells (Fig. 3.5c, f, i) even VPS35 was marked in each of the MCF7 cell lines (Fig. 3.5b, e, h). Since MCF7 cells showed no binding and no detectable specific bindings, this suggested the PTH is not binding the receptor and is not functional.

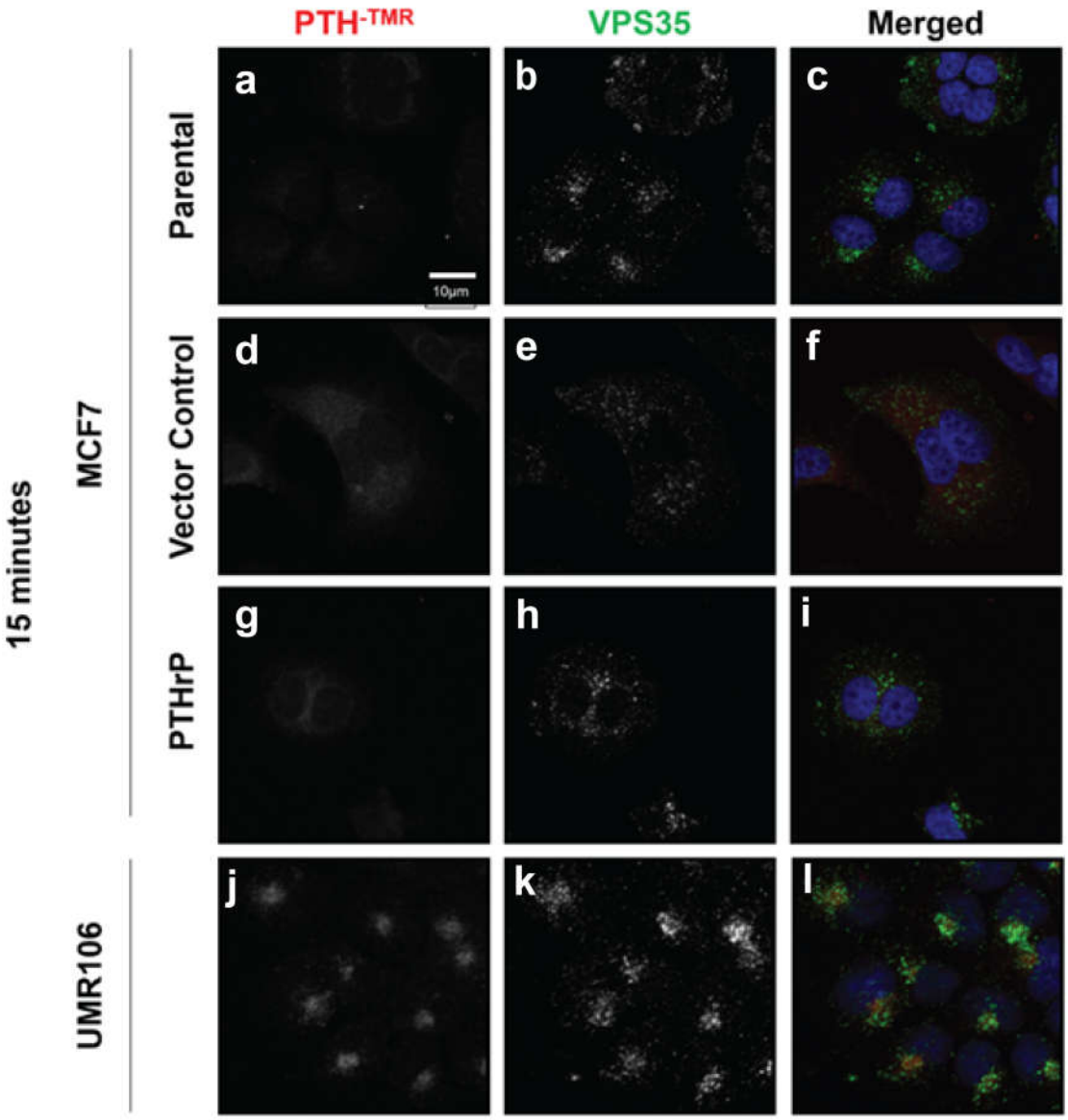

Figure 3.4. MCF7 cells do not express sufficient PTHR1 on the cell surface to bind detectable amounts of PTH through confocal microscopy. MCF7 cells and UMR106-01 cells were cultured on poly-l-lysine-coated glass coverslips and serum starved for 1 hour prior to the addition of Tetramethylrhodamine-labelled PTH(1-34) (PTH^{TMR}, 100nM) for 15 mins at 37°C. Cells were then fixed in 4% PFA, and immune-stained for endogenous retromer subunit, vacuolar protein sorting-associated protein 35 (VPS35) and imaged for PTH^{TMR} (a, d, g, j), VPS35 (b, e, h, k) and DAPI(c, f, i, l) using a Nikon A1Si confocal microscope. Scale bar, 10µm. Representative of $n = 3$ from independent experiments.

3.4 Multiple signalling pathways are upregulated in MCF7 parathyroid hormone-related protein-overexpressing cells

To identify significantly enriched pathways that have been increased due to the overexpression of PTHrP, STRING analysis (Szklarczyk, Gable *et al*. 2018) was carried out on the RNA-Seq data based on the MCF7 cells overexpressing full-length PTHrP (MCF7_PTHrP) over MCF7_pcDNA vector control (Section 3.1.1). To identify the interacting partners regulated by PTHrP overexpression in the dataset, the top 250 up- and 250 down-regulated genes (all $p < 0.05$) sorted in order of the largest $\log_2$ fold change; a total of 500 genes analysed. STRING pathway analysis of this RNA-Seq data showed that the most significantly enriched pathways (false discovery rate = 0.0081–0.0324) in MCF7 cells overexpressing PTHrP (in comparison to parental cells as controls and across all 500 genes) were the calcium signalling pathway, cytokine–cytokine receptor interaction, chemokine signalling pathway, inflammatory mediator regulation of transient receptor potential (TRP) channels, and circadian entrainment pathway (Fig. 3).

Table | KEGG BIOLOGICAL PATHWAY (Up-regulated)

Name	Gene count	False discovery rate
Calcium signaling pathway	6	0.0081
Cytokine-cytokine receptor interaction	7	0.0081
Chemokine signaling pathway	6	0.0081
Inflammatory mediator regulation of TRP channels	5	0.0081
Circadian entrainment	4	0.0324

Figure 3.5. Multiple signalling pathways are upregulated in MCF7 parathyroid hormone-related protein-overexpressing cells. KEGG biological pathways significantly enriched for in the STRING analysis of the top 250 upregulated genes. There were no significantly enriched KEGG biological pathways for the top 250 downregulated genes. Data was adapted from Dr. Rachelle Johnson's.

3.4.1 The calcium signalling pathway is significantly enriched downstream of parathyroid hormone-related protein (PTHrP) overexpression in MCF7 cells.

Calcium pathways and TRP channels are high selectivity particle channels for Ca^{2+} (Ramsey, Delling et al. 2006), suggesting calcium is dramatically modified with PTHrP overexpression. The "calcium signalling pathway" and "TRP channel pathway" from the STRING analysis results (*P2RX6* was specific for the calcium signalling pathway (Gandla, Lomada *et al*. 2017)) with 5/6 genes overlapped (Fig. 3.7A); no unique TRP channel pathway genes were characterised. Messenger RNA levels for *PTHLH* (control), *BDKRB1* (Tsukagoshi, Shimizu et al. 1999), and *CALML3* (Strehler 2011; Fig. 3.7B–D) confirmed RNA-Seq datasets in MCF7 PTHrP-overexpressing cells.

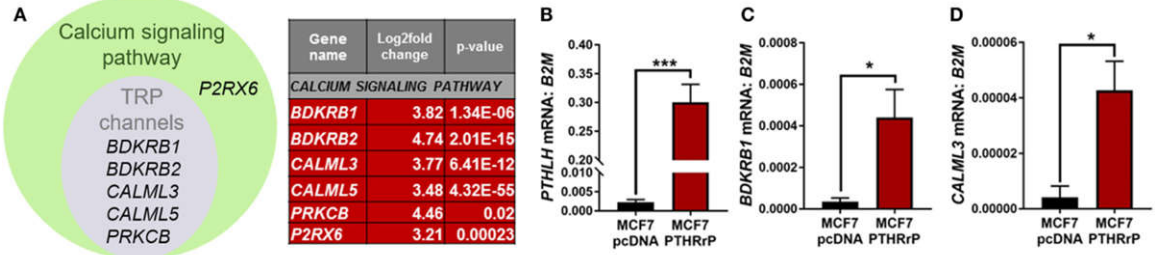

Figure 3.6. The calcium signalling pathway is significantly enriched in MCF7 cells overexpressing PTHrP. (A) Venn diagram indicating the calcium signalling pathway and transient receptor potential (TRP) channel genes that were significantly upregulated in PTHrP-overexpressing cells (green). One significantly enriched gene that was unique to the calcium signalling pathway: *P2RX6* (green). (B) *PTHLH* mRNA levels in MCF7pcDNA control or MCF7 PTHrP-overexpressing cells, shown as a control for PTHrP overexpression. (C,D) qPCR for mRNA levels of calcium signalling pathway genes (*BDKRB1* and *CALML3*) in MCF7pcDNA or MCF7 PTHrP-overexpressing cells. Bar graph height = mean ± SEM. n = 3 replicates from independent experiments. *p < 0.05, ***p < 0.001 by Unpaired Student's t-test. Data from B, C and D was from Dr. Rachelle Johnson.

3.5 Preparation of MCF7 cells overexpressing *PTHLH* mutants

In order to identify the non-canonical actions influencing gene expression in MCF7 breast cancer cells, I generated MCF7 cells overexpressing mutant forms of PTHrP. I used PTHrP isoform constructs established by Patricia Ho with different alignment of PTH1R-independent domains. These were previously used study the secretion of PTHrP in osteocytes (Ansari, Ho *et al*. 2018), and are as follows: $PTHrP^{FL}$ (-36–139) to produce and secrete full length (139 aa), $PTHrP^{\Delta NLS\Delta C}$ (-36–67) to produce and secrete PTHrP lacking the NLS and the C- terminus domain, $PTHrP^{\Delta Sec}$(1–139) to produce full length PTHrP that is not secreted but is retained within the cells, and $PTHrP^{\Delta NLS}$ to produce full length protein that lacks the NLS but is secreted (Section 2.4.5).

To compare how different domains within the PTHrP molecule can influence gene expression in MCF7 cells, I generated these MCF7 cells expressing each of these mutant forms. I have performed the validation of the PTHrP gene products using region specific primers and PTHrP RIA (Fig. 3.8). All of these procedures are described in Chapter 2.

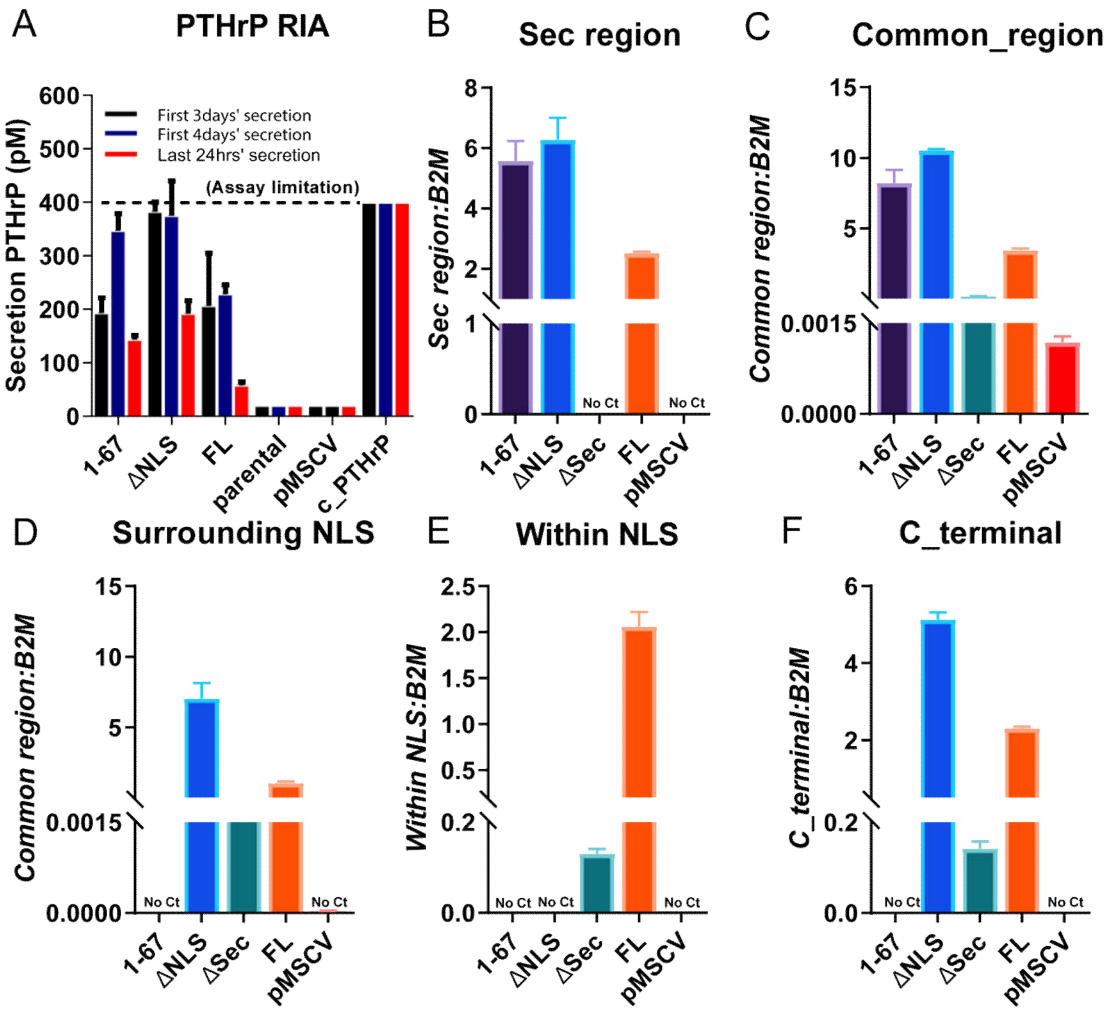

Figure 3.7. Confirmation of Pthlh overexpressing constructs in MCF7 cells. (A) Analysis of conditioned media from transfected cells, assayed by measuring PTHrP RIA. The first 3 or 4 days as well as the last 24 hours of conditioned medium from each of the MCF7 cell lines were collected and subjected to the PTHrP RIA assay. 1-67: MCF7 overexpressing PTHrP but lacks the NLS and C-terminus region; ΔNLS: MCF7 overexpressing PTHrP but lacks NLS region; FL: MCF7 overexprssing PTHrP full length; parental: MCF7 wild-type parental cells; pMSCV: MCF7 overexpressing pMSCV vector control; c_PTHrP: MCF7 overexpressing PTHrP full length (MCF7_PTHrP). Data shown as mean +SEM; n=3 replicates of three independent experiments. (B-F) validation of overexpression of PTHLH leader sequence (B), common region (C), region surrounding NLS (D), region within NLS (E) and C terminal (F) by real-time PCR. Graphs = mean + SEM. Each of these primer sets and gene products will be described in section 4.2.1 and Figure 4.1.

In order to show that PTHrP had been continuously produced, secreted PTHrP concentrations in the first three or four days as well as the last 24 hours of conditioned medium from each of the MCF7 cell lines were quantified by a N-terminal radioimmunoassay. My analysis showed the first four days secretion of PTHrP from the secreted cell lines (Fig 3.8D) had the highest concentration of PTHrP (around 250~380 pM). The first three days secretion in each of the cell lines showed a similar amount of PTHrP compared with that collected within the first four days.

Primer sets designed to amplify specific regions within PTHrP cDNA (Ansari, Ho *et al*. 2018) plus a C-terminus region primer set were used to detect mRNA products from the PTHrP constructs. As shown in Fig. 3.7 B–F, all the four secreted isoforms have generated correct and similar amount of genes transcription levels. Overall, these suggested that all the stable cell lines that overexpress the PTHrP and PTHrP mutant forms are bearing enough secretion of PTHrP thus can be used for further study. Having validated these cells, they were sent to our collaborator Dr. Johnson (Vanderbilt University) for RNA-Seq analysis. The results of that analysis are not included in this thesis.

3.6 Discussion

Although human breast cancer cells (MCF7) were found to express receptors for calcitonin and PGE_2 associated with adenylyl cyclase activation, no such activities could be measured in response to treatment with PTH(1–34; Findlay, deLuise *et al*. 1980). I have confirmed this observation and showed that PTHrP(1–141) also does not promote adenylyl cyclase activity in these cells. In addition, neither PTH(1–34) nor PTHrP(1–141) had any effects on activation of a CREB reporter compared with control. This means that other

non-cAMP/CREB mediated pathways must play a role in the action of PTHrP in MCF7 cells to metastasise.

This work showed that although PTHrP has the ability to induce major changes in gene expression and activities in MCF7 cells, it does not signal through the PTH1R to activate the cAMP pathway in these cells. Although PTH1R was detected by qPCR and Western blot, no cAMP response was detected, and no CRE-luciferase activities were detected. In addition, out of all the known cAMP responsive genes, only two of 32 were upregulated in an RNA-Seq analysis. In contrast, PTHrP overexpression in these cells upregulated genes regulated by the calcium signalling pathway, including TRP channel genes.

The only two cAMP responsive genes that were significantly upregulated with PTHrP overexpression in MCF7 cells by RNA-Seq: *AREG* and *NRP1*. This could suggest a positive feedback loop and PTHrP formation via AREG since an autocrine loop of AREG-EGFR signalling has been reported to activate *PTHLH* transcription in MDA-MB-231 breast cancer cells (Gilmore, Scott *et al*. 2008). This could be a factor in the reduced dormancy of PTHrP -overexpressing cells, which might promote *PTHLH* transcription in MCF7 cells as well. The increased level of NRP1 production in MCF7 breast cancer cells is also a potential link with the potential to metastasise, perhaps due to PTHrP formation and action. *NRP1* has been shown to promote tumorigenesis in breast cancer cells by enhancing angiogenesis (Miao, LEE *et al*. 2000) and NRP1-positive lung cancer cells have been reported to have tumour-initiating properties (Jimenez-Hernandez, Vazquez-Santillan *et al*. 2018).

I performed qPCR on an independent set of RNA samples to those used for RNA-Seq, which allowed me to validate both the technique and the biological results. qPCR was used to validate RNA-Seq results. Of the six mRNAs analysed, five were consistently regulated in both techniques; *NR4A1*, however, showed a significant increase in MCF7_PTHrP cells compared

to the control by qPCR but it was not significantly regulated by RNA-Seq. The upregulation of *NR4A1* mRNA, a known cAMP target gene in MCF7 cells overexpressing PTHrP, as determined by PCR, allowed us to consider whether there might be some cAMP-independent interaction between *NR4A1* and PTHrP. Zhou, Drabsch *et al.* (2014) identified that NR4A1 promoted breast cancer cell invasion and metastasis by stimulating TGF-β signalling and facilitating Smad7 degradation. This suggests that NR4A1 might be important for an invasive cancer phenotype; such a condition is associated with the aggressive phenotype of MCF7 cancer cells. Since we saw no cAMP activation, upregulation of these genes may result from indirect effects independent of cAMP, however, the possibility needs to be further investigated. For example, effects through other signalling pathways, including the calcium signalling pathway, were observed in my analysis when PTHrP was overexpressed.

Overexpression and exogenous treatment with PTHrP constructs containing the N-terminal domain both induced a significant increase in cAMP in osteoblast lineage cells, and overexpression increased the CREB responsive genes, *Nr4a1* and *Rgs2* (Ansari, Ho *et al*. 2018) confirming that these forms of PTHrP are capable of inducing a CREB response, but not in MCF7 cells. The PTHrP induction of *AREG* mRNA and the CREB-responsive gene *NR4A1* that I observed from PCR results in MCF7 cells was much lower than its induction with the positive controls for cyclic AMP activation (PGE2 and sCT). This further confirms that MCF7 cells do not have a PTHrP receptor functionally linked to adenylyl cyclase, as PTHrP has greatly reduced capacity to induce mRNA for CREB genes. In a separate analysis, I tested the recombinant PTHrP(1–141) used in this experiment in OCY454 cells; an osteocyte cell line that expresses the PTH1R (Ansari, Ho *et al*. 2018) to confirm that the protein was active and could induce expression of CREB genes.

My data also indicates that PTH, which has the same capacity to bind to the PTH1R as PTHrP, had virtually no binding to MCF7 cells, as revealed by PTH^{TMR} confocal imaging. This method applied to UMR106.01 cells showed that PTH^{TMR} is capable of PTH1R binding and forms complexes internalised into early endosomes (Chan, Clairfeuille *et al*. 2016). This makes use of PTH binding as a surrogate for PTHrP binding. The lack of detectable binding suggests that the PTH1R in MCF7 cells detected by Western blot lacks normal binding affinity. However, it must be conceded that PTHrP might bind to PTH1R at levels below my recognition limits, even though this seems unlikely.

It can be seen from above studies that functional PTH1R is absent in MCF7 cells. Hence, changes of expression in genes of PTHrP-overexpressing cells must be a consequence of autocrine or intracrine effects of PTHrP based on transduction of signals from other regions of the molecule (e.g. nuclear localisation sequence, NLS) or C-terminus region unrelated to PTH1R actions. The cell lines I have now generated overexpressing full-length PTHrP and mutant PTHrP were established to understand how PTHrP affects cell signalling and how these activities affect PTHrP function in promoting cells out of dormancy. This will facilitate future research on the increasingly appreciated non-canonical actions and pathways of PTHrP using RNA-Seq and other approaches.

This study pointed out that the substantial influences of PTHrP overexpression on gene expression in MCF7 cells are likely to occur through domains other than the PTH1R-mediated activation of cAMP/PKA/CREB. In my analysis, a number of other pathways were regulated in the PTHrP overexpressing cells, including the calcium signalling pathway, cytokine–cytokine receptor interaction, chemokine signalling pathway, inflammatory mediator regulation of transient receptor potential (TRP) channels, and circadian entrainment pathway. PTHrP overexpression in MCF7 cells has resulted in significantly enriched gene expression

downstream of calcium signalling pathways and TRP channels, and both these pathways are highly selective for intracellular Ca^{2+} (Ramsey, Delling *et al*. 2006). It has been demonstrated that upregulation of Ca^{2+} pathways can contribute to the development and proliferation of breast tumours in the MMTV-PymT transgenic mouse model of breast cancer and in human breast cancer cells (Kim, Takyar *et al*. 2016). Moreover, some components of the Ca^{2+} signalling pathway have been increased in breast, prostate, colon, pancreas, and lung tumours (Tsavaler, Shapero *et al*. 2001, El Hiani, Lehen'kyi *et al*. 2009, Dhennin-Duthille, Gautier *et al*. 2011). These data suggest intracellular calcium is dramatically modified with PTHrP overexpression, and these two pathways may contribute in ways to be determined to increased growth of PTHrP-overexpressing MCF7 cells in breast cancer metastasis, as shown by Johnson R W, *et al.* (Johnson, Finger *et al*. 2016).

My findings suggest that PTHrP overexpression in MCF7 cells drives calcium signalling, which may change the concentration of internal Ca^{2+}. Here I suggest there could be a positive feedback loop since the increased Ca^{2+} intracellular concentration may have an influence on concentration release, which affects the extracellular Ca^{2+} levels, exerting functions on CaSR to stimulate PTHrP. PTHrP stimulated by CaSRs can prevent nuclear accumulation of apoptosis-inducing factors, which mainly occurs under high Ca^{2+} concentration, by lowering the expression level of p27Kip1 (Kim, Takyar *et al*. 2016). In addition, Mamillapalli, VanHouten *et al*. (2008) confirmed that CaSR stimulates PTHrP production through Gαs signalling in MCF7 breast cancer cells. The CaSR-calcium signalling interactions with PTHrP have never been previously linked to the PTHrP-induced metastatic bone destruction phenotype. Although a role for the calcium signalling pathway in PTHrP's action to force cells to exit from dormancy to invasion has been suggested by Johnson *et al.* (2016), it remains essential to carry out an *in vivo* experiment to disclose the role of the CaSR-calcium signalling interaction in activation and proliferation of dormant tumour cells in bones.

Johnson and colleagues (Johnson, Finger *et al*. 2016) noted twelve pro-dormancy genes were downregulated (assayed by qPCR) in MCF7 cells overexpressing PTHrP. Using a second method, I confirmed these findings. However, I have noted only four of these genes (*AMOT*, *PAHA1*, *HIST1H2BK*, and *SELENBP1*) were significantly changed in cells overexpressing PTHrP. The reason for this may relate to slightly different culture conditions.

3.7 Conclusion

In conclusion, MCF7 human breast cancer cells lack a functional PTH1R linked to the cAMP/PKA pathway. Since many genes are regulated either up or down in MCF7 cells when PTHrP is overexpressed, this regulation must result from actions of PTHrP independent of PTH1R. These signals may come from other domains within the molecule, such as the nuclear localisation sequence (NLS) or the C-terminal region. The RNA-Seq analysis provided potential pathways through which PTHrP may function to downregulate gene regulations. Experiments to determine the mechanism of calcium signalling pathway in tumour dormancy would need to be conducted in the future to determine whether this is the pathway through which PTHrP promotes breast cancer cells out of dormancy.

3.8 Future Direction

Johnson R W, *et al.* (Johnson, Finger *et al*. 2016) demonstrated that PTHR1 mRNA levels were detectable across all human breast cancer, and mouse mammary carcinoma cell lines. These are cell lines （MDA-MB-231, MDA-MB-231b, 4T1, 4T1BM2, and D2A1) with great metastatic potential that can aggressively set the bone after intracardiac injection, or lung after tail vein inoculation, and cell lines (MCF7, SUM159, D2.0R, and PyMT) with low metastatic potential that do not colonize or proliferate very slowly after inoculation. The mRNA of PTH1R in these above cell lines were detected but did not correspond to the metastatic potential of the cell lines. It will be interesting to detect the PTH1R mRNA

difference, and compared in different represent different molecular subtypes, like ER-positive (ER+, MCF-7) and ER-negative (ER-, MDA-MB-231) breast cancer cell lines. Using some of the methods in this chapter, it will allow us to validate the finding in other cell lines (like ER+, ER-, and UMR106.01), and identify PTH1R differences between ER+ and ER- cell lines.

CHAPTER 4: Identification of PTHrP receptor-independent domain functions using RNA-Seq

4.1 Introduction

In the last chapter I provided evidence from breast cancer cells that PTHrP actions arise from domains beyond the amino-terminal region. My particular interest is the action of PTHrP in bone, where it is known to act canonically through the PTH1R (Zhao, Brauer *et al*. 2002, Datta and Abou-Samra 2009). However, given the aforementioned conclusion in the previous chapter, the possibility that actions arise from other domains should be explored. The target chosen to look at is the osteocyte. Osteocytes are terminally differentiated osteoblasts (Bruder and Caplan 1990, Birmingham, Niebur *et al*. 2012), but become trapped within mineralised bone (Heino and Hentunen 2008), with cells growing in individual lacunae and communicating with each other and with the surface cells (Aarden, Nijweide *et al*. 1994). My lab showed many years ago by immunostaining that osteocytes produce PTHrP (Kartsogiannis, Udagawa *et al*. 1998). More recently they have used an immortalised osteocyte cell line to show that these cells have a functional PTH1R since they respond in a specific and sensitive manner by increasing cAMP in response to PTHrP (Ansari, Ho *et al*. 2018).

The importance of osteoblast-derived PTHrP in the control of bone remodelling has been established though mouse genetic experiments, and a role for osteocytes is shown in the recent work from my lab in which PTHrP has been knocked-down from osteocytes by crossing PTHrP floxed mice with mice with a Cre linked to promoter for the osteocyte-specific protein, DMP1 (Ansari, Ho *et al*. 2018). It has been demonstrated that osteocyte-derived PTHrP maintains trabecular bone mass (Ansari, Ho *et al*. 2018). This mouse model with knockdown of PTHrP in osteocytes demonstrated significantly lower femoral trabecular bone volume and a

25% reduction in ultimate deformation by three-point bending tests of adult femora. This highlights the importance of osteocyte-derived PTHrP as a determinant of bone strength. Of much interest to us though was the work of another group who prepared mice with the same DMP1 Cre, but with knockout of the PTH1R (Delgado‐Calle, Tu *et al*. 2017). This resulted in a phenotype of increased trabecular bone, the reverse of my finding, so raised the question of actions of the PTHrP in osteocytes that are achieved by means other than through PTH1R.

Although the PTH1R-dependent pathway and the cAMP-PKA signalling are now well defined, the mechanisms by which intracellular PTHrP, the PTHrP C-terminus, and nuclear PTHrP control cell function are still incompletely known. I aimed therefore in this chapter to determine the effects in osteocytes of PTHrP domains compared to the N-terminus that signals through PTH1R. The data led to the striking conclusion that many more genes are regulated by $PTHrP^{\Delta NLS\Delta C}$ than by $PTHrP^{FL}$. To examine this further, I have found that the absence of PTHrP C-terminus increases gene expression in both numbers and magnitude change, particularly those genes regulated through the PTH1R.

4.2 Methods

In order to identify the specific region impacts on influencing gene expression in OCY454 osteocytes, I used OCY454 cells overexpressing PTHrP isoform constructs with different mutants of PTH1R-independent domains. These are as follows: $PTHrP^{FL}$ (-36–139) is to produce secreted full length PTHrP, $PTHrP^{\Delta NLS\Delta C}$ (-36–67) to produce and secrete PTHrP lacking the NLS and the C-terminus domain, $PTHrP^{\Delta Sec}$(1–139) to produce full length PTHrP that is not secreted but is retained within the cells, and $PTHrP^{\Delta NLS}$ to produce full length protein that lacks the NLS but is secreted. These cell lines have been published (Ansari, Ho *et al.* 2018) and will allow me to compare how different domains within the PTHrP molecule can influence gene expression in the cells.

I first identified that the gene numbers were primarily increased in $PTHrP^{\Delta NLS\Delta C}$. To examine further, I extracted the common genes regulated by $PTHrP^{FL}$ and $PTHrP^{\Delta NLS\Delta C}$ using the function in Venny (see a method in Section 2.10.5), and compared the difference of magnitude change in the two separate cell lines. In this way, I have confirmed that deletion of NLS and/or C terminus would change gene regulation magnitude since there is a significant increase in $PTHrP^{\Delta NLS\Delta C}$ compared to $PTHrP^{FL}$. However, when I made a similar comparison on the $PTHrP^{FL}$ and $PTHrP^{\Delta NLS}$, there was no change. Heatmaps (see the method in Section 2.10.5) were used to show most of the genes were regulated in the same direction. This suggests the gene regulation from $PTHrP^{FL}$ was not affected by deletion of NLS, but the absence of C-terminus. The deletion of the PTHrP C-terminus promotes gene expression in both numbers and magnitude change by regulated by PTHrP in OCY454 cells (see methods in Section 2.10.4 and 2.10.5) and determined NLS region may be essential for the absence of C-terminus in gene regulatory effect (see methods in Section 2.10.4 and 2.10.5). Importantly, I also confirmed that the absence of the C-terminus increases the number of cAMP/CREB-responsive genes, but not their response magnitude using the method in Section 2.10.5. I next identified that $PTHrP^{\Delta Sec}$ form did not modify PTHR1 signalling since the common genes regulated by all the cell lines are likely to behave differently in the regulation direction in the $PTHrP^{\Delta Sec}$ form vs the other forms. The PTHR1 associated genes were identified by uploading the 277 common genes regulated by all the cell lines to the STRING (see the method in Section 2.10.5). Thus, I have identified that OCY454 $PTHrP^{\Delta Sec}$ did not act through PTH1R. Using DAVID and its KEGG functions, I also determined that $PTHrP^{\Delta Sec}$ uniquely regulated nuclear localisation or function GO items associated genes and ubiquitination protein degradation pathway.

4.3 Evidence that deletion of the PTHrP C-terminus promotes gene expression by PTHrP in OCY454 cells

4.3.1 Validation of the OCY454 osteocytes overexpressing mutant PTHrP

The OCY454 stable cell lines were confirmed to overexpress PTHrP (Ansari, Ho *et al*. 2018), and I thawed fresh aliquots to confirm their PTHrP expression. Following infection of OCY454 cells with the PTHrP constructs shown in Figure 2.2, specific region primers (see Table 2.6 in Chapter 2) were employed with qPCR to demonstrate that approximately the same amount of *Pthlh* mRNA is produced in the separate cell lines (Fig. 4.1A).

All four PTHrP cell lines overexpressed PTHrP relative to the vector control cells, as determined by qPCR of mRNA using mid-region primer sets (Fig. 4.1A). Using primers to detect the products around the NLS region, all cell lines produced gene products except for the 1-67 ($PTHrP^{\Delta NLS\Delta C}$), which was expected because it does not possess a NLS region. However, $PTHrP^{\Delta Sec}$ showed a very low level of this product, indicating $PTHrP^{\Delta Sec}$ gene expression was not induced highly enough. Three cells lines expressed signal sequence normally, however, $PTHrP^{\Delta Sec}$ cells (with signal sequence deletion) showed a significantly weaker qPCR signal, which confirmed the initial expectation.

Fig. 4.1B shows the protocol of how to estimate the amount of PTHrP secreted by OCY454 cells. Samples of conditioned medium from each cell line were collected and used to treat UMR106.01 cells to assay cAMP because UMR106.01 cells have many PTH1R receptors. With PTH(1–34) used as a standard (Everhart-Caye, Inzucchi *et al*. 1996), the amounts of PTHrP activity in the media were approximately equivalent to 150 nM PTH(1–34) for the three secreted PTHrP cell lines. No biological activity was obtained with the non-secreted form, *Pthlh*(1–139; Fig. 4.1C). All these results were consistent with results by (Ansari, Ho *et al*. 2018).

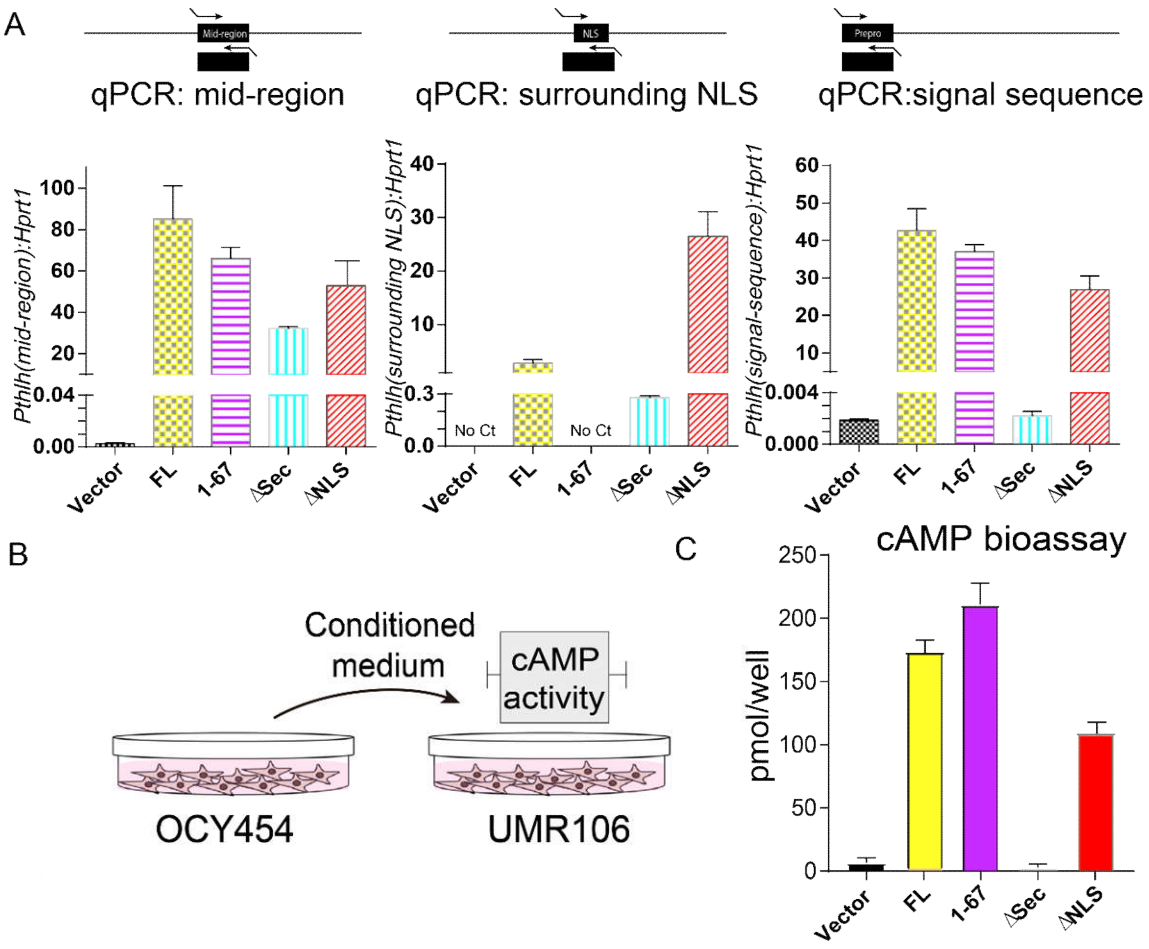

Figure 4.1. Validation of the OCY454 osteocytes overexpressing mutant PTHrP. (A)qRT- PCR for the mid region, surrounding NLS as well as the leader sequence of PTHrP. (B) Acquisition of cAMP production caused by PTHrP protein secreted by OCY454 cell lines overexpressing FL and mutant PTHrP. Confluent monolayers of UMR106.01 cells were maintained in solution containing 100 µM IBMX, a phosphodiesterase inhibitor, treated with conditional medium collected from OCY454 cells. The amount of cAMP was quantified by immunoassay and normalised to the amount of total protein. (C) Levels of cAMP increased by activated PTHrP from OCY454 cells appear not to vary markedly within each cell line.

4.3.2 Deletion of PTHrP C-terminus increased gene expression responses in OCY454

4.3.2.1 Deletion of C terminus increased gene expression response numbers

To give an overview of how many genes were regulated by each PTHrP construct, the total number of differentially expressed (DE) genes (including both up- and down-regulated genes) were quantified and compared: $PTHrP^{FL}$ regulated 1,413 genes; $PTHrP^{\Delta Sec}$ regulated 2,082 genes, whereas $PTHrP^{\Delta NLS}$ regulated 1,741 DE genes (Fig. 4.2A). These three cell lines regulated a similar number of genes (~1,400-2,000) in comparison to the vector, however, $PTHrP^{\Delta NLS\Delta C}$ regulated a strikingly greater number of genes, 4,463, more than twice the number regulated by each of the other three. This suggests that deletion of the PTHrP C-terminus magnifies the number of genes regulated by PTHrP in OCY454 osteocytes.

The number of unique and common DE genes were compared in a Venn diagram in Figure 4.2. More specifically, numbers of genes were shown in intersections (of four separate DEG lists: $PTHrP^{FL}$, $PTHrP^{\Delta NLS\Delta C}$, $PTHrP^{\Delta Sec}$, and $PTHrP^{\Delta NLS}$), which revealed gene numbers that are commonly regulated by different OCY454 cell lines or satisfy different conditions (FL, *Δ*NLS*Δ*C, *ΔSec* and *ΔNLS*. 277 genes were significantly regulated by PTHrP overexpression in all four transfected cell lines. 193 genes were uniquely regulated by $PTHrP^{FL}$, 667 uniquely regulated by $PTHrP^{\Delta Sec}$ and 265 uniquely regulated by $PTHrP^{\Delta NLS}$. The greater number of genes regulated by $PTHrP^{\Delta NLS\Delta C}$ was mainly made up of 2,283 genes that were uniquely regulated by overexpression of the PTHrP form lacking the C-terminus.

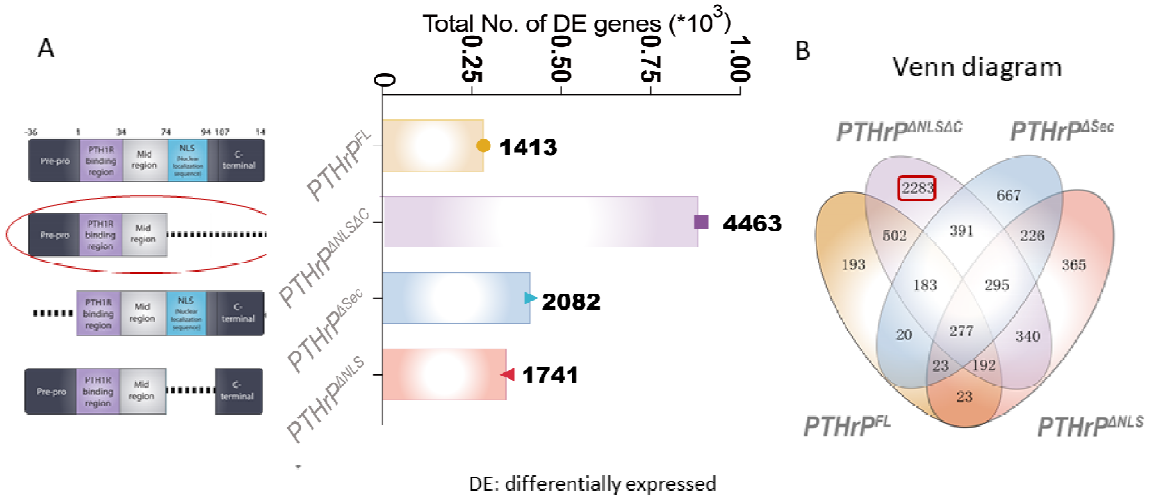

Figure 4.2. Genes regulated by OCY454 cells overexpressing four different forms of PTHrP. (A) The left part of the panel shows the expression constructs aligned with each construct name. The total number of differentially expressed (DE) genes compared to Ocy454 cells expressing vector are shown for each construct. (B) The Venn diagram shows the genes from panel A, and how they overlap between each of the constructs. Numbers in the regions indicate the total number of genes regulated by each cell line, including common and unique genes. The colours used in panel A and B are matched for each of the four OCY454 cell lines.

In summary, the schematic diagram (Fig. 4.3) illustrates the finding that full-length PTHrP expresses approximately 1,400 genes, but there are many more genes that are expressed when both the NLS and C-terminus regions are deleted. This illustrates the hypothesis that the C-terminus reduces the number of regulated genes. Relative numbers of regulated genes are shown for each of three OCY454 cell lines ($PTHrP^{FL}$, $PTHrP^{\Delta NLS\Delta C}$ and $PTHrP^{\Delta NLS}$). The number of black curved lines, representing mRNA molecules, beside each construct indicates that construct's transcript number levels. Comparing $PTHrP^{\Delta NLS\Delta C}$ and $PTHrP^{FL}$, a double deletion of NLS and C-terminus, up-regulates all the gene output. However, a single deletion of the NLS region resulted in a similar number of genes expressed in both $PTHrP^{\Delta NLS}$ and $PTHrP^{FL}$. Since deletion of NLS did not change many DE genes, the increased transcription numbers can be attributed mainly to absence of the PTHrP C-terminus. This also suggests that

the C-terminus domain might limit gene expression response numbers compared to that exerted by full-length PTHrP in OCY454.

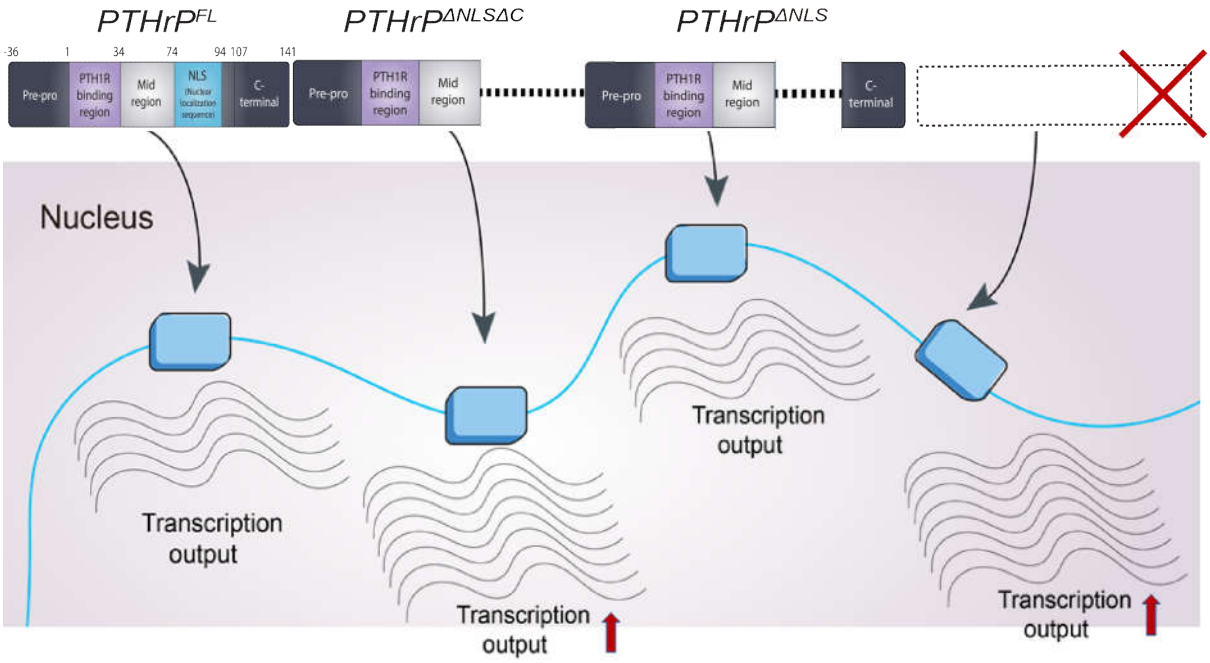

Figure 4.3. IIustration of the theory for deletion of C terminus in increasing the gene regulation numbers. Relative gene transcription output change (regulation number levels) are shown for each of three OCY454 cell lines (*PTHrP*^{FL}, *PTHrP*$^{\Delta NLS\Delta C}$ and *PTHrP*$^{\Delta NLS}$). The number of curved lines (mRNA molecules) next to each construct represents its transcript number levels. Comparing *PTHrP*$^{\Delta NLS\Delta C}$ versus *PTHrP*^{FL}, a double deletion of NLS and C-terminus, up-regulates all the gene output. However, a single deletion of NLS region showed the same gene regulation numbers when comparing the *PTHrP*$^{\Delta NLS}$ versus *PTHrP*^{FL}. Thus, there is evidence for the absence of C-terminus in altering the expression for the entire gene regulatory numbers regulated by *PTHrP*^{FL}.

4.3.2.2 Cells over-expressing PTHrP lacking the C-terminus exhibited more differentially expressed genes compared to control cells than those expressing full-length PTHrP

Next, to determine whether absence of the C-terminus can also limit the magnitude of gene responses from PTH/PTHrP signalling, I plotted the magnitude of change in commonly regulated genes that were regulated by $PTHrP^{FL}$ and the same genes regulated by $PTHrP^{\Delta NLS\Delta C}$. A heatmap (Fig. 4.4A) shows that the majority of these genes are regulated in the same direction by both constructs. I also observed that the proportion of differentially expressed genes shared between $PTHrP^{FL}$ and $PTHrP^{\Delta NLS\Delta C}$ were significantly ($P=0.0008$) regulated, more strongly in $PTHrP^{\Delta NLS\Delta C}$ compared to the $PTHrP^{FL}$ strain, suggesting that deletion of PTHrP-NLS and/or PTHrP C-terminus may have released an indusive effect of these regions of the molecule on gene expression (Fig. 4.4A). Further, this indicates that the NLS or C-terminus (or both together) may inhibit the effects on gene regulation of full-length PTHrP.

When I carried out a similar analysis on the genes commonly regulated by $PTHrP^{FL}$ and $PTHrP^{\Delta NLS}$, genes were also regulated in the same direction when genes with colour codes were plotted on a heatmap. More specifically, a comparison of genes commonly regulated by $PTHrP^{FL}$ and $PTHrP^{\Delta NLS}$ revealed no significant difference ($P=0.5592$), which indicated that the NLS region does not promote this gene regulation phenotype (Fig. 4.4B). This suggests that the deleted C-terminus of PTHrP, rather than NLS region, may have a negative impact on genes regulated through the PTH1R.

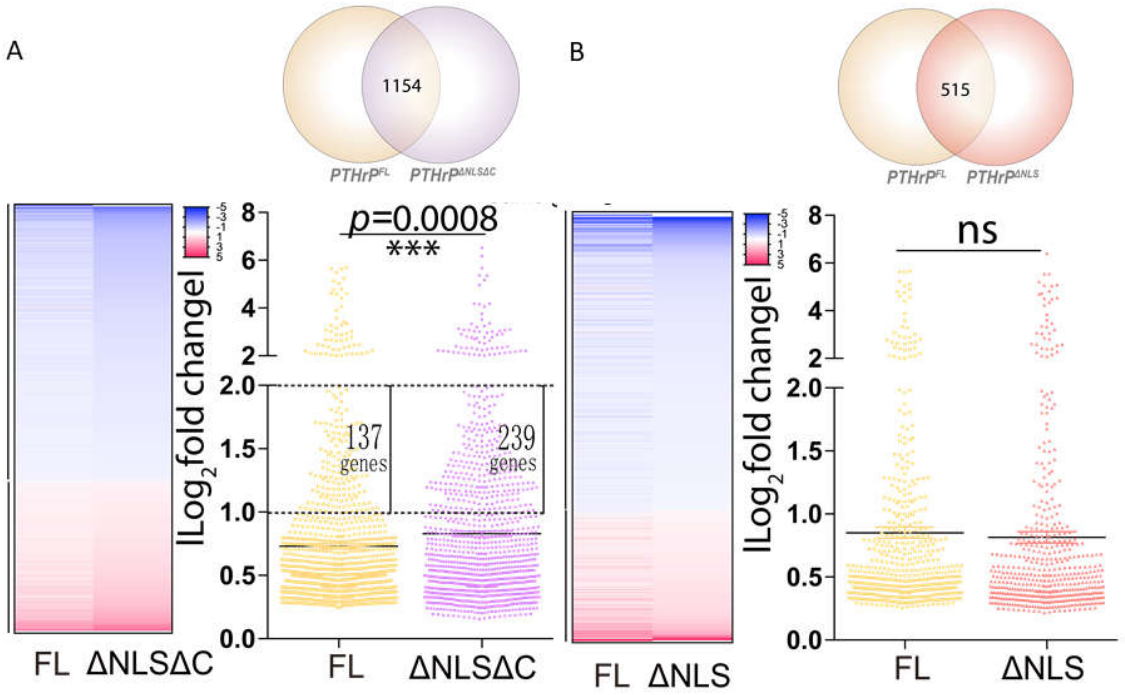

Figure 4.4. Lack of PTHrP C-terminus significantly increases a cohort of genes expression The absolute magnitude of difference in DEGs regulated by both *PTHrP*^{FL} and *PTHrP*$^{\Delta NLS\Delta C}$ (A) condition and by both (B) *FL* and *ΔNLS*. (A)Venn diagram summarising the overlap between DE genes regulated by *FL* (left circle) and DE genes regulated by *1–67 (ΔNLSΔC)* (right circle). 1154 genes called by both cell lines is indicated by the overlap between the two circles. It also contains the numbers of up/down-regulated genes for each set in the Venn-Diagram. Heatmap showing the significance of all of genes commonly regulated between the two groups. Magnitude change of genes that are commonly regulated were compared and plotted. *1–67 (ΔNLSΔC)* exhibited significantly higher gene magnitude changes than *FL*. Graphs = mean ± SEM. n = 1154 replicates. *p < 0.05, ***p < 0.001 by Unpaired Student's T-test. (B) Venn diagram summarising the overlap between DE genes regulated by *FL* (left circle) and DE genes regulated by *ΔNLS* (right circle). 515 genes called by both cell lines is indicated by the overlap between the two circles. Heatmap showing the significance of all of genes commonly regulated between the two groups. Magnitude change of genes that are commonly regulated were compared and plotted. Magnitude change of genes regulated by *ΔNLS* were unaffected than that regulated by *FL*. Graphs = mean ± SEM. n = 515 replicates. *p < 0.05, ***p < 0.001 by Unpaired Student's T-test. ns means not significant (P≥0.1).

To summarise this, the schematic diagram (Fig. 4.5) illustrates that when deleting both NLS and C-terminus regions, common DE genes in $PTHrP^{\Delta NLS\Delta C}$ and $PTHrP^{\Delta NLS}$ are expressed at a higher degree compared to $PTHrP^{FL}$. Since deletion of NLS did not change the level of DE genes, the greater level of genes regulated is attributed to the absence of the C-terminus. This also suggested C-terminus may limit gene expression response magnitude levels compared to that exerted by full-length PTHrP in OCY454 cells.

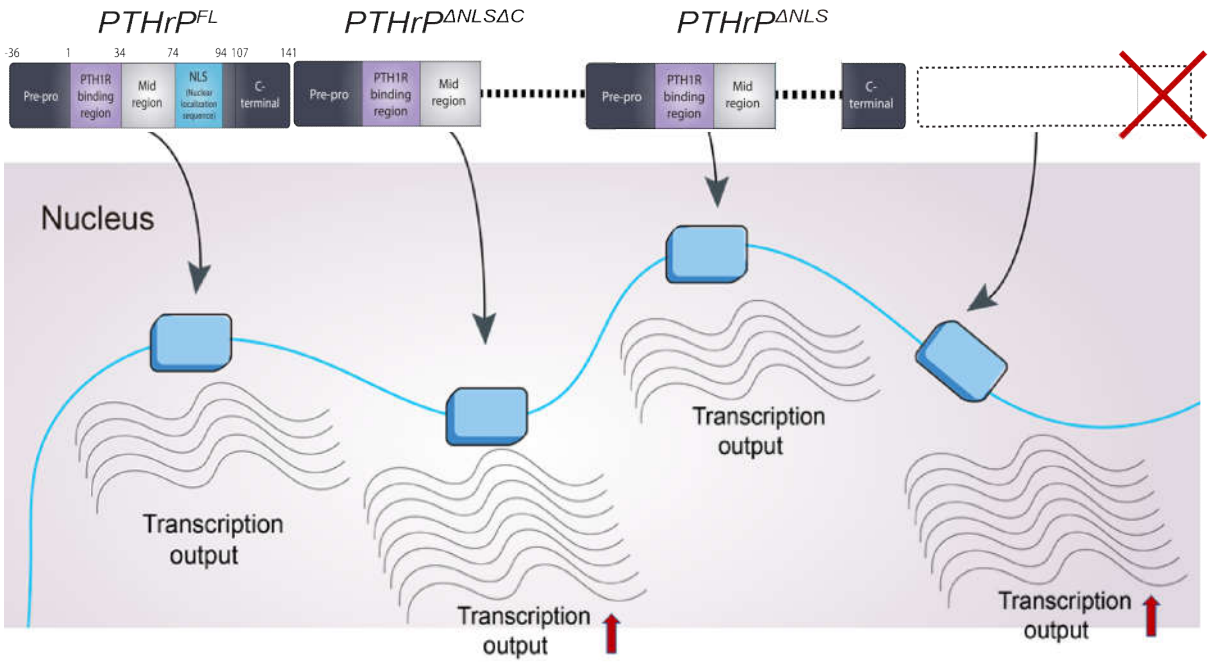

Figure 4.5. IIustration of the theory for deletions of C-terminus in increasing the gene regulation magnitude levels. Relative gene regulation transcript levels are shown for each of three OCY454 cell lines ($PTHrP^{FL}$, $PTHrP^{\Delta NLS\Delta C}$ and $PTHrP^{\Delta NLS}$). The magnitude level of curved lines (mRNA molecules) next to each construct represents its transcript levels. Compairing $PTHrP^{\Delta NLS\Delta C}$ versus $PTHrP^{FL}$, a double deletion of NLS and C-terminus, up-regulates all the gene regulation magnitude changes. However, a single deletion of NLS region showed the same gene regulation levels when comparing the $PTHrP^{\Delta NLS}$ versus $PTHrP^{FL}$. Thus, there is evidence for the absence of C-terminus in up-regulating the expression magnitude change for the entire gene lists regulated by $PTHrP^{FL}$.

I identified the 50 most up- and 50 most down- regulated DE genes induced by deletion of the C-terminus PTHrP in the cells by using the method in section 4.2, defined as C-terminus effect genes. To identify the C-terminus effect genes in the cells, gene expression results were transformed into magnitude change to assess the difference between $PTHrP^{FL}$ and $PTHrP^{\Delta NLS\Delta C}$ expression magnitude (Fig. 4.6). The top 50 genes of down-(A) and top 50 genes of up-(B) regulated with the most variable deleting C-terminus -induced expression were identified by ranking differences of magnitude change in the two cell lines. The top 50 (A) downregulated and (B) upregulated genes with the strongest C-terminus effect are listed in Fig. 4.6.

In making a Venn diagram, I am interested in the intersection of two sets—the gene items are shared between $PTHrP^{FL}$ and $PTHrP^{\Delta NLS\Delta C}$ categories. In this diagram, the area covers a, b, c and d (where $PTHrP^{FL}$ with a yellow circle and $PTHrP^{\Delta NLS\Delta C}$ with a purple circle overlap) represents the intersection of $PTHrP^{FL}$ and $PTHrP^{\Delta NLS\Delta C}$, or $PTHrP^{FL} \cap PTHrP^{\Delta NLS\Delta C}$. These are the genes that regulated by both cells overexpressing full length PTHrP and cells overexpressing PTHrP mutant when NLS and C terminus regions were deleted. As mentioned above, there are 1154 genes that were regulated by $PTHrP^{FL}$, but their gene magnitude changes were significantly increased by $PTHrP^{\Delta NLS\Delta C}$.

	FL Log2fc	ΔNLSΔC Log2fc	FL |Log2fc|	ΔNLSΔC |Log2fc|	Ranked by magnitude difference
4damts18	-3.28121	-5.34691	3.281214	5.346908	2.065695
Myom3	-2.93733	-4.95621	2.937326	4.956208	2.018882
B4galnt3	-3.33951	-5.35809	3.339512	5.358092	2.01858
Rarres1	-0.83615	-2.27611	0.836155	2.276115	1.43996
Mbp	-1.44574	-2.7706	1.445739	2.770602	1.324863
Inhbb	-0.74926	-2.06032	0.749264	2.060323	1.311059
Itih2	-1.48084	-2.74197	1.480841	2.741969	1.261129
Cyp2j9	-1.72755	-2.9156	1.727548	2.915603	1.188055
Enpp1	-0.69191	-1.81471	0.691915	1.814706	1.122791
Sulf1	-0.63891	-1.7509	0.638908	1.7509	1.111992
C3	-1.18502	-2.21449	1.185024	2.214485	1.029461
Srpx	-0.82141	-1.8485	0.821406	1.848502	1.027095
Mamdc2	-0.9293	-1.91209	0.929301	1.912088	0.982786
Il1rl1	-0.70689	-1.65132	0.706891	1.651319	0.944428
Serpina3g	-0.46923	-1.39156	0.469226	1.39156	0.922334
Ly6a	-0.37597	-1.19618	0.375966	1.196183	0.820217
Itgb8	-0.55261	-1.3412	0.552613	1.341196	0.788582
Abca1	-0.75226	-1.53048	0.75226	1.530481	0.778221
Clec2d	-0.45956	-1.22986	0.459558	1.229857	0.770299
Sp140	-0.69206	-1.44153	0.692063	1.44153	0.749467
Clip4	-0.96089	-1.69054	0.960887	1.690545	0.729658
Galnt13	-0.40117	-1.12388	0.401167	1.123881	0.722714
Enpp2	-0.42761	-1.13682	0.427609	1.136824	0.709215
Ptpn3	-0.73731	-1.43819	0.737312	1.438189	0.700877
Ngef	-1.41197	-2.0984	1.411969	2.0984	0.686431
Sfmbt2	-1.07247	-1.7567	1.072472	1.7567	0.684228
Psd3	-0.71059	-1.39259	0.710595	1.392592	0.681997
Cdh13	-0.88064	-1.55607	0.880641	1.556071	0.67543
Ghr	-0.49305	-1.16583	0.493048	1.165832	0.672784
H2-T23	-0.48549	-1.15646	0.485492	1.156455	0.670963
Serpinb8	-0.71847	-1.37946	0.718471	1.379455	0.660985
Ica1	-1.25776	-1.91405	1.257765	1.91405	0.656285
Sgk1	-0.37465	-1.02243	0.374653	1.022427	0.647773
Deptor	-0.6338	-1.27955	0.633796	1.279548	0.645751
Slpi	-2.12895	-2.77147	2.128948	2.771467	0.642519
Cntf	-1.56443	-2.20689	1.56443	2.20689	0.64246
Gas7	-0.93635	-1.57385	0.936346	1.573849	0.637503
Gsdmd	-0.64051	-1.27406	0.64051	1.274061	0.633551
Casp1	-0.86978	-1.49688	0.869779	1.49688	0.627101
Cp	-0.80498	-1.42953	0.804984	1.42953	0.624547
Atp8b1	-1.03123	-1.6482	1.031231	1.648202	0.616971
Pkhd1l1	-1.09671	-1.70765	1.096714	1.707649	0.610935
Styk1	-0.52307	-1.13299	0.523075	1.132992	0.609918
Oaf	-0.57232	-1.17479	0.572321	1.174788	0.602467
Mark1	-0.95749	-1.55829	0.957494	1.558292	0.600799
Wisp2	-0.31823	-0.91226	0.31823	0.91226	0.59403
Ifih1	-0.77579	-1.36873	0.775791	1.368732	0.592941
Nov	-0.43671	-1.02351	0.436709	1.023511	0.586802
Lgr6	-0.72199	-1.3036	0.721992	1.303599	0.581607
Fbn1	-0.58111	-1.16195	0.581111	1.161949	0.580838

	FL Log2fc	ΔNLSΔC Log2fc	FL |Log2fc|	ΔNLSΔC |Log2fc|	Ranked by magnitude difference
Bglap	1.804347	3.004458	1.804347	3.004458	1.200111
Dlx5	0.92467	1.837124	0.92467	1.837124	0.912454
Bglap2	2.033007	2.910902	2.033007	2.910902	0.877895
Chodl	5.649254	6.515089	5.649254	6.515089	0.865835
Sntg1	2.400099	3.239663	2.400099	3.239663	0.839564
Zcchc5	1.963183	2.784264	1.963183	2.784264	0.821081
Atoh8	1.288633	2.106787	1.288633	2.106787	0.818154
Fgfr3	0.785249	1.594015	0.785249	1.594015	0.808766
Gprc5c	0.616078	1.350864	0.616078	1.350864	0.734786
Clec11a	0.50672	1.227545	0.50672	1.227545	0.720824
Plekhg1	1.275648	1.995241	1.275648	1.995241	0.719593
Gdf15	0.627962	1.339658	0.627962	1.339658	0.711696
Col11a1	1.366749	2.059299	1.366749	2.059299	0.69255
Tmem252	0.755464	1.437803	0.755464	1.437803	0.682339
Gm26857	1.484352	2.121018	1.484352	2.121018	0.636666
Asb4	2.355777	2.974622	2.355777	2.974622	0.618845
Ndufa4l2	1.038997	1.654853	1.038997	1.654853	0.615856
Actg2	1.602273	2.211024	1.602273	2.211024	0.608751
Sdc3	0.448614	1.05438	0.448614	1.05438	0.605766
Adamts9	1.034264	1.636688	1.034264	1.636688	0.602424
Eya1	1.318358	1.913313	1.318358	1.913313	0.594954
Wnt4	2.425981	3.006572	2.425981	3.006572	0.580591
Efnb1	0.747072	1.302678	0.747072	1.302678	0.555606
Insc	0.801811	1.353611	0.801811	1.353611	0.5518
Plekha5	0.503614	1.041052	0.503614	1.041052	0.537437
Hcfc1r1	0.423233	0.955809	0.423233	0.955809	0.532576
Rap1gap	0.784027	1.308506	0.784027	1.308506	0.524478
4damtsl3	0.367479	0.881186	0.367479	0.881186	0.513707
Vasn	0.442766	0.954089	0.442766	0.954089	0.511323
Glis3	0.534957	1.041095	0.534957	1.041095	0.506138
Tnfrsf19	1.404431	1.908653	1.404431	1.908653	0.504221
Selenbp1	0.514136	1.014966	0.514136	1.014966	0.50083
3-111G16	0.671448	1.171272	0.671448	1.171272	0.49982
Fat3	0.978443	1.473957	0.978443	1.473957	0.49551
Ctnna2	5.686899	6.174953	5.686899	6.174953	0.48805
Cxcl14	1.36379	1.839061	1.36379	1.839061	0.47527
Thsd4	0.833342	1.308247	0.833342	1.308247	0.47490
Pgm5	0.739712	1.211444	0.739712	1.211444	0.47173
Ptn	1.390806	1.862159	1.390806	1.862159	0.47135
Fgfr2	0.922614	1.393112	0.922614	1.393112	0.47049
Ackr4	1.705467	2.175579	1.705467	2.175579	0.47011
Arvcf	0.486397	0.944083	0.486397	0.944083	0.45768
Kcnk5	0.712486	1.163969	0.712486	1.163969	0.45148
Npnt	2.889252	3.334518	2.889252	3.334518	0.44526
Dlx6	1.045567	1.490037	1.045567	1.490037	0.4444
Thbd	0.340904	0.783775	0.340904	0.783775	0.4428
Plagl1	0.933265	1.365731	0.933265	1.365731	0.43246
Tnn	0.468597	0.893793	0.468597	0.893793	0.42519
S1pr1	0.727561	1.147162	0.727561	1.147162	0.41960
Zfp951	1.050065	1.46356	1.050065	1.46356	0.41349

Figure 4.6. The top 50 (A) downregulated and (B) upregulated genes with strongest C terminal effect. Heatmaps showing the expression of individual genes regulated with the most variable deleting C-terminus -induced expression sorted by the ranking of difference of magnitude change among the two cell lines. The first two columns show *FL* and *1-67* cell lines' original $\log_2$ fold change normalised by pMSCV counts, with the following two columns representing the magnitude changes. Genes are ranked by magnitude differences revealed in the last lane in each form.

4.2.2.3 NLS region is perhaps important for the absence of C-terminus in gene regulatory effect

To determine whether the effect of C-terminus deletion depends on deletion of the NLS, I analysed the magnitude change in genes regulated by both $PTHrP^{FL}$ and $PTHrP^{\Delta NLS\Delta C}$, according to whether they were also regulated by $PTHrP^{\Delta NLS}$, $PTHrP^{\Delta Sec}$, or were unique to $PTHrP^{FL}$ and $PTHrP^{\Delta NLS\Delta C}$. I have analysed the gene magnitude difference within the intersections (labelled with B, C, D, and E) compared between $PTHrP^{FL}$ and $PTHrP^{\Delta NLS\Delta C}$. The intersection of all three (region D, and E), $PTHrP^{FL} \cap PTHrP^{\Delta NLS\Delta C} \cap PTHrP^{\Delta NLS}$, has been represented as D and E, since all three cell lines commonly regulated those genes. The magnitude changes of genes in B, C, D, and E regions were extracted separately and were compared between $PTHrP^{FL}$ and $PTHrP^{\Delta NLS\Delta C}$. Such significant difference were maintained when genes were extracted in both region B and C. However, there were not any difference in comparison of gene in region D, and E when "ΔNLS" condition is shared by region D and E whereas region B and C does not have the "ΔNLS" condition. In another word, the genes in region B and C satisfy $PTHrP^{FL} \cap PTHrP^{\Delta NLS\Delta C}$ conditions, however, the genes in region D and E require a further condition of $PTHrP^{\Delta NLS}$. This suggest "ΔNLS" condition has abolished the difference of gene inhibitory effects. The greater magnitude of gene regulation by $PTHrP^{FL}$ and $PTHrP^{\Delta NLS\Delta C}$ was not observed in those genes that were also regulated by $PTHrP^{\Delta NLS}$ (Figure 4.7). This suggests that the NLS region may be required for the effect of PTHrP C-terminus deletion on gene regulation.

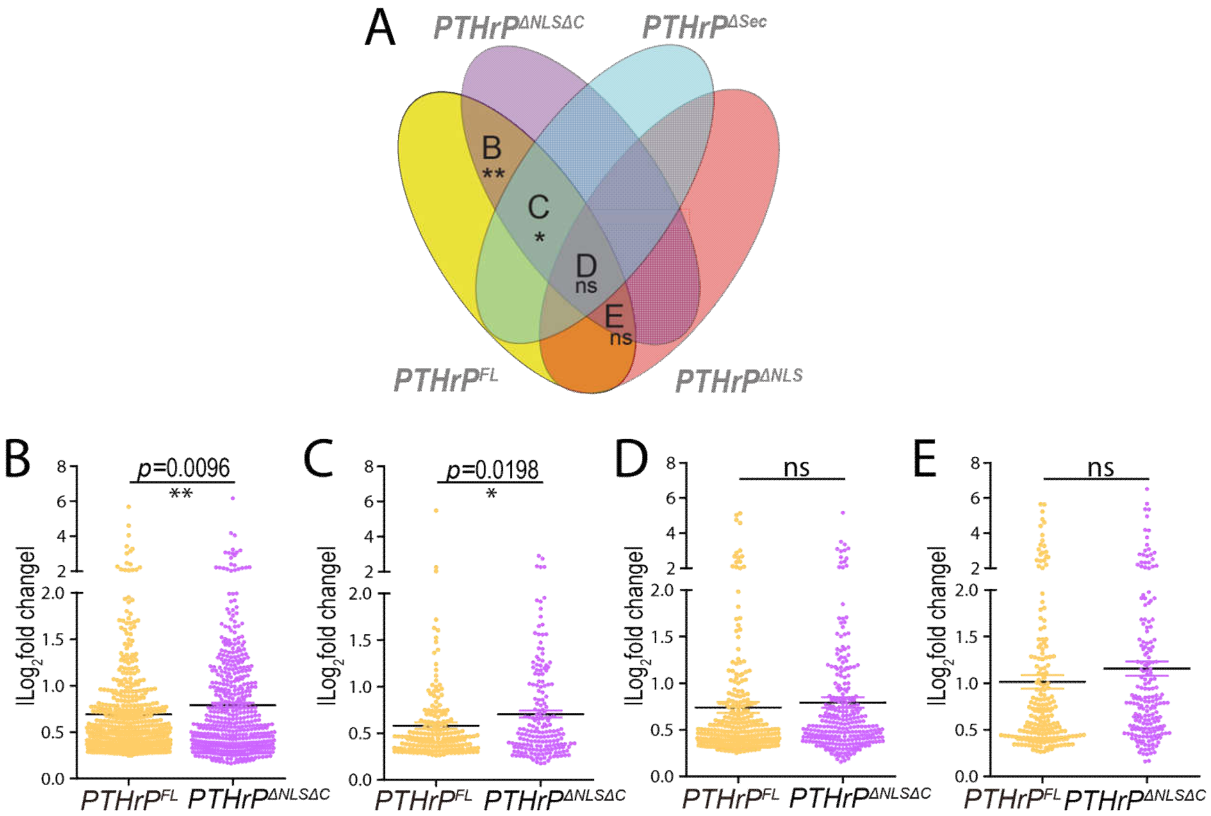

Figure 4.7. NLS region is essential for the absence of C-terminus in gene regulatory effect. (A) B, C, D, and E labelled intersection represent genes commonly regulated by $PTHrP^{FL}$ and $PTHrP^{\Delta NLS\Delta C}$. (B-D) The gene magnitude change comparison between $PTHrP^{FL}$ and $PTHrP^{\Delta NLS\Delta C}$ within in the intersection of region B (Figure B), region C (Figure C), region D (Figure D) and region E (Figure E). Regions D and E mapped in Venn showed genes regulated by cells overexpressing $PTHrP^{\Delta NLS}$, simultaneously overlapped with the intersection of $PTHrP^{FL} \cap PTHrP^{\Delta NLS\Delta C}$. ΔNLS conditions abolished the difference of gene inhibitory effects exerted from the absence of the C-terminus region, indicating that the NLS is perhaps important for the gene regulatory effect. Graphs = mean ± SEM. n = 502, 183, 277 and 192 (from region a, b, c and d separately) replicates. *p < 0.05, ***p < 0.001 by Unpaired Student's T-test. ns means not significant (P≥0.1).

4.2.3 Absence of the C-terminus increases the number of cAMP/CREB genes but not their response magnitude

The cAMP/CREB-responsive genes described in Chapter 3 were screened and compared among the four cell lines. $PTHrP^{\Delta NLS\Delta C}$ regulated many more cAMP/CREB-responsive genes compared to $PTHrP^{FL}$ and $PTHrP^{\Delta NLS}$ (Fig. 4.8A). That is, $PTHrP^{\Delta NLS\Delta C}$ regulated 19 out of 33 CREB-responsive genes whereas the other two forms only regulated seven CREB-responsive genes (Fig. 4.8B). This suggests C-terminus-deficient PTHrP induces more CREB-responsive genes. I also compared the commonly regulated genes that are shared by $PTHrP^{FL}$ and $PTHrP^{\Delta NLS\Delta C}$, however, the commonly regulated gene magnitude changes were not different between $PTHrP^{FL}$ and $PTHrP^{\Delta NLS\Delta C}$ (Fig. 4.8C). The detailed regulation information is listed in Fig. 4.9. This indicates that absence of the C-terminus domain increases the number of responsive of genes in the cAMP/PKA/CREB pathway but not their response magnitude.

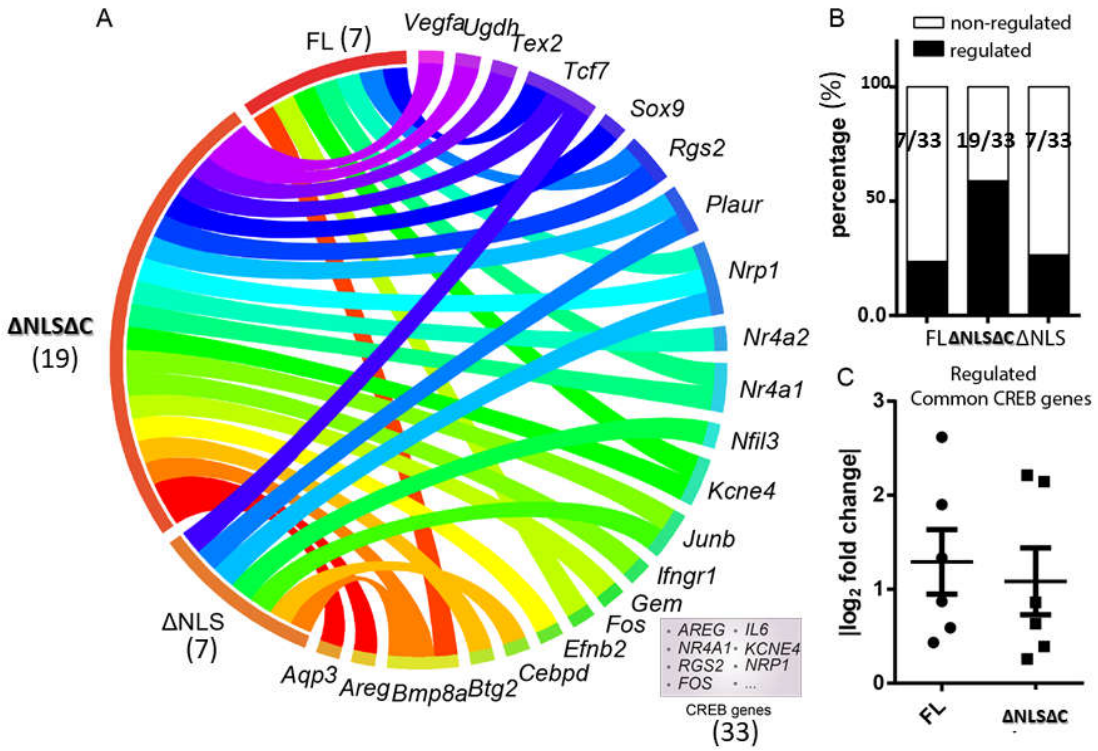

Figure 4.8. Deletion of the C terminus increases the number of cAMP/ CREB genes regulated, but not the magnitude of their response. (A) Circos plot incorporating evaluated 33 cAMP/CREB differential gene expression. (B) Distribution of cAMP/CREB responsive genes among *FL*, *1–67 (ΔNLSΔC)* and *ΔNLS*. *1–67 (ΔNLSΔC)* certainly regulated more genes than the other isoforms. (C) The magnitude change of common regulated genes between *FL* and *1–67(ΔNLSΔC)* was not significantly altered. Graphs = mean ± SEM. n = 7 replicates. *p < 0.05, ***p < 0.001 by Unpaired Student's T-test. ns means not significant (P≥0.1).

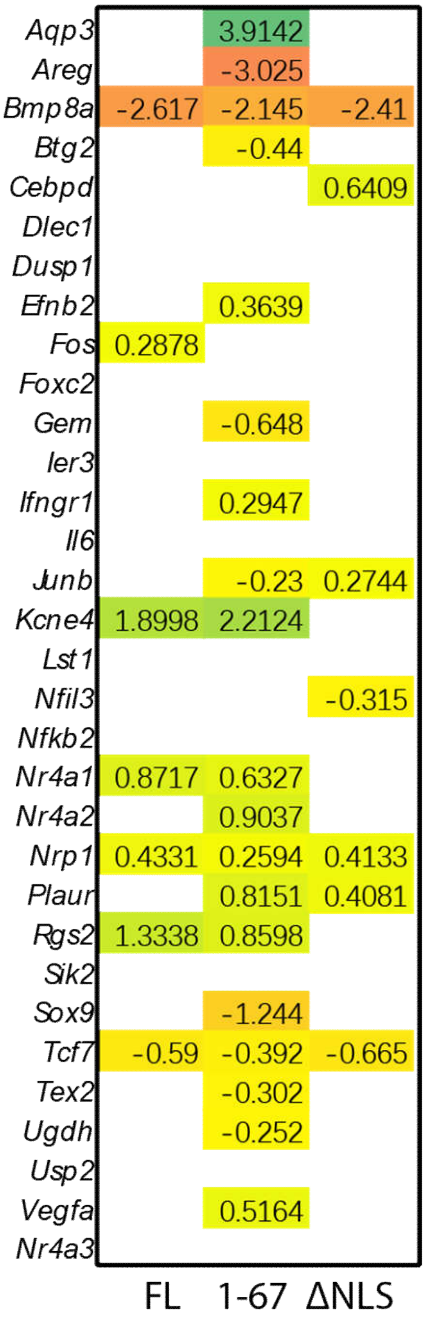

Figure 4.9. Heatmap showing CREB-responsive genes transcription levels detected in RNA-Seq among *FL*, *1–67(ΔNLSΔC)* and *ΔNLS*. Genes with Log_2fc normalised by vector control cells have been listed in the heatmap.

4.3 Identifying OCY454 *PTHrP$^{\Delta Sec}$* as a model for unveiling PTHrP receptor-independent pathways

4.3.1 Identifying differences in gene expression between OCY454 cells expressing different forms of PTHrP

In this section, I have used the OCY454 system as a model to further explore the mechanism of action through which PTHrP uses non-receptor mediated pathways. I was interested in defining the signal peptide deletion mutants *PTHrP$^{\Delta Sec}$* that have the desirable propery of being unable to exit the cell via the secretory pathway, to examine the intracellular signalling. When compared by heatmap, cell lines overexpressing the secreted PTHrP isoforms (*PTHrP^{FL}*, *PTHrP$^{\Delta NLS}$* and *PTHrP$^{\Delta NLS\Delta C}$*) appeared to modify gene expression in similar ways (277 commonly regulated genes are shown in the heat map in Fig. 4.10A). Twenty-six out of 277 genes including *Pth1r* have been identified to be regulated in the same directions in all the secreted forms but regulated in the opposite direction in *PTHrP$^{\Delta Sec}$* (Fig. 4.10B). I have carried out STRING analysis based on these 277 genes and found five genes were PTH1R associated (*Pth1r*, *Ibsp*, *Thfrsf11b*, *Itg10,* and *Mmp13*) and four of them have the same regulation direction in secreted PTHrP cell lines but not in *PTHrP$^{\Delta Sec}$*. These four PTH1R related transcriptomes have been plotted in Fig. 4.10C. This shows that the OCY454 cells overexpressing secreted PTHrP and the non-secretive mutant *PTHrP$^{\Delta Sec}$* have two distinct patterns of gene expression.

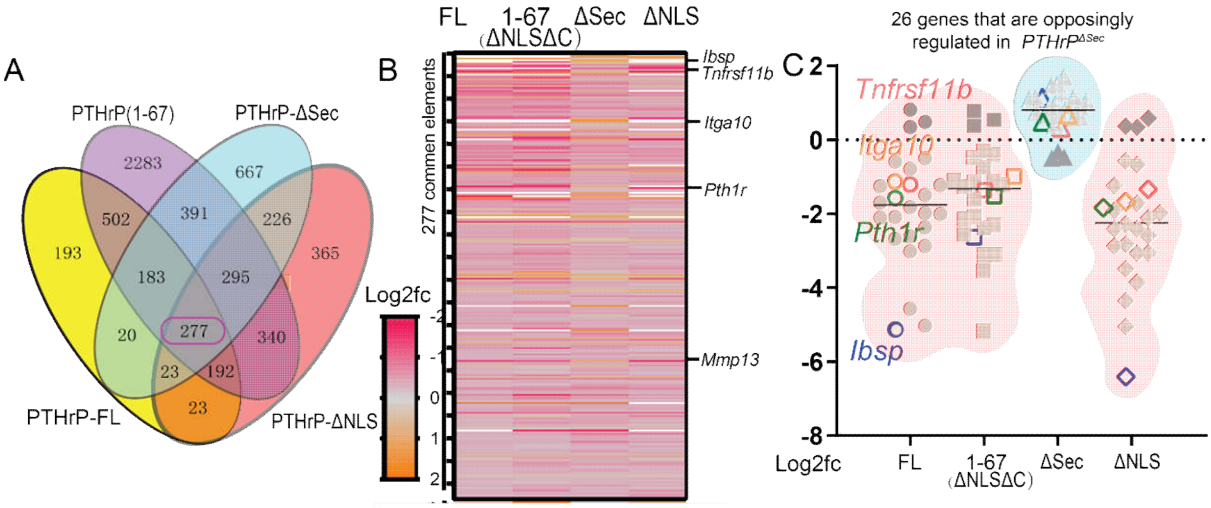

Figure 4.10. PTH1R signalling was not modified by the ΔSec form and *OCY454$^{\Delta Sec}$* did not act through PTH1R (A) Venn diagram to present global comparison of gene expression by OCY454 cell lines overexpressing *PTHrP^{FL}*, *PTHrP(1-67)*(*PTHrP$^{\Delta NLS\Delta C}$*), *PTHrP$^{\Delta Sec}$* and *PTHrP$^{\Delta\ NLS}$*, depicting unique and common DEGs (FDR<0.05). The 667 genes uniquely regulated by non-secreted form of PTHrP represent genes modified exclusively through intracellular pathways. (B) The proportion of elements (277 cluster) shared among the 3 secreted PTHrP strains represent genes influenced through actions via PTH1R. *Ibsp*, *Tnfrsf11b*, *Itg10*, *Pth1r* and *Mmp13* are known to be PTH1R related genes suggested by STRING analysis when 277 genes were regarded as input. (C) The secreted PTHrP(*PTHrP^{FL}*, PTHrP$^{\Delta NLS\Delta C}$ and *PTHrP$^{\Delta\ NLS}$*) have two distinct patterns of gene expression by clustering analysis. Five known PTH1R related transcriptomes are highlighted.

4.3.2 OCY454 cells overexpressing *PTHrP*$^{\Delta Sec}$ showed accumulated PTHrP inside the nucleus

When cells were examined by confocal immunofluorescence for PTHrP using an antibody targeted to PTHrP C-terminus, cells bearing the pMSCV vector control showed very faint staining in both nucleus and cytoplasm (Fig. 4.11A), whereas there is intense positive nuclear staining in *PTHrP*$^{\Delta Sec}$. *PTHrP*$^{\Delta Sec}$ was mainly presented and accumulated greatly in the nuclei while *PTHrP*^{FL} appeared mainly in the cytoplasm. Cells bearing the vector constructs showed less punctate staining than those with *PTHrP*^{FL}.

The confocal result was consistent with the GO analysis (Section 2.5.5) of the 667 genes uniquely regulated by *PTHrP*$^{\Delta Sec}$, which showed highest levels of regulation in nuclear, nucleoplasmic, nucleolus, cytoplasmic, and intracellular GO items (Fig. 4.11B); the first three of which are nucleus-associated.

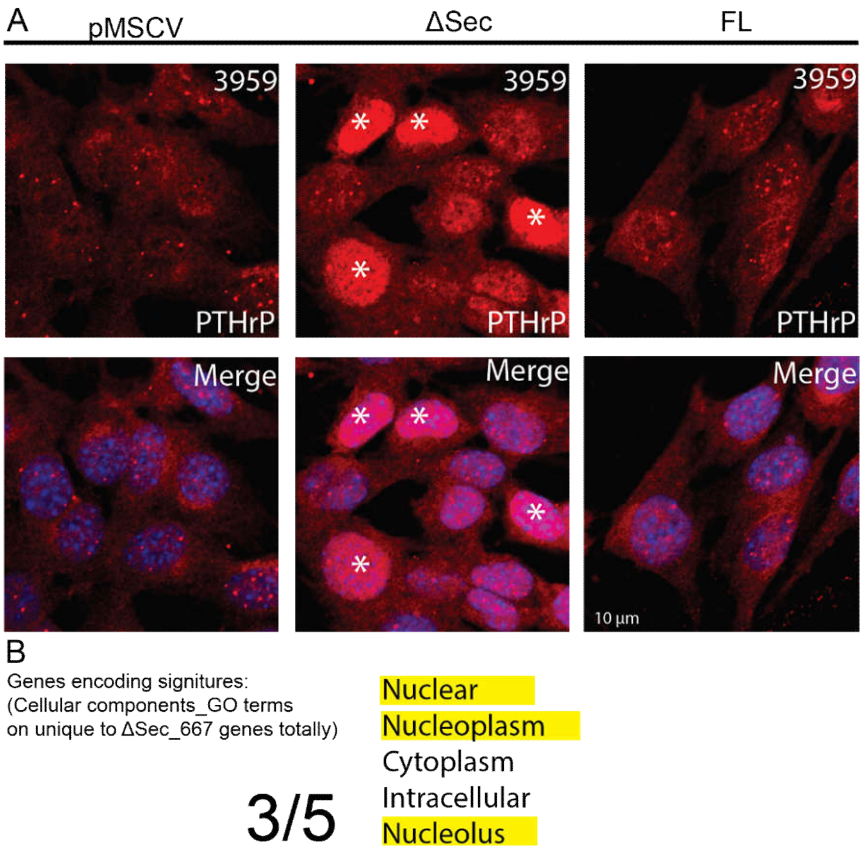

Figure 4.11. OCY454 cells overexpressing the non-secreted form of PTHrP showed large accumulations of PTHrP inside the nucleus. (A) Confocal images of OCY454 cells showing subcellular accumulation of PTHrP in the absence of secretion region and presence of full length PTHrP. Stars point to the nucleus in most panels. (A) PTHrP transfected cells show fluorescence in the cytoplasm and nucleus. *PTHrP*$^{\Delta Sec}$ infected cells show fluorescence in nucleus and perinuclear aggregate. (B) Annotate functions of GO enrichment analysis on proteins encoded by 667 transcripts uniquely regulated by the "non-secreted PTHrP" cell lines are enriched in cellular components associated with nucleus mostly. Bars in all images represent 10 µm.

Because of the high level of nuclear expression of *PTHrP*$^{\Delta Sec}$, I then focused on a Kyoto Encyclopedia of Genes and Genomes (KEGG; Kanehisa, Goto *et al*. 2009) analysis to identify what may be occurring based on all genes regulated by *PTHrP*$^{\Delta Sec}$. KEGG is a database that integrates genomic chemical and systemic functional information. Using this method (see Section 2.5.5) it revealed that *PTHrP*$^{\Delta Sec}$ had differently regulated expression of genes in five major pathways: Protein processing in endoplasmic reticulum, Ubiquitin mediated proteolysis, PI3K-Akt signalling pathway, Focal adhesion, and Central carbon metabolism in cancer (Fig. 4.9A). Using KEGG means clustering algorithm in Cytoscape software (Kohl, Wiese *et al*. 2011; Section 2.5.5) functional clusters were generated. Genes regulated in *PTHrP*$^{\Delta Sec}$ can be grouped and are associated with thiol-dependent ubiquitin-specific protease activity, ubiquitin-like protein binding, steroid hormone receptor activity, and amino acid transmembrane transporter activity based on the molecular function annotations in DAVID (Huang, Sherman *et al*. 2009, Fig. 4.9B). The results indicated that OCY454 *PTHrP*$^{\Delta Sec}$ contains abundant mRNAs encoding classes of ubiquitin-associated pathways. Further, the molecular function (MF) and biological process (BP) terms that include “ubiquitination” or “ubiquitin” labels were over-represented in an Alluvial Diagram with the transcripts contributing to the functional annotation (Fig. 4.9C). Using a Venn diagram (Section 2.5.5), some ubiquitination-associated genes were also regulated by the other constructs (Fig. 4.9D). Thus, there appears to be a ubiquitin-associated regulation signalling pathway for *PTHrP*$^{\Delta Sec}$.

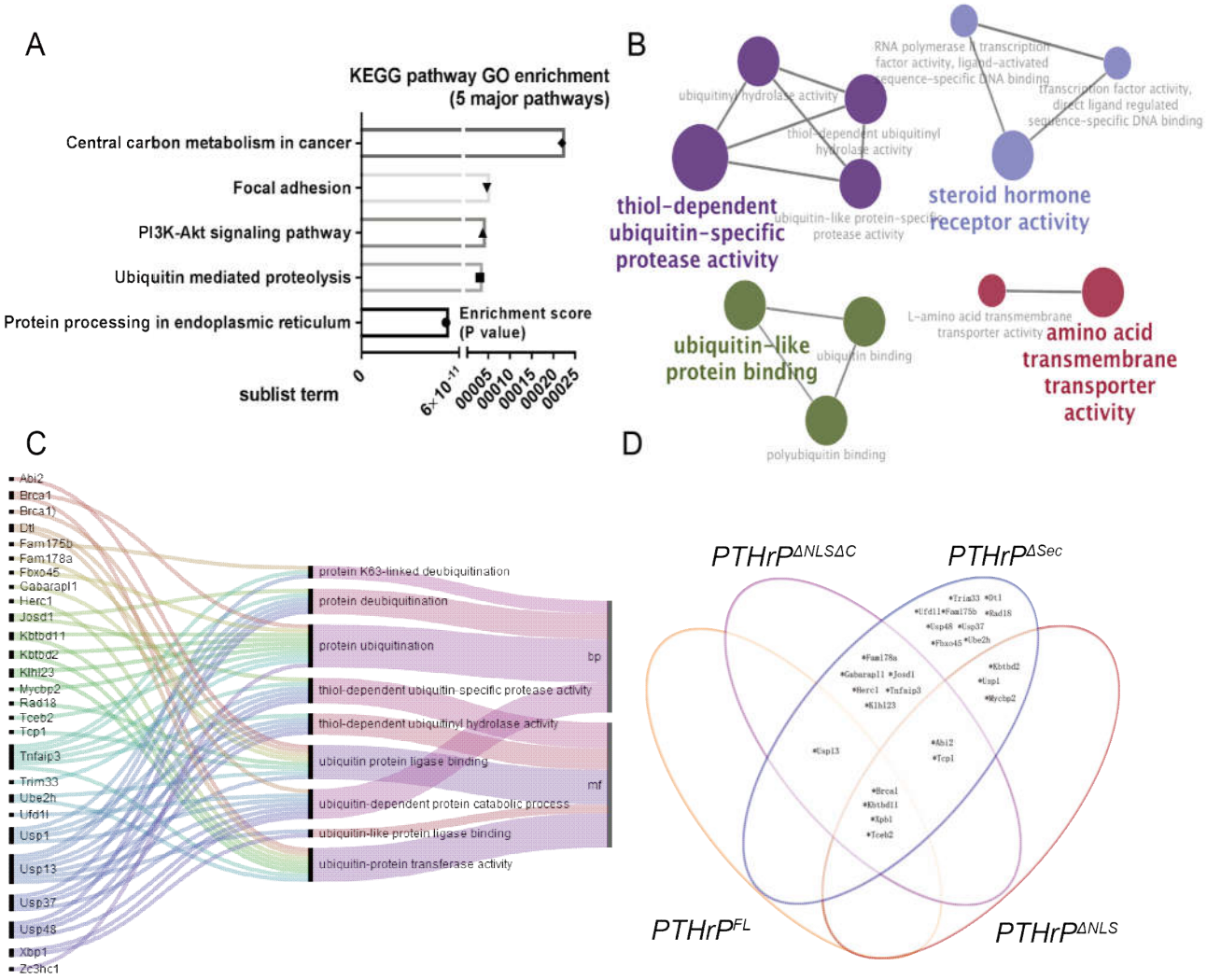

Figure 4.12. Gene-enrichment analysis result of *PTHrP$^{\Delta Sec}$* (A) Top 5 statistically enriched KEGG pathway (DAVID). (B) Representative biomolecular function enrichment against enrichment against KEGG database. (C) Alluvial diagram illustrating the GO (mf: molecular functions; bp: biological process) terms that include "ubquitination" or "ubiquitin" based on DAVID functional annotation. (D) Distribution of ubiquitin related genes in different conditions.

My analysis also showed that genes encoding clusters of proteins including E3 enzymes *Herc1* (Chong-Kopera, Inoki *et al*. 2006) and *Trim33* (Meroni and Diez‐Roux 2005), K family proteins (Dhanoa, Cogliati *et al*. 2013, Shibata, Zhang *et al*. 2013) *Kbtb11*, *Kbtbd2*, *Kctd9*, *Klhdc1,* and *Klhl23* coupled with deubiquitinating enzymes (DUBs), *Josd1* (Seki, Gong *et al*. 2013), *Usp1* (García-Santisteban, Peters *et al*. 2013), *Usp12* (Moretti, Chastagner *et al*. 2012), *Usp37* (Tanno, Shigematsu *et al*. 2014), and *Usp48 (*Uckelmann, Densham *et al*. 2018) that trigger ubiquitin proteolysis are downregulated by *PTHrP*$^{\Delta Sec}$ (Fig. 4.10). These genes were detected at a significant level in my RNA-Seq profile, indicating that these genes regulated by *PTHrP*$^{\Delta Sec}$ may be required for cells to degrade proteins in OCY454 osteocytes. This also suggested that protein degradation pathway has been repressed and proteins cannot be degraded via ubiquitination pathway due to the deletion of the secretion region.

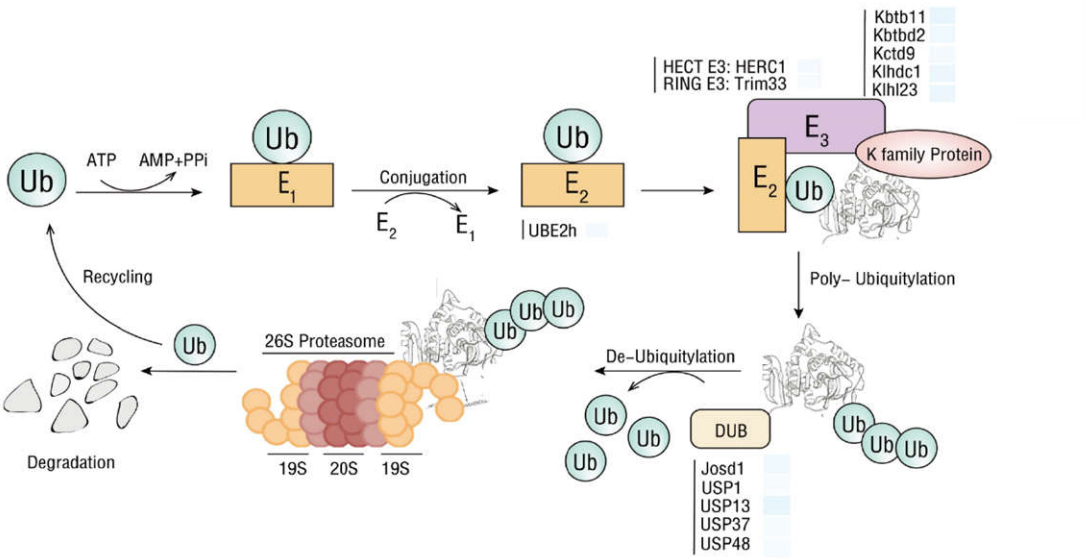

Figure 4.13. Proposed the ubiquitin protein degradation system identified by RNA-Seq data mapped with assigned genes. Schematic illustration of the ubiquitin proteasome pathway with DE genes at OCY454 *PTHrP*$^{\Delta Sec}$. Gene symbols are listed in heatmap and grouped in conditions. Blue code represents the genes that to be down regulated.

4.4 Discussion

In the present study, using osteocytes engineered to express PTHrP of differing lengths, I have shown that gene expression in response to N-terminal PTHrP overexpression is more strongly induced in the absence of the PTHrP C-terminal domain. RNA-Seq combined with multiple bioinformatic software analyses revealed that absence of the PTHrP C-terminus more strongly regulates gene expression in both absolute number and magnitude in OCY454 osteocytes compared to cells overexpressing PTHrP containing the C-terminus. This suggests the PTHrP C-terminus may limit gene expression induced by PTHrP signalling.

C-terminus deletion induced more pronounced increases and decreases, in both absolute and relative terms, in a cohort of genes, compared to those targeted by full-length PTHrP overexpression. However, NLS deficiency did not result in any significant differences. Those genes regulated by full-length PTHrP were selectively regulated more strongly in cells overexpressing C-terminus deficient PTHrP.

There are a number of studies of actions of exogenous C-terminus in gene regulation, but no endogenous effect of C-terminus has ever been described. A report has shown that exogenous C-terminus treatment stimulated Ca^{2+}signalling more strongly than PTHrP(1–36) in rat osteoblastic osteosarcoma UMR106 cells (ValÍn, Guillén *et al*. 2001). Increased *Il6* and *Fos* messenger RNA, markers of PKA activity induced by PTHrP(1–36), were inhibited when cells were preincubated with PTHrP(107–139). However, such gene expression was not affected when cells were treated with a PKA inhibitor, indicating that stimulation of intracellular Ca^{2+} on induction of *Il6* and *Fos* by exogenous C-terminus is not dependent on PTH1R receptor signalling through cAMP (ValÍn, Guillén *et al*. 2001). Another research group, Lozano *et. al* found that exposure of the osteoblastic cell line MC3T3-E1 to PTHrP

C-terminus stimulated gene expression of osteoblast differentiation markers, such as Runt-related transcription factor 2 (*Runx2)*, Bone gamma-carboxyglutamate protein (*Bglap*) and Osterix (*Sp7,* Lozano, Fernández‐de‐Castro *et al*. 2011). Such effects were not observed when cells were subjected to C-terminus antiserum, suggesting these are mediated by exogenous C-terminal PTHrP. Overall, these pharmacological experiments could suggest exogenous PTHrP C-terminus exerts intracellular effects on gene expression, but they do not provide evidence of a physiological role for PTHrP C-terminus. No effects of intracellular endogenous C-terminus on gene regulation have been described. The identification of endogenous C-terminus functions from my bioinformatic analysis are important because this is the first time that any endogenous C-terminus function has been described. Gene expression affected by absence of the C-terminus needs to be further validated by various experiments, such as detection of gene suppression in cells overexpressing the C-terminus, using qPCR.

Given that absence of the C-terminus significantly increased the expression level of a cohort of genes, the PTHrP C-terminus may act as a negative regulatory domain against full-length PTHrP, targeting more than one transcriptional substrate. In this way, PTHrP C-terminal may normally antagonise signalling in response to full-length PTHrP. This will be investigated in the next chapter.

Despite the evidence that PTHrP C-terminus can act as a negative regulatory domain against full-length PTHrP in gene targeting, no such effects were found in comparing data between $PTHrP^{\Delta NLS}$ and $PTHrP^{FL}$ overexpressing cells. This indicates that absence of the NLS region alone does not alter expression of PTHrP-induced genes. However, while comparing the magnitude of changes in subgroups among the genes commonly regulated by $PTHrP^{FL}$ and $PTHrP^{\Delta NLS\Delta C}$, I noted that the presence of ΔNLS cancelled out the effect of C-terminus

deletion. This raises the possibility that the C-terminus effect is dependent on the NLS region. This suggests an interaction between the NLS region and the C-terminus region. It is possible that the C-terminus may be transported to and exert its effects in the nucleus. It remains to be determined whether C-terminus' role in regulating gene expression is dependent on the absence of NLS, and this begins to be investigated in the next chapter.

Each of the secreted PTHrP isoforms, but not $PTHrP^{\Delta Sec}$, regulated mRNA of target genes known to be regulated through the cAMP/PKA pathway in OCY454 cells, validating earlier qPCR results in the cases of *Pth1r*, *Tnfsf11*, *Tnfrsf11b*, *Bglap1*, *Nr4a1*, and *Rgs2* (Ansari, Ho *et al*. 2018). This finding fulfils my prediction that the cells expressing a non-secreted form of PTHrP do not participate in PTH1R receptor-mediated actions in the cAMP pathway. The OCY454 cells secreted PTHrP which was tested in the cell culture medium by using a PTHrP cAMP bioassay. However, Ocy454 cells expressing $PTHrP^{\Delta Sec}$ did not produce any detectable bioactivity of PTHrP. This is consistent with García-Martín *et al.* (2014) who used another osteoblastic cell line, MC3T3-E1, to demonstrate that deletion of the PTHrP secretory region impaired PTHrP secretion process (Garcia-Martin, Ardura *et al*. 2014). Moreover, in that earlier study, PTH1R remained inactive on the cell membrane of osteoblastic MC3T3-E1 when cells overexpressed the non-secreted form of PTHrP (Garcia-Martin, Ardura *et al.* 2014). All these observations confirm that without the PTHrP secretory region, osteoblast and osteocyte-like cells are unable to secrete PTHrP and their PTH1R remains inactivated because of the lack of ligand.

I demonstrated by immunostaining that $PTHrP^{\Delta Sec}$ isoforms accumulated within the nucleus. There was an intense positive nuclear staining in $PTHrP^{\Delta Sec}$ while $PTHrP^{FL}$ appeared mainly in the cytoplasm. This suggests that without PTHrP secretion region/signal domain, $PTHrP^{\Delta Sec}$ isoforms promote a great nuclei transport rather than secretion or targeting cytoplasm. The

PTHrP secretion region/signal domain allows translocation into the endoplasmic reticulum (ER) in the cytoplasm where it can be cleaved for secretion (Nguyen, He *et al.* 2001). The alternative initiation of translation within this region from one of the four alternate start sites of PTHrP mRNA has been demonstrated to result in defective ER targeting (Nguyen, He *et al.* 2001). Subsequent study confirmed that transcription from these alternate start sites leads to lower levels of PTHrP protein in the cytoplasm or ER targeting but improves the trafficking capacity of PTHrP to the nucleus (Amaya, Nakai *et al.* 2015). Amizuka *et al*. suggest that it appeared that when translation started from CUGs, PTHrP largely translocated to the nucleus, however, when translation began with AUGs, it localised in both the Golgi apparatus and the nucleus (Amizuka, Oda *et al.* 2002). The shift initiating from AUG and CUG clearly makes a difference in subcellular localisation of PTHrP. These results are consistent with mine, and I have shown that the deletion of secretion region leads to greater levels of $PTHrP^{\Delta Sec}$ localisation in nuclei than other subcellular localisations. This indicates that deletion of the secretory region of PTHrP stimulates PTHrP to escape the requirement for intracellular translocation into the ER, where it can be cleaved for secretion.

However, the biological importance of the secretion region and its role in affecting pathways for intracellular trafficking and nuclear localisation remain to be explained. Two pathways are associated with nuclear localisation of PTHrP: translocation of PTHrP through the nuclear pore complex in which the NLS region interacts with other factors, or internalisation of PTHrP-PTH1R complex due to endocytosis (Soki, Park *et al.* 2012). PTHrP NLS domain was confirmed and defined as contained within residues 67–94 of PTHrP based on its ability to interact with karyophillic importin proteins (importins) and the nuclear pore complex (Lam, Briggs *et al*. 1999, Lam, Thomas *et al*. 2000) but other residues were suggested by others to contribute to nuclear import (Henderson, Amizuka *et al*. 1995). Cingolani *et al.* (2002) undertook a co-crystallisation of PTHrP with importin-β to identify the fragment that was

capable of recognising importin-β, and this resulted in identification of specific PTHrP (67–94) that interacts with importin-β. PTHrP NLS region binds importin-β directly but not importin-α, which suggests that PTHrP is directly transported into the nucleus in an importin β mediated manner (Lam, Briggs *et al*. 1999, Zhang, Li *et al*. 2019). Whether the great levels of $PTHrP^{\Delta Sec}$ localisation in nuclei induced by deletion of PTHrP secretion region is mediated by an importin β mediated manner remains unknown. It also has been hypothesised that nuclear PTHrP localisation increased survival of chondrocytes under conditions that promote apoptotic cell death (Janet, Norio *et al*. 1995). However, how this localisation may modulate programmed cell death remain to be defined. Further to this, nuclear PTHrP localisation has been suggested to promote vascular smooth muscle cell proliferation (Massfelder, Dann *et al.* 1997, De Miguel, Fiaschi-Taesch *et al.* 2001). Since there have been no reports on the PTHrP nuclei localisation in osteocytes, it might be useful to know whether the nuclear translocation induced by deletion of the secretion region would also drive an increase in osteocyte cell survival.

Bioinformatics analysis showed that a cohort of genes encoding clusters of proteins that trigger ubiquitin proteolysis were downregulated in cells overexpressing $PTHrP^{\Delta Sec}$, indicating protein degradation has been repressed by loss of the secretory region. This result is consistent with that $PTHrP^{\Delta Sec}$ isoforms accumulated within the nucleus by immunostaining observation. However, the mechanism for the phenomenon is yet to be demonstrated. PTHrP can be ubiquitinated and serves as a substrate for proteasome degradation (Meerovitch, Wing *et al.* 1997, Meerovitch, Wing *et al.* 1998). This suggests the proteasome inhibitor can interfere with the degradation, which causes accumulation of PTHrP. It is plausible that the ubiquitin-dependent proteolytic pathway is associated with regulation of the metabolic trafficking of cytosolic PTHrP and that ubiquitin components ligating to PTHrP are a requirement for its degradation. Failure of ubiquitin-dependent

protein degradation may contribute to accumulation of *PTHrP*$^{\Delta Sec}$. When the PTHrP secretion region was truncated, the proteins were not able to be secreted or degraded. No further investigation was performed to address this process in this project because of my concern that the very great abundance of PTHrP nuclear protein does not represent any likely normal PTHrP function.

4.5 Future directions and Conclusion

The most significant effect that I observed is the increased regulation (in both number and magnitude) of PTH1R-associated genes by deletion of the PTHrP C-terminus. This implies that the C-terminus has a function in limiting gene expression that is regulated through PTH1R. This will be investigated in the next chapter.

Chapter 5: Activation by PTHrP in the osteocyte is profoundly inhibited by the PTHrP C-terminal domain.

5.1 Introduction

The PTHrP C-terminal region (107–139, Fig.1B) has been proposed to exist as a separate circulating peptide that cleaved off by prohormone thiol protease (PTP) in lung cancer cells (Hook, Burton *et al.* 2001). Fenton *et al.* (1991) were the first suggest that the native C-terminus may be important in bone because it exogenously inhibited osteoclast-mediated bone resorption by directly interacting with osteoclasts. However, no receptors have yet been identified.

A number of *in vitro* studies revealed actions of C-terminal PTHrP associated with human osteoblastic cells survival by activating specific pathways (Alonso, De Gortazar *et al.* 2008, García‐Martín, Acitores *et al.* 2013). However, no endogenous C-terminus effects have been clearly clarified and no functional characterisation has been performed to determine the relationship between C-terminus and PTH/PTHrP signalling. In addition, the actions of PTHrP on osteoblasts, osteocytes are understood to occur primarily through PTH1R and the cAMP/CREB signalling (Yavropoulou, Michopoulos *et al*. 2017). In this chapter, my primary aim is to determine whether the C terminal limits PTH/PTHrP signalling and whether this is mediated through PTH1R/cAMP-dependent pathways.

To clarify whether PTHrP C terminus might exert its effects by limiting the extent of effects on gene expressions, two C-terminus constructs were established and transfected into UMR106.01 cells. Then I chose to focus on one example to look further into the gene suppression phenotype by C-terminus. By working out the genes with the most variable expression following deletion of C-terminus in the cells, *Bglap* family genes which were known to have multi-functions in osteoblast and osteocyte, were selected for further study.

Here I have shown that *Bglap* mRNA was reduced in the cells overexpressing the C terminus, measured by qPCR in the UMR 106.01 cells under the treatment of PTHrP(1-141) or PTH(1-34). Based on multiple assays combined with bioinformatic analysis, my results suggested *Bglap* gene expression is up-regulated by deleting of PTHrP C-terminus without any dependence on differentiation in OCY454 osteocytes. Further analysis showed that the decrease in *Bglap* expression via C-terminus in UMR106.01 cells is not through upstream mechanistic overlap with cAMP/PKA signalling. Moreover, it is potentially that the *Bglap* suppression by the C terminal is dependent on the induction of Wnt signalling.

5.2 Methods

I first set out to confirm *Bglap1/2* family genes are the most significantly differentially expressed genes between OCY454 $PTHrP^{\Delta NLS\Delta C}$ and $PTHrP^{FL}$ (see methods in Section 2.10.5). To examine whether a lack of exogenous PTHrP C-terminus influences *Bglap* expression, I compared *Bglap* transcription in OCY454 wild-type cells treated with hPTHrP(1–141) to hPTHrP(1–84) (see methods in Section 2.5.2). Importantly, the effect of C-terminal PTHrP expression on *Bglap* regulation by PTH/PTHrP was determined in UMR106.01 cells stably overexpressing PTHrP(107–141) (UMR $PTHrP^{107\text{-}141}$) and PTHrP 68–141 (UMR $PTHrP^{68\text{-}141}$), which were established (see methods in Section 2.4.6), seeded, and analysed by qPCR for *Bglap* mRNA (Section 2.5.3). *Bglap* is not regulated by phosphorylated Runx2 binding to the OSE2 cis-regulatory elements, determined by using reporter genes carrying OG2-OSE2 elements (methods see Section 2.7). UMR106.01 cells were seeded and CREB genes were analysed (Section 2.5.4). I use cAMP assay (Section 2.6.1), qPCR (Section 2.9.2) and western blot (Section 2.11) to check CREB responsive gene alterations, and CREB phosphorylation, respectively, in response to exogenous PTHrP treatment in cells overexpressing the C-terminus. Top flash-luciferase assay (methods see Section 2.7), analysis on Wnt target genes by qPCR (Section 2.9.2) combined with bioinformatic analysis (Section

2.10) were used to determine that the reduction of *Bglap* targeted by PTH/PTHrP might be dependent on Wnt signalling.

5.3 OCY454 cells overexpressing PTHrP(1-67) induce greater levels of *Osteocalcin (Bglap1/2)*

5.3.1 *Bglap1/2* family genes were identified as the most significantly differentially expressed genes between OCY454 $PTHrP^{\Delta NLS\Delta C}$ and $PTHrP^{FL}$

In the last chapter, I have identified the top 50 up- and the top 50 down- regulated genes resulting from C-terminus-induced expression in the cells, termed "C-terminus effect genes". To further address the roles of the C-terminus, I have compared and plotted the magnitude change differences of these genes. The top 50 downregulated (Fig. 5.1A) and top 50 upregulated (Fig. 5.1B) genes were regulated to a greater extent (induced to a level ~ one fold greater) in $PTHrP^{\Delta NLS\Delta C}$ compared with the common genes in $PTHrP^{FL}$. It is noted that *Bglap* family genes (containing *Bglap1* and *Bglap2*) were identified as the most significantly differentially expressed up-regulated genes (see the last chapter, Fig. 4.6) between OCY454 $PTHrP^{\Delta NLS\Delta C}$ and $PTHrP^{FL}$ when comparing the magnitude changes of common genes between these two groups.

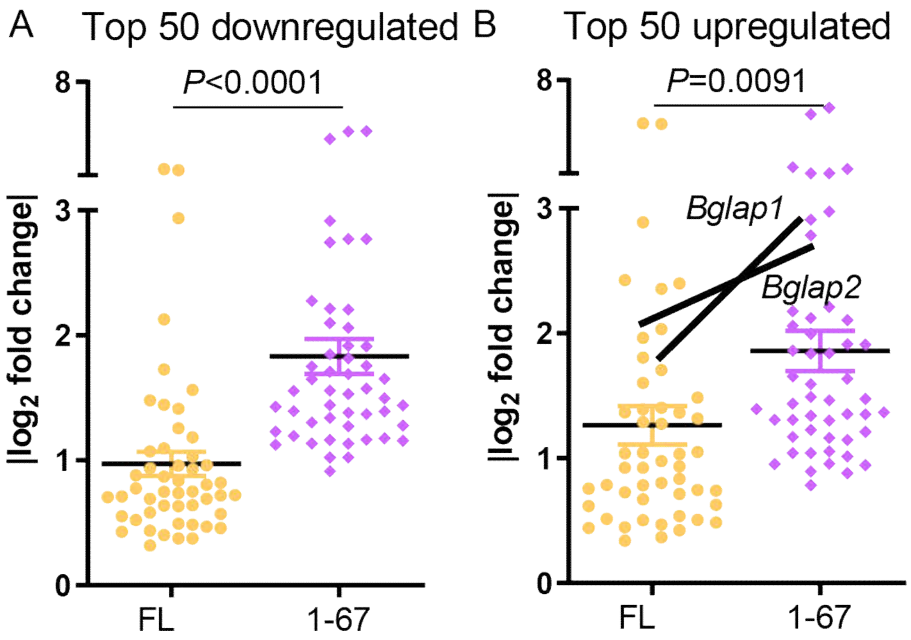

Figure 5.1. Regulatory difference from overlapped genes between *FL* and *1-67(ΔNLSΔC)* based on (A) top 50 downregulated genes where genes were all down-regulated in both *FL* and *1-67* (presented in Fig. 4.6A) and (B) top 50 upregulated genes when genes were all up-regulated (see Fig. 4.6B) with C terminal inhibitory effects. Magnitude change of genes that are commonly regulated were compared and plotted. *1-67 (ΔNLSΔC)* exhibited significantly higher gene magnitude changes than *FL*. Graphs = mean ± SEM. n = 50 replicates. *p < 0.05, ***p < 0.001 by Unpaired Student's T-test. ns means not significant (P≥0.1)."

5.3.2 *Bglap* gene expressions are up-regulated by deleting PTHrP C-terminal without any dependence on differentiation in OCY454 osteocytes

qPCR was used to validate the RNA-Seq findings on the *Bglap* expression pattern among the OCY454 overexpressing full-length and other mutant PTHrP forms. As shown in the Fig. 5.2A, $PTHrP^{\Delta NLS\Delta C}$ had induced *Bglap* to a significantly greater level than any other cell line ($PTHrP^{FL}$, $PTHrP^{\Delta NLS}$, and the pcDNA vector control). However, this pattern of *Bglap*

expression was not seen in NLS-truncated PTHrP (*PTHrP*$^{\Delta NLS}$) in OCY454 at day 14 (Fig. 5.2A).

Thus, *PTHrP*$^{\Delta NLS\Delta C}$ which lacks the last 35 C-terminal amino acids and 28 NLS amino acids, not only still retains the ability to induce *Bglap1/2* but also induces a higher level of transcription. Overall, this suggests that NLS region might be required for *Bglap* induction but deleting the C-terminus is sufficient to induce much higher *Bglap* levels (a two-fold increase) under the condition of NLS deficiency (Fig. 5.2A). This observation for the *Bglap* gene expression among the cells bearing functional PTHrP isoforms is summarised in Figure 5.2B. Importantly, this indicates that PTHrP C-terminal region might have an inhibitory effect on *Bglap* induction in OCY454 osteocytes.

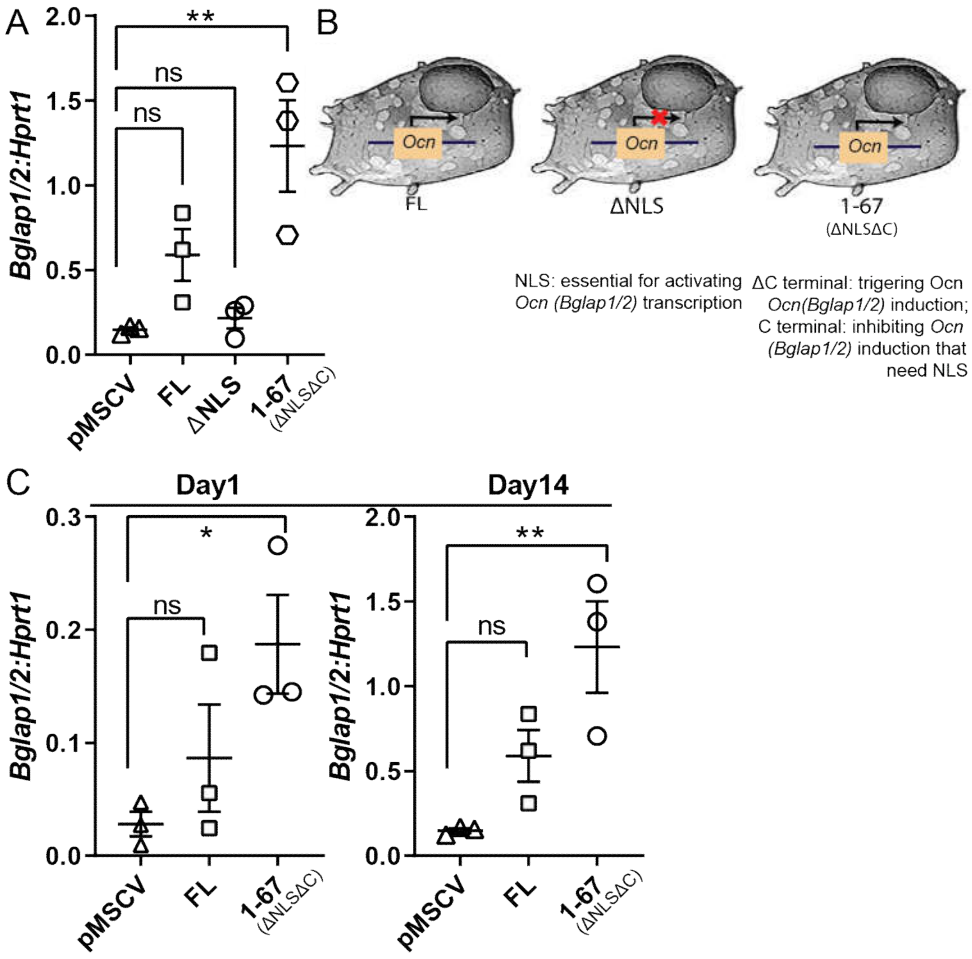

Figure 5.2. Lack of C-terminus PTHrP significantly induces expression of *Ocn* (*Bglap*1/2) endogenously. RT-PCR analysis of gene expression of *Bglap* for OCY454 cells with overexpressing with different PTHrP isoforms (14 days). Data were expressed as mean ± SEM (n = 3) Note: *indicates $p < 0.05$ compared with control (One-way ANOVA). (B) Working model of the repression exerted by C terminal on *Ocn* (*Bglap*) transcription. Activation of *Bglap* gene transcription mediated by PTHrP full length. Repression of *Bglap* gene transcription mediated by ΔNLS, indicates NLS is essential for activating *Bglap* transcriptions. Since additionally ΔC will trigger *Bglap* induction, the occupancy of C terminal will repress transcription that needs NLS. (C) *Bglap* expression inhibited by PTHrP C terminal in osteocytes is not dependent on differentiation. *Bglap* transcription regulated by pMSCV, FL and 1-67 (ΔNLSΔC) are having the same regulatory patterns in day1 and day14. The data are expressed as the mean ±SEM of triplicate determinations, each being repeated at least three times. *, P 0.05; **, P 0.01; ***, P 0.001 (compared with vehicle control, One-way ANOVA). ns means not significant (P≥0.1).

Bglap was used as a last-stage osteogenic differentiation phenotype marker, and was highly expressed at day 14 in OCY454 cells (Ansari, Ho *et al*. 2018). To understand whether the *Bglap* expression regulated by the C-terminus was dependent on the cell differentiation stage, transcription of *Bglap* was identified among the OCY454 cell lines at day one when the cells were not differentiated. Figure 5.2C shows that day one undifferentiated OCY454 cells with a deleted C-terminus were still able to induce greater *Bglap* induction, even though transcription levels were low. The $PTHrP^{\Delta NLS\Delta C}$ induced a two-fold increase of *Bglap* compared with that regulated in $PTHrP^{FL}$ which had induced *Bglap* expression but not significantly (Fig. 5.2C left panel). This is the same regulation pattern that was observed at day 14, suggesting the role of PTHrP C-terminal in repression of *Bglap* is independent of cell differentiation (Fig. 5.2C right panel).

5.3.3 Effects of exogenous treatment with hPTHrP(1–84) lacking the C-terminus and full-length hPTHrP(1–141) peptides on *Bglap1/2* gene transcription in OCY454 osteocytes

Since I observed a greater induction of *Bglap* transcription phenotype by C-terminus deletion in previous RNA-Seq and qPCR validation experiments, I then sought to understand whether exogenous treatment with C-terminus lacking peptides might limit *Bglap1/2* transcription induced by full-length PTHrP.

Since PTHrP is secreted, it can exert an exogenous effect in an autocrine or paracrine manner. To examine whether lack of exogenous PTHrP C-terminal influences *Bglap* expression, I compared *Bglap* transcription in OCY454 wild-type cells treated with hPTHrP(1–141) and hPTHrP(1–84), which lacks the C-terminal region. After one hour of treatment, hPTHrP(1–141), hPTHrP(1–84), and PTH increase *Bglap* induction but not significantly compared with the non-treatment (NT). At six hours, both hPTHrP(1–141) and PTHrP(1–84)

induced *Bglap* expression significantly more than NT. PTH also induced a greater *Bglap* transcription level but not significantly. After 24 hours, all three treatments induced diminished levels of *Bglap* compared to NT. In all three timepoints, hPTHrP(1–84) did not differ significantly from hPTHrP(1–141) in the effect on *Bglap* (Fig. 5.3). PTHrP(1–84) cannot reproduce *Bglap* transcription differently from 1–141 at different timepoint treatments, demonstrating that lack of an exogenous C-terminus is not sufficient to result in a greater level of *Bglap in* OCY454. Therefore, any effect of PTHrP C-terminus may be exerted through an intracrine effect – acting within the cell.

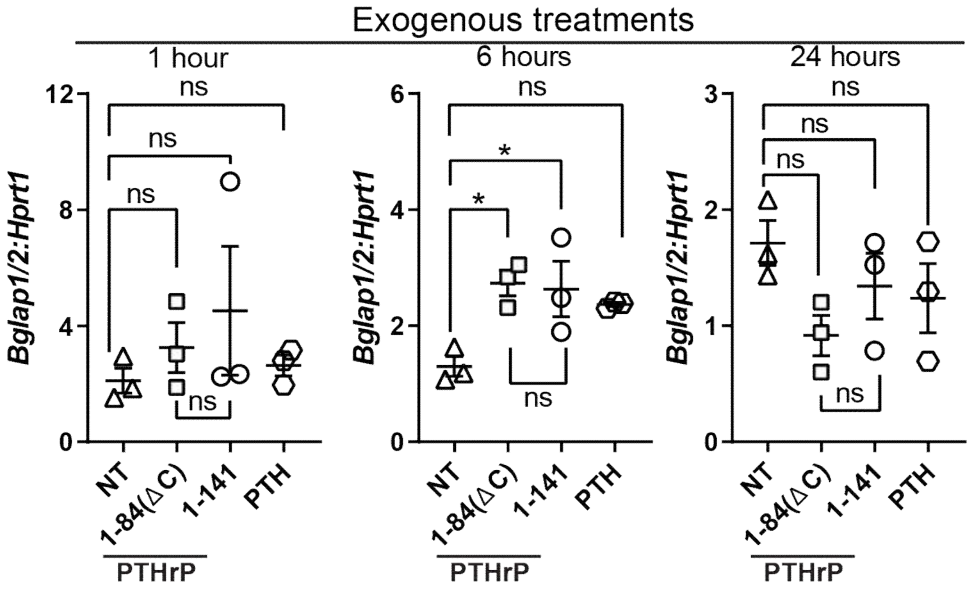

Figure 5.3. Effect of hPTHrP(1-141) and hPTHrP(1-84) on the *Bglap* gene expression at 1, 6 and 24 hours treatment in OCY454 osteocytes. The mRNA contents were measured by qRT-PCR. Despite significant induction of *Bglap* levels in hPTHrP(1–141) (10 nM) and hPTHrP(1-84) (10 nM) treated cells at 6 hours timepoint incubation, no significant difference of *Bglap* was observed between hPTHrP(1–141) and hPTHrP(1-84) treatments. For other timepoints, the overall results were similar with and without normalisation with the *Hprt1* mRNA content. The data are expressed as the mean ±SEM of triplicate determinations in one independent experiment. *, P 0.05 **, P 0.01; ***, P 0.001 (compared with vehicle control, One-way ANOVA). ns means not significant (P≥0.1).

5.4 The effect of PTHrP C-terminus domain on *Bglap* induced by PTH/PTHrP signalling in rat osteogenic cell line UMR106.01

5.4.1 qPCR validations have confirmed the C-terminus stably overexpressed in UMR106.01

I postulated that the PTHrP C-terminus might antagonise the PTH1R-mediated induction of *Bglap* induced by full-length PTHrP signalling. To test this, I generated UMR106.01 cells stably overexpressing PTHrP amino acids 107–141 ($PTHrP^{107\text{-}141}$) and PTHrP68-141 ($PTHrP^{68\text{-}141}$). Gene fragments were synthesised that correspond to amino acids 68–141, which contains the NLS region and C-terminus region in $PTHrP^{68\text{-}141}$. $PTHrP^{107\text{-}141}$ were established, corresponding only to the C-terminus.

qPCR was used to confirm stable expression of PTHrP C-terminus constructs, and gene expression was significantly increased in both cell lines. Fig. 5.4 showed the C-terminus gene products were produced in both of these two cell lines when using primer sets targeting the C-terminus transcription region. NLS gene product was only produced in $PTHrP^{107\text{-}141.}$

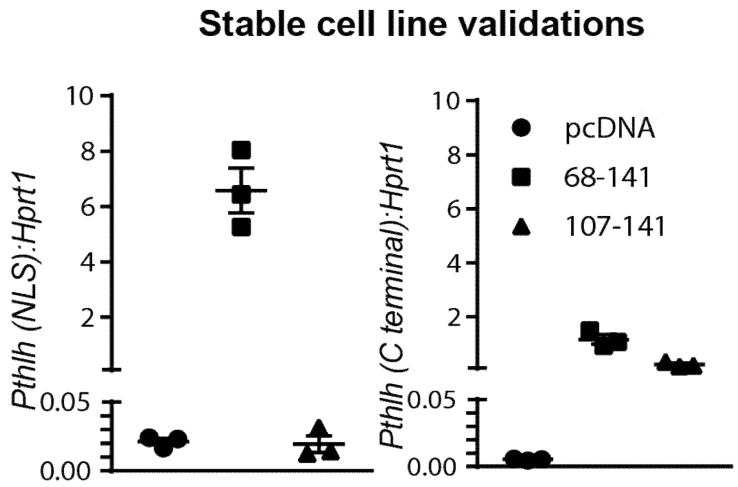

Figure 5.4. qRT-PCR validation of PTHrP two C terminal constructs in UMR 106.01 stable cell lines. C-terminus gene products were detected in both of these two cell lines when using primer sets targeting C terminus transcription region. NLS gene product was only produced in *PTHrP*$^{68\text{-}141}$. The data are expressed as the mean±SEM of triplicate determinations, each being repeated at least three times.

5.4.2 Overexpression of C-terminus inhibited *Bglap* targeted by PTH/PTHrP treatments

To understand the functions of transfected C-terminus in regulating *Bglap* transcription levels, both of these cells were treated with PTHrP(1-141). To test this, I stimulated UMR106.01 cells bearing pcDNA vector control and two C-terminus constructs with PTHrP(1-141) at 2nM, as shown in the Figure 5.5. When the cells were treated with PTHrP(1-141) all three cell lines (UMR106.01 pcDNA, *PTHrP*$^{68\text{-}141}$, and *PTHrP*$^{107\text{-}141}$) increased *Bglap* transcription after eight hours of incubation. However, only the cell line overexpressing solely C-terminal peptide successfully inhibited *Bglap* induction induced by PTHrP.

To test the specificity of PTHrP signalling antagonised by the PTHrP C-terminal, I examined the ability of the PTHrP C-terminal to inhibit the elevation of *Bglap* transcription by treating the cells with PTH(1–34), to mimic PTHrP signalling. The results were the same as those treated with PTHrP (Fig. 5.5). Together these data showed that the PTHrP C-terminus domain, but not NLS region, restricted the ability of PTHrP or PTH signalling involved in promoting *Bglap* transcription.

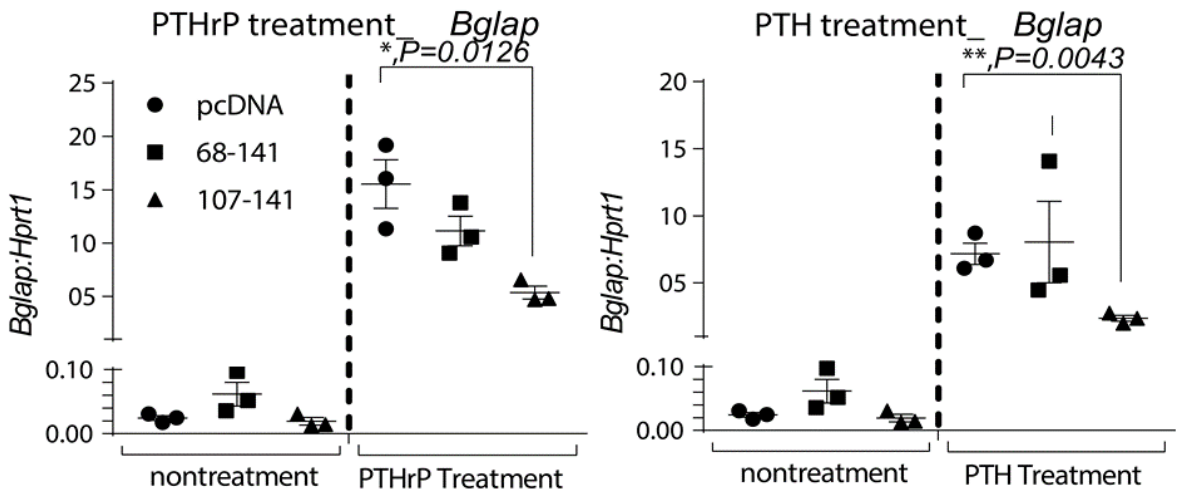

Figure 5.5. Effect of PTHrP C terminal on *Bglap* mRNA abundance in UMR-106 cells. *Bglap* has been significantly repressed by C terminal but not NLS when *Bglap* has been induced by PTHrP treatment (2nM) (left) and PTH treatment (2nM) (right) for 8hours. The data are expressed as the mean±SEM of triplicate determinations, each being repeated at least three times. *, P 0.05; **, P 0.01; ***, P 0.001 (compared with vehicle control, One-way ANOVA).

5.4.3 The activation of the OSE2 promoter region is not inhibited in UMR *PTHrP*$^{107-141}$ or UMR *PTHrP*$^{68-141}$

Runt-related transcription factor 2 (Runx2) is an upstream factor that regulates *Bglap* transcription by binding cis-regulatory elements OSE2 (Ducy, Zhang *et al*. 1997, Franceschi and Xiao 2003, Stein, Lian *et al*. 2004, Martin, Zielenska *et al*. 2010). To determine whether the PTHrP-C terminal inhibits *Bglap* transcription by acting directly on the Runx2-binding element OSE2 (Osteoblast-specific element 2) within the *Bglap* promoter, I used reporter genes carrying OG2-OSE2 elements (Ducy and Karsenty 1995, Saito, Ochiai *et al*. 2011). The UMR106.01 *PTHrP*$^{68-141}$, *PTHrP*$^{107-141}$, and pcDNA stable cell lines were transiently transfected with an OSE2 reporter plasmids containing six tandem copies (Section 2.7). After exposure to 2nM or 20nM PTH for four hours, the reporter activities of OG2-OSE2 increased (five-fold with 2nM and 12-fold with 20nM PTH (Fig. 5.6). This induction was not changed in UMR *PTHrP*$^{107-141}$ and UMR *PTHrP*$^{68-141}$ cells, indicating that the reduction of *Bglap* transcription by the C-terminus is not due to the impaired activities of the OSE2 gene at the promoter site.

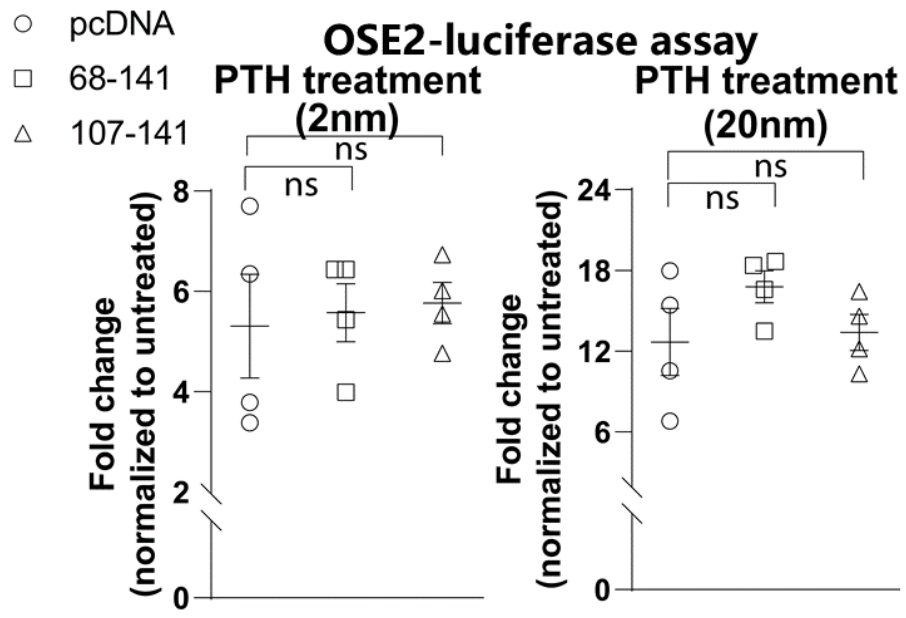

Figure 5.6. OSE2 activation is not mediated by the C-terminus. OSE2 luciferase assay result in UMR pcDNA. UMR *PTHrP*$^{68\text{-}141}$ and *PTHrP*$^{107\text{-}141}$ when cells are treated with PTH (2nM, 20nM). The data are expressed as the mean±SEM of triplicate determinations, each being repeated at least three times. **, P 0.01; ***, P 0.001 (compared with vehicle control, One-way ANOVA). ns means not significant (P≥0.1).

5.5 The effect of PTHrP C-terminus domain on *Bglap* induction by PTHrP is not through PTH1R/PKA signalling

Since the RNA-Seq data (Section 4.1.2) indicates that the PTHrP C-terminus decreases the number of cAMP/CREB responsive genes, I next investigated the role of the C-terminus in regulating the cAMP/PKA pathway.

5.5.1 Exogenous hPTHrP(1-84) and hPTHrP(1-141) do not exert different effects on CREB-responsive gene transcription

Apart from the analysis done in the stable UMR106.01 cell lines overexpressing the C-terminus, I have used the OCY454 WT cells and treated the cells with exogenous hPTHrP(1-84) and hPTHrP(1-141). Both treatments induce high transcription levels of CREB genes (Fig. 5.7). However, the five CREB responsive genes (*Rgs2*, *Nr4a2*, *Nr4a1*, *Efnb2*, and *Btg2*) expression did not differ significantly in cells treated with PTHrP(1-84) and PTHrP(1-141). This suggests that absence of exogenous C-terminus does not change CREB responsive transcription. In other words, the C-terminus of exogenous PTHrP does not modify CREB responsive genes.

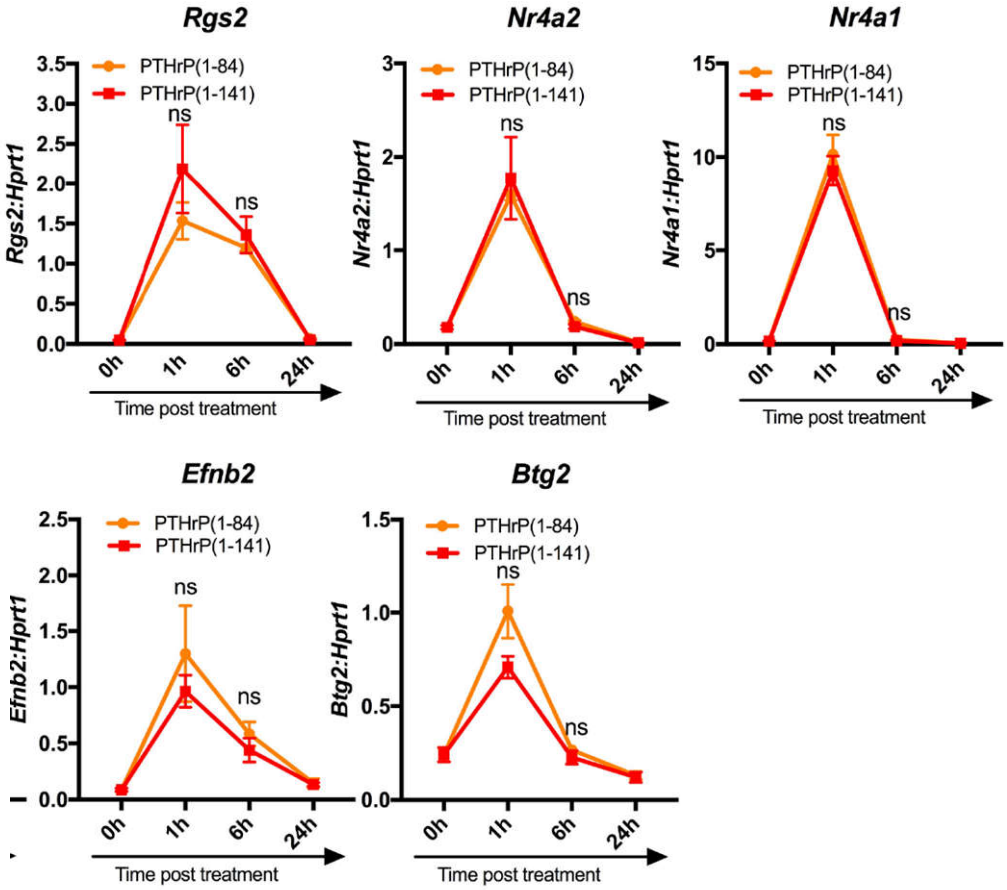

Figure 5.7. qRT-PCR analysis of CREB responsive genes in OCY454 wild-type cells treated with PTHrP(1-141) and PTHrP((1-84), ΔC). Graphs = mean ± SEM. n = 3 replicates from three independent experiments. *p < 0.05, ***p < 0.001 by Unpaired Student's T-test. ns means not significant (P≥0.1).

5.5.2 PKA/cAMP/CREB response is not involved in cytosolic action of the PTHrP C-terminus to suppress *Bglap* transcription

In order to detect whether second messenger cAMP induced by exogenous PTHrP is reduced by the cytosolic action of the PTHrP C-terminus, I have assessed cAMP accumulation in UMR *PTHrP*$^{107-141}$ and UMR *PTHrP*$^{68-141}$cells in response to treatment with PTH and PTHrP. Cells overexpressing the C-terminus did not show a different production in intracellular cAMP in response to PTH hormone concentrations (10nM and 100nM) compared to pcDNA (Fig. 5.8). Similarly, each of the two stable cell lines overexpressing the C-terminus showed no significant difference in accumulation of cAMP compared to control in response to treatment with PTHrP, consistent with the PTH treatment (Fig. 5.8).

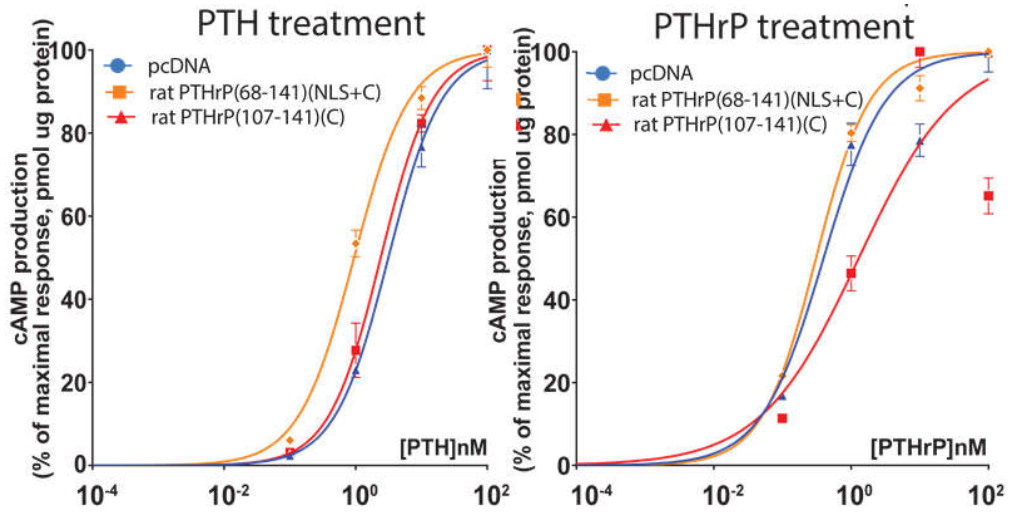

Figure 5.8. C-terminus did not alter cAMP accumulation. Dose-response curves for PTH/PTHrP-induced cAMP accumulation in UMR106.01 cells transfected with vector, *PTHrP*$^{68-141}$, *PTHrP*$^{107-141}$. Response is expressed as percentage of maximal PTH(A) or PTHrP(B) induced response. Results are the means±SEM of triplicate determinations in one independent experiment.

To ascertain whether the C-terminus affects CREB signalling, expression constructs for *PTHrP*$^{107\text{-}141}$ and *PTHrP*$^{68\text{-}141}$ were transiently co-transfected with CRE-Luc reporter construct into UMR106 WT cells respectively, and the luciferase activities were compared. Exogenous treatments with either PTH or PTHrP provoked a large increase in luciferase activity, confirming CREB responsiveness of the reporter (Fig. 5.9A). Luciferase activity in UMR cells transfected with the two PTHrP-C terminal peptides (107–141 and 68–141) remained elevated under the stimulation of different dosages of PTH and PTHrP but did not behave differently (Fig. 5.9A). Thus, the C-terminus domain does not significantly affect CRE-Luc functioning activities in UMR *PTHrP*$^{68\text{-}141}$ and *PTHrP*$^{107\text{-}141}$. This indicates that cytosolic PTHrP C-terminus does not directly regulate the CRE-Luc activity that follows PKA activation.

To obtain further evidence whether cAMP-dependent protein kinase A (PKA) was activated by the C-terminus domain, I checked the level of phosphorylated CRE-binding protein (pCREB) levels in UMR cells treated with PTHrP, using western blotting. pCREB activity was tested after 15 mins and 30 mins as well as nontreatment conditions. Overexpression of PTHrP(68–141) or PTHrP(107–141) did not alter phospho-CREB compared with pcDNA at different time points in UMR cells (Fig. 5.9B), suggesting the role of the C-terminus is not associated with CREB activity under either PTH or PTHrP signalling.

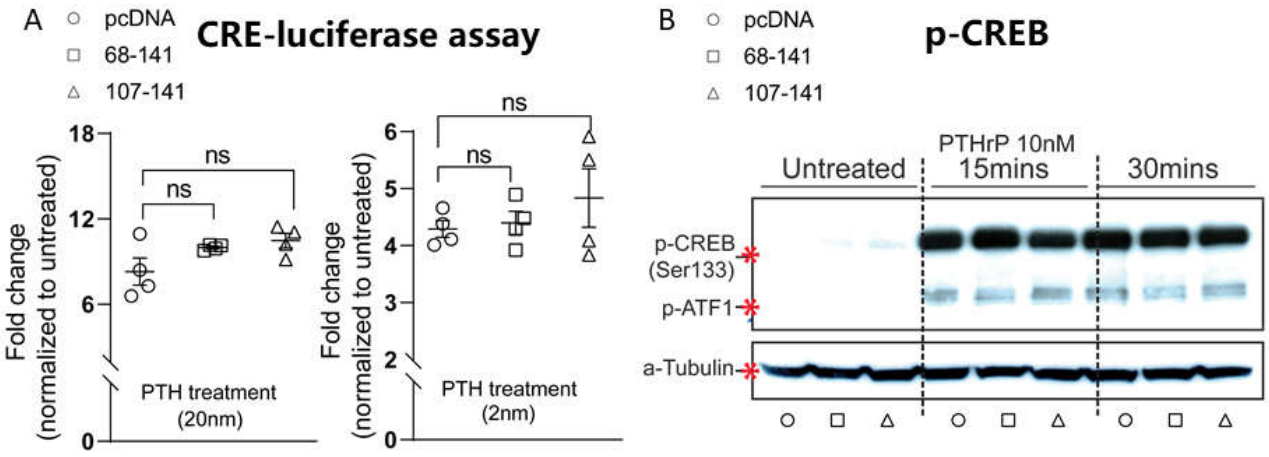

Figure 5.9. C-terminus does not modify CRE-luciferase activities nor pCREB levels. (A) Luciferase reporter assays in UMR106.01 cells with pcDNA vector control, PTHrP68-141 and PTHrP107-141. Cells were co-transfected with a luciferase reporter fused to a CRE. Cells were stimulated with PTH (2nM, 20nM) as indicated in the Materials and Methods section. Graphs = mean ± SEM. n = 3 replicates from independent experiments. *p < 0.05, ***p < 0.001 by One-way ANOVA. ns means no significant (P≥0.1). (B) Effect of C-terminus on pCREB. Representative Western blot using total protein lysates from UMR106.01 cells with pcDNA vector control, *PTHrP*$^{68\text{-}141}$ and *PTHrP*$^{107\text{-}141}$ treated with PTHrP for 15 mins and 30 mins. Lysis were blotted with anti–-tubulin (1:2500), anti-pCREB (1:500). The anti-pCREB antibody also detects the phosphorylated form of the CREB-related protein, ATF-1 (activating transcription factor). This Western blot is based on one independent result.

5.5.3 C-terminus expression does not change CREB target genes transcription.

I next tested whether endogenous overexpression of the PTHrP C-terminus modifies expression levels of CREB responsive genes in cells treated with PTH(1–34). Figure 5.10A,B showed expression of *Nr4a2* and *c-fos* were elevated by the treatment of PTH and PTHrP but there is no detectable effect in cells presented with $PTHrP^{68\text{-}141}$ or $PTHrP^{107\text{-}141}$. It is concluded that C-terminus or NLS domains do not inhibit the CREB gene response to treatment with PTH or PTHrP proteins.

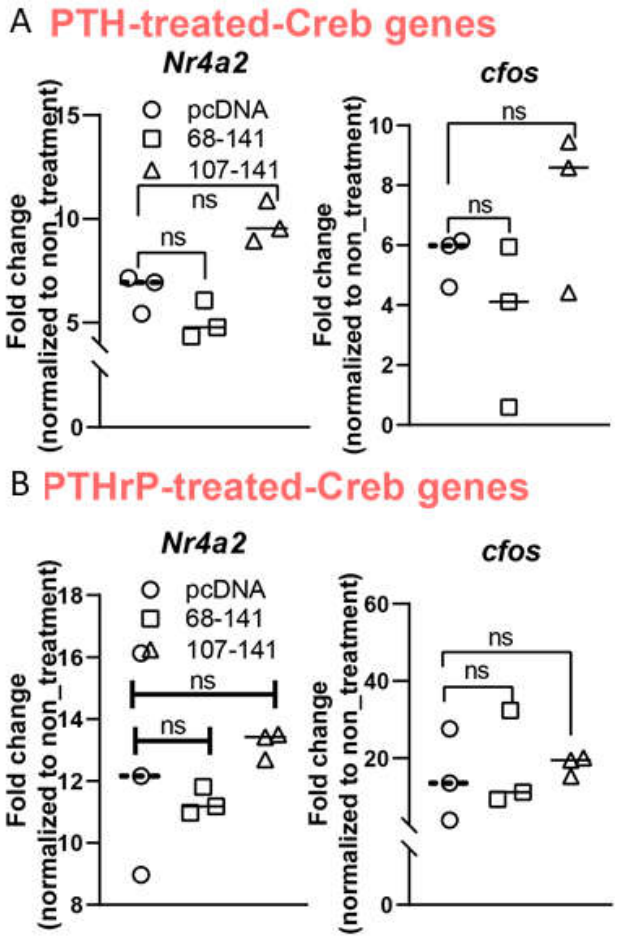

Figure 5.10. qRT-PCR analysis of CREB responsive genes in UMR106.01 cells overexpressing with *PTHrP*$^{68-141}$ and *PTHrP*$^{107-141}$. (A) PTH treated; fold change normalised to untreated; (B) PTHrP treated; fold change normalised to untreated. Data are represented as mean ± SEM; *P < 0.05 by one-way ANOVA, n = 3 in each group. ns means no significant (P≥0.1).

5.6 The PTHrP C-terminus may modify the Wnt signalling pathway

Understanding any relationship between the PTHrP C-terminus and its possible involvement of *Bglap* will require identification of candidate pathways. To begin exploring the mechanism of *Bglap* suppression by the C-terminus, I performed DAVID bioinformatic analysis on the RNA-Seq data to identify significant pathways due to the C-terminus effect in OCY454. I have analysed the top 50 up- and top 50 down-regulated genes with a stronger regulation when the C-terminus was deleted. The results of DAVID analysis are presented in Figure 5.11. Functional annotations of proteins encoded by genes with C-terminus effect showing significantly ($P<0.05$) increased or decreased enrichment compared with controls, were classified according to their associated biological processes (BP), cellular components (CC), and molecular functions (MF). GO analysis indicated that the molecular functions of the majority of the genes identified as C-terminus effect genes were associated with cell-cell signalling, cell differentiation and regulation of the Wnt signalling pathway in the biological process (BP) functioning database. At the level of cellular components (CC), there were significant differences between proteins encoded by genes with C-terminus effects associated with the extracellular space, proteinaceous extracellular matrix, extracellular region, and cell surface (Fig. 5.11). Analysis according to molecular function (MF) revealed significant differences between enrichment of encoded proteins associated with growth factor activity, integrin binding, heparin binding, calcium ion binding, structural constituent of bone, etc. (Fig. 5.11).

A number of Wnt targeting genes changed in transcriptional profile based on our RNA-seq dataset (highlighted in red in Fig. 5.11). Wnt signalling plays an important role in PTHrP action (Kulkarni, Halladay *et al*. 2005), and the data suggest Wnt signalling is altered with

absence of the C-terminus in OCY454. Since Wnt signalling plays an important role in transcription of *Bglap*, it will be important to investigate further the effect of Wnt signalling on regulation of *Bglap* mediated by the PTHrP C-terminus.

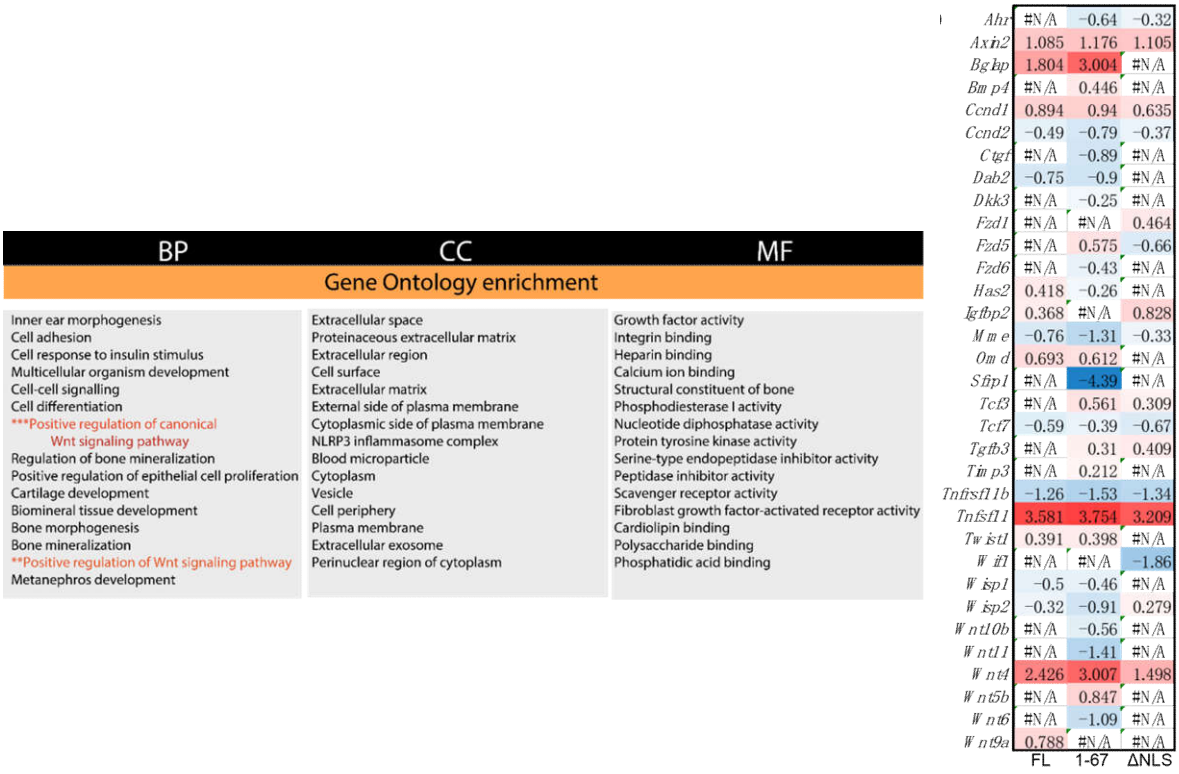

Figure 5.11. Bioinformatic data showed C terminus is regulating Wnt signalling pathway. GO enrichment analysis using both top 50 upregulated and 50 downregulated genes with C-terminus effect. Genes encoding Wnt Signalling pathways were significantly altered by PTHrP C terminal identified in the biological process (BP) database (left panel). Wnt signalling associated genes were listed in a heapmap, showing genes that were regulated by OCY454 $PTHrP^{FL}$ (FL), $PTHrP^{\Delta NLS\Delta C}$ (1-67) and $PTHrP^{\Delta NLS\Delta C}$ (ΔNLS) (right panel).

To detect whether the C-terminus modifies the response to exogenous PTH treatment, the assay for this exploited the Wnt signalling pathway reporter Top flash (TCF optimal promoter), which comprises multimerised TCF-binding sites involved in the expression of cDNA that encodes the firefly luciferase gene (DasGupta, Kaykas *et al*. 2005). PTH promotes Wnt pathway activity, as determined with the Top-Flash reporter: PTH induced Top-flash luciferase activity in cells in a dose-dependent manner (four-fold at 2nM; six-fold at 20nM; Fig. 5.12). No significant change to this occurred when UMR cells had NLS and C-terminus proteins overexpressed compared to the control. This indicates that *PTHrP* does not affect the Top-flash luciferase activation at these conditions (PTH 2nM, 20nM). However, there was significant enhancement of Top-flash-Luc activity due solely to the presence of the PTHrP C-terminus when cells were treated at a lower dose of PTH (Fig. 5.12). The result was based on three repeated independent experiments.

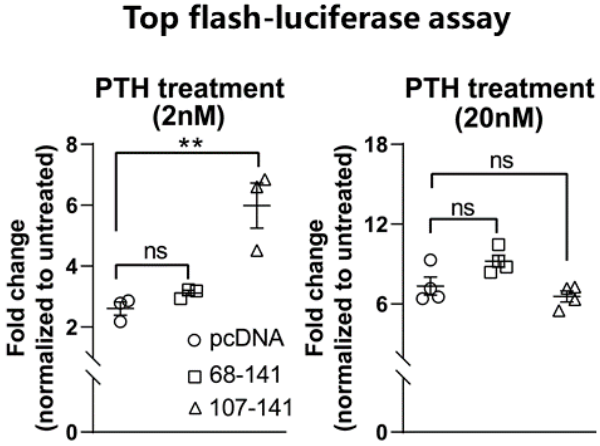

Figure 5.12. PTHrP C terminus transfection but not NLS increases Wnt/β-catenin signalling in response to PTH (2nM). UMR106.01 cell lines (pcDNA, 68-141, and 107-141) were transiently co-transfected with Top-flash plasmid DNA with Renilla Luciferase plasmid DNA. Cells were treated with different concentrations of PTH (2 and 20 nM) for 4 hours. Activity of Wnt/β-catenin signalling pathway was quantified by measuring relative firefly luciferase activity units (RLU) normalised to Renilla luciferase. PTHrP C terminus deficiency but not that of NLS induces Wnt/β-catenin signalling when cells were treated with 2 nM PTH. Graphs = mean $\pm$ SEM. n = 3 replicates from at least three independent experiments. *p < 0.05, **p<0.05, ***p < 0.001 by one-way ANOVA. ns means no significant (P≥0.1).

To gain insights into possible alternative mechanisms governing this phenomenon, mRNA expressions of Wnt target genes *Wnt4* (Arnold, Stappert *et al*. 2000), *Wisp1* (Xu, Corcoran *et al*. 2000, Maeda, Ono *et al*. 2015), *Wisp2* (Grünberg, Hammarstedt *et al*. 2014) and *Lef1* (Eastman and Grosschedl 1999) in UMR106.01 cells treated with PTH were measured. In the cells expressing $PTHrP^{107\text{-}141}$, PTH treatment significantly increased Wnt ligand *Wnt4* levels compared to levels in the pcDNA control UMR cells (Fig. 5.13A), but the *Wnt 4* effect was significantly reduced in cells expressing $PTHrP^{107\text{-}141}$ compared to the pcDNA vector control (Fig. 5.13A). Both $PTHrP^{68\text{-}141}$ and $PTHrP^{107\text{-}141}$ cells expressed higher levels of *Wisp1*. *Tnfsf11* expression was not changed by presence of the pcDNA vector control but was highly induced in $PTHrP^{68\text{-}141}$ *and* $PTHrP^{107\text{-}141}$ when compared to levels in pcDNA UMR106.01 cells. Expression of *Wisp2* and *Lef1* behaved similarly to gene regulation patterns of other Wnt target genes (Fig. 5.13B). In both $PTHrP^{68\text{-}141}$ and $PTHrP^{107\text{-}141}$, *Tnfrsf11* was decreased in response to PTH treatment (Fig. 5.13C). Overexpression of C-terminus PTHrP significantly reduced Wnt signalling pathway inhibitor *Sclerostin* (*Sost)* mRNA when cells treated with PTH (Fig. 5.13D). The other inhibitor *Dickkopf* (*Dkk1*; Holdsworth, Slocombe *et al*. 2012) was also repressed but not significantly. Together, the data suggests that the PTHrP C-terminus, but not NLS, induces Wnt signalling when cells are treated with PTH.

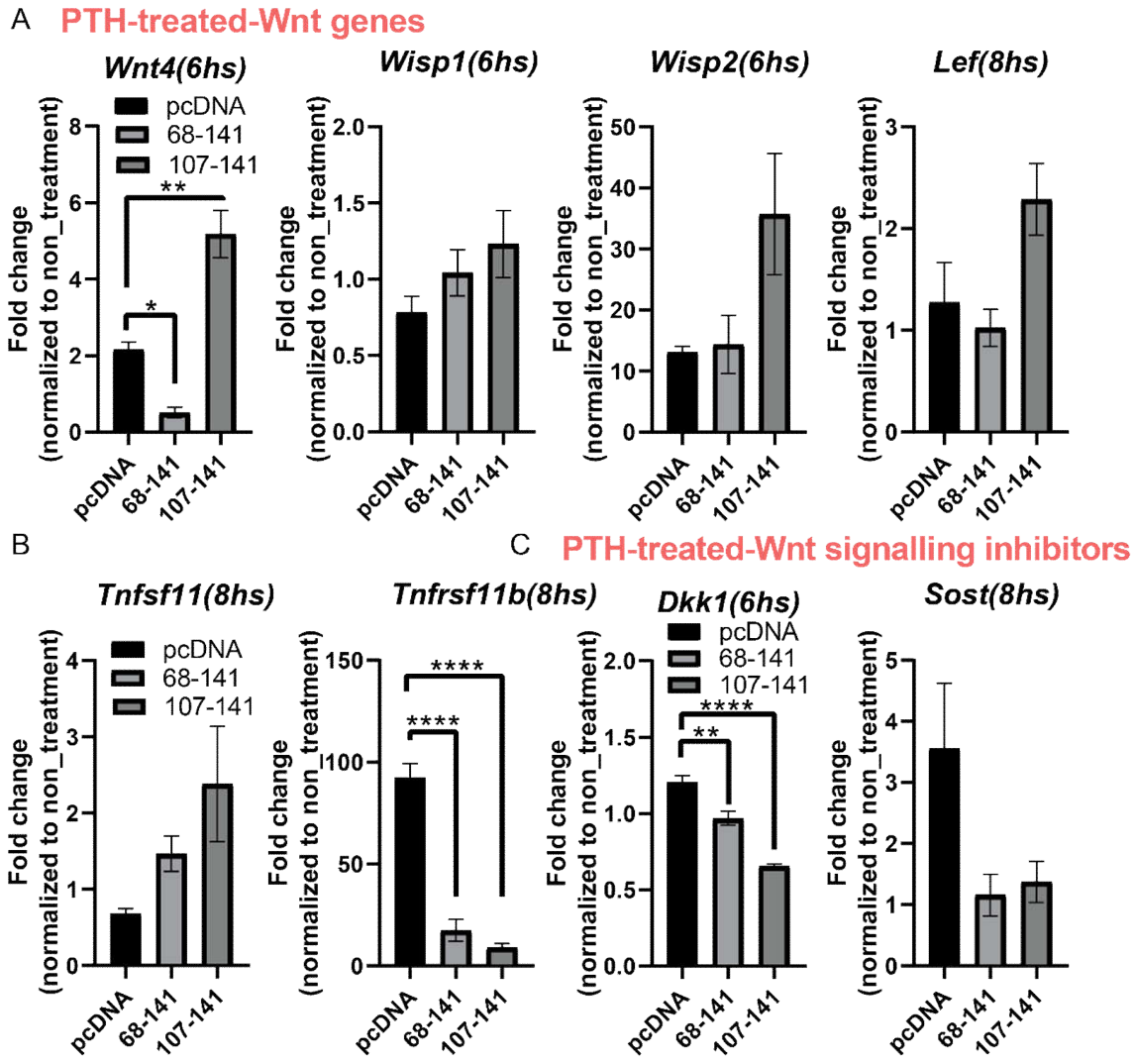

Figure 5.13. PTHrP C-terminus but not NLS induces Wnt/β-catenin signalling. Validation of RNA-seq-discovered candidate genes by qPCR. Transcripts collected from *PTHrP* and *PTHrP*$^{107\text{-}141}$ were compared with control (UMR 106.01 pcDNA). (A) *PTHrP*$^{107\text{-}141}$ significantly increased *Wnt4* levels compared with levels in pcDNA control UMR cells. PTHrP significantly reduced *Wnt4* levels in compared with pcDNA vector control. Both PTHrP and PTHrP$^{107\text{-}141}$ expressed much higher levels of *Wisp1* and *Tnfsf11* when compared with levels in pcDNA. *Wisp2* and *Lef1* are not changed by PTHrP but largely induced by *PTHrP*$^{107\text{-}141}$, behaving the similar gene regulation patterns with other Wnt targeting genes. (C)*PTHrP*$^{68\text{-}141}$ and *PTHrP*$^{107\text{-}141}$ both reduced the *Tnfrsf11b* expression, which is the responsive gene of *Tnfsf11*, supposed to be targeted by Wnt signalling. (D)Both of the two C-terminus overexpressing cells significantly reduced Wnt signalling pathway inhibitors Dkk1 when cells treated with PTH. *Sost* has also been repressed but not

significantly. *P<0.1, **P<0.05; ns, not significant (P≥0.1); One-way ANOVA. Data are represented as mean ± SEM of triplicates at least in one independent experiment.

5.7 Discussion

Of the genes regulated by PTHrP overexpression, *Bglap* family genes (containing *Bglap1* and *Bglap2*) were selected for further study because they were the most significantly differentially expressed genes of all those upregulated by overexpression of $PTHrP^{\Delta NLS\Delta C}$ and $PTHrP^{FL}$ in Ocy454 cells (see the last chapter, Fig. 4.6). Secondly, *Bglap* family genes were selected because they are known to have multiple functions in osteoblasts and osteocytes. In this chapter, my results suggest that the PTHrP C-terminus may inhibit the effect of exogenous PTHrP on *Bglap* transcription. This action is not mediated through CREB activation since there were no changes in cAMP response, CREB responsive genes or CREB phosphorylation when cells overexpressing the PTHrP C-terminus were treated with exogenous PTHrP. However, this effect is intracellular, since there was no difference in the effects of exogenously supplied C-terminal PTHrP compared to full length PTHrP. The action did not occur through OSE2 promoter binding.

When UMR106.01 cells were treated with PTH/PTHrP, *Bglap* mRNA levels were increased in all three cell lines (pcDNA, $PTHrP^{68–141}$, and $PTHrP^{107-141}$), however, this response was less substantial in the cells overexpressing $PTHrP^{107-141}$. This indicates that the PTHrP C-terminus ($PTHrP^{107-141}$) inhibits the effect of exogenous PTH/PTHrP on PTHR1-mediated increase *Bglap* transcription. In contrast, the response to exogenous PTH/PTHrP was not modified in UMR106.01 cells overexpressing $PTHrP^{68–141}$. Compared with $PTHrP^{68–141}$, $PTHrP^{107–141}$ lacks the NLS region, which suggests that the PTHrP C-terminus reduces PTHR1-mediated increase in *Bglap* response via a cytosolic action, not requiring nuclear activity or nuclear translocation activity associated with NLS region. In addition, the data showed that in cells overexpressing $PTHrP^{68–141}$ the suppression of the *Bglap* effect observed in cells overexpressing $PTHrP^{107-141}$ was not found, suggesting the NLS region might suppress

the C-terminus' ability to suppress gene expression. However, this is only one example of gene regulation and it is plausible that several more genes are regulated by the C-terminus and by the C-terminus interaction with the NLS region.

Mice have three complex osteocalcin loci, but only two, *Bglap1* and *Bglap2*, are expressed in bone (Desbois, Hogue *et al*. 1994). My RNA-Seq data has confirmed that *Bglap3* is not expressed in Ocy454 cells. The initial RNA-Seq finding that deletion of the PTHrP C-terminus increases PTH1R-mediated gene expression responses in OCY454 (Chapter 4), further suggests that the C-terminus of PTHrP reduces the induction of both *Bglap1* and *Bglap2*, induced by exogenous PTHrP. These two murine *Bglap* family genes have 99% similarity with each other such that qPCR cannot distinguish them.

The C-terminus' inhibition of *Bglap* mRNA levels may provide evidence into how PTHrP promotes bone formation, and could lead to a therapeutic approach for treating osteopenia and osteoporosis. The role of osteocalcin (*Bglap*, *Ocn, Osc* gene product) in regulating bone formation was originally estimated by using osteocalcin-null mice (Osc^{m1}/Osc^{m1} mice) with both *Bglap1* and *Bglap*2 genes deleted (Ducy, Desbois, et al. 1996), which exhibited increased bone formation. These six-month-old osteocalcin-deficient mice exhibited increased cortical thickness and density relative to their wild littermates. These mice also developed a high bone strength tested by strength testing (four-point bending biomechanical measures), revealed by a significant increase in failure load. Consistent with this, using an osteocalcin-null rat model, Lambert et al. (2016) found that the *Bglap* gene depleted rats showed a high trabecular bone volume compared with the controls. These data suggest that the therapeutic reduction of osteocalcin expression could prevent osteoporosis in humans.

However, its effects on bone mass remain controversial in the literature (Diegel C R, Hann S, et al. 2020, Moriishi T, Ozasa R, et al. 2020), showing that osteocalcin is not involved in the

regulation of bone mass. Neither Moriishi el al. (2020) nor Diegel el al. (2020) can explain the differencebetween their findings in bone mass phenotype exerted from osteocalcin deficiency and those from Ducy et al.'s (1996). Genetic background, modifier genes, and differences in the molecular genetics of the knockout alleles remain possible explanations for the discrepancies (Manolagas S C. 2020). However, consistent with Ducy et al. (1996), Diegel C R et al. (2020) showed an increased bone crystal size and mineral maturity in newly generated osteocalcin-null mice (Bglap/2dko/dko mice) with a double knockout allele for *Bglap* and *Bglap2*. Moriishi et al. (2020) showed that another new strain of osteocalcin-null mice (Ocn–/–mice) in which *Bglap* and *Bglap2* are deleted exhibited a disrupted c-axis orientation of biological apatite along the femur longitudinal axis. This suggests that osteocalcin depletion may affect the mineral crystallographic orientation to collagen fibrils. Overall, these data suggest that osteocalcin may regulate collagen fibrils, bone crystal size, as well as mineral maturity in animals. It is essential to investigate the impact of osteocalcin deficiency on bone strength and confirm the suppression of osteocalcin has a beneficial on treating osteoporosis by adjusting the crystal size or mineral.

My data showed that PTHrP might inhibit *Bglap* mRNA levels using its C terminus. Combined with current research on osteocalcin, even though it is still controversial, a PTHrP-C-terminus based therapy may increase bone mass, bone formation, or bone strength by adjusting bone composition (such as collagen fibrils, bone crystal size and mineral maturity) through suppression of osteocalcin (or *Bglap* mRNA inhibition). In Chapter 6, I will investigate the effect of PTHrP as well as its C-terminus in regulating bone composition.

Boileau *et al.* (2001) observed that the PTHrP C-terminus serves as a substrate and can be cleaved off into four fragments by Phosphate regulating endopeptidase homolog X-linked (PHEX) endopeptidase. However, osteocalcin can inhibit this activity and prevent the

C-terminus from being degraded (Boileau, Tenenhouse *et al*. 2001). Though this was observed in kidney, PHEX is predominantly expressed in bone (Du, Desbarats *et al*. 1996; Beck, Soumounou *et al*. 1997; Guo and Quarles 1997), and thus this effect may also be relevant in bone tissues. There was no further characterisation of how osteocalcin disrupts this, however, my finding of the C-terminus in inhibiting *Bglap* gene expression indicates that a lack of osteocalcin reduces the potential for PHEX cleavage of the C-terminus. This complicated regulatory loop needs to be further examined so that it may be explained how the C-terminus exerts inhibitory effects to limit gene expression induced by PTHrP.

My analysis showed no change in cAMP response, CREB responsive gene alterations nor CREB phosphorylation in response to exogenous PTHrP treatment in cells overexpressing the C-terminus, nor any difference in the effects of exogenous absence of C-terminus compared to full-length PTHrP. This suggests the CREB gene regulatory phenotype and *Bglap* regulation by PTHrP C-terminus are not mediated by cAMP/PKA signalling. My initial hypothesis that the C-terminus might inhibit PTH1R-signalling through cAMP/CREB was based on work demonstrating that when PTHrP activates the cAMP/CREB axis pathway, the NH_2-terminal regions of both PTH(1–34) and PTHrP(1–34) have the capacity to interact specifically with PTH1R (Kemp, Moseley *et al.* 1987; Juppner, Abou-Samra *et al.* 1991). The PTHrP C-terminus binding to the N-domain of PTH1R results in increased interactions of the J-domain with the NH2-terminal (Hoare, Gardella *et al*. 2001), promoting cAMP production. However, my data have shown that PKA/cAMP/CREB response is not involved in cytosolic action of the PTHrP C-terminus to suppress *Bglap* transcription, suggesting that this gene regulation effect exerted by C-terminus is not dependent on C-terminus binding to the N-domain of PTH1R. Understanding any relationship between PTHrP C-terminus and its possible involvement with *Bglap* will require identification of candidate pathways. Some from my analysis on the biological process and molecular function so far indicated PTHrP

C-terminus may regulate genes associated with cell-cell signalling, cell differentiation, regulation of the Wnt signalling pathway, growth factor activity, integrin binding, heparin binding, calcium ion binding, and structural constituent of bone (Fig. 5.11). These may be involved and need to be further explored.

Runx2 has been suggested to function as the upstream factor that regulates *Bglap* transcription by binding to OSE2 sites (Ducy, Zhang *et al*. 1997, Cohen Jr 2009). However, I found OSE2-reporter activities were not changed when the two cell lines overexpressing PTHrP C-terminus were treated with PTH. Thus, the PTHrP C-terminus does not act on the OSE2 promoter site nor does it modify its interaction with Runx2. My OCY454 RNA-Seq data also supported this conclusion because Runx2 transcription levels were not significantly altered by $PTHrP^{\Delta NLS\Delta C}$. However, I cannot exclude the possibility that the reduction of *Bglap* is regulated by the interaction of Runx2 with other promoter sites, such as the *Bglap* association with OSE1 (Ochiai *et al*. 2011), an osteoblast-specific cis-acting element. The other possibility is that another *Bglap* upstream related gene, *AdipoR1* (Tangseefa, Martin *et al*. 2018), which is not related to OSE2, interacts with *Bglap*. This needs to be investigated.

I observed that PTH increased Wnt signalling pathway reporter TOP-flash (TCF optimal promoter) activity. This result is consistent with that from O'Brien, Plotkin *et al*. (2008) and Baron and Kneissel (2013), suggesting that PTH1R action in osteocytes increases the activation of Wnt signalling. My analysis showed that TOP-flash-Luciferase activity induced by PTH was further increased in UMR106.01 cells overexpressing the $PTHrP^{107\text{-}141}$ but was not modified by overexpression of $PTHrP^{68\text{-}141}$. This is consistent with my other result that the data (Section 5.4.2) showed that the suppression of the *Bglap* effect observed in cells overexpressing PTHrP107-141 was not found in cells overexpressing PTHrP68–141. This

suggests the NLS region might abolish the C-terminus' ability to suppress gene expression, and repress the Wnt signalling induced by C-terminus.

Further to this, DAVID analysis showed transcriptional changes in a number of Wnt associated genes including *Bglap* (See Fig. 5.11) were regulated by deletion of the C-terminus. This suggests Wnt signalling is altered by the absence of the C-terminus in OCY454 cells. However, whether C-terminus stimulates or suppresses the pathway is not obvious.

The Wnt target gene *Wnt4* was significantly increased in UMR106.01 overexpressing the C-terminus (107-141) but was repressed in UMR106.01 tranfected to express PTHrP containing both the C-terminus and the NLS region. Other Wnt target genes, *Wisp2* and *Lef1* both showing a large increase in cells overexpressing PTHrP C-terminus (107-141) but none when they overexpressed $PTHrP^{68\text{-}141}$ (68-141). Like the TOP-Flash result, this suggests that the PTHrP C-terminus promotes Wnt signalling when cells are treated with PTH, and that this may be suppressed by the NLS. It has been demonstrated previously that Wnt signalling plays an important role in the transcription of *Bglap* since induction of LEF1 by stimulating Wnt signalling represses *Bglap* (Kahler and Westendorf 2003). Since my data showed that expression of *Lef1* behaved similarly to gene regulation patterns of other Wnt target genes, it is important to know whether presence of the C-terminus in suppression of *Bglap* is dependent on Wnt signalling via LEF1 or by other components in the future.

In my study, I found the C-terminus effect was not dependent on osteocyte differentiation since *Bglap* transcription regulation by OCY454 pMSCV, $PTHrP^{FL}$, and $PTHrP^{\Delta NLS\Delta C}$ have the same regulatory patterns in day 1 when cells were not differentiated and in day 14 when cells were fully differentiated (Section 5.2.2). However, since my analysis showed that Wnt signalling may be modified by the C-terminus, the C-terminus might also regulate osteoblast

to osteocyte differentiation since Wnt signalling activation promotes cell osteogenic differentiation (Baron, Rawadi *et al*. 2006).

It is important to know whether the PTHrP C-terminus, if associated with Wnt signalling, perhaps via *Sost*, which is a Wnt signalling inhibitor known to suppress bone formation. My preliminary data showed that UMR106.01 cells, which express high levels of a Wnt inhibitor, *Sost* (Keller H, Kneissel M. 2005), but *Sost* mRNA was much more largely repressed with the presence of the PTHrP C-terminus by treatment with PTH (Section 5.5, Fig. 5.13) compared with the vector control. This suggests that the ability of the C-terminus to suppress the PTH-induced increase in *Bglap* may depend on Wnt signalling, via *Sost*. Therefore, the next step in understanding how the C-terminus regulates *Bglap* expression will need to focus on whether the Wnt inhibitor sclerostin can rescue C-terminus-induced inhibition of *Bglap*.

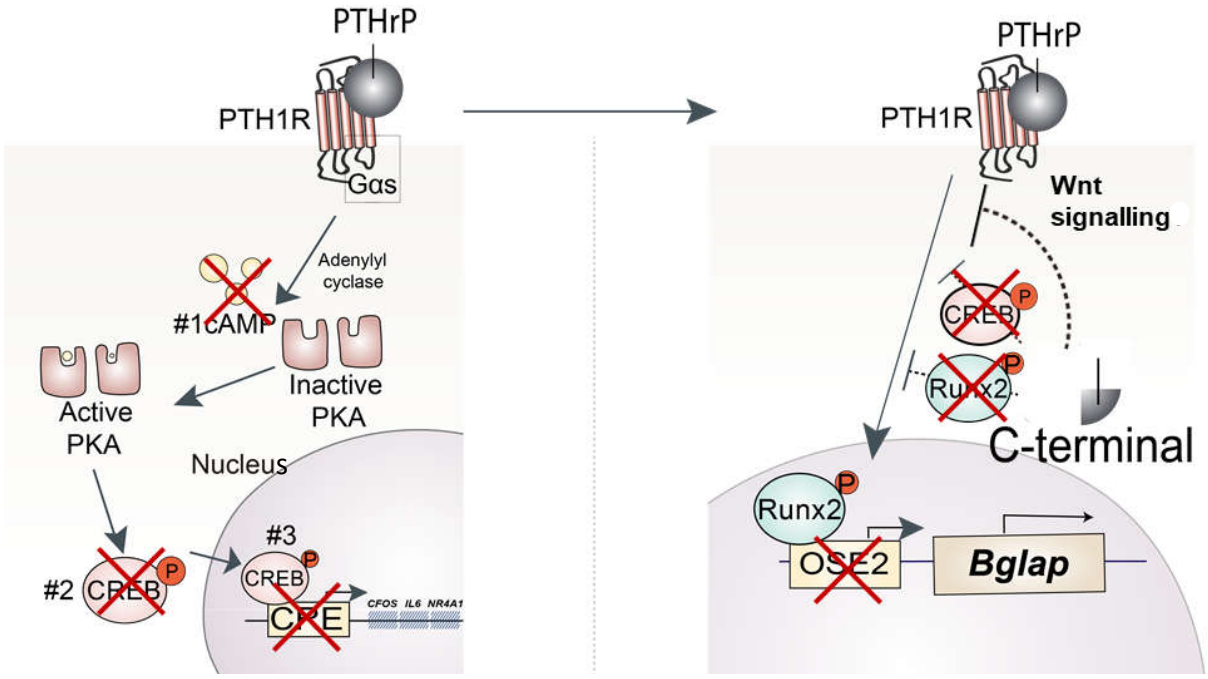

Figure 5.14. Model showing how PTHrP actions in the osteocyte may be inhibited by the PTHrP C-terminus. Our data indicates that any actions of the C-terminus to suppress PTHrP effects on gene expression are intracrine, and are beyond CREB action. The left panel shows pathways excluded through experimental work in this thesis: multiple assays have confirmed that the PTHrP C-terminus does not affect cAMP production (#1, left panel) nor CREB activity (#2, left panel). The C-terminus also did not modify binding to a CRE promoter construct; this CRE is found in the promoter of target genes *CFOS, IL6,* and *NR4A1* (#3, left panel). The right panel pictures my new hypothesis. Although the PTHrP C-terminus can inhibit the magnitude of *Bglap* transcription induced by PTHR1 signalling, this is not dependent on CREB, nor its OSE2 promoter site in interacting with Runx2 transcription factors. Since the PTHrP C-terminus can induce Wnt signalling, it is possible that the C-terminus exerts its functions via induction of Wnt signalling.

Using multiple assays, work in this chapter has shown that (Figure 5.14) the ability of the PTHrP C-terminus to inhibit PTHR1-mediated stimulation of *Bglap* gene expression does not occur by modifying cAMP/CREB activation nor is it regulated by phosphorylated Runx2 binding to the OSE2 cis-regulatory elements. Intracellular PTHrP C-terminus suppressed the *Bglap* response in UMR106.01 cells, which is consistent with the result in OCY454 cells, since

OCY454 *PTHrP*$^{\Delta NLS\Delta C}$ increases the transcription of *Bglap*. This suggests that PTHrP C-terminus mediated *Bglap* reduction is not regulated by a canonical OSE2 interaction with Runx2 pathway but can be subjected to other signalling or by other regulating elements. The reduction of *Bglap* targeted genes by PTH/PTHrP might be dependent on Wnt signalling regulation, cell-cell signalling, cell differentiation, etc based on my RNA-Seq GO analysis. In particular, the Wnt signalling requires further study.

It must be noted that these experiments are limited to stable cell lines which express high levels of PTHrP proteins, which could bring about other alterations of cell function. To confirm these findings, a strategy to avoid this may be to use cells from the mouse to generate with a knocked-in C-terminus in osteocytes to see if whether gene regulations are repressed in osteocytes isolated from mice administered by PTH or PTHrP.

5.8 Future directions

Overexpression of the PTHrP C-terminus attenuated PTHrP-induced expression of *Bglap* without affecting OSE2 promoter sites. It is necessary to examine whether OSE1 sites are required for the action of the C-terminus in inhibiting Bglap. For this experiment, 6XOSE1-luc reporter construct could be transfected into UMR106.01 cells stably overexpressing the C-terminus constructs described in this chapter.

Another necessary direction is to look for binding partners for the PTHrP C-terminus within the cells. Yeast two-hybrid screening with expression of C-terminus (122–141) as a bait and co-transfection of β-arrestin, has demonstrated that the C-terminus interacts with β-arrestin fragments, suggesting a role for PTHrP in the β-arrestin/MAPK pathway, perhaps in the modulation of the cellular response to extracellular proliferative signals (Conlan, Martin *et al*. 2002). Yeast two-hybrid screening with expression of the C-terminus (107-141) as a bait will

help to investigate more binding partners in the cytosol, and it is important to know the direct interaction of C-terminus in regulating gene expressions induced by PTH/PTHrP.

5.9 Conclusion

In conclusion, I have shown that the PTHrP C-terminus inhibition of PTHR1 signalling, which stimulates *Bglap* gene expression, does not require activation of cAMP/CREB. *Bglap* is not regulated by phosphorylated Runx2 binding to the OSE2 cis-regulatory elements. This suggests that PTHrP C-terminus mediated *Bglap* reduction is not regulated by a canonical OSE2 interaction with Runx2 pathway but can result other signalling or by other regulating elements. My preliminary data showed that the reduction of *Bglap* targeted by PTH/PTHrP might be dependent on Wnt signalling. In particular, the latter requires further study.

Chapter 6 Conditional deletion of PTHrP in late osteoblasts and osteocytes compromise bone matrix mineral composition or maturation

6.1 Introduction

Same as that in osteoblasts, PTHrP is produced in newly embedded osteocytes identified *by in situ* hybridisation (Kartsogiannis, Udagawa *et al*. 1998). Osteocytes, have been identified as mechanical sensors of the skeleton that modulate bone remodelling and bone mineral homeostasis, and they comprise 90–95% of all bone cells in adult skeleton (Aarden, Nijweide *et al*. 1994, Nicolella, Moravits *et al*. 2006). Not only is PTHrP important in osteoblasts but it also has essential roles in osteocytes. Our laboratory has recently shown that conditional knock-down of PTHrP in osteocytes results in mice with a phenotype of reduced bone strength (Ansari, Ho *et al*. 2018). Neither bone size nor bone shape was shown to be the effector of changing bone strength, leading to the conclusion that other factors must contribute to the lessening of bone strength, such as defects in the amount and structure of skeletal material (Ansari, Ho *et al*. 2018). *Osteocalcin* (*Bglap*), which is a well-characterised late marker of osteoblast differentiation and mineralisation (Gu, Fu *et al*. 2017), was strongly attenuated in *PTHrP* knock down OCY454 cells differentiated for seven and 14 days (Ansari, Ho *et al*. 2018). Moreover, it has been demonstrated that expression not only of *Bglap*, but also mineralisation gene markers *Alpl*, *Dmp1* are decreased up to day 14 in PTHrP knock down OCY454 cultures (Ansari, Ho *et al*. 2018), indicating that PTHrP is likely to be involved in bone mineralisation. However, whether such mineralisation gene changes in *Dmp1Cre.Pthlh*$^{f/f}$ is because of the change in surrounding matrix is not yet well understood. It has also been suggested by Ansari *et al*. (2018) that PTHrP affects cortical strength through a

non-receptor-mediated pathway because mice administrated PTH did not develop compromised bone matrix mineral composition or maturation (Vrahnas, Pearson *et al*. 2016). Consistent with this, my RNA-Seq result has also suggested that OCY454 cells overexpressing full length and mutant PTHrP may regulate the mineralisation process. Genes participate in the bone mineralisation biological process are involved in regulation of mineralisation from the Biological Process Annotations dataset, suggesting these mineralisation genes are regulated by overexpression of PTHrP in OCY454 *in vitro*. Thus, it is necessary to further characterise the effect of PTHrP in regulating bone composition involving in mineralisation, collagen compaction and the carbonate ration. Both *in vivo* and *in vitro* assays have confirmed that PTHrP is essential for proper formation of mineral content by the osteocytes. However, further study is needed to illustrate in what other factors may be affected by PTHrP in regulating mineralisation.

Fourier transform infrared (FTIR) spectroscopy provides information about bone composition and can also determine the amount of substance. For this reason, FTIR spectroscopy may be used to diagnose certain bone diseases characterised by poor bone strength. In this research, I established the contribution of mineral and collagen properties to PTHrP defects through FTIR spectroscopy, analysing the biochemical profile differences between femoral strength of *Dmp1Cre.Pthlh*$^{f/f}$ mice and *Dmp1Cre.Pthlh*$^{w/w}$ mice.

6.2 Methods

Genes important for the mineralisation process were selected for my bioinformatic analysis based on the methods of section 2.10.5 and 2.10.6. To determine whether adult *Dmp1Cre.Pthlh*$^{f/f}$ mice exhibit a modification in bone composition, high resolution synchrotron-based Fourier Transform Infrared (FTIR) microspectroscopy (Rey, Collins *et al*. 1989, Bi, Li *et al*. 2005, Fuchs, Allen *et al*. 2008) was used in a region of non-remodelling

cortical bone of 12-week-old *Dmp1Cre.Pthlh*$^{f/f}$ mice compared with *Dmp1Cre.Pthlh*$^{w/w}$ littermate bone samples. Mineralisation and composition were measured by FTIR microspetroscopy from the most immature bone on the periosteal to the end of endosteal edge, which allowed multiple measurements of progressive changes in bone matrix during the maturation (Rey, Collins *et al*. 1989, Bi, Li *et al*. 2005, Fuchs, Allen *et al*. 2008) explained in Methods section 2.11.

Spectra were collected at 1,500 μm, from the medial side of tibiae, across the full width of cortex from the base of the hypertrophic zone of the growth plate (Vrahnas, Pearson *et al*. 2016, Vrahnas, Buenzli *et al*. 2018). I set the starting point for FTIR measurement on the periosteal site and continued to measure the regions of interest through the width of bone. I collected at least five to eight measurements using FTIR and analysed the data using OPUS, depending on bone width, with each measurement taken at 10 μm intervals. For analysis of spectra I defined the first periosteal and endosteal regions by the characteristic height and shape of phosphate peak. If there was not a clear and obvious peak, I excluded the spectrum from the dataset. For example, in my analysis, I have excluded the data when the mineral to matrix ratio is below 3.0 based on my data; meantime excluded the data when the phosphate shape is not obvious.

For qPCR analysis on the bone samples, data from zero to five animals were excluded during analysis of gene expression in male and female femora when flushed of bone marrow in WT and PTHrP-deficient mice, when there was contamination during PCR handing or when the data was zero, which was not detected.

6.3 RNA-Seq identified mineralisation genes are regulated by overexpression of PTHrP in osteocyte

Using all the DE genes (P<0.05) from the OCY454 *PTHrP*^{FL} for DAVID Functional Annotation Bioinformatics Microarray Analysis, I assessed fifteen major GO annotations

associated with different biological process (Fig. 6.1A). This data showed that two out of the top fifteen GO terms are related to the bone mineralisation process.

Genes that are involved in these two GO terms with Log_2 fc values regulated in OCY454 *PTHrP*^{FL} compared to the vector control are shown in Fig. 6.1B and Fig. 6.1C. Thirteen genes participate in the bone mineralisation biological process (GO:0030282) and 12 are involved in regulation of mineralisation (GO:0030500) from the GO Biological Process Annotations dataset, suggesting these mineralisation genes are regulated by overexpression of PTHrP in OCY454 *in vitro*.

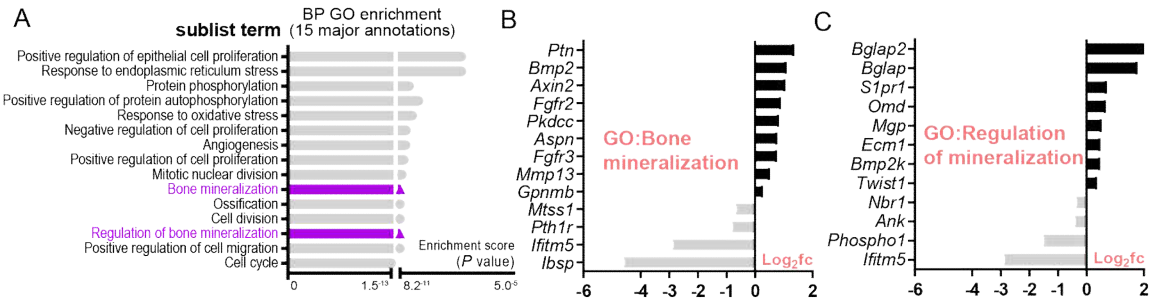

Figure 6.1. GO analysis output revealed bone mineralisation genes are regulated by PTHrP overexpression in OCY454 osteocytes. (A) Enriched GO Terms in biological process showing 15 top - ranked biological processes (BP) GO categories. Two out of fifteen GO terms are pointing to bone mineralisation regulation. (B) Genes in the bone mineralisation and (C) Regulation of bone mineralisation categories are shown in $\log_2$ scale.

6.4 Determination of the mineral defects of osteocytic PTHrP deletion on bone structure *in vivo*

6.4.1 *Dmp1Cre.Pthlh$^{f/f}$* induced a mild change in carbonate content in female bone compared with *Dmp1Cre.Pthlh$^{w/w}$*

As proof of the validity of FTIR microspectroscopy to measure mineralisation (Vrahnas, Pearson *et al*. 2016, Vrahnas, Dite *et al*. 2018), I observed that phosphate (mineral): amide I (matrix) ratio increased significantly with increasing depth into the bone *Dmp1Cre.Pthlh$^{f/f}$* and *Dmp1Cre.Pthlh$^{w/w}$* tibial section (Fig. 6.2A), with increases reaching a plateau in the centre. However, there were no significant differences in mineral:matrix ratio between the *Dmp1Cre.Pthlh$^{f/f}$* and *Dmp1Cre.Pthlh$^{w/w}$* group (Fig. 6.2A, B), suggesting the mineral content, the amount of matrix, or both, were not affected.

In contrast, the amount of carbonate incorporated within hydroxyapatite mineral crystal lattice (carbonate: mineral ratio) measured in *Dmp1Cre.Pthlh$^{f/f}$* mice showed a significantly different carbonate to mineral ratio compared with the values in the control group (Fig. 6.2C, D). Although the *Dmp1Cre.Pthlh$^{w/w}$* mice showed an lower increase in carbonate to mineral ratio from the immature periosteal edge to the centre (compared to periosteal region P-one to P-three), the *Dmp1Cre.Pthlh$^{f/f}$* bone had a lower carbonate:mineral ratio overall compared to *Dmp1Cre.Pthlh$^{w/w}$* (P-four to P-six). Because the relative difference between *Dmp1Cre.Pthlh$^{w/w}$* and *Dmp1Cre.Pthlh$^{f/f}$* reverses when comparing lower periosteal regions to higher ones, the overall difference between *Dmp1Cre.Pthlh$^{w/w}$* and *Dmp1Cre.Pthlh$^{f/f}$* is minimal. A post-hoc test of all six periosteal regions simultaneously is therefore unable to identify a significant difference between the two groups.

There was no significant difference in the amide I:II suppression, which is used to ascertain collagen compaction (Vrahnas, Pearson *et al*. 2016), nor in interaction between genotype and

region, suggesting that no significant effects of *Dmp1Cre.Pthlh*$^{f/f}$ were exerted on molecular collagen compaction (Fig. 6.2E,F). However, *Dmp1Cre.Pthlh*$^{f/f}$ animal had a lower amide I:II ratio in the last region from endocortical edge (Fig. 6.2E).

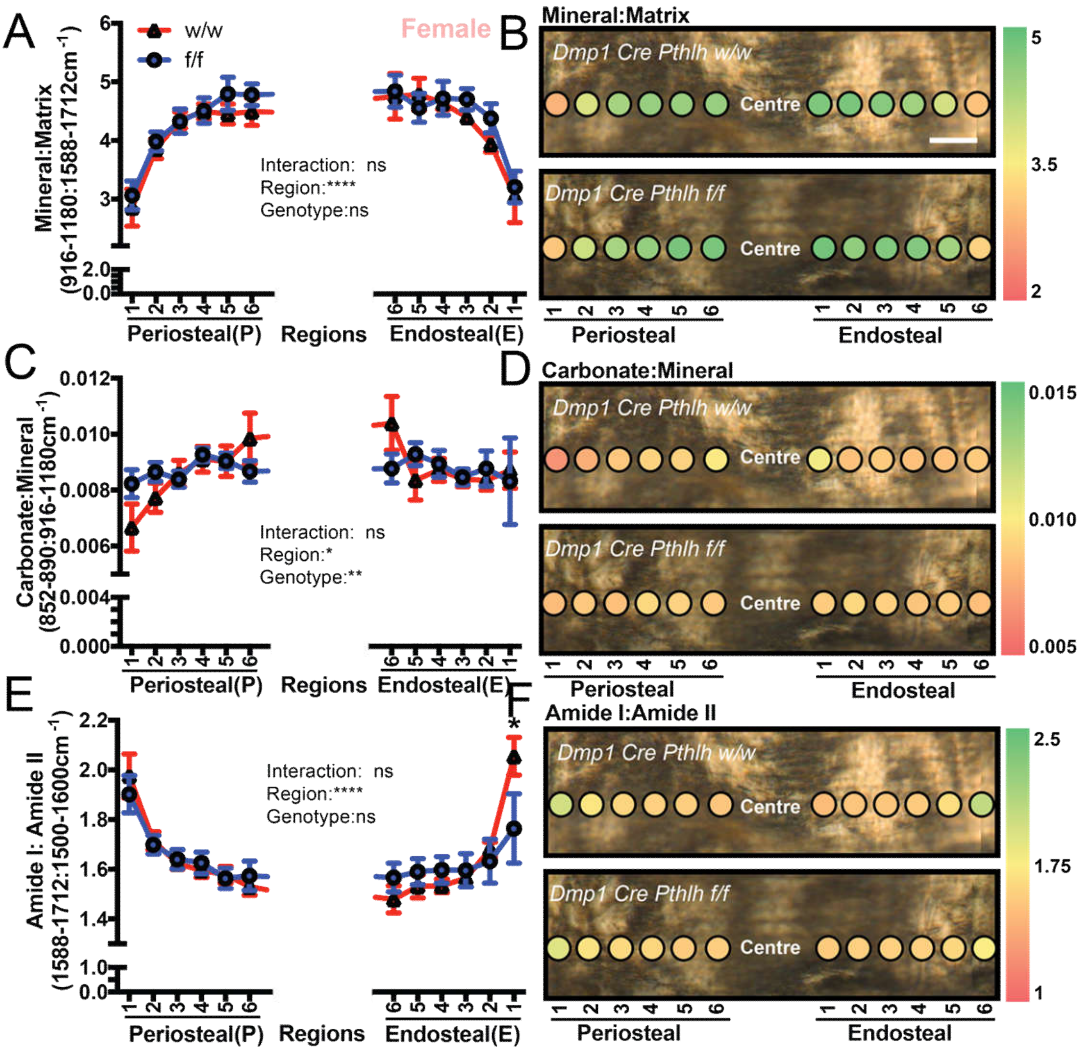

Figure 6.2. PTHrP knock out induced a mild increase in carbonate content in female mice. FTIR microspectroscopy -derived female animals mineral:matrix (A), carbonate: mineral (C), amide I:II (E) ratios in regions 1-6 (from periosteal and endosteal edges) of *Dmp1Cre.Pthlh*$^{w/w}$ and *Dmp1Cre.Pthlh*$^{f/f}$ tibiae. Data are represented as mean ± SEM, n = (6-10)/group. *p<0.05, **p<0.01, ***p<0.001 vs *Dmp1Cre.Pthlh*$^{w/w}$ in the same region (genotype effect). Two-way ANOVA followed by Fisher's LSD *post hoc* test at all regions. (B,D,F) Heatmaps of values identified in mineral:matrix (B), carbonate: mineral (D), amide I:II (F) ratios in regions 1-6 of *Dmp1Cre.Pthlh*$^{w/w}$ and *Dmp1Cre.Pthlh*$^{f/f}$ tibiae.

6.4.2 Male *Dmp1Cre.Pthlh$^{f/f}$* mice exhibited greater amide I:II ratios compared to controls

To examine whether impaired bone strength in 12-week old *Dmp1Cre.Pthlh$^{f/f}$* male mice was due to altered bone composition, region-based FTIR microspectroscopy was performed from the periosteal edge through to mature regions of the tibia, as was performed for the female group. In male bone, a significantly lower level of mineral to matrix ratio was detected in *DMP1Cre.Pthlh$^{f/f}$* mice compared to their controls (Fig. 6.3A). This indicates that the mineral content is significantly decreased in male *Dmp1Cre.Pthlh$^{f/f}$* mice. I observed this decreased mineral content phenotype in *Dmp1Cre.Pthlh$^{f/f}$* in every single region compared to the *Dmp1Cre.Pthlh$^{w/w}$*, as represented visually in Fig. 6.3B. Mineral content in both *Dmp1Cre.Pthlh$^{f/f}$* and *Dmp1Cre.Pthlh$^{w/w}$* increases towards the centre (region six) of the bone. Mineral content in both *Dmp1Cre.Pthlh$^{f/f}$* and *Dmp1Cre.Pthlh$^{w/w}$* increases towards the centre (region six) of the bone.

Unlike females, there was no significant difference between *Dmp1Cre.Pthlh$^{f/f}$* and *Dmp1Cre.Pthlh$^{w/w}$* bone in the carbonate:mineral ratio (Fig. 6.3C,D), suggesting this ratio is not changed in male *Dmp1Cre.Pthlh$^{f/f}$* mice.

The amide I:II ratio was determined to be 25% greater at the periosteal and endosteal edges than at the centre of the bone, as previously observed in the female group, in both *Dmp1Cre.Pthlh$^{w/w}$* and *Dmp1Cre.Pthlh$^{f/f}$* samples (Fig. 6.3E,F). However, the ratio was significantly higher in *Dmp1Cre.Pthlh$^{f/f}$* mice (Fig. 6.3E,F). A post-hoc test at all regions was done but not informative for the reason mentioned previously. This is the most significant effect that I have seen in the male group.

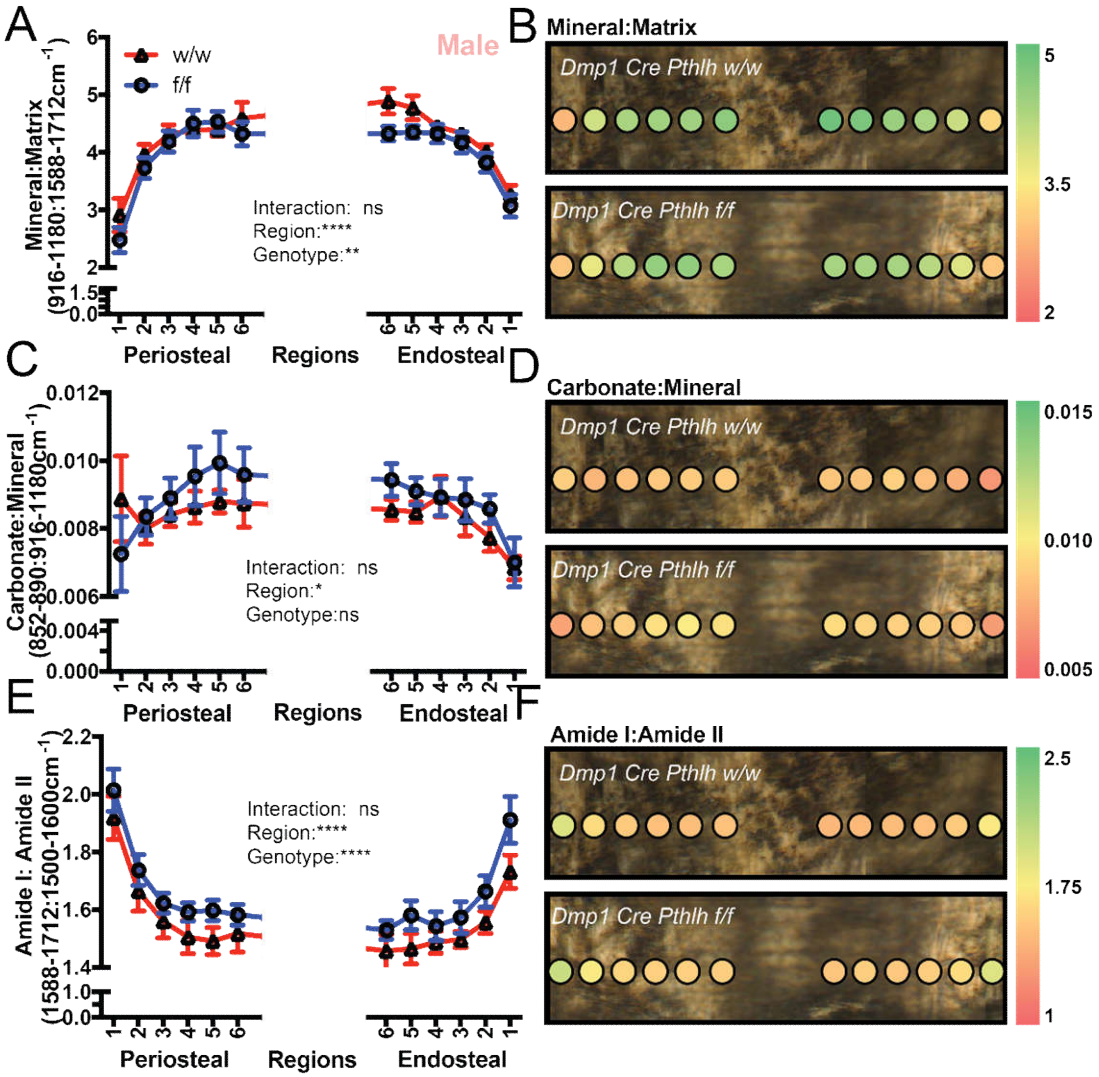

Figure 6.3. A lower level of mineral to matrix ratio has been detected in male PTHrP knock-out mice. FTIR microspectroscopy-derived Male animals mineral:matrix. (A), carbonate: mineral (C), amide I:II (E) ratios in regions 1-6 (from periosteal and endosteal edges) of *Dmp1Cre.Pthlh*$^{w/w}$ and *Dmp1Cre.Pthlh*$^{f/f}$ tibiae. Data are represented as mean ± SEM, n = (6-10)/group. *p<0.05, **p<0.01, ***p<0.001 vs *Dmp1Cre.Pthlh*$^{w/w}$ in the same region (genotype effect). Two-way ANOVA followed by Fisher's LSD *post hoc* test at all regions. (B,D,F) Heatmaps of values identified in mineral: matrix (B), carbonate:mineral (D), amide I:II (F) ratios in regions 1-6 of *Dmp1Cre.Pthlh*$^{w/w}$ and *Dmp1Cre.Pthlh*$^{f/f}$ tibiae.

6.5 Male *Dmp1Cre.Pthlh$^{f/f}$* resulted in canalicular network defects

During mineralisation osteocytes form long dendritic processes that are believed to allow them to communicate with other osteocytes and with the periosteum, endosteum, and vasculature on the bone surface (Kamioka, Honjo *et al*. 2001, Sugawara, Kamioka *et al.* 2005, Kerschnitzki, Kollmannsberger *et al*. 2013). The processes also allow osteocytes access to sufficient nutrients including oxygen (Dallas, Prideaux *et al*. 2013) during the mineralisation process. In order to identify whether canalicular networks are modified by PTHrP, I used silver nitrate stain to visualise the osteocyte lacuno-canalicular network. Regions were analysed commencing from the growth plate. Representative images were taken for each microscope view. Male *Dmp1Cre.PTHrP$^{f/f}$*, prepared by Ansari *et al.* (2018), exhibited impaired and low density canalicular structure in cortical bones at 12 weeks age. In some areas the structure was comparable to that in *Dmp1Cre.Pthlh$^{w/w}$*, whereas in other areas the tissue stained very poorly and canalicular networks were meandering or apparently absent. Additionally, of all the regions from the microscope field of view that I measured, only one region of all measured regions revealed a difference between *Dmp1Cre.PTHrP$^{f/f}$* and *Dmp1Cre.Pthlh$^{w/w}$*. After calculation of the position of this specific region, I found the region was at the same position as I have measured for detecting the bone composition by FTIR microspectroscopy (~1,500 μm down from the growth plate; Fig. 6.4). These preliminary data suggest that PTHrP may be an important factor in maintaining the normal osteocyte canalicular network associated with the mineralisation process.

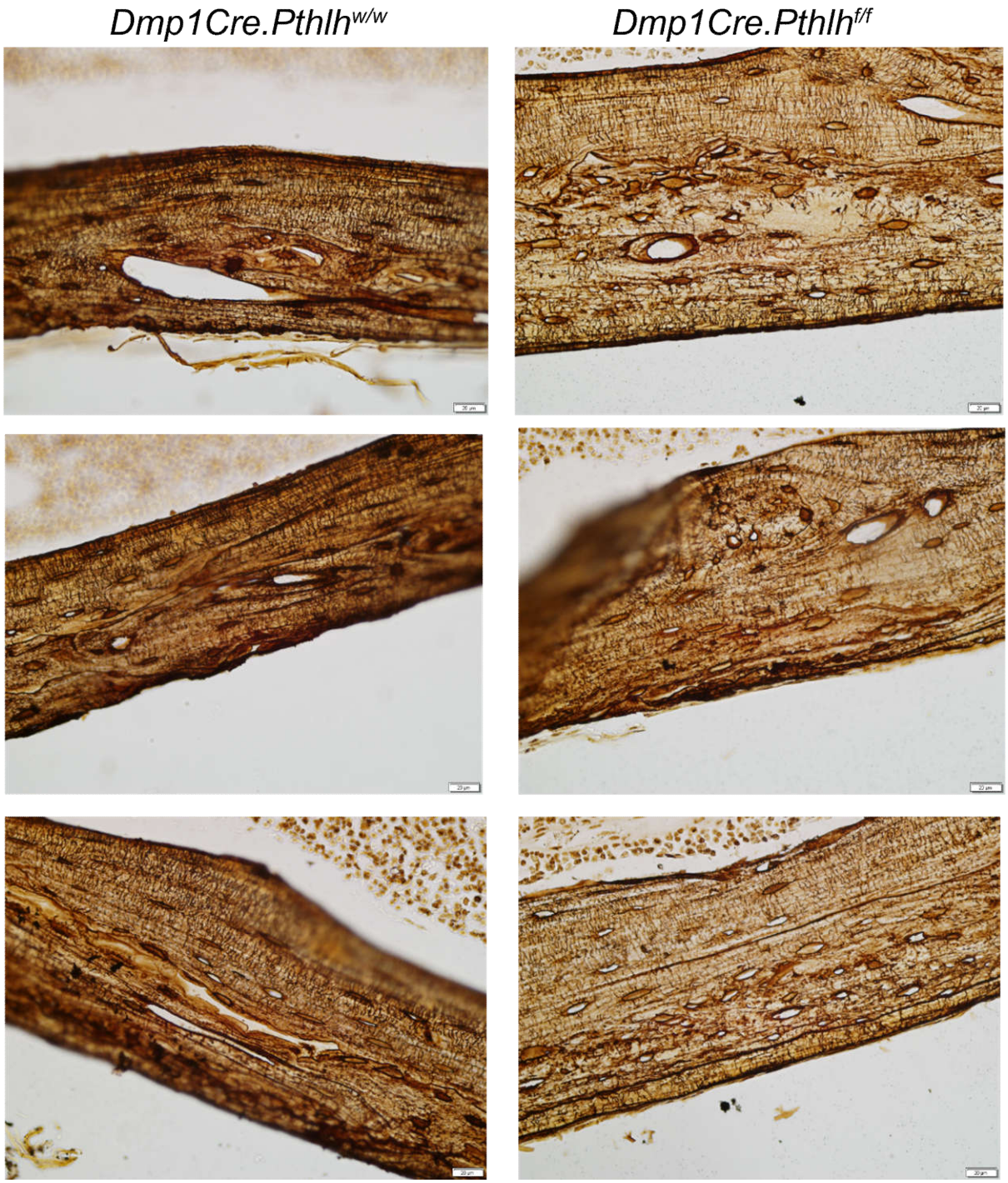

Figure 6.4. Network morphogenesis and canaliculi formation are impaired in male *Dmp1Cre.PTHrP$^{f/f}$* cortical bone**.** Silver nitrate staining of osteocytic canaliculi in the young (12-week-old) cortical femurs. *Dmp1Cre.Pthlh$^{w/w}$* mice feature straighter canaliculi and stronger silver nitrate staining than *Dmp1Cre.PTHrP$^{f/f}$* mice; this indicates the impaired, lower-density canalicular structure present in *Dmp1Cre.PTHrP$^{f/f}$* mice. Scale bars = 20 µm. Each row represents an individual animal.

6.6 Bone mineralisation defects were not associated with systematic changes in known mineralisation genes

To determine alterations in mineralisation genes, RNA from flushed tibiae from both *Dmp1Cre.Pthlh*$^{f/f}$ and *Dmp1Cre.Pthlh*$^{w/w}$ were used to assess mineralisation gene expression (Section 2.16). Only *Secreted Phosphoprotein 1* (*Spp1*; Peacock, Huk *et al.* 2011) decreased in the *Dmp1Cre.Pthlh*$^{f/f}$ female group (Fig. 6.6F) and the remaining gene transcripts *Integrin Binding Sialoprotein* (*Ibsp;* Bouleftour, Boudiffa *et al.* 2014), *Interferon Induced Transmembrane Protein 5* (*Ifitm;* Hanagata 2016*;* Hanagata and Nobutaka 2016), *Sphingolipid Transporter 2 (Spns2*; Bougault, El Jamal *et al.* 2017*,* Spiegel, Maczis *et al.* 2019), *Phosphoethanolamine/Phosphocholine Phosphatase 1 (Phospho1*; Houston, Stewart *et al.* 2004), *Ectonucleotide Pyrophosphatase/Phosphodiesterase 1* (*Enpp1*; Kato, Nishimasu *et al.* 2012, Kato, Nishimasu *et al.* 2012) do not behave significantly differently from that in *Dmp1Cre.Pthlh*$^{w/w}$ mice. *Spp1* was not significantly regulated in male *Dmp1Cre.Pthlh*$^{f/f}$ compared to *Dmp1Cre.Pthlh*$^{w/w}$. This suggests that the *Dmp1Cre.PTHrP*$^{f/f}$ bone mineralisation defects are not likely associated with any significant change in expression of known mineralisation genes.

Thus, the above FTIR data indicates that a lack of PTHrP could interfere the amide I:II ratio in male mice, suggesting PTHrP modifies the collagen matrix. Both male and female overall mineral contents significantly changed, as explained previously. The above mineralisation genes did not provide any further explanation, so to ascertain whether PTHrP regulates the mineralisation process, I subsequently identified the role of PTHrP by in vivo examination.

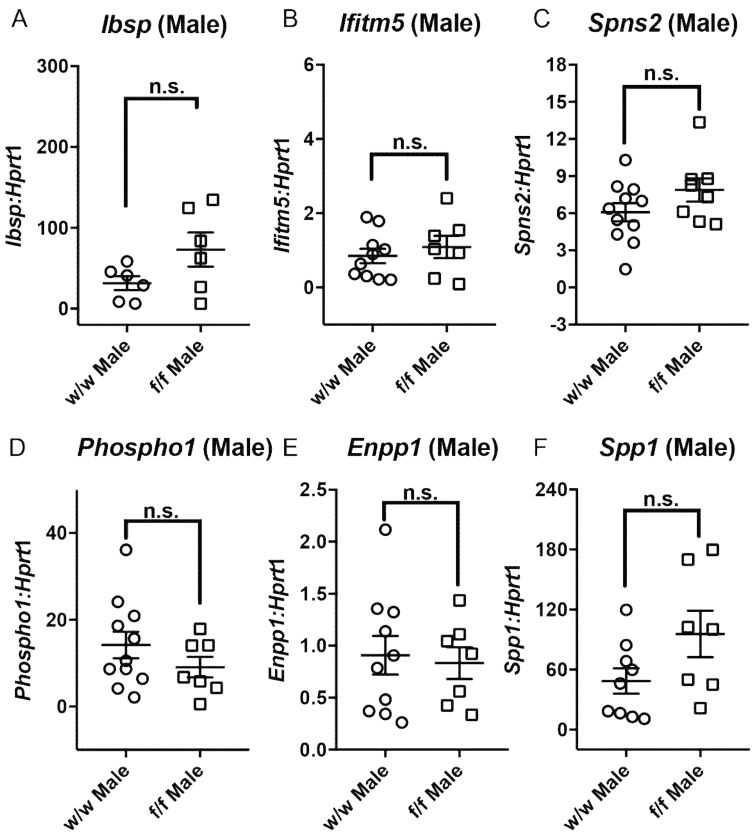

Figure 6.5. qPCR analysis of the gene expression in the Male femurs when flushed for bone marrow in WT and PTHrP-deficient mice. Total RNA was extracted from homogenised marrow-flushed bone, and RT-PCR was performed using primer sets for murine *Ibsp* (A), *Ifitm5* (B), *Spns2* (C), *Phospho1* (D), *Enpp1* (E) and *Spp1* (F) genes. The data are expressed as the mean±SEM, n=6-10. *, P 0.05; **, P 0.01; ***, P 0.001 (compared with vehicle control, One-way ANOVA). n.s. means not signicant.

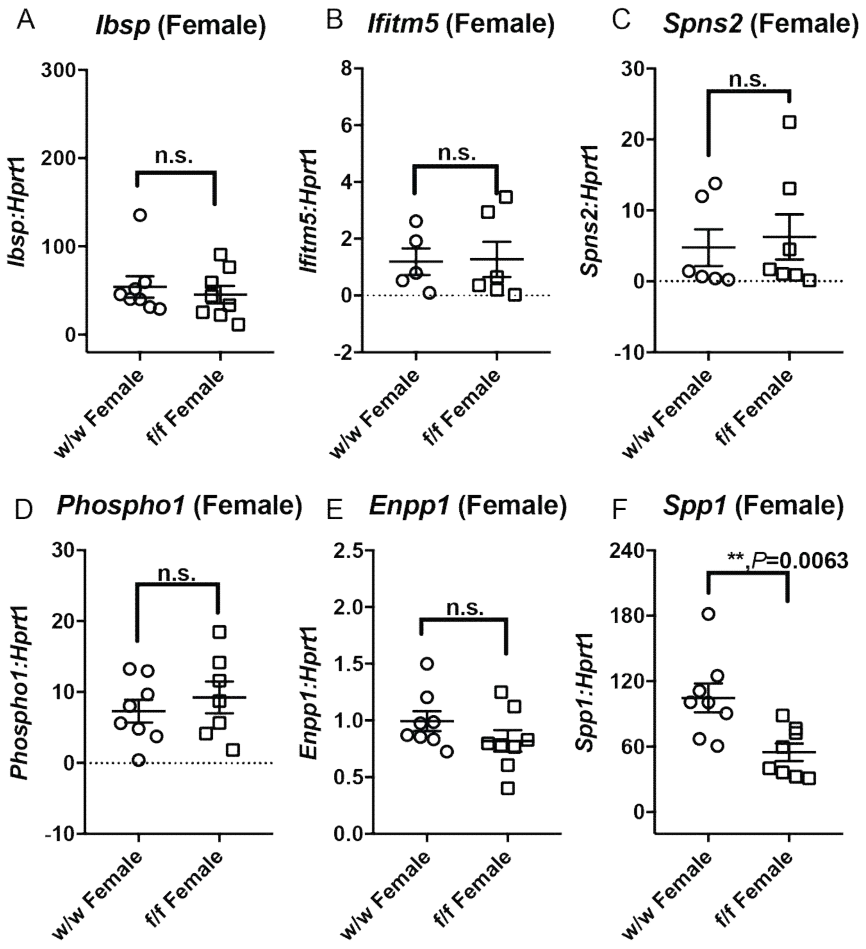

Figure 6.. qPCR analysis of the gene expression in the Female femurs when flushed for bone marrow in WT and PTHrP-deficient mice. Total RNA was extracted from homogenised marrow-flushed bone, and RT-PCR was performed using primer sets for murine *Ibsp* (A), *Ifitm5* (B), *Spns2* (C), *Phospho1* (D), *Enpp1* (E) and *Spp1* (F) genes. The data are expressed as the mean±SEM, n=5-10. *, P 0.05; **, P 0.01; ***, P 0.001 (compared with vehicle control, One-way ANOVA). n.s. means not significant.

6.7 Both PTHrP overexpression and PTHrP knock-down in OCY454 cells exhibited bone mineralisation defects *in vitro*

To detect whether mineralised calcium-rich deposits were affected by PTHrP *in vitro*, Alizarin red S (ARS) staining was used for further analysis at day zero, four, and seven in OCY454 cells (Section 2.9). The OCY454 Luc Ctrl vector control cells (Luc Ctrl vector control) had a greater amount of staining compared to the PTHrP knock-down cells (PTHrP KD), indicating the PTHrP deficiency had delayed the induction of proper mineral content (Fig. 6.7A,B,C). However, this is preliminary data as the mineralisation assay of OCY454 PTHrP knock-down cells and the control cells were only performed once each. Further replication is needed. In the mineralisation assay I detected a decreased level of positive staining in $PTHrP^{FL}$ compared to the pMSCV vector control (Fig. 6.7D,E,F). The quantification of the positive areas showed a significant induction of deposits in pMSCV over $PTHrP^{FL}$ (n=3). Inset images in Figure 6.7C and Figure 6.7F show parts of the surface of non-classical osteoblast-like mineralised nodules at day 7, at 20x magnification. Overall, this suggests that both PTHrP knock-down and overexpression in osteocytes impairs the mineralisation process.

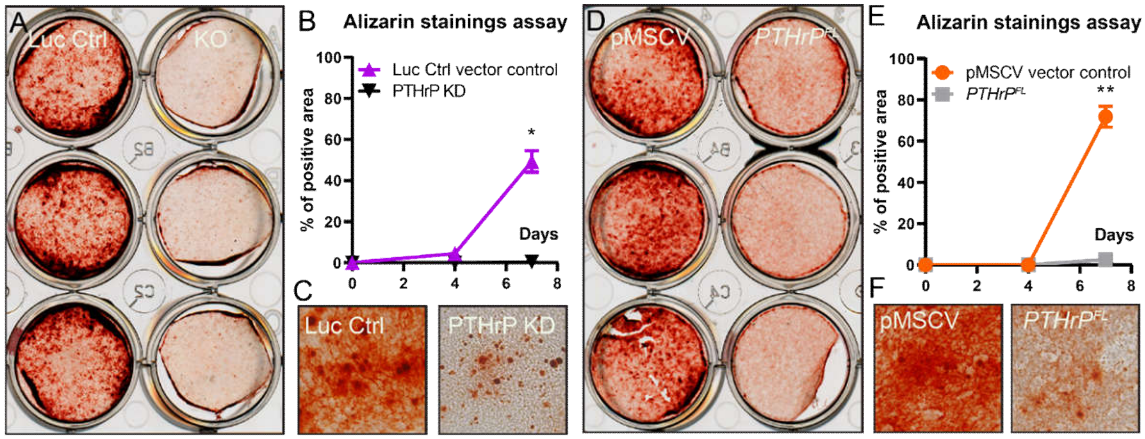

Figure 6.6. Overexpression and knock down of PTHrP significantly represses osteocytes mineralisation. Stained calcium deposition of Luc Ctrl vector control vs PTHrP-KD (A) and pMSCV vector control vs *PTHrP*^{FL} (D) by Alizarin Red S at day 7. (B,E) Alizarin Red-S staining of mineralised nodules under osteogenic condition for 0, 4 and 7 days. Mineralisation area was quantitated through image J to get % of positive area of total to represent stained mineral deposits. Results from A-C are mean ± SEM of the three replicates in three independent experiments, *P<0.05. Results from D-F are mean ± SEM, n=3 replicates of one independent experiment. (C, F) Insets images at 20x magnification of mineral at day 7.

6.8 Mineralisation genes were down-regulated in OCY454 overexpressing PTHrP but up-regulated in PTHrP-KD cells

Since mineralised deposits were disrupted by PTHrP overexpression, I then checked the mineralisation genes' regulation patterns. Five mineralisation genes (*Ifitm5*, *Ibsp*, *Spns2*, *Alpl*, and *Spp1*) were chosen for study of their regulation patterns, as these genes were not analysed by Ansari et al. (2018). *Ifitm5*, *Ibsp*, *Spns2*, and *Alpl* were significantly down-regulated by PTHrP overexpression (Fig. 6.8). *Spp1* was also down-regulated but not significantly.

Ifitm5 and *Ibsp* were both significantly up-regulated in PTHrP knock down osteocytes. *Spns2* and *Alpl* were up-regulated but not significantly in OCY454 with PTHrP knocked-down. *Spp1* was down-regulated significantly. These findings suggest the mineralisation genes were down-regulated by PTHrP overexpression, but absence of PTHrP can almost rescue the gene regulation phenotype.

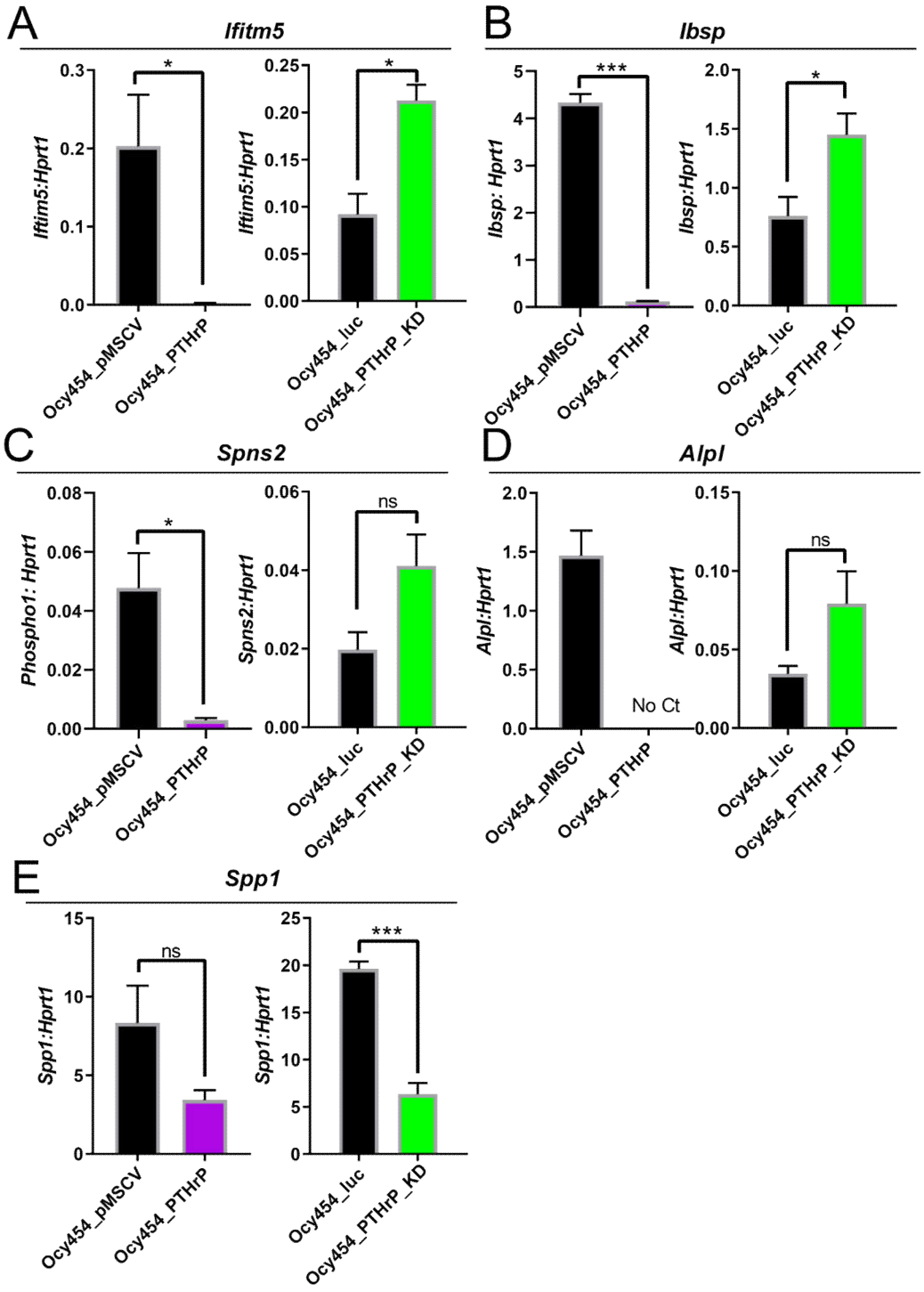

Figure 6.7. PTHrP regulates expression of mineralisation genes in OCY454 osteocytes. The relative mRNA expression of *Ifitm5*, *Ibsp*, *Spns2*, *Alpl* and *Spp1* were measured by qRT-PCR at days 14. *Hprt1* was used as an internal control. All of the data represent means ± SEM of three biological samples in at least one independent experiment. * $p < 0.05$, ** $p < 0.01$, *** $p < 0.001$. Unpaired Student's t test. OCY454_pMSCV: OCY454 vector control; OCY454_PTHrP: OCY454 PTHrP overexpressing; OCY454_luc: OCY454 vector control; OCY454_PTHrP_KD: OCY454 with PTHrP knocked-down. (Section 2.4.1)

6.9 OCY454 *PTHrP*^{FL} regulates differentiation markers for the development from osteoblasts to osteocytes

Since *PTHrP*^{FL} did not harbour an opposing mineralisation defect to PTHrP knock-down cells *in vitro,* I next investigated whether PTHrP overexpression caused a change in the osteocyte differentiation process. It is established that during the first steps of commitment pre-osteoblasts express ALP, COL1, RUNX2, and osterix (Huang, Yang *et al.* 2007, Sims, White *et al.* 1997, Miron and Zhang 2012). Soon after, osteoblast express markers: ALP, COL1, Osteocalcin, Osteopontin, and Bone sialoprotein (Huang, Yang *et al.* 2007, Sims, White *et al.* 1997, Miron and Zhang 2012). These genes assiociated are listed in Fig.6.9A.

To more clearly demonstrate that the PTHrP and PTHrP functional regions are participating in OCY454 differentiation, I decided to return to my RNA-Seq data to assess the genes involved in differentiation development (Fig. 6.9A) in OCY454 overexpressing full-length or mutant PTHrP. A list of differentiation markers for pre-osteoblasts, osteoblasts, and osteocytes during osteoblast differentiation to osteocytes is shown in Fig. 6.9A. Overall expression of differentiation genes (including *Alpl*, *Col1a1*, *Runx2*, *Bglap*, *Spp1*, and *Ibsp*) in RNA-Seq of osteocytes overexpressing full-length and mutant forms of PTHrP (*PTHrP*$^{\Delta NLS\Delta C}$, *PTHrP*$^{\Delta NLS}$, and *PTHrP*$^{\Delta Sec}$) revealed different overall gene regulation patterns distributed within different isoforms of PTHrP (Fig. 6.9B,C). The normalised mean of the degree of differentiation gene marker expression in full-length PTHrP, *PTHrP*$^{\Delta NLS\Delta C}$, and *PTHrP*$^{\Delta NLS}$ is one-Log2 fold change greater than the vector control, whereas the *PTHrP*$^{\Delta Sec}$ is one-fold lower. This suggests the PTHrP and PTHrP functional regions may have important roles in the process of differentiation from osteoblast to osteocyte.

Osteocytes have less osteoblast markers but express DMP1 (Feng, Ward *et al.* 2006, Zhu, Mackenzie *et al.* 2011), MEPE (Nampei, Hashimoto *et al.* 2004, Zhu, Mackenzie *et al.* 2011), PHEX (Ruchon, Tenenhouse *et al.* 2000) and SOST (Zhu, Mackenzie *et al.* 2011), thereby representing osteocyte gene expression markers as they become embedded in the mineralising osteoid matrix *in vivo* (Ansari *et al.* 2018). It has been suggested by Ansari. et al. (2018) by qPCR that the effect of PTHrP knockdown was associated with an early increase in all three osteocyte markers: *Sost* and *Dmp1* mRNA levels were expressed ~three-fold greater in PTHrP knockdown OCY454 than control cells at day seven and fourteen of differentiation, while *Mepe* mRNA was two-fold greater in PTHrP knockdown cells compared to control at day fourteen. I then decided to assess these three genes expression in RNA-Seq data in OCY454 overexpressing full-length or mutant PTHrP. However, none of these genes were significantly regulated by the four OCY454 PTHrP overexpressing cell lines, indicating PTHrP overexpression in OCY454 does not affect osteocyte differentiation markers.

As mentioned in the last section, different studies have shown the importance of *Alpl* and *Ibsp*, not only in cell mineralisation but also in osteoblast cell differentiation. These two markers were extremely down-regulated by full-length PTHrP overexpression using qPCR (Fig. 6.8B, D), which confirmed a disruption of the gene patterns of osteoblast differentiation. Therefore, the mineralisation defects that were observed in OCY454 $PTHrP^{FL}$ may occur due primarily to a failure to differentiate at osteoblast stage rather than to mineralise the matrix.

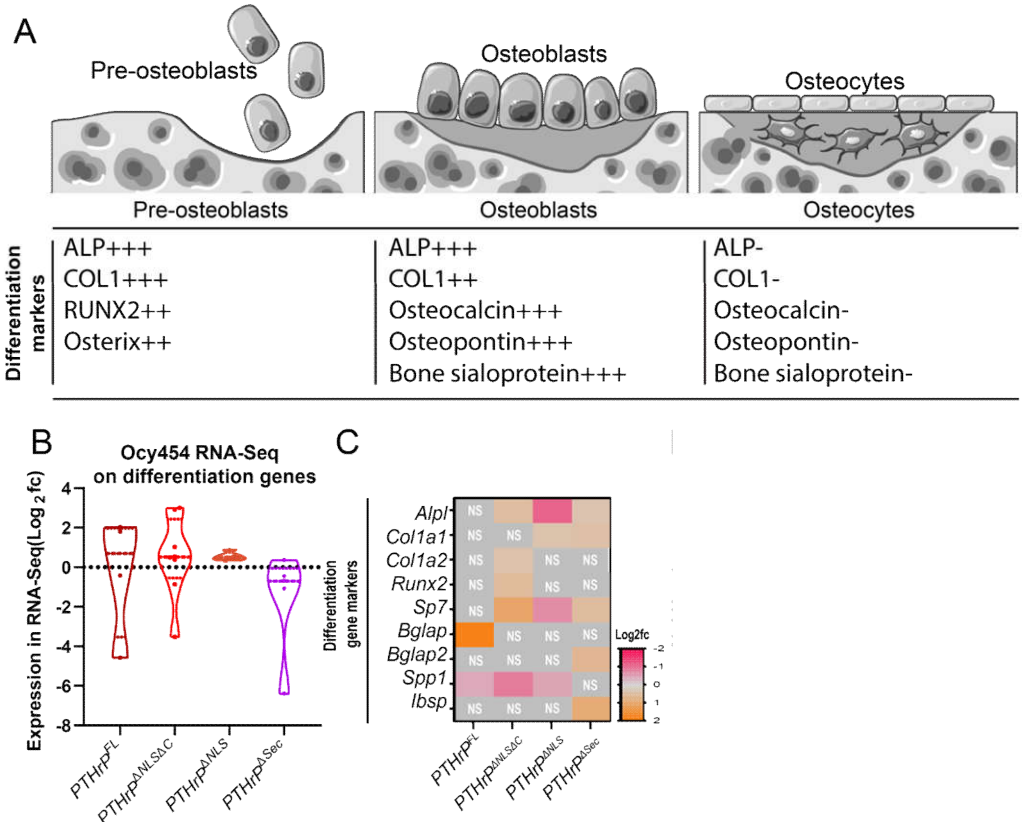

Figure 6.8. OCY454 differentiation has been compromised in *PTHrP*^{FL}. (A) A list of differentiation markers for pre-osteoblasts, osteoblasts, and osteocytes during osteoblast differentiation to osteocytes. (B) Violin plots showing the mean and variance difference on differentiation genes among the OCY454 four cell lines. Differentiation genes have been regulated in *PTHrP*^{FL}. (C) Expression level of overall differentiation gene markers in OCY454 overexpressing PTHrP full length and mutant forms in RNA-Seq. (D) Details of expression level in OCY454 RNA-Seq data.

6.10 Discussion

In this chapter I showed that osteocytes overexpressing full length PTHrP (OCY454 *PTHrP*^{FL} cells) exhibited regulation of GO-identified mineralisation genes. This led me to study the bone composition in mice with PTHrP knockdown (*Dmp1Cre.Pthlh*$^{f/f}$). This identified a significantly higher amide I:II ratio in male *Dmp1Cre.Pthlh*$^{f/f}$ bone, suggesting significantly less collagen compaction. Male *Dmp1Cre.Pthlh*$^{f/f}$ also exhibited a significant change in mineral to matrix ratio compared to *Dmp1Cre.Pthlh*$^{w/w}$, but this was only consistent on endocortical regions. This suggests a requirement of PTHrP for both collagen organisation and mineral formation. Surprisingly, preliminary *in vitro* results showed that both PTHrP knocked-down cells and overexpression cells had a low mineralised deposit phenotype.

Vrahnas *et al*. (2016) found a significant decline in the amide I:II ratio with increasing distance towards the centre of the bone. My results are consistent with Vrahnas *et al*. (2016), and I found that the amide I:II ratio was determined to be 25% greater at the (relatively immature) periosteal and endocortical edges than at the (relatively mature) centre of the bone, as observed in both male and female group, in both *Dmp1Cre.Pthlh*$^{f/f}$ and *Dmp1Cre.Pthlh*$^{w/w}$ samples. This suggests that the bones of *Dmp1Cre.Pthlh*$^{f/f}$ have less mature composition than *Dmp1Cre.Pthlh*$^{w/w}$.

Amide I:II suppression is used to ascertain collagen compaction (Vrahnas, Pearson *et al*. 2016). The decline in the amide I:II ratio observed towards the maturing centre of the bone means that mature bone has more compact collagen. My *in vivo* study showed a significantly higher amide I:II ratio in male *Dmp1Cre.Pthlh*$^{f/f}$, suggesting a significant decrease in collagen compaction in *Dmp1Cre.Pthlh*$^{f/f}$. The amide I:II ratio reflects peptide bond vibrations in collagen molecules (McCreadie, Morris *et al*. 2006). Amide I (C = O stretch) and amide II (C–N, N–H bend)

vibrations, move parallel and perpendicular respectively, to the axis of the collagen triple helix axis. Vrahnas *et al*. (2016) suggested two possibilities for this result in maturing bone matrix: that collagen fibres are more stretched (hence greater distance between C and N atoms) parallel to the fibre axis, or that the collagen is more compressed in width (hence lesser distance between C and O atoms). This suggests that this less mature bone is composed of collagen fibres that are either less stretched in parrallel or less compressed in width. To elucidate whether higher amide I:II ratios in male *Dmp1Cre.Pthlh*$^{f/f}$ mice are specific to collagen fibres running longitudinally or transversely across the bone, polarised Fourier-transform infrared imaging (pFTIRI) under 0° and the 90° polarising filters could be used to determine this.

Whether the increase in the amide I:II ratio is due to a defect in collagen deposition/production is not known, but the collagen type I alpha 1 (*Col1a1*): collagen type I alpha 2 (*Col1a2*) mRNA ratio can be an indicator of collagen I production(Couchourel, Denis, *et al*. 2009). The aberrant ratio observed in *DMP1Cre.gp130*$^{f/f}$ was the result of significantly reduced *Col1a1*:*Col1a2* mRNA expression, which implies the collagen I triple helix was malformed in *DMP1Cre.gp130*$^{f/f}$ mice (Johnson, Brennan et. al 2014). To analyse my data thoroughly to understand the mechanisms, I also analysed *Col1a1* and *Col1a2* mRNA levels in OCY454 RNA-Seq data, however, neither of these two genes were regulated by PTHrP overexpression in the cells. Therefore, the *Col1a1*:*Col1a2* mRNA ratio is unknown in OCY454 when PTHrP are overexpressed, suggesting PTHrP does not regulate collagen mRNA directly. This further suggests that the less compacted collagen in male *Dmp1Cre.Pthlh*$^{f/f}$ mice may not be due to a defect of collagen deposition, but other defects of the collagen.

Vrahnas *et al*. (2016) demonstrated a low level of mineralisation, in early stages of bone maturation, is associated with a high amide I:II ratio. Importantly, my results showed a high amide I:II ratio in male *Dmp1Cre.Pthlh* $^{f/f}$ and *Dmp1Cre.Pthlh* $^{w/w}$ at the initial stage of bone

maturation (at the endocortical edge), which is consistent with a low mineral:matrix ratio. Ansari *et al*. (2018) showed that male *Dmp1Cre.Pthlh*$^{f/f}$ femora were physically compromised, showing bone strength defects. My data showed both higher amide I:II ratio and lower mineral:matrix ratio in male *Dmp1Cre.Pthlh* $^{f/f}$ compared to the controls but it is not clear whether the defects in bone strength are due to production of under-mineralised matrix, or to an improper development of compacted collagen within the bone.

However, it is important to understand how PTHrP deficiency disturbed the ratio of mineral and matrix and how it affects the bone mechanical properties. Mineral to matrix ratio reflects the level of mineralisation relative to the volume of organic matrix in the sample analysed (Fredericks, Bennett *et al*. 2012, Gamsjaeger, Mendelsohn *et al*. 2014). While increases in mineralisation are suggested to result in a more brittle, fragile bone (Tommasini, Nasser *et al*. 2008), the greater mineralisation in controls increases their resistance to damage. Delayed mineralisation in *OsxCre.Efnb2*$^{f/f}$ causes the development of more elastic, less brittle bone. This suggests that mineralisation is essential for determining proper bone strength (Tonna, Stephen, *et al*. 2014). The lower mineral to matrix ratio in the male *Dmp1Cre.Pthlh* $^{f/f}$ model in my results suggest a decrease in mineralisation, which is expected to promote a less brittle bone. However, with three-point bending tests, male *Dmp1Cre.Pthlh*$^{f/f}$ femora showed lower ultimate deformation, ultimate force, and displacement at yield than controls, which indicates a more brittle bone phenotype. In other words, if collagen was normal and mineralistaion was low, the bones would be more flexible and would be able to deform more, resulting in an increase of the deformation, rather than a reduction. This suggests even though male *Dmp1Cre.Pthlh*$^{f/f}$ possess low mineralisation, it does not fully explain the bone strength defect.

As a consequence, this suggests that the absence of PTHrP in osteocytes *in vivo* might contribute to the decreased ultimate stress and yield stress in whole-bone strength via reduced

collagen compaction. It has been demonstated that haphazard collagen fibre organisation contributes to woven bone, characterised by mechanically weak property (Currey 2002). It is important to know whether there is a disorganisation of collagen fibres in *Dmp1Cre.Pthlh*$^{f/f}$ mice, which might be a significant contributor to the PTHrP-deficient strength phenotype.

My FTIRM data has shown that male *Dmp1Cre.Pthlh*$^{f/f}$ bone exhibits less mineralisation than controls. However, my PCR data showed that mineralisation gene profiles of *Dmp1Cre.Pthlh*$^{f/f}$ bones were only partially changed *in vivo*. This suggests that the *Dmp1Cre.Pthlh*$^{f/f}$ mineralisation phenotype observed is not due to the regulation of known mineralisation gene changes in bone tissues. *Ifitm5* (Moffatt *et al.* 2008; Hanagata *et al.* 2011), *Ibsp* (Kerr *et al.* 1993), *Spns2* (El Jamal *et al.* 2019), and *Phospho1 (*Houston, Stewart *et al.* 2004*),* are all genes involved in promoting bone mineralisation, whereas *Enpp1*(Kato, Nishimasu *et al.* 2012, Kato, Nishimasu *et al.* 2012) and *Spp1* (Steitz, Susan A., *et al*. 2002) are mineralisation inhibitors. I expected to see mineralisation genes regulated in bone of PTHrP knocked-down animals, however, only *Spp1* (Peacock, Huk *et al*. 2011) was decreased in the *Dmp1Cre.Pthlh*$^{f/f}$ female group. *Spp1* was not significantly regulated in male *Dmp1Cre.Pthlh*$^{f/f}$ compared to *Dmp1Cre.Pthlh*$^{w/w}$. Wassen *et al*. (2000) suggested that specific collagen orientations are essential in facilitating the mineralisation process. Since the most obvious change in males was the greater amide I:II ratio, it is plausible that a less compacted collagen phenotype results in decreased mineralisation via a regulation of collagen orientations in *Dmp1Cre.Pthlh*$^{f/f}$ mice. Overall, this suggests bone mineralisation defects are not associated with systematic changes in known mineralisation genes, but a less compacted collagen phenotype, which may result in decreased mineralisation. I have observed that a normal osteocyte canalicular network is dependent on PTHrP. However, whether the phenotype is associated with the mineralisation process need further explanations. This need to be further investigated.

Consistent with the *Dmp1Cre.Pthlh*$^{f/f}$ phenotype, my preliminary data showed that cultured OCY454 cells with PTHrP knocked down have fewer mineralised deposits *in vitro* than controls. However, surprisingly, OCY454 cultures overexpressing PTHrP (OCY454 *PTHrP*^{FL}) also showed less mineral content *in vitro* (at day 7, compared to the control). This suggests some other mechanism is affecting mineralisation other than the collagen compaction factor; mentioned above. For example, PTHrP's influence on osteocyte cell differentiation may affect mineralisation, in that low concentration of PTHrP in cells may promote differentiation. Ansari *et al*. (2018) have already shown that the osteocyte differentiation markers, *Dmp1*, *Mepe*, and *Sost*, are upregulated in PTHrP knockdown osteocytes. Perhaps this suggests that in low concentration of PTHrP, the cells differentiate too quickly such that they do not deposit enough mineral during this short differentiation period. I therefore assessed these three genes in RNA-Seq data in OCY454 overexpressing full-length or mutant PTHrP. However, none of these genes were significantly regulated by the four OCY454 PTHrP overexpressing cell lines, indicating PTHrP overexpression in OCY454 does not affect osteocyte differentiation markers. However, my data showed that OCY454 *PTHrP*^{FL} does regulate a number of differentiation markers (including *Alpl*, *Col1a1*, *Runx2*, *Bglap*, *Spp1*, and *Ibsp*) for the development from osteoblasts to osteocytes, showing different regulation patterns in osteocytes overexpressing full-length and mutant forms of PTHrP (*PTHrP*$^{\Delta NLS\Delta C}$, *PTHrP*$^{\Delta NLS}$, and *PTHrP*$^{\Delta Sec}$). This suggests the PTHrP and PTHrP functional regions may have important roles in the regulation of osteoblast development into osteocytes. Overall, these data suggest low concentration of PTHrP in cells may promote differentiation, but PTHrP overexpression in OCY454 regulates osteoblast development into osteocytes rather than the later process of osteocyte differentiation. A precisely regulated bone mineralisation process is essential for normal hardness and strength of bone (Yeni *et al*., 1998). If mineralisation neither is sufficient nor is excessive, the quality of bone tissue can be

compromised. Pathological mineralisation is observed in a range of bone diseases (such as Fibrous osteodystrophy, Osteomalacia and osteogenesis imperfecta), and recent studies have suggested that changes in matrix composition may also be associated with bone fragility in patients with normal bone mineral density (Boskey A L, 2013; Osterhoff G, Morgan E F *et al.* 2016).

My data suggests that any effect of PTHrP on mineralisation does not occur via known mineralisation genes. *Ifitm5* (Moffatt *et al.* 2008; Hanagata *et al.* 2011), *Ibsp* (Kerr *et al.* 1993), *Spns2* (El Jamal *et al.* 2019), and *Alpl* (Narisawa *et al.* 2003) are all genes involved in promoting bone mineralisation, and all were modified by PTHrP knockdown and/or overexpression. *Spp1* (Steitz, Susan A., *et al*. 2002) is a mineralisation inhibitor. These four genes that promote mineralisation were downregulated when PTHrP was overexpressed but upregulated when PTHrP was knocked-down. *Spp1* was downregulated with both PTHrP knockdown and overexpression. This illustrates that PTHrP might not directly modify bone mineralisation through these genes. I will discuss each of these genes in turn.

When I assessed PTHrP overexpressing cells, the gene *Alpl*, which encodes alkaline phosphatase (ALP), was significantly decreased to the point that there was no signal detected. ALP is a calcium-binding enzyme (Anderson 2003) that controls the first stage of mineralisation where matrix vesicles accumulate phosphate and calcium (Anderson 1995, Boskey 2007). ALP promotes bone mineralisation by breaking down extracellular mineralisation inhibitors (Golub and Boesze-Battaglia 2007). The dramatic suppression of *Alpl* mRNA in PTHrP overexpressing cells may mean that the cells are less able to break down extracellular mineralisation inhibitors, which would delay the mineralisation process. This is consistent with the lower level of mineral:matrix ratio detected in male *Dmp1Cre.Pthlh*$^{f/f}$ bones *in vivo* and decreased mineral deposits in OCY454 *PTHrP*^{FL}

compared with controls. However, upregulation in *Alpl* expression in PTHrP knockdown cells vs vector control did not correspond to the alterations in the mineralisation assay which showed a decreased mineralisation phenotype. Therefore, this indicates that PTHrP may not regulate mineralisation via *Alpl*.

Like *Alpl*, another gene downregulated by PTHrP overexpression was *Ifitm5,* a transmembrane protein expressed in the initial stage of bone mineralisation. Moffatt and Gaumond *et al*. (2018) determined the expression phenotype and localisation of *Ifitm5*, both *in vitro* and *vivo*, and its role in matrix mineralisation *in vitro*. In my analysis of mineralisation gene mRNA profiles, in comparison to vector controls, *Ifitm5* was significantly less abundant under the condition of PTHrP overexpression, which suggests PTHrP overexpression suppresses *Ifitm5* transcription. However, the *in vitro* mineralisation result showed decreased mineral deposits in the cells with knocked-down PTHrP, which is not consistent with the upregulation of the gene in PTHrP knockdown cells. This suggests that PTHrP may not regulate mineralisation via *Ifitm5*.

Other gene regulation patterns also did not fit with the observed pattern of mineralisation deposits. This suggests none of the known mineralisation genes that I have detected were directly regulated by PTHrP and directly caused the defects of mineralisation. Ansari *et al*. (2018) found that mineralisation genes *Dmp1* (*Dentin matrix protein 1*) and *Mepe* (*Matrix Extracellular Phosphoglycoprotein*) are up-regulated in osteocytes with PTHrP knocked-down, which also does not fit with the decreased mineralisation I observed in cells with PTHrP knocked-down. This suggests those two genes that essential for phosphorylation of the matrix proteins in the bone mineralisation process (Strom, Francis *et al*. 1997, Blair, Gormally *et al*. 1998) are not involved in regulation of mineralisation by PTHrP directly. I did not look at these two genes in *Dmp1Cre.Pthlh*$^{f/f}$ bone samples but my RNA-Seq data also showed these two

genes are not regulated by PTHrP overexpression in OCY454. Overall, these data further support the notion that PTHrP may not regulate the mineralisation process through these known mineralisation genes directly, but rather, through a different process.

Given that osteocyte canalicular networks are hypothesised to be associated with bone mineralisation, a low density canalicular structure in male *Dmp1Cre.Pthlh*$^{f/f}$ mice may be a cause of reduced mineral accumulation, but this needs to be further explored. The first transmission electron microscopy of normal bone revealed that the osteocyte cellular bodies are connected with each other. Such a network may play a role in the mineralisation of the bone matrix due to its network position between the layer of osteoblasts and the mineralised matrix (Nijweide, Van der Plas *et al*. 1981). Osteocyte cells became flattened against the mineralisation surface, and osteocyte body morphology changed with its dendrites radiating only to the mineralisation surface (Palumbo, Palazzini *et al*. 1990). Palumbo *et al*. (1990) have thus hypothesised that the osteocyte canalicular network is perhaps important in facilitating intercellular communication and may help to regulate mineralisation, but there is no data to support this with certainty. My preliminary analysis showed there may be abnormal osteocyte canalicular networks and dendrites within cortical bone of *Dmp1Cre.Pthlh*$^{f/f}$ compared to controls. Silver nitrate staining visualisation of cortical bone identified one particular region in male *Dmp1Cre.PTHrP*$^{f/f}$ that exhibited impaired and low density canalicular structure with poorly stained parts or with meandering networks, compared to the osteocytes embedded in control bones. Overall, this suggests that PTHrP may be a factor in maintaining the normal osteocyte canalicular network associated with the mineralisation process, but more detailed work is required.

There was a sex difference in the effect of the *Dmp1Cre.Pthlh*$^{f/f}$ genotype on matrix composition. While in male mice, I observed a significantly greater amide I:II ratio in

Dmp1Cre.Pthlh$^{f/f}$ bone, the collagen compaction (amide I:II ratio) was not significantly changed in females. My data also showed that male *Dmp1Cre.Pthlh*$^{f/f}$ bone exhibits a significant mineralisation difference compared to *Dmp1Cre.Pthlh*$^{w/w}$ (10 out of 12 regions along the periosteal to endosteal exhibited attenuated mineral: matrix ratio in *Dmp1Cre.Pthlh*$^{f/f}$ compared to *Dmp1Cre.Pthlh*$^{w/w}$). However, there was not a significant difference in the female group. This could be relevant to the fact , as shown by Ansari *et al*. (2018) , that male *Dmp1Cre.Pthlh*$^{f/f}$ femora were physically compromised, with three-point bending tests revealing lower ultimate deformation, ultimate force, and displacement at yield than controls. In contrast although no clear reductions were detected in ultimate strain, energy to failure, and ultimate force in female *Dmp1Cre.Pthlh*$^{f/f}$ mice compared to controls, the statistical analysis in that study suggested that female mice may have a milder defect in cortical strength. My data suggests that knockdown of PTHrP in osteocytes may have a sex-specific role in regulating matrix composition and cortical strength at a whole tissue level and it is likely that this reduction of PTHrP is more important in male mice than females.

6.11 Limitations of the work

One limitation of the work is that the canalicular network information is limited to silver nitrate images, and is not quantified, but there is no standard method to quantify this. Many other publications suggest it would be helpful to explore this network in future studies by using phalloidin staining as markers for actin cytoskeleton formation imaged by confocal microscope, which would give a way to show osteocyte cellular dendrites that are easily to be quantified (Tanaka‐Kamioka, Kamioka *et al*. 1998, Dallas and Bonewald 2010). This is because the integration of osteocyte cell projection and networks require the actin cytoskeleton to form osteocyte dendritic processes (Tanaka‐Kamioka, Kamioka *et al*. 1998, Dallas and Bonewald 2010). In addition to an assessment of actin organisation, qPCR test on genes *Mmp2* (Keiichi, Yuko *et al*. 2006), *Sod2* (Keiji, Hidetoshi *et al*. 2015) that were

previously reported to regulate osteocytic canalicular formation by knockout animals, could provide more insight into whether changes in mineralisation level in *Dmp1Cre.Pthlh*$^{f/f}$ mice are associated with changes in this network.

I observed high variability in my sFTIRM studies; this may reflect low sample numbers available for this study. In one group only six samples could be analysed out of an intended total of ten; four samples had to be excluded due to incorrect sampling for FTIR measurements; nfortunately there was not time to repeat these measurements due to limited Synchrotron access. Given the variability, a power calculation, using standard inputs (power = 0.8, effect size = 0.5), determined that at least 17 samples would be needed to detect whether the change I observed in the carbonate ratio was significant. The data could also have been refined by investigating multiple positions rather than focussing on only one site on the bone.

6.12 Future directions

It is possible that unknown mineralisation genes do in fact regulate mineralisation, or that PTHrP regulates collagen rather than mineralisation itself, or that PTHrP indirectly changes mineralisation by changing collagen, as mentioned above. RNA-Seq could be done in the future on bone samples from *Dmp1Cre.Pthlh*$^{f/f}$ mice as we have the RNA available to help determine what has changed.

As mentioned above, my data suggest that the less compacted collagen in male *Dmp1Cre.Pthlh*$^{f/f}$ mice may be due to a range of defects of the collagen. We could further investigate the amount of collagen protein in the bone to see whether the change of collagen compaction is because of a change in collagen production. This could be achieved via a collagen assay of PTHrP knocked-down osteocytes *in vitro*, or by analysis of whole bone from the mouse model. It has been demonstrated that Matrix metallopeptidase (MMP-9) deficiency impairs collagen compaction (Whatling, Carl *et al*. 2004). Further studies are needed,

including the investigation of the potential effects of genetic deficiency of *Mmp9* mRNA levels on compaction in bone samples.

6.13 Conclusion

Overall, my findings show that male *Dmp1Cre.Pthlh*$^{f/f}$ bone exhibits an increased amide I:II ratio and attenuated mineralisation compared to *Dmp1Cre.Pthlh*$^{w/w}$, thus demonstrating the requirement of PTHrP for normal bone composition. PTHrP is likely to contribute to bone strength via proper deposition and compaction of collagen, and by modifying osteocyte differentiation. PTHrP does not appear to regulate mineralisation directly via known mineralisation genes.

Chapter 7 General discussion

This project began with the aim of confirming and understanding PTHrP receptor (PTH1R)-independent pathway transduction signalling pathways in the contexts of both breast cancer and bone. Although PTHrP significantly promotes aggressive growth and invasion by breast tumour MCF7 cells in bone, I showed that the effect exerted by PTHrP is not dependent only on PTH1R-cAMP mediated activities. In addition, I showed that in the osteocyte the PTHrP C-terminus is likely to down-regulate a number of genes that are induced by PTH/PTHrP, including *Bglap1/2*, through mechanisms that are beyond the CREB activation. Moreover, I also found osteocyte-derived PTHrP has an essential role regulating collagen and mineral composition in bone.

In Chapter 3 my studies show that cancer cell-derived PTHrP does not trigger only classical (canonical) PTH1R stimulation. The downstream genes identified by RNA-Seq in MCF7 breast cancer cells include other pathways, such as the calcium signalling pathway and TRP channel pathway. However, these are not under the influence of the PTH1R-cAMP/PKA axis since I found no functional PTH1R in MCF7 cells. Given that PTHrP has a role of driving breast cancer cells out of dormancy, it is important for us to understand how PTHrP acts on these cells and what has altered PTHrP signalling. More effort will be put into investigating the pathways regulated by PTHrP signalling through mechanisms other than through the PTH1R.

Although I showed that the MCF7 cells lack specific PTH1R binding and cAMP production, PTH1R protein was detected in the MCF7 cells, which suggests that PTH1R in these cells is almost entirely not functional in response to PTHrP, at least in any detectable way. The reason for this inactive phenotype is not known, as Western blot showed no size shift or quantitative

alteration, which could have revealed a mutation or expression alteration of the receptor, respectively. This does not exclude the possibility that the PTHrP receptor is not modified by other effectors/ elements. For example, White *et al.* demonstrated that extracellular calcium binds to the first extracellular loop of the PTH1R receptor and functions as a positive allosteric modulator of PTH1R signalling by increasing ligand residence time on the receptor and magnifying the sustained cAMP production (White, Fang *et al*. 2019). In that study, extracellular Ca^{2+} can stabilise the agonist-bound PTH1R in an active conformation due to the magnitude of PTH1R activation resulted from increasing calcium concentration. It is possible that these changes of Ca^{2+} signalling, with impacts on extracellular Ca^{2+} concentration and on the concentration gradient across the cell membrane, result in a more transient cAMP response that was too transient to detect.

In Chapter 3 I determined that PTHrP action arises from domains beyond the amino-terminal region, using breast cancer cells. The possibility that actions arising from other domains should be explored. I therefore decided to study osteocytes, where PTHrP is known to act canonically through the amino-terminal region with PTH1R (Zhao, Brauer *et al*. 2002; Datta and Abou-Samra 2009). This was the focus of Chapters 4-6.

It has been shown (Ansari, Ho *et al*. 2018) that osteocytic PTHrP is essential for maintenance of bone mass during remodelling, extending the previous observation that PTHrP in the osteoblast lineage maintains trabecular bone mass (Miao, He *et al*. 2005). The finding of Ansari *et al*. of a similar phenotype of lower trabecular bone mass in *Dmp1Cre.Pthlh*$^{f/f}$ mice, however, is contrasted with that in mice with deletion of PTH1R in osteocytes (Saini, Marengi *et al*. 2013, Delgado‐Calle, Tu *et al*. 2017). This suggests that, in addition to PTH1R-mediated activities of PTHrP, some osteocyte-derived PTHrP actions may be independent of PTH1R. Although the PTH1R-dependent pathway through cAMP-PKA

signalling is well defined, the mechanisms by which intracellular PTHrP, the PTHrP C-terminus, and nuclear PTHrP control cell function are still incompletely known. This led to my next two experimental chapters which used my RNA-Seq datasets on OCY454 cells overexpressing PTHrP and mutant isoforms (Section 4.2) to determine the effects in osteocytes of PTHrP domains compared to the N-terminus that signals through PTH1R. My data led to the striking finding that many more genes are regulated by a form of PTHrP lacking both the nuclear localising sequence and C-terminus of (*PTHrP*$^{\Delta NLS\Delta C}$) than by full length PTHrP (*PTHrP*^{FL}). To examine this further, in Chapter 4 I found that the absence of the PTHrP C-terminus leads to a greater regulation of genes regulated through the PTH1R, both in terms of the number or genes and the magnitude change. This suggests that the PTHrP-C terminal may inhibit a cohort of genes that are targeted by PTH/PTHrP signalling.

A number of studies have shown that exogenous treatment with C-terminus PTHrP promotes human osteoblast survival (Alonso, De Gortazar *et al*. 2008, García‐Martín, Acitores *et al*. 2013). However, no intracellular C terminus activities have been previously described in osteoblasts.

Among genes regulated by PTHrP overexpression, the osteocytic gene *Bglap* was studied further because it showed the greatest difference in regulation between OCY454 osteocytes expressing the full length and C-terminus lacking forms of PTHrP. UMR106.01 cells treated with PTH or PTHrP featured increased *Bglap* mRNA transcription even when C-terminus PTHrP constructs were overexpressed endogenously. The *Bglap* mRNA response was significantly weaker when the C-terminus (*PTHrP*$^{107\text{-}141}$) was overexpressed, suggesting that it inhibits the effect of exogenous PTH/PTHrP on the PTHR1-mediated increase in *Bglap* transcription. However, the *Bglap* response to exogenous PTH/PTHrP was not modified in UMR106.01 cells that overexpress the C-terminus containing the nuclear localising sequence

(*PTHrP*$^{68–141}$). This indicates that the PTHrP C-terminus lowers the PTHR1-mediated increase in *Bglap* response, not via NLS-associated nuclear activity nor nuclear translocation activity, but rather, via intracellular actions that remain to be determined. Furthermore, this indicates that the NLS region could act to inhibit the C-terminus' suppression of gene expression. It should be noted, however, that additional genes may be suppressed by the C-terminus and may also be affected by interaction of the C-terminus with the NLS region. The latter needs further study.

My present study has suggested the gene regulation exerted by the absence of C-terminus is not mediated by cAMP/PKA signalling. There was no change in cAMP response, CREB responsive gene alterations nor CREB phosphorylation in response to exogenous PTHrP treatment in cells overexpressing the C-terminus, nor any difference in the effects of exogenous PTHrP lacking the C-terminus compared to full-length PTHrP. In order to investigate the mechanisms, I assessed the Wnt signalling gene profile in OCY454 cells overexpressing PTHrP and noted regulation of some genes in that pathway. Overexpression of the PTHrP C-terminus in UMR106.01 resulted in induction of some Wnt targeting genes under the treatment of PTH. The result was consistent with Wnt reporter activation, showing that the PTHrP C-terminus up-regulated Wnt reporter activity when cells were treated at a lower dose of PTH. In addition to this, I found that the Wnt inhibitor, *Sost*, was largely repressed by the overexpression of PTHrP C-terminus in UMR106.01, under the treatment of PTH compared to vector controls (Section 5.5). This indicates that the C-terminus' suppression of *Bglap* may depend on Wnt signalling, via Sost. Answering this question fully will require first understanding whether the Wnt inhibitor Sclerostin can rescue C-terminus-induced inhibition of *Bglap*.

Since complete absence of osteocalcin protein caused increased trabecular bone volume (Lambert, Challa *et al*. 2016) it is important to understand how osteocalcin plays negative roles in bone formation. These osteocalcin deficient rats also had increased the insulin sensitivity even though body weight and composition were not changed. This is consistent with the mouse model when osteocalcin deficiency showed increased bone formation (Ducy, Desbois *et al*. 1996) and other studies characterising osteocalcin have demonstrated that it can act as a mediator of skeletal modulation of metabolism (Lee, Sowa *et al*. 2007) and fertility (Oury, Ferron *et al*. 2013). Moreover, *in vitro* studies have also suggested that osteocalcin might increase differentiation of osteoclast precursors into osteoclasts (Malone, Teitelbaum *et al*. 1982, Mundy and Poser 1983, Chenu, Colucci *et al*. 1994), which suggested another role of osteocalcin in regulating bone modelling and remodelling. Understanding the molecular mechanism of how the PTHrP C-terminus inhibits *Bglap* expression may therefore have implications for the treatment osteopenia and osteoporosis.

It is useful to understand the functions of the PTHrP C-terminus, which may explain how endogenous PTHrP limits PTHrP signalling through the PTH1R receptor. Prior studies in *Pthlh*$^{+/-}$ mice indicated that PTHrP might limit the anabolic effects of PTH (Miao, He *et al*. 2005) but the cellular source was still unknown. Since PTH and PTHrP share the PTH1R receptor, deletion of endogenous osteocytic C-terminus PTHrP might enhance the anabolic efficacy of PTH. In another words, PTHrP C terminus may limit some effects though PTH1R by inhibiting gene expressions. However, this needs to be investigated in future studies, perhaps by using mice genetically modified to overexpress the C-terminus. This would indicate whether the effects of the C-terminus are associated with anabolism of bone tissue.

In Chapter 6, using relevant GO terms, I identified that full length PTHrP regulated genes associated with mineralisation in OCY454 osteocyte cells. This led to my study of PTHrP

knockdown (*Dmp1Cre.Pthlh*$^{f/f}$) bone composition to see the change in bone mineralisation. However, the associations of PTHrP with regulating mineralisation have not been thoroughly investigated. The only evidence that PTHrP may change bone material was found by Ansari *et al*. 2018, who showed that *Dmp1Cre.Pthlh*$^{f/f}$ femurs with PTHrP knocked-down osteocytes featured changes in a few mineralisation genes and poorer material strength. Neither bone size nor bone shape was shown to be the effector to change the bone strength, which suggested that material defect due to PTHrP knockdown restricts the bone strength in these mice (Ansari, Ho *et al*. 2018). My *in vivo* FTIR microspectroscopy studies showed that male *Dmp1Cre.Pthlh*$^{f/f}$ mice exhibited a significantly higher amide I:II ratio (i.e. less collagen compaction) and lower mineral:matrix ratio compared to controls. This suggests a requirement of PTHrP for proper promotion of mineralisation and proper collagen alignment.

Whether bone strength defects are caused by poorly-mineralised matrix production, or by aberrant development of compact collagen, is important to understand. The mineral to matrix ratio is an indicator of the degree of mineralisation in proportion to the volume of organic matrix (Fredericks, Bennett *et al*. 2012; Gamsjaeger, Mendelsohn *et al*. 2014). While increases in mineralisation are suggested to result in a more brittle, fragile bone (Tommasini, Nasser *et al*. 2008), the greater mineralisation in controls increases their resistance to damage. Delayed mineralisation in *OsxCre.Efnb2*$^{f/f}$ caused development of more elastic, less brittle bone. This provides confirmation that mineralisation is essential for determining proper bone strength (Tonna, Stephen, *et al*. 2014). The lower mineral to matrix ratio in the male *Dmp1Cre.Pthlh*$^{f/f}$ model in my results suggest a decrease in mineral incorporation, which is expected to produce a less brittle bone. However, in three-point bending tests from Ansari *et al*. (2018), male *Dmp1Cre.Pthlh*$^{f/f}$ femora showed lower ultimate deformation, ultimate force, and displacement at yield than controls, suggesting a more brittle bone phenotype. In other words, if mineralisation alone were defective the bones would be more flexible and would be able to

deform more, resulting in an increase of deformation, rather than a reduction. This suggests even though male *Dmp1Cre.Pthlh*$^{f/f}$ possess low mineralisation, it is not enough to promote this bone strength defect. The absence of PTHrP, *in vivo*, may therefore have contributed to the decreased ultimate stress and yield stress in whole-bone strength, via a decrease in collagen compaction within the matrix. It has been demonstated that haphazard collagen fibre organisation contributes to woven bone, which is mechanically weak (Currey 2002). A disorganisation of collagen fibres in *Dmp1Cre.Pthlh*$^{f/f}$ mice, might be a significant contributor to the PTHrP-deficient strength phenotype.

My *in vitro* results show that PTHrP deficient cells have a low mineralised deposit phenotype which is consistent with the *in vivo* data. However, overexpression of PTHrP did not rescue this, but showed decreased mineral content, implying the presence of other mechanisms that affect the process. Wassen *et al*. (2000) proposed that the correct orientation of collagen is essential in facilitating mineralisation. As the most marked change as I have observed in males was a greater amide I:II ratio, it is possible that a less compacted collagen phenotype decreases mineralisation by regulating collagen orientation in *Dmp1Cre.Pthlh*$^{f/f}$ mice. In addition, Ansari *et al*. (2018) demonstrated that the osteocyte differentiation markers (*Dmp1*, *Mepe*, and *Sost*) are upregulated in osteocytes that have PTHrP knocked-down. This may indicate that when concentration of PTHrP is low, the cells differentiate too rapidly to deposit enough mineral. My data shows that overexpression of PTHrP in the OCY454 osteocyte cell line regulates many differentiation markers associated with osteoblast–osteocyte development and different regulation patterns in osteocytes overexpressing full-length and mutant forms of PTHrP (*PTHrP*$^{\Delta NLS\Delta C}$, *PTHrP*$^{\Delta NLS}$, and *PTHrP*$^{\Delta Sec}$). This suggests that the mineralisation defects observed in cultured OCY454 osteocytes may occur primarily due to a compromised differentiation of development from osteoblast to osteocyte as a result of PTHrP overexpression. Overall, these data suggest a lower than normal level of endogenous PTHrP

may promote osteocyte differentiation whereas overexpressing PTHrP may affect an earlier stage when osteoblasts develop into osteocytes. These two processes and the effect of PTHrP on collagen production may all play a role in regulating mineralisation.

Ansari *et al*. (2018) suggested that PTHrP affects cortical strength through a non-PTH1R-mediated pathway because mice administered exogenous PTH, which must use PTH1R, did not develop compromised bone matrix mineral composition or compromised maturation (Vrahnas *et al*. 2016). Thus, PTHrP is presumably important for bone mineralisation, however, the signalling pathway of osteocytic-PTHrP independent of PTH1R in regulating bone mineralisation has not yet been examined.

In conclusion, my study showed that PTHrP acts through non-canonical pathways associated with regions of the molecule other than the PTH1R binding region in both osteocytes and breast cancer cells. Although PTHrP modifies gene expression substantially and promotes breast tumour MCF7 cells growth in bone, this is not dependent on PTH1R/cAMP/PKA activation. In addition, in osteocyte-like cells, which express PTHR1, the PTHrP C-terminus appears to inhibit *Bglap1/2* transcription induced by PTH/PTHrP and this occurs through intracellular pathways independent of PTH1R/cAMP/PKA. In closing, PTHrP is likely important for the proper promotion of mineralisation, contributing to bone strength via compaction of collagen; these may occur independently of PTH1R, both *in vivo* and *in vitro*.

This research in future will focus on identification of PTHrP non-canonical signals/ligand responsible for the action of PTHrP to promote metastasis in breast cancer; this may provide information that could lead to ways to suppress PTHrP metastasis. The ability of PTHrP C-terminus to modify the action of PTH receptor signalling in osteocytes (including stimulation of *Bglap* mRNA) may provide insights into how PTHrP acts physiologically to promote bone formation, and how pharmacological treatment of osteoporosis by PTH may be

limited by endogenous PTHrP in osteocytes. Endogenous PTHrP in osteocytes also modifies bone mineral composition. Together understanding these processes could lead to new therapeutic approaches for treating bone fragility, including osteopenia and osteoporosis. Whether it is possible for the C-terminus of PTHrP to inhibit the non-canonical action of PTHrP in breast cancer cells, in the same way it acts on osteocytes, remains to be determined.

Appendix in Endocrinology

ORIGINAL RESEARCH
published: 16 May 2018
doi: 10.3389/fendo.2018.00241

Parathyroid Hormone-Related Protein Negatively Regulates Tumor Cell Dormancy Genes in a PTHR1/Cyclic AMP-Independent Manner

Rachelle W. Johnson[1], Yao Sun[2,3], Patricia W. M. Ho[2], Audrey S. M. Chan[4], Jasmine A. Johnson[1], Nathan J. Pavlos[4], Natalie A. Sims[2,3] and T. John Martin[2,3]*

[1]Department of Medicine, Division of Clinical Pharmacology, Vanderbilt Center for Bone Biology, Vanderbilt University Medical Center, Nashville, TN, United States, [2]Bone Biology and Disease Unit, St. Vincent's Institute of Medical Research, Fitzroy, VIC, Australia, [3]Department of Medicine at St. Vincent's Hospital, University of Melbourne, Melbourne, VIC, Australia, [4]Cellular Orthopaedic Laboratory, School of Biomedical Sciences, The University of Western Australia, Crawley, WA, Australia

OPEN ACCESS

Edited by:
Chandi C. Mandal, Central University of Rajasthan, India

Reviewed by:
Han Qiao, Shanghai Jiao-Tong University School of Medicine, China
Petra Simic, Massachusetts Institute of Technology, United States

***Correspondence:**
Rachelle W. Johnson
rachelle.johnson@vanderbilt.edu

Specialty section:
This article was submitted to Bone Research, a section of the journal Frontiers in Endocrinology

Received: *27 January 2018*
Accepted: *26 April 2018*
Published: *16 May 2018*

Citation:
Johnson RW, Sun Y, Ho PWM, Chan ASM, Johnson JA, Pavlos NJ, Sims NA and Martin TJ (2018) Parathyroid Hormone-Related Protein Negatively Regulates Tumor Cell Dormancy Genes in a PTHR1/Cyclic AMP-Independent Manner. Front. Endocrinol. 9:241. doi: 10.3389/fendo.2018.00241

Parathyroid hormone-related protein (PTHrP) expression in breast cancer is enriched in bone metastases compared to primary tumors. Human MCF7 breast cancer cells "home" to the bones of immune deficient mice following intracardiac inoculation, but do not grow well and stain negatively for Ki67, thus serving as a model of breast cancer dormancy *in vivo*. We have previously shown that PTHrP overexpression in MCF7 cells overcomes this dormant phenotype, causing them to grow as osteolytic deposits, and that PTHrP-overexpressing MCF7 cells showed significantly lower expression of genes associated with dormancy compared to vector controls. Since early work showed a lack of cyclic AMP (cAMP) response to parathyroid hormone (PTH) in MCF7 cells, and cAMP is activated by PTH/PTHrP receptor (PTHR1) signaling, we hypothesized that the effects of PTHrP on dormancy in MCF7 cells occur through non-canonical (i.e., PTHR1/cAMP-independent) signaling. The data presented here demonstrate the lack of cAMP response in MCF7 cells to full length PTHrP(1–141) and PTH(1–34) in a wide range of doses, while maintaining a response to three known activators of adenylyl cyclase: calcitonin, prostaglandin E_2 (PGE_2), and forskolin. PTHR1 mRNA was detectable in MCF7 cells and was found in eight other human breast and murine mammary carcinoma cell lines. Although PTHrP overexpression in MCF7 cells changed expression levels of many genes, RNAseq analysis revealed that PTHR1 was unaltered, and only 2/32 previous PTHR1/cAMP responsive genes were significantly upregulated. Instead, PTHrP overexpression in MCF7 cells resulted in significant enrichment of the calcium signaling pathway. We conclude that PTHR1 in MCF7 breast cancer cells is not functionally linked to activation of the cAMP pathway. Gene expression responses to PTHrP overexpression must, therefore, result from autocrine or intracrine actions of PTHrP independent of PTHR1, through signals emanating from other domains within the PTHrP molecule.

Keywords: parathyroid hormone-related protein, cyclic AMP, MCF7, breast cancer, calcium signaling

INTRODUCTION

Parathyroid hormone-related protein (PTHrP, gene name *PTHLH/Pthlh*) is a cytokine with functions in both pathology and physiology (1, 2). Although it was identified as the circulating factor responsible for humoral hypercalcemia of malignancy (3), it more commonly acts in a paracrine manner: in breast cancer cells it promotes their metastasis (4, 5), in bone (osteoblasts and osteocytes) it stimulates bone formation (6, 7), and in cartilage cells (chondrocytes) it controls proliferation and hypertrophy (8).

In breast cancer cells that lay dormant in bone (9) we have previously shown that overexpression of PTHrP enables otherwise dormant human MCF7 breast cancer cells to aggressively colonize the bone marrow and induce osteolysis (5). Consistent with enhanced bone colonization, we recently reported that such overexpression of PTHrP in MCF7 cells results in the downregulation of several pro-dormancy genes (9).

The best understood actions of PTHrP are those that are mediated by its binding to the G protein-coupled receptor that it shares with parathyroid hormone (PTH) (PTHR1). Upon ligand binding to the receptor, cyclic AMP (cAMP) is activated, followed by protein kinase A (PKA) activation, cAMP responsive element binding protein (CREB) phosphorylation, and transcription of CREB target genes (10–13). This PTHR1-dependent signaling pathway is shared between PTH and PTHrP due to high sequence homology in their amino-terminal domains; the portion of the molecule that interacts with the receptor (14). Early work showed that MCF7 cells failed to respond to PTH treatment with any increase in cAMP or activation of cAMP-dependent protein kinase, suggesting that PTHR1 in those cells is not functionally linked to adenylyl cyclase (15). In contrast, MCF7 cells possess specific, high affinity receptors for calcitonin linked to adenylyl cyclase activation, and activate cAMP in response to prostaglandin E_2 (15, 16). These data suggest that the effect of PTHrP overexpression on tumor dormancy in MCF7 cells may occur through PTHR1-independent actions of the PTHrP molecule.

Using multiple assays, we report here that MCF7 cells, and many other breast cancer cell lines, express PTHR1 mRNA but do not bind PTH, nor do they activate cAMP formation or subsequent cAMP signaling events in response to PTH or PTHrP. Our RNAseq analyses identify many genes induced by PTHrP overexpression in MCF7 cells, and several potential alternative pathways, notably those related to calcium signaling.

MATERIALS AND METHODS

Cell Culture

Human MCF7 cells were obtained from ATCC and grown in DMEM supplemented with 10% FBS and penicillin/streptomycin (P/S). MCF7pcDNA and MCF7 PTHrP-overexpressing cells were generated as described previously (5) and grown in the same conditions as MCF7 cells; we utilized strains grown and maintained at two separate institutions to validate findings. All breast cancer and mouse mammary carcinoma cell lines were obtained and grown as previously described (9). The rat osteosarcoma (UMR106-01) cell line was maintained in DMEM supplemented with 10% FBS and P/S as described in Ref. (17). MC3T3-E1 cells were maintained in α-MEM supplemented with 10% FBS as described in Ref. (18).

cAMP Response Assay

Briefly, MCF7 cells were cultured in 12-well plate in cell culture media containing 1 mM isobutylmethylxanthine. Cells were then treated for 12 min with either PTH (100 nM) (sourced from Bachem, Bubendorf, Switzerland), PTHrP(1–141) (100 nM) [expressed in *Escherichia coli* and purified in house (7)], or the known agonists forskolin (10 μM) (sourced from Sigma), prostaglandin E_2 (1 μM) (sourced from Sigma), or salmon calcitonin (sCT) (1 μM) (kindly gifted by the late Dr. M Azria, Novartis AG, Basel, Switzerland). The cells were washed, acidified ethanol was added, and after air drying was reconstituted in assay buffer and cAMP formation assayed as previously (19).

CRE-Luciferase Assay

MCF7 cells were transiently transfected with cAMP response element (pCRE)-luciferase (Clontech), a vector containing multiple copies of CRE binding sequences. Fugene (Promega) was used to transfect cells. Four hours after agonist stimulation, cells were lysed, substrate (Promega) was added, and signal was measured using a Polarstar Optima.

Real-Time Quantitative PCR

Cell lines were harvested in TRIzol (Life Technologies) or TriSure (Bioline) for phenol/chloroform extraction of RNA, DNAse digested (TURBO DNA-free kit, Life Technologies), and cDNA was synthesized from 200 ng–1 μg RNA (iScript cDNA synthesis kit, Bio-Rad or Tetro cDNA synthesis kit, Bioline) per the manufacturer's instructions as previously described (9). Real-time PCR was performed on either a Quantstudio5 384-well plate format (Thermo Fisher) or Stratagene MX3000P (Agilent) with the following cycling conditions: 2 min at 50°C, 10 min at 95°C, (15 s at 95°C, 1 min at 60°C) × 40 cycles, and dissociation curve (15 s at 95°C, 1 min at 60°C, 15 s at 95°C) or 10 min at 95°C, (30 s at 95°C, 1 min at 60°C) × 40 cycles, and dissociation curve (1 min at 95°C, 30 s at 55°C, 30 s at 95°C). Primers for mouse *PTHR1* were previously published (20) and human *PTHR1* primer sequences were sourced from MGH Primerbank (F: CTGGGCATGATTTACACCGTG, R: CAGTG CAGCCGCCTAAAGTA). Human *PTHLH* primers were previously published (21) and human *HPRT1*, *RGS2*, *CREB*, *PRKAR1*, *AREG*, and *NR4A1* primers were previously published (22). Primer sequences for human *BDKRB1* and *CALML3* were designed using PrimerBLAST (*BDKRB1* F: AATGCTACGGCCTGTGACAA, R: TCCCTAGGAGGCCGAAGAAA; *CALML3* F: TGGTTGAT TCAGCCCACCTC, R: TCCGTGTCATTCAGACGAGC). Gene expression between samples was normalized to *B2M* expression or *B2M*: *HPRT1* geometric mean. Relative expression was quantified using the comparative CT method [$2^{-(\text{Gene Ct}-\text{Normalizer Ct})}$].

Confocal Microscopy

Antibodies and Reagents

Tetramethylrhodamine (TMR)-labeled PTH(1–34) (PTH^{-TMR}) was synthesized as previously described (23). Anti-VPS35 mouse

monoclonal was purchased from Santa Cruz Biotechnology Inc., USA. Alexa Fluor 488 anti-mouse secondary antibody was purchased from Molecular Probes®, Invitrogen, USA.

Imaging

MCF7 and UMR106-01 cells were cultured as described above, and seeded on poly-L-lysine-coated glass coverslips at 1×10^4 cells/well (96-well plate) for 24–48 h prior to agonist stimulation. Cells were then serum starved for 1 h prior to the addition of PTH-^{TMR} (100 nM) for 15 min at 37°C. Cells were then washed in ice-cold 1× PBS and fixed in 4% PFA at room temperature, permeabilized with 0.1% Triton X-100 for 5 min, washed in 0.2% BSA-PBS, and blocked in 3% BSA-PBS for 30 min. Cells were then incubated with anti-VPS35 antibody (Santa Cruz Biotechnology Inc.) for 1 h at room temperature, and washed in 0.2% BSA-PBS and 1× PBS prior to incubation with Alexa Fluor 488 anti-mouse secondary antibody (Molecular Probes®, Invitrogen), for 45 min at room temperature. Cells were then stained with DAPI stain and mounted in ProLong® Diamond Antifade (Molecular Probes®, Invitrogen). Detection of immunofluorescence was performed using a Nikon A1Si confocal microscope running NIS-C Elements Software (Nikon Corp., Japan). A 40× oil immersion objective lens (Nikon, Japan) was used, where serial optical sections (z-stack) of 0.5–1 μm were used to reconstruct 2D projections in FIJI (NIH, USA).

RNA Sequencing and Bioinformatics

RNA samples of MCF7pcDNA control and MCF7 PTHrP-overexpressing cells ($n = 3$ independent replicates/group) were submitted to the Stanford Functional Genomics Facility and analyzed for RNA integrity using a Bioanalyzer (Eukaryote Total RNA Nano, Agilent) and all samples had a RNA integrity number of 9.50–10 (10 is highest quality possible). RNA samples were sequenced on an Illumina NextSeq with coverage of approximately 40 million reads per sample. Sequence alignment and RNAseq bioinformatics analysis was performed by the Vanderbilt Technologies for Advanced Genomics Analysis and Research Design (VANGARD) core at Vanderbilt University Medical Center. RNAseq files are available in the GEO repository (GEO accession number GSE110713).

Statistics

All data are presented as the mean of $n = 3$ biological replicates obtained from three independent experiments (one biological replicate, with three technical replicates per experiment). For all graphs error bars indicate the SEM. Statistical tests used are indicated in the figure legends, and p-values were considered significant at $p < 0.05$.

RESULTS

PTHR1 mRNA Is Detected in Breast Cancer Cells

PTHR1 mRNA levels varied but were detectable across all human breast cancer and mouse mammary carcinoma cell lines tested (**Figure 1**). The panel included cell lines termed "high metastatic potential" [that aggressively colonize the bone after intracardiac inoculation or lung after tail vein inoculation (9)], and cell lines termed "Low metastatic potential" (9) [that do not colonize, or proliferate very slowly after inoculation (9)]. PTHR1 mRNA levels did not correspond to the metastatic potential of the cell lines. 4T1 and D2A1 cells had the lowest expression of PTHR1, which was nearly undetectable (4T1: Ct values = 33–39; D2A1: Ct values = 33–34). All breast cancer cell lines had at least 10-fold lower *PTHR1* mRNA levels than MC3T3-E1 cells, which have a robust cAMP response to exogenous PTH and PTHrP treatment (24).

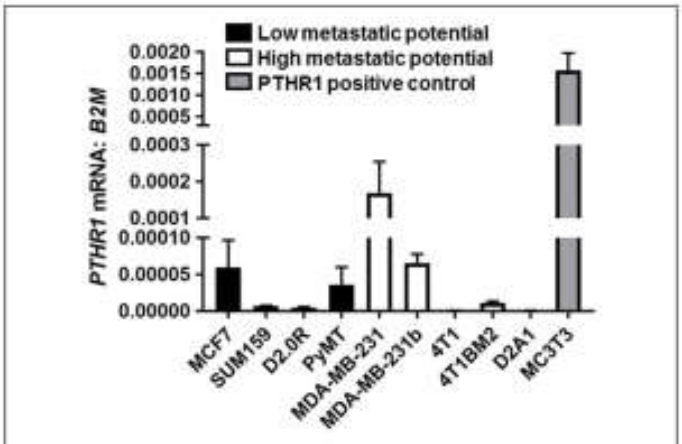

FIGURE 1 | PTHR1 is expressed by breast cancer cells. *PTHR1* mRNA levels in human breast cancer cell lines [MCF7, SUM159, MDA-MB-231, MDA-MB-231b [bone metastatic clone (25, 26)]], mouse mammary carcinoma cell lines [D2.0R, PyMT, 4T1, 4T1BM2 [bone metastatic clone (27)], D2A1], classified according to metastatic potential, and PTHR1/cyclic AMP responsive MC3T3-E1 cells. mRNA levels were normalized to β-2-microglobulin (*B2M*) housekeeping gene. Graphs = mean + SE. $n = 3$ replicates from independent experiments.

Neither PTH nor PTHrP Stimulates cAMP in Breast Cancer Cells

MCF7 cells robustly induced cAMP formation in response to forskolin, PGE_2, and sCT, but treatment with high dose PTH(1–34) or PTHrP(1–141) elicited no cAMP response (**Figure 2A**). This confirmed the lack of a cAMP response to PTH in MCF7 cells as reported at the time of discovery of the functional calcitonin receptor (15). In order to investigate later cellular responses, MCF7 cells were transiently transfected with a cAMP response element (CRE)-luciferase construct (CRE-Luc). Treatment with either sCT or PGE_2 resulted in substantial activation of the CRE-Luc reporter, with no detectable effect of PTH(1–34). All were used at multiple doses in repeated experiments, with no measureable effects detected (**Figure 2B**).

Tetramethylrhodamine-labeled PTH (PTH-^{TMR}) has proven useful for monitoring the surface binding and internalization of amino-terminal PTH upon its target cells through the PTHR1 (23). Vacuolar protein sorting 35 (VPS35) is an essential subunit of the mammalian retromer trafficking complex, where retromer coordinates both retrograde (endosome-to-Golgi) and recycling (endosome-to-plasma membrane) of many cell surface receptors

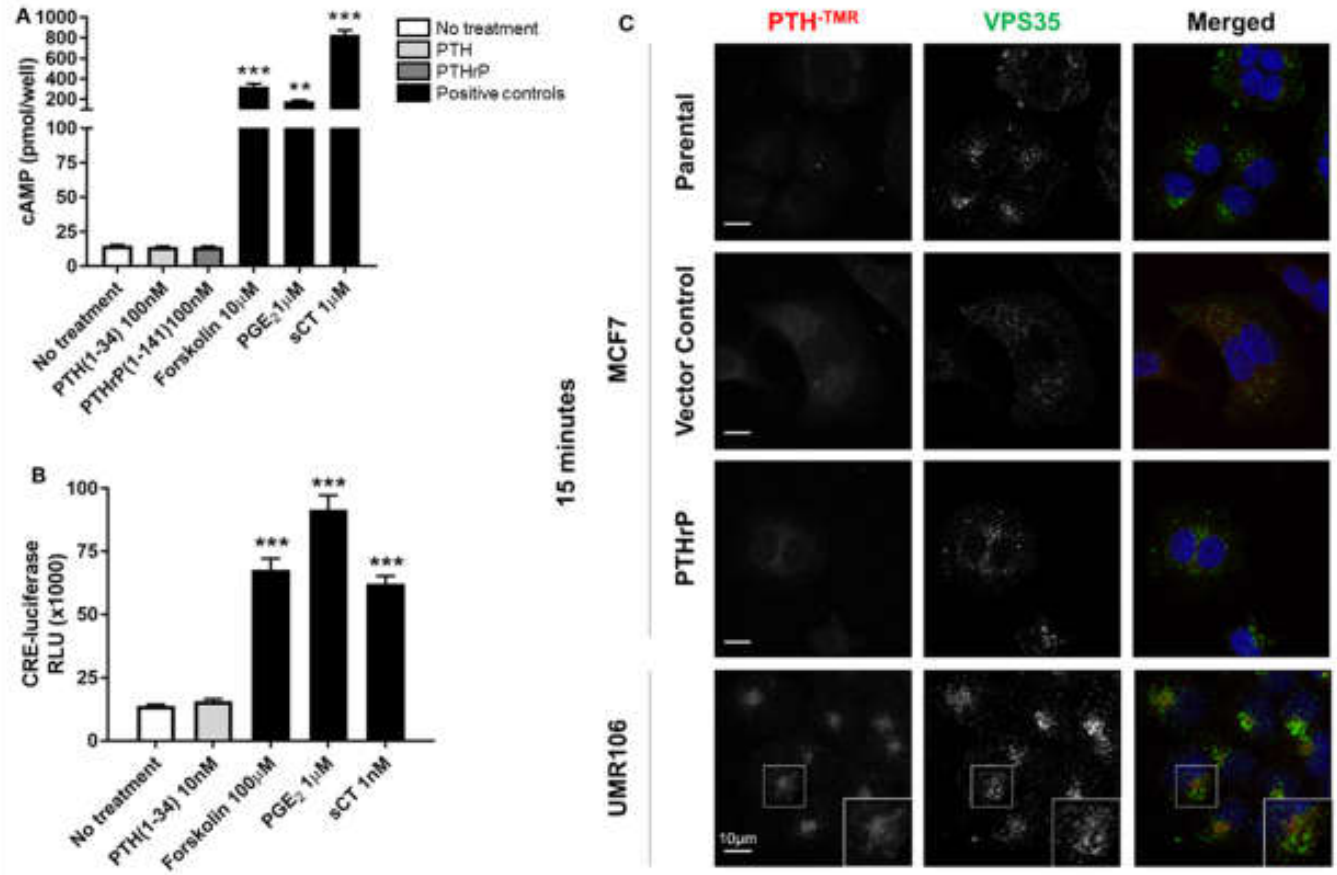

FIGURE 2 | Neither parathyroid hormone (PTH) nor parathyroid hormone-related protein (PTHrP) bind to/activate cyclic AMP (cAMP) in MCF7 cells. **(A)** cAMP production in MCF7 cells following 12 min stimulation with PTH(1–34) or PTHrP(1–141), or positive controls forskolin, prostaglandin E_2 (PGE_2), or salmon calcitonin (sCT). Graphs = mean + SE. $n = 3$ replicates from independent experiments. $^{**}p < 0.01$, $^{***}p < 0.001$ vs no treatment by one-way ANOVA with multiple comparisons. **(B)** cAMP response element (CRE)-luciferase signal following 4 h stimulation with PTH or positive controls forskolin, prostaglandin E_2 (PGE_2), or sCT. Graphs = mean + SE. $n = 3$ replicates from independent experiments. $^{***}p < 0.001$ vs no treatment by one-way ANOVA with multiple comparisons. **(C)** Confocal images of stable MCF7 and UMR106-01 cells cultured on poly-L-lysine-coated glass coverslips and serum starved for 1 h prior to the addition of tetramethylrhodamine-labeled PTH(1–34) (PTH^{-TMR}, 100 nM) for 15 min at 37°C. Cells were fixed in 4% PFA and immunostained for the endogenous retromer subunit, vacuolar protein sorting 35 (VPS35). Scale bar, 10 μm. Representative of $n = 3$ independent experiments.

(28), including PTHR1 (23, 29) along the endocytic pathway. VPS35, therefore, serves as a marker of internalized PTH^{-TMR}–PTHR1 ligand-receptor complexes following their sequestration into early endosomes (23). Accordingly, the addition of PTH^{-TMR} at saturating conditions (100 nM) for 15 min to UMR106-01 cells, was sufficient to visualize encapsulated ligand–receptor complexes in early endosomes, as determined by its co-localization with VPS35 (**Figure 2C**). This event coincides with the generation of cAMP following stimulation with either PTH and PTHrP peptides with identical dose responses (19). In contrast, neither PTH^{-TMR} internalization nor co-localization with VPS35 was detected in MCF7 parental, vector-transfected, or PTHrP-transfected cells (**Figure 2C**).

Lack of cAMP Gene Response in MCF7 Cells

In order to identify novel dormancy genes regulated by PTHrP, we used RNAseq to analyze which pathways are activated in response to PTHrP overexpression in MCF7 cells. We identified >2,500 genes differentially regulated with a $\log_2$ fold change >1 and $p < 0.05$ in MCF7 PTHrP-overexpressing vs MCF7 control cells (**Figure 3A**). Consistent with our finding that neither PTH nor PTHrP induce cAMP formation or early post-receptor activation events in MCF7 cells, RNAseq analysis confirmed that only 2 of a previously described panel of 32 CREB-responsive genes (22) were significantly upregulated in MCF7 PTHrP-overexpressing cells (**Table 1**). Three CREB-responsive genes were significantly downregulated, and the remaining 27 were not altered by PTHrP over-expression, confirming that even long term overexpression of PTHrP does not induce genes that result from cAMP signaling in MCF7 cells.

Validation of several candidate CREB-responsive genes in MCF7 PTHrP-overexpressing cell lines maintained at a separate institution was consistent with our RNAseq findings (**Figures 3B–E**). The one exception was *NR4A1*, which was found to be unaltered by RNAseq, but was significantly upregulated in

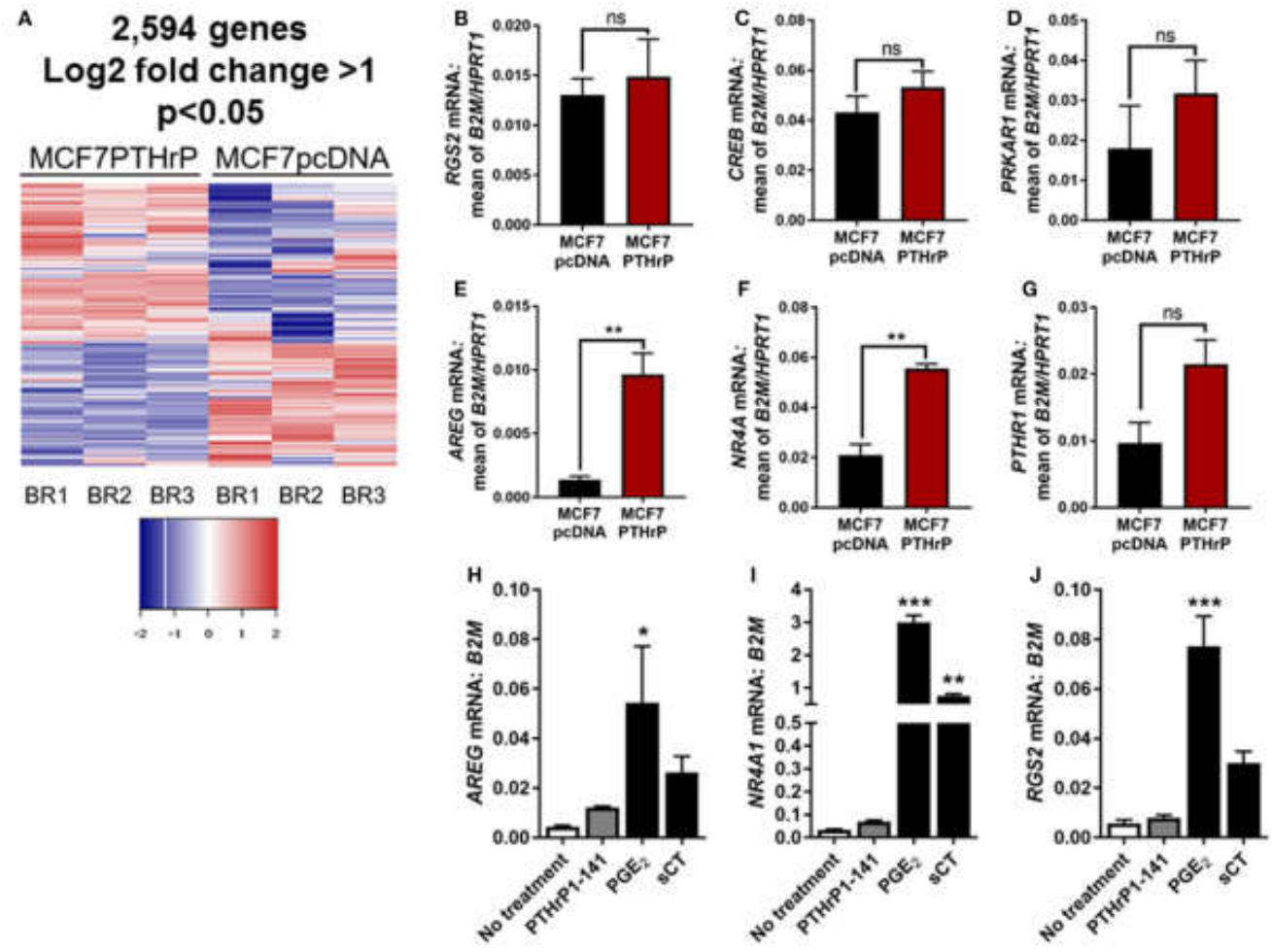

FIGURE 3 | Parathyroid hormone-related protein (PTHrP) overexpression does not induce cyclic AMP (cAMP) target genes. **(A)** Heat map of gene expression with 95% confidence intervals in MCF7pcDNA (empty vector control) or MCF7 PTHrP-overexpressing cells. BR1 = biological replicate 1, BR2 = biological replicate 2, BR3 = biological replicate 3. **(B–G)** qPCR for cAMP target genes in MCF7pcDNA or MCF7 PTHrP-overexpressing cells. mRNA levels were normalized to the geometric mean of *B2M* and *HPRT1* housekeeping genes. Graphs = mean + SE. $^{**}p < 0.01$ by unpaired Student's *T*-test. **(H–J)** qPCR for cAMP target genes in MCF7 cells following stimulation with PTHrP(1–141) or positive controls prostaglandin E_2 (PGE_2) or salmon calcitonin (sCT). Graphs = mean + SE. $n = 3$ replicates from independent experiments. $^{*}p < 0.05$, $^{**}p < 0.01$, $^{***}p < 0.001$ vs no treatment by one-way ANOVA with multiple comparisons.

PTHrP-overexpressing cells by real-time PCR (**Figure 3F**). We also confirmed that *PTHR1* is not downregulated with PTHrP overexpression (**Figure 3G**). In addition, treatment with positive controls PGE_2 and sCT induced significantly greater mRNA levels of CREB-responsive genes *AREG*, *NR4A1*, or *RGS2*, but exogenous treatment with PTHrP(1–141) had no significant effect (**Figures 3H–J**).

RNAseq Confirms PTHrP Overexpression Reduces Pro-Dormancy Genes

We previously reported that PTHrP overexpression in MCF7 cells significantly reduced the pro-dormancy genes *LIFR*, *SOCS3*, *TPM1*, *AMOT*, *P4HA1*, *HIST1H2BK*, *SELENBP1*, and *QSOX1* (9). RNAseq analysis confirmed that 6/8 of these genes were downregulated in MCF7 PTHrP-overexpressing cells (**Table 2**).

Calcium-Related Pathways Are Activated in Response to PTHrP Overexpression in MCF7 Cells

We next performed STRING analysis on the RNAseq data to identify significantly enriched pathways. We separately analyzed the 250 upregulated and downregulated genes (all $p < 0.05$) with the largest $\log_2$ fold change, a total of 500 genes analyzed (**Figures 4A,B**). STRING pathway analysis of this RNAseq data revealed that the most significantly enriched pathways (false discovery rate = 0.0081–0.0324) in MCF7 cells overexpressing PTHrP in comparison to parental MCF7 cells and across all 500 genes, were the calcium signaling pathway, cytokine–cytokine receptor interaction, chemokine signaling pathway, and inflammatory mediator regulation of transient receptor potential (TRP) channels (**Figure 4C**).

TABLE 1 | Cyclic AMP (cAMP) signaling is not induced by parathyroid hormone-related protein (PTHrP) in MCF7 cells.

Gene name	Log_2 fold change	*p*-Value	Direction
AREG	3.58	1.25E-07	Up
NRP1	0.75	5.12E-04	Up
FOS	−0.74	0.03	Down
AQP3	−1.07	1.14E-03	Down
CEBPD	−0.83	0.03	Down
SOX9	−0.41	0.41	–
NR4A3	−0.07	0.93	–
BTG2	−0.29	0.53	–
UGDH	0.06	0.87	–
DUSP1	−0.12	0.75	–
NR4A2	0.14	0.69	–
GEM	−0.47	0.66	–
RGS2	−0.12	0.93	–
TCF7	0.19	0.56	–
VEGFA	−0.03	0.96	–
NR4A1	0.52	0.53	–
TEX2	0.04	0.88	–
IFNGR1	0.07	0.88	–
EFNB2	0.53	0.10	–
SIK2	−0.16	0.49	–
PLAUR	0.39	0.34	–
BMP8A	0.14	0.82	–
JUNB	0.15	0.72	–
IER3	0.83	0.17	–
USP2	−0.38	0.40	–
NFIL3	0.02	0.95	–
NFKB2	0.08	0.75	–
DLEC1	0.25	0.65	–
FOXC2	0.67	0.65	–
LST1	−0.05	0.97	–
KCNE4	0.25	0.56	–
IL6	0.60	0.81	–
PTHR1	0.01	0.99	–

RNAseq values for 32 known cAMP target genes (22) and PTHR1 (bottom of table) in MCF7 PTHrP-overexpressing cells compared to MCF7 vector controls.
Red = significantly up-regulated, green = significantly down-regulated, gray = no significant change.

TABLE 2 | Dormancy genes are downregulated by parathyroid hormone-related protein (PTHrP) in MCF7 cells.

Gene name	Log_2 fold change	*p*-Value
LIFR	−0.57	$p = 0.09$
SOCS3	−1.18	$p = 0.01^{*}$
AMOT	−0.45	$p = 0.04^{*}$
FHL1	−0.54	$p = 0.02^{*}$
HIST1H2BK	−0.61	$p = 0.003^{**}$
SELENBP1	−0.65	$p = 2.92 \times 10^{-6****}$
TPM1	0.02	$p = 0.945$
QSOX1	−0.35	$p = 0.13$

RNAseq values for eight pro-dormancy genes (9) in MCF7 PTHrP-overexpressing cells compared to MCF7 vector controls.
Green = significantly down-regulated, gray = no significant change.
$^{*}p < 0.05$, $^{**}p < 0.01$, $^{****}p < 0.0001$.

The calcium signaling pathway and TRP channels are ion channels with high selectivity for Ca^{2+} (30), indicating calcium signaling is dramatically altered with PTHrP overexpression. There was overlap of 5/6 regulated genes in the "calcium signaling pathway" and "regulation of TRP channel pathway" from STRING analysis (*P2RX6* was specific for the calcium signaling pathway) (**Figure 5A**); there were no unique TRP channel pathway genes that were regulated. mRNA levels for *PTHLH* (control), *BDKRB1*, and *CALML3* (**Figures 5B–D**) confirmed the RNAseq findings in MCF7 PTHrP-overexpressing cells.

DISCUSSION

This work provides extensive evidence that PTHrP, although it is capable of inducing substantial changes in gene expression and behavior in MCF7 cells, does not signal through the PTHR1 to activate the cAMP pathway in these cells. Although PTHR1 is detected by qPCR, no cAMP response was detected, and no activity was observed in a CREB reporter assay. Furthermore, out of all the known cAMP responsive genes, only 2 of 32 were regulated in a positive direction by RNAseq analysis. In contrast, PTHrP overexpression in these cells upregulated genes associated with the calcium signaling pathway.

When human breast cancer cells were found to express functional receptors for calcitonin and PGE_2 linked to adenylyl cyclase activation, no such activation could be detected in response to PTH(1–34) (15). We confirm this observation in the present experiments and show that PTHrP(1–141) also lacks this activity. In addition, we report that PTH(1–34) has no effect on activation of a CREB reporter construct that is readily activated by either sCT or PGE_2. The latter two agonists, unlike PTH and PTHrP, also promoted expression of genes known to be regulated by the PKA–CREB pathway. There were only two cAMP responsive genes that were significantly upregulated with PTHrP overexpression by RNAseq: *AREG* and *NRP1*. Both of these genes have been implicated in cancer. *AREG* is essential for estrogen receptor-targeted therapeutic response (31). *NRP1* has been previously shown to promote tumorigenesis by enhancing angiogenesis (32) and NRP1-positive cells have been reported to have tumor-initiating properties (33). Thus the upregulation of these genes may result from indirect effects independent of cAMP, a possibility we will investigate. It is also worth noting that the PTHrP induction of *AREG* mRNA, and the CREB-responsive gene *NR4A1*, in MCF7s is much lower than its induction with the positive controls prostaglandin E_2 (PGE_2) and sCT. In a separate study, we have tested the same secreted form of PTHrP, and the same preparation of recombinant PTHrP(1–141) in Ocy454 cells, an osteocyte cell line that expresses the PTHR1 (7). Overexpression and exogenous treatment both induced a significant increase in cAMP in these cells, and overexpression increased the CREB responsive genes, *Nr4a1* and *Rgs2* (7) confirming that these forms of PTHrP are capable of inducing a CREB response, but not in MCF7 cells.

Our data also indicate that PTH, which shares with PTHrP the same ability to bind to the PTHR1, does not bind to MCF7 cells in any detectable manner. This is illustrated by use of the PTH^{-TMR} reagent, which requires functional PTHR1 for CREB activation and internalization into early endosomes. This suggests that the action of overexpressed PTHrP that suppresses dormancy and results in major changes in gene expression and osteolytic destruction of bone, is not only not cAMP-mediated, but is also not elicited through the PTHR1. However, we have not excluded the possibility that PTHrP binds to PTHR1 at levels below our detection limits, and initiates cAMP-independent signaling.

KEGG BIOLOGICAL PATHWAY (UP-REGULATED)	Gene count	False discovery rate
Calcium signaling pathway	6	0.0081
Cytokine-cytokine receptor interaction	7	0.0081
Chemokine signaling pathway	6	0.0081
Inflammatory mediator regulation of TRP channels	5	0.0081
Circadian entrainment	4	0.0324

FIGURE 4 | Multiple signaling pathways are upregulated in MCF7 parathyroid hormone-related protein-overexpressing cells. **(A)** STRING network analysis of the top 250 upregulated genes (with $\log_2$ fold change >1 and $p < 0.05$). Colors of each node correspond to the KEGG pathway indicated in **(C)**. **(B)** STRING network analysis of the top 250 downregulated genes (with $\log_2$ fold change <−1 and $p < 0.05$). **(C)** KEGG biological pathways significantly enriched for in the STRING analysis of the top 250 upregulated genes. There were no significantly enriched KEGG biological pathways for the top 250 downregulated genes. Colors correspond to the nodes in **(A)**.

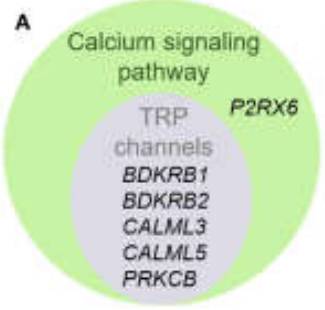

Gene name	Log2fold change	p-value
CALCIUM SIGNALING PATHWAY		
BDKRB1	3.82	1.34E-06
BDKRB2	4.74	2.01E-15
CALML3	3.77	6.41E-12
CALML5	3.48	4.32E-55
PRKCB	4.46	0.02
P2RX6	3.21	0.00023

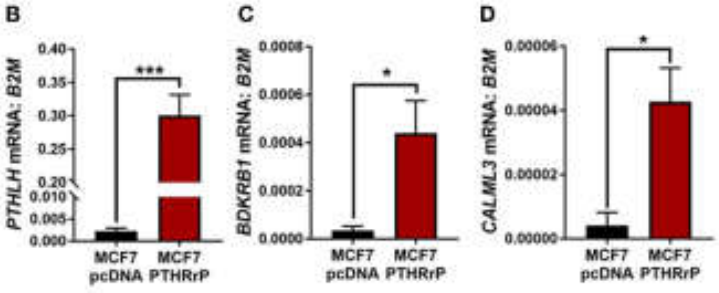

FIGURE 5 | The calcium signaling pathway is significantly enriched downstream of parathyroid hormone-related protein (PTHrP) in MCF7 cells. **(A)** Venn diagram indicating the calcium signaling pathway and transient receptor potential (TRP) channel genes that were significantly upregulated in PTHrP-overexpressing cells (gray circle). There was also one significantly enriched gene that was unique to the calcium signaling pathway, P2RX6 (green circle). **(B)** *PTHLH* mRNA levels, shown as a control for PTHrP overexpression, in MCF7pcDNA control or MCF7 PTHrP-overexpressing cells **(C,D)**. qPCR for mRNA levels of calcium signaling pathway genes in MCF7pcDNA or MCF7 PTHrP-overexpressing cells. Graphs = mean + SE. $n = 3$ replicates from independent experiments. $^*p < 0.05$, $^{***}p < 0.001$ by Unpaired Student's *T*-test.

Parathyroid hormone and PTHrP have identical amino acids in 8 of their first 13 residues, but other similarities within the sequences are no more than would be expected by chance (1, 3). In PTHR1-bearing target cells, recombinant PTHrP(1–141) and synthetic shorter amino-terminal forms were equipotent on a molar basis with each other and with PTH(1–34) in their ability to promote cAMP activity (19). In exerting this function, PTHrP and PTH were shown to share actions upon a common receptor, PTHR1 (14). These functions are absent in MCF7 cells. Instead, our findings suggest that the major changes in gene expression

in MCF7 cells in response to PTHrP must occur through PTHrP actions mediated by domains of PTHrP distinct from the (1–34) region known to act on the cAMP–PKA pathway through PTHR1.

A number of biological activities have been ascribed to domains of PTHrP beyond the amino-terminal region, but although these domains have been defined on the basis of the primary amino acid sequence, no receptors for these responses have yet been identified. For example, (i) the mid-molecule portion, between residues 35 and 84, is responsible for placental calcium transport, (ii) many pharmacologic studies have shown biological effects of the C-terminal domain, beginning at residue 107, and (iii) a nuclear localizing sequence mediates transport of PTHrP to the nucleus in many cell types [reviewed in Ref. (1)]. These many biological activities within the PTHrP molecule led to it being regarded as a multifunctional cytokine (34, 35) but the specific intracellular pathways that mediate these non-PTHR1-mediated actions remain unknown. These possibilities have been raised recently with respect to the role of PTHrP in bone remodeling (7), since mice lacking PTHrP in osteocytes exhibit a bone phenotype that is markedly different from mice lacking the PTHR1 (36).

Thus in this work, where substantial effects of PTHrP overexpression on gene expression in MCF7 cells seem to be unrelated to PTHR1-mediated actions though cAMP/PKA/CREB activation, these other domains of PTHrP need to be considered. This question begins to be addressed with the findings from the RNAseq data, which identified the calcium signaling pathway as significantly upregulated by PTHrP overexpression. In cancer, upregulation of Ca^{2+} channels and pumps promotes tumor proliferation and drives tumorigenesis. Several of these signaling pathway components have been reported as overexpressed in breast, prostate, colon, pancreas, and lung tumors (37–39). It has also been shown that PTHrP nuclear action downstream of the calcium-sensing receptor (CaSR) promotes proliferation and reduces $p27^{Kip1}$ levels in breast cancer cells, ultimately preventing nuclear accumulation of apoptosis-inducing factor and the cell death that normally occurs when Ca^{2+} levels are in excess (40). While these actions have never been directly linked to PTHrP-induced bone destruction, our findings are consistent with the known roles for the calcium signaling pathway in cancer. These data suggest that CaSR acts upstream of PTHrP, and our data raise the possibility that PTHrP further promotes calcium signaling, possibly in a feed-forward loop.

We previously reported that PTHrP overexpression in MCF7 cells downregulates eight pro-dormancy genes (9) and our RNAseq analysis now provides a potential pathway through which PTHrP may function to downregulate these genes. Experiments to determine the functional significance of the calcium signaling pathway in tumor dormancy *in vivo* will be necessary to determine whether this is the pathway through which PTHrP enables dormant tumor cells to aggressively colonize the bone.

AUTHOR CONTRIBUTIONS

RJ, YS, PH, AC, and JJ performed experiments and analyzed data. RJ, NP, NS, and TM interpreted the data. RJ, NS, and TM wrote the manuscript. YS, PH, AC, JJ, and NP edited the manuscript.

ACKNOWLEDGMENTS

A portion of these data were previously published as a conference paper supplement (41). The authors wish to acknowledge the expert technical support of the VANGARD core facilities. RJ is supported in part by NIH award R00CA194198 (RJ). Experiments performed at Vanderbilt were supported in part by scholarship funds from NIH award P30CA068485 Vanderbilt-Ingram Cancer Center Support Grant. Experiments performed at SVI were supported in part by NHMRC grant 1081242 to NS and TM, and SVI receives support from the Victorian Government OIS Program. AC was supported in part by an Australian and New Zealand Bone and Mineral Society Christine & T. Jack Martin Research Travel Grant and NHMRC grant 1078280 to NP.

REFERENCES

1. Martin TJ. Parathyroid hormone-related protein, its regulation of cartilage and bone development, and role in treating bone diseases. *Physiol Rev* (2016) 96(3):831–71. doi:10.1152/physrev.00031.2015
2. McCauley LK, Martin TJ. Twenty-five years of PTHrP progress: from cancer hormone to multifunctional cytokine. *J Bone Miner Res* (2012) 27(6):1231–9. doi:10.1002/jbmr.1617
3. Suva LJ, Winslow GA, Wettenhall RE, Hammonds RG, Moseley JM, Diefenbach-Jagger H, et al. A parathyroid hormone-related protein implicated in malignant hypercalcemia: cloning and expression. *Science* (1987) 237(4817):893–6. doi:10.1126/science.3616618
4. Powell GJ, Southby J, Danks JA, Stillwell RG, Hayman JA, Henderson MA, et al. Localization of parathyroid hormone-related protein in breast cancer metastases: increased incidence in bone compared with other sites. *Cancer Res* (1991) 51(11):3059–61.
5. Thomas RJ, Guise TA, Yin JJ, Elliott J, Horwood NJ, Martin TJ, et al. Breast cancer cells interact with osteoblasts to support osteoclast formation. *Endocrinology* (1999) 140(10):4451–8. doi:10.1210/endo.140.10.7037
6. Martin TJ. Osteoblast-derived PTHrP is a physiological regulator of bone formation. *J Clin Invest* (2005) 115(9):2322–4. doi:10.1172/JCI26239
7. Ansari N, Ho PW, Crimeen-Irwin B, Poulton IJ, Brunt AR, Forwood MR, et al. Autocrine and paracrine regulation of the murine skeleton by osteocyte-derived parathyroid hormone-related protein. *J Bone Miner Res* (2018) 33(1):137–53. doi:10.1002/jbmr.3291
8. Kobayashi T, Chung UI, Schipani E, Starbuck M, Karsenty G, Katagiri T, et al. PTHrP and Indian hedgehog control differentiation of growth plate chondrocytes at multiple steps. *Development* (2002) 129(12):2977–86.
9. Johnson RW, Finger EC, Olcina MM, Vilalta M, Aguilera T, Miao Y, et al. Induction of LIFR confers a dormancy phenotype in breast cancer cells disseminated to the bone marrow. *Nat Cell Biol* (2016) 18(10):1078–89. doi:10.1038/ncb3408
10. Kemp BE, Moseley JM, Rodda CP, Ebeling PR, Wettenhall RE, Stapleton D, et al. Parathyroid hormone-related protein of malignancy: active synthetic fragments. *Science* (1987) 238(4833):1568–70. doi:10.1126/science.3685995
11. Pizurki L, Rizzoli R, Moseley J, Martin TJ, Caverzasio J, Bonjour JP. Effect of synthetic tumoral PTH-related peptide on cAMP production and Na-dependent Pi transport. *Am J Physiol* (1988) 255(5 Pt 2):F957–61. doi:10.1152/ajprenal.1988.255.5.F957
12. Fukayama S, Bosma TJ, Goad DL, Voelkel EF, Tashjian AH Jr. Human parathyroid hormone (PTH)-related protein and human PTH: comparative biological activities on human bone cells and bone resorption. *Endocrinology* (1988) 123(6):2841–8. doi:10.1210/endo-123-6-2841
13. Ebeling PR, Adam WR, Moseley JM, Martin TJ. Actions of synthetic parathyroid hormone-related protein(1-34) on the isolated rat kidney. *J Endocrinol* (1989) 120(1):45–50. doi:10.1677/joe.0.1200045

14. Juppner H, Abou-Samra AB, Freeman M, Kong XF, Schipani E, Richards J, et al. A G protein-linked receptor for parathyroid hormone and parathyroid hormone-related peptide. *Science* (1991) 254(5034):1024–6. doi:10.1126/science.1658941
15. Martin TJ, Findlay DM, MacIntyre I, Eisman JA, Michelangeli VP, Moseley JM, et al. Calcitonin receptors in a cloned human breast cancer cell line (MCF 7). *Biochem Biophys Res Commun* (1980) 96(1):150–6. doi:10.1016/0006-291X(80)91193-6
16. Findlay DM, deLuise M, Michelangeli VP, Ellison M, Martin TJ. Properties of a calcitonin receptor and adenylate cyclase in BEN cells, a human cancer cell line. *Cancer Res* (1980) 40(4):1311–7.
17. Martin TJ, Ng KW, Partridge NC, Livesey SA. Hormonal influences on bone cells. *Methods Enzymol* (1987) 145:324–36. doi:10.1016/0076-6879(87)45019-2
18. Mulcrone PL, Campbell JP, Clement-Demange L, Anbinder AL, Merkel AR, Brekken RA, et al. Skeletal colonization by breast cancer cells is stimulated by an osteoblast and beta2AR-dependent neo-angiogenic switch. *J Bone Miner Res* (2017) 32(7):1442–54. doi:10.1002/jbmr.3133
19. Hammonds RG Jr, McKay P, Winslow GA, Diefenbach-Jagger H, Grill V, Glatz J, et al. Purification and characterization of recombinant human parathyroid hormone-related protein. *J Biol Chem* (1989) 264(25):14806–11.
20. Allan EH, Hausler KD, Wei T, Gooi JH, Quinn JM, Crimeen-Irwin B, et al. EphrinB2 regulation by PTH and PTHrP revealed by molecular profiling in differentiating osteoblasts. *J Bone Miner Res* (2008) 23(8):1170–81. doi:10.1359/jbmr.080324
21. Richard V, Luchin A, Brena RM, Plass C, Rosol TJ. Quantitative evaluation of alternative promoter usage and 3' splice variants for parathyroid hormone-related protein by real-time reverse transcription-PCR. *Clin Chem* (2003) 49(8):1398–402. doi:10.1373/49.8.1398
22. Walia MK, Ho PM, Taylor S, Ng AJ, Gupte A, Chalk AM, et al. Activation of PTHrP-cAMP-CREB1 signaling following p53 loss is essential for osteosarcoma initiation and maintenance. *Elife* (2016) 5:e13446. doi:10.7554/eLife.13446
23. Chan AS, Clairfeuille T, Landao-Bassonga E, Kinna G, Ng PY, Loo LS, et al. Sorting nexin 27 couples PTHR trafficking to retromer for signal regulation in osteoblasts during bone growth. *Mol Biol Cell* (2016) 27(8):1367–82. doi:10.1091/mbc.E15-12-0851
24. Yamada H, Tsutsumi M, Fukase M, Fujimori A, Yamamoto Y, Miyauchi A, et al. Effects of human PTH-related peptide and human PTH on cyclic AMP production and cytosolic free calcium in an osteoblastic cell clone. *Bone Miner* (1989) 6(1):45–54. doi:10.1016/0169-6009(89)90022-6
25. Guise TA, Yin JJ, Taylor SD, Kumagai Y, Dallas M, Boyce BF, et al. Evidence for a causal role of parathyroid hormone-related protein in the pathogenesis of human breast cancer-mediated osteolysis. *J Clin Invest* (1996) 98(7):1544–9. doi:10.1172/JCI118947
26. Johnson RW, Nguyen MP, Padalecki SS, Grubbs BG, Merkel AR, Oyajobi BO, et al. TGF-beta promotion of Gli2-induced expression of parathyroid hormone-related protein, an important osteolytic factor in bone metastasis, is independent of canonical Hedgehog signaling. *Cancer Res* (2011) 71(3):822–31. doi:10.1158/0008-5472.CAN-10-2993
27. Kusuma N, Denoyer D, Eble JA, Redvers RP, Parker BS, Pelzer R, et al. Integrin-dependent response to laminin-511 regulates breast tumor cell invasion and metastasis. *Int J Cancer* (2012) 130(3):555–66. doi:10.1002/ijc.26018
28. Gallon M, Cullen PJ. Retromer and sorting nexins in endosomal sorting. *Biochem Soc Trans* (2015) 43(1):33–47. doi:10.1042/BST20140290
29. Feinstein TN, Wehbi VL, Ardura JA, Wheeler DS, Ferrandon S, Gardella TJ, et al. Retromer terminates the generation of cAMP by internalized PTH receptors. *Nat Chem Biol* (2011) 7(5):278–84. doi:10.1038/nchembio.545
30. Ramsey IS, Delling M, Clapham DE. An introduction to TRP channels. *Annu Rev Physiol* (2006) 68:619–47. doi:10.1146/annurev.physiol.68.040204.100431
31. Peterson EA, Jenkins EC, Lofgren KA, Chandiramani N, Liu H, Aranda E, et al. Amphiregulin is a critical downstream effector of estrogen signaling in ERalpha-positive breast cancer. *Cancer Res* (2015) 75(22):4830–8. doi:10.1158/0008-5472.CAN-15-0709
32. Miao HQ, Lee P, Lin H, Soker S, Klagsbrun M. Neuropilin-1 expression by tumor cells promotes tumor angiogenesis and progression. *FASEB J* (2000) 14(15):2532–9. doi:10.1096/fj.00-0250com
33. Jimenez-Hernandez LE, Vazquez-Santillan K, Castro-Oropeza R, Martinez-Ruiz G, Munoz-Galindo L, Gonzalez-Torres C, et al. NRP1-positive lung cancer cells possess tumor-initiating properties. *Oncol Rep* (2018) 39(1):349–57. doi:10.3892/or.2017.6089
34. Philbrick WM, Wysolmerski JJ, Galbraith S, Holt E, Orloff JJ, Yang KH, et al. Defining the roles of parathyroid hormone-related protein in normal physiology. *Physiol Rev* (1996) 76(1):127–73. doi:10.1152/physrev.1996.76.1.127
35. Martin TJ, Moseley JM, Williams ED. Parathyroid hormone-related protein: hormone and cytokine. *J Endocrinol* (1997) 154(Suppl):S23–37.
36. Saini V, Marengi DA, Barry KJ, Fulzele KS, Heiden E, Liu X, et al. Parathyroid hormone (PTH)/PTH-related peptide type 1 receptor (PPR) signaling in osteocytes regulates anabolic and catabolic skeletal responses to PTH. *J Biol Chem* (2013) 288(28):20122–34. doi:10.1074/jbc.M112.441360
37. El Hiani Y, Lehen'kyi V, Ouadid-Ahidouch H, Ahidouch A. Activation of the calcium-sensing receptor by high calcium induced breast cancer cell proliferation and TRPC1 cation channel over-expression potentially through EGFR pathways. *Arch Biochem Biophys* (2009) 486(1):58–63. doi:10.1016/j.abb.2009.03.010
38. Tsavaler L, Shapero MH, Morkowski S, Laus R. Trp-p8, a novel prostate-specific gene, is up-regulated in prostate cancer and other malignancies and shares high homology with transient receptor potential calcium channel proteins. *Cancer Res* (2001) 61(9):3760–9.
39. Dhennin-Duthille I, Gautier M, Faouzi M, Guilbert A, Brevet M, Vaudry D, et al. High expression of transient receptor potential channels in human breast cancer epithelial cells and tissues: correlation with pathological parameters. *Cell Physiol Biochem* (2011) 28(5):813–22. doi:10.1159/000335795
40. Kim W, Takyar FM, Swan K, Jeong J, VanHouten J, Sullivan C, et al. Calcium-sensing receptor promotes breast cancer by stimulating intracrine actions of parathyroid hormone-related protein. *Cancer Res* (2016) 76(18):5348–60. doi:10.1158/0008-5472.CAN-15-2614
41. Johnson RW, Sun Y, Ho PWM, Sims N, Martin TJ. 2017 Annual Meeting of the American Society for Bone and Mineral Research, Colorado Convention Center, Denver, CO, USA – September 8–11, 2017. *J Bone Miner Res* (2017) 32:S1–432. doi:10.1002/jbmr.3363

Conflict of Interest Statement: The authors declare that the research was conducted in the absence of any commercial or financial relationships that could be construed as a potential conflict of interest.

Bibliography

Aarden, E. M., *et al*. (1994). "Function of osteocytes in bone." Journal of cellular biochemistry **55**(3): 287-299.

Aarts, M., *et al*. (1999). "The nucleolar targeting signal (NTS) of parathyroid hormone related protein mediates endocytosis and nucleolar translocation." Journal of Bone and Mineral Research **14**(9): 1493-1503.

Aarts, M. M., *et al*. (2001). "Parathyroid hormone-related protein promotes quiescence and survival of serum-deprived chondrocytes by inhibiting rRNA synthesis." Journal of Biological Chemistry **276**(41): 37934-37943.

Addison, W. N., *et al*. (2010). "Phosphorylation-dependent inhibition of mineralization by osteopontin ASARM peptides is regulated by PHEX cleavage." Journal of Bone and Mineral Research **25**(4): 695-705.

Alonso, V., *et al*. (2008). "Parathyroid hormone-related protein (107–139) increases human osteoblastic cell survival by activation of vascular endothelial growth factor receptor-2." Journal of cellular physiology **217**(3): 717-727.

Altarejos, J. Y. and M. Montminy (2011). "CREB and the CRTC co-activators: sensors for hormonal and metabolic signals." Nature reviews Molecular cell biology **12**(3): 141.

Amaya, Y., *et al*. (2015). "Evolutionary well-conserved region in the signal peptide of parathyroid hormone-related protein is critical for its dual localization through the regulation of ER translocation." The Journal of Biochemistry **159**(4): 393-406.

Amizuka, N., *et al*. (1996). "Haploinsufficiency of parathyroid hormone-related peptide (PTHrP) results in abnormal postnatal bone development." Developmental biology **175**(1): 166-176.

Amizuka, N., *et al*. (2002). "Biological action of parathyroid hormone (PTH)-related peptide (PTHrP) mediated either by the PTH/PTHrP receptor or the nucleolar translocation in chondrocytes." Anatomical science international **77**(4): 225-236.

Anderson, H. C. (1995). "Molecular biology of matrix vesicles." Clinical orthopaedics and related research(314): 266-280.

Anderson, H. C. (2003). "Matrix vesicles and calcification." Current rheumatology reports **5**(3): 222-226.

Ansari, N., *et al*. (2018). "Autocrine and paracrine regulation of the murine skeleton by osteocyte-derived parathyroid hormone-related protein." Journal of Bone and Mineral Research **33**(1): 137-153.

Arnold, S. J., *et al*. (2000). "Brachyury is a target gene of the Wnt/β-catenin signalling pathway." Mechanisms of development **91**(1-2): 249-258.

Atkins, G., *et al*. (2009). "Strontium ranelate treatment of human primary osteoblasts promotes an osteocyte-like phenotype while eliciting an osteoprotegerin response." Osteoporosis International **20**(4): 653-664.

Atkins, G. J., *et al*. (2007). "Metabolism of vitamin D3 in human osteoblasts: evidence for autocrine and paracrine activities of 1α, 25-dihydroxyvitamin D3." Bone **40**(6): 1517-1528.

Atkins, G. J., *et al*. (2011). "Sclerostin is a locally acting regulator of late-osteoblast/preosteocyte differentiation and regulates mineralization through a MEPE-ASARM-dependent mechanism." Journal of Bone and Mineral Research **26**(7): 1425-1436.

Atkins, G. J., *et al*. (2009). "Vitamin K promotes mineralization, osteoblast-to-osteocyte transition, and an anticatabolic phenotype by γ-carboxylation-dependent and-independent mechanisms." American Journal of Physiology-Cell Physiology **297**(6): C1358-C1367.

Bala Y, Farlay D, Boivin G. Bone mineralization: from tissue to crystal in normal and pathological contexts[J]. Osteoporosis International, 2013, 24(8): 2153-2166.

Baron, R. and M. Kneissel (2013). "WNT signaling in bone homeostasis and disease: from human mutations to treatments." Nature medicine **19**(2): 179.

Baron, R., *et al*. (2006). "Wnt signaling: a key regulator of bone mass." Current topics in developmental biology **76**: 103-127.

Barragan-Adjemian, C., *et al*. (2006). "Mechanism by which MLO-A5 late osteoblasts/early osteocytes mineralize in culture: similarities with mineralization of lamellar bone." Calcified tissue international **79**(5): 340-353.

Bellido, T., *et al*. (2013). "Effects of PTH on osteocyte function." Bone **54**(2): 250-257.

Bendre, M., *et al*. (2003). "Breast cancer metastasis to bone - It is not all about PTHrP." Clinical Orthopaedics & Related Research **415**(415 Suppl): S39-45.

Bergmann, P., *et al*. (1990). "Release of parathyroid hormonelike peptides by fetal rat long bones in culture." Journal of Bone and Mineral Research **5**(7): 741-753.

Berrettoni, B. A. and J. R. Carter (1986). "Mechanisms of cancer metastasis to bone." JBJS **68**(2): 308-312.

Bhatia, V., *et al*. (2009). "Nuclear PTHrP targeting regulates PTHrP secretion and enhances LoVo cell growth and survival." Regulatory peptides **158**(1-3): 149-155.

Bianco, P., *et al*. (1991). "Expression of bone sialoprotein (BSP) in developing human tissues." Calcified tissue international **49**(6): 421-426.

Birmingham, E., *et al*. (2012). "Osteogenic differentiation of mesenchymal stem cells is regulated by osteocyte and osteoblast cells in a simplified bone niche." European Cells and Materials **23**: 13-27.

Biswas, S., *et al*. (2011). "Anti-transforming growth factor ss antibody treatment rescues bone loss and prevents breast cancer metastasis to bone." PloS one **6**(11): e27090.

Bi X, Li G, Doty S B, *et al*. A novel method for determination of collagen orientation in cartilage by Fourier transform infrared imaging spectroscopy (FT-IRIS)[J]. Osteoarthritis and cartilage, 2005, 13(12): 1050-1058.

Blair, H. J., *et al*. (1998). "Mouse mutants carrying deletions that remove the genes mutated in Coffin-Lowry syndrome and lactic acidosis." Human molecular genetics **7**(3): 549-555.

Blair Jr, A. J., *et al*. (1973). "Ectopic hyperparathyroidism in a patient with metastatic hypernephroma." Metabolism **22**(2): 147-154.

BOILEAU, G., *et al*. (2001). "Characterization of PHEX endopeptidase catalytic activity: identification of parathyroid-hormone-related peptide107–139 as a substrate and osteocalcin, PPi and phosphate as inhibitors." Biochemical Journal **355**(3): 707-713.

Boskey, A. L. (2007). "Mineralization of bones and teeth." Elements **3**(6): 385-391.

Bougault, C., *et al*. (2017). "Involvement of sphingosine kinase/sphingosine 1-phosphate metabolic pathway in spondyloarthritis." Bone **103**: 150-158.

Bouleftour, W., *et al*. (2014). "Skeletal Development of Mice Lacking Bone Sialoprotein (BSP) - Impairment of Long Bone Growth and Progressive Establishment of High Trabecular Bone Mass." PloS one **9**.

Boskey A L. Bone composition: relationship to bone fragility and antiosteoporotic drug effects[J]. BoneKEy reports, 2013, 2.

Brandt, D. W., *et al*. (1994). "Parathyroid hormone-like protein: alternative messenger RNA splicing pathways in human cancer cell lines." Cancer research **54**(3): 850-853.

Broadus, A. E., *et al*. (1988). "Humoral hypercalcemia of cancer." New England Journal of Medicine **319**(9): 556-563.

Bruder, S. P. and A. Caplan (1990). "Terminal differentiation of osteogenic cells in the embryonic chick tibia is revealed by a monoclonal antibody against osteocytes." Bone **11**(3): 189-198.

Burtis, W. J., *et al*. (1990). "Immunochemical characterization of circulating parathyroid hormone–related protein in patients with humoral hypercalcemia of cancer." New England Journal of Medicine **322**(16): 1106-1112.

Burton, D., *et al*. (1994). "Parathyroid hormone-related protein in the cardiovascular system." Endocrinology **135**(1): 253-261.

Care, A., *et al*. (1990). "Stimulation of ovine placental transport of calcium and magnesium by mid-molecule fragments of human parathyroid hormone-related protein." Experimental Physiology: Translation and Integration **75**(4): 605-608.

Chan, A. S., *et al*. (2016). "Sorting nexin 27 couples PTHR trafficking to retromer for signal regulation in osteoblasts during bone growth." Molecular biology of the cell **27**(8): 1367-1382.

Cazalbou S, Combes C, Eichert D, *et al*. Poorly crystalline apatites: evolution and maturation in vitro and in vivo[J]. Journal of bone and mineral metabolism, 2004, 22(4): 310-317.

Chen, C., et al. (2004). "Impact of the mitogen-activated protein kinase pathway on parathyroid hormone-related protein actions in osteoblasts." Journal of Biological Chemistry **279**(28): 29121-29129.

CHEN, K. H., *et al*. (2005). "Calcification of senile cataractous lens determined by Fourier transform infrared (FTIR) and Raman microspectroscopies." Journal of microscopy **219**(1): 36-41.

Chenu, C., *et al*. (1994). "Osteocalcin induces chemotaxis, secretion of matrix proteins, and calcium-mediated intracellular signaling in human osteoclast-like cells." The Journal of cell biology **127**(4): 1149-1158.

Chepelev, I., *et al*. (2009). "Detection of single nucleotide variations in expressed exons of the human genome using RNA-Seq." Nucleic acids research **37**(16): e106-e106.

Chong-Kopera, H., *et al*. (2006). "TSC1 stabilizes TSC2 by inhibiting the interaction between TSC2 and the HERC1 ubiquitin ligase." Journal of Biological Chemistry **281**(13): 8313-8316.

Coats, A., *et al*. (2003). "Polarization artefacts of an FTIR microscope and the consequences for intensity measurements on anisotropic materials." Journal of microscopy **211**(1): 63-66.

Cohen Jr, M. M. (2009). "Perspectives on RUNX genes: an update." American journal of medical genetics Part A **149**(12): 2629-2646.

Conlan, L. A., et al. (2002). "The COOH-terminus of parathyroid hormone-related protein (PTHrP) interacts with β-arrestin 1B 1." FEBS letters 527(1-3): 71-75.

Couchourel, Denis, *et al*. "Altered mineralization of human osteoarthritic osteoblasts is attributable to abnormal type I collagen production." Arthritis & Rheumatism 60.5 (2009): 1438-1450.

Croucher, P. I., *et al*. (2016). "Bone metastasis: the importance of the neighbourhood." Nature Reviews Cancer **16**(6): 373.

Currey "The Structure of Bone Tissue", in Bones: Structure and Mechanics (2002): 12–14. Princeton University Press. Princeton, NJ. ISBN 9781400849505.

Dallas, S. L. and L. F. Bonewald (2010). "Dynamics of the transition from osteoblast to osteocyte." Annals of the New York Academy of Sciences **1192**: 437.

Dallas, S. L., *et al*. (2013). "The osteocyte: an endocrine cell… and more." Endocrine reviews **34**(5): 658-690.

DasGupta, R., *et al*. (2005). "Functional genomic analysis of the Wnt-wingless signaling pathway." Science **308**(5723): 826-833.

Datta, N. S. and A. B. Abou-Samra (2009). "PTH and PTHrP signaling in osteoblasts." Cellular signalling **21**(8): 1245-1254.

de Castro, L. F., *et al*. (2012). "Comparison of the skeletal effects induced by daily administration of PTHrP (1–36) and PTHrP (107–139) to ovariectomized mice." Journal of cellular physiology **227**(4): 1752-1760.

De Miguel, F., *et al*. (2001). "The C-terminal region of PTHrP, in addition to the nuclear localization signal, is essential for the intracrine stimulation of proliferation in vascular smooth muscle cells." Endocrinology **142**(9): 4096-4105.

Delgado-Calle, J., *et al*. (2017). "Role and mechanism of action of sclerostin in bone." Bone **96**: 29-37.

Delgado-Calle, J., *et al*. (2017). "Control of bone anabolism in response to mechanical loading and PTH by distinct mechanisms downstream of the PTH receptor." Journal of Bone and Mineral Research **32**(3): 522-535.

Desbois, C., *et al*. (1994). "The mouse osteocalcin gene cluster contains three genes with two separate spatial and temporal patterns of expression." Journal of Biological Chemistry **269**(2): 1183-1190.

Dhanoa, B. S., *et al*. (2013). "Update on the Kelch-like (KLHL) gene family." Human genomics **7**(1): 13.

Dhennin-Duthille, I., *et al*. (2011). "High expression of transient receptor potential channels in human breast cancer epithelial cells and tissues: correlation with pathological parameters." Cellular Physiology and Biochemistry **28**(5): 813-822.

Diegel CR, Hann S, Ayturk U, Hu JCW, Lim K, et al. (2020) An osteocalcin-deficient mouse strain with-out endocrine abnormalities. PLoS Genetics. 16:e1008361.

Drozdov, I., *et al*. (2011). "Gene network inference and biochemical assessment delineates GPCR pathways and CREB targets in small intestinal neuroendocrine neoplasia." PloS one **6**(8): e22457.

Ducy, P., *et al*. (1996). "Increased bone formation in osteocalcin-deficient mice." Nature **382**(6590): 448.

Ducy, P. and G. Karsenty (1995). "Two distinct osteoblast-specific cis-acting elements control expression of a mouse osteocalcin gene." Molecular and cellular biology **15**(4): 1858-1869.

Ducy, P., *et al*. (1997). "Osf2/Cbfa1: a transcriptional activator of osteoblast differentiation." cell **89**(5): 747-754.

Eastman, Q. and R. Grosschedl (1999). "Regulation of LEF-1/TCF transcription factors by Wnt and other signals." Current opinion in cell biology **11**(2): 233-240.

Ecarot-Charrier, B., *et al*. (1983). "Osteoblasts isolated from mouse calvaria initiate matrix mineralization in culture." The Journal of cell biology **96**(3): 639-643.

El Hiani, Y., *et al*. (2009). "Activation of the calcium-sensing receptor by high calcium induced breast cancer cell proliferation and TRPC1 cation channel over-expression potentially through EGFR pathways." Archives of biochemistry and biophysics **486**(1): 58-63.

Everhart-Caye, M., *et al*. (1996). "Parathyroid hormone (PTH)-related protein (1-36) is equipotent to PTH (1-34) in humans." The Journal of Clinical Endocrinology & Metabolism **81**(1): 199-208.

Falzon, M. and P. Du (2000). "Enhanced growth of MCF-7 breast cancer cells overexpressing parathyroid hormone-related peptide." Endocrinology **141**(5): 1882-1892.

Feng, J. Q., *et al*. (2006). "Loss of DMP1 causes rickets and osteomalacia and identifies a role for osteocytes in mineral metabolism." Nature genetics **38**(11): 1310.

Fenton, A., *et al*. (1991). "A POTENT INHIBITOR OF OSTEOCLASTIC BONE RESORPTION WITHIN A HIGHLY CONSERVED PENTAPEPTIDE REGION OF PARATHYROID HORMONE-RELATED PROTEIN; PTHrP [107–lll]." Endocrinology **129**(6): 3424-3426.

Fenton, A. J., *et al*. (1991). "A carboxyl-terminal peptide from the parathyroid hormone-related protein inhibits bone resorption by osteoclasts." Endocrinology **129**(4): 1762-1768.

Findlay, D. M., *et al*. (1980). "Properties of a calcitonin receptor and adenylate cyclase in BEN cells, a human cancer cell line." Cancer research **40**(4): 1311-1317.

Forrest, S., *et al*. (1985). "Characterization of an osteoblast-like clonal cell line which responds to both parathyroid hormone and calcitonin." Calcified Tissue International **37**(1): 51-56.

Franceschi, R. T. and G. Xiao (2003). "Regulation of the osteoblast-specific transcription factor, Runx2: Responsiveness to multiple signal transduction pathways." Journal of cellular biochemistry **88**(3): 446-454.

Franz-Odendaal, T. A., *et al*. (2006). "Buried alive: how osteoblasts become osteocytes." Developmental dynamics: an official publication of the American Association of Anatomists **235**(1): 176-190.

Fredericks, J. D., *et al*. (2012). "FTIR spectroscopy: A new diagnostic tool to aid DNA analysis from heated bone." Forensic Science International: Genetics **6**(3): 375-380.

Fuchs R K, Allen M R, Ruppel M E, *et al*. In situ examination of the time-course for secondary mineralization of Haversian bone using synchrotron Fourier transform infrared microspectroscopy[J]. Matrix Biology, 2008, 27(1): 34-41.

Gamsjaeger, S., *et al*. (2014). "Vibrational spectroscopic imaging for the evaluation of matrix and mineral chemistry." Current osteoporosis reports **12**(4): 454-464.

Gandla, J., *et al*. (2017). "miR-34c-5p functions as pronociceptive microRNA in cancer pain by targeting Cav2. 3 containing calcium channels." Pain **158**(9): 1765.

Garcia-Martin, A., *et al*. (2014). "Functional roles of the nuclear localization signal of parathyroid hormone-related protein (PTHrP) in osteoblastic cells." Molecular Endocrinology **28**(6): 925-934.

García-Santisteban, I., *et al*. (2013). "USP1 deubiquitinase: cellular functions, regulatory mechanisms and emerging potential as target in cancer therapy." Molecular cancer **12**(1): 91.

García-Martín, A., *et al*. (2013). "Src kinases mediate VEGFR2 transactivation by the osteostatin domain of PTHrP to modulate osteoblastic function." Journal of cellular biochemistry **114**(6): 1404-1413.

Gardella, T. J. and H. Jüppner (2001). "Molecular properties of the PTH/PTHrP receptor." Trends in Endocrinology & Metabolism **12**(5): 210-217.

Gilmore, J. L., *et al*. (2008). "Amphiregulin-EGFR signaling regulates PTHrP gene expression in breast cancer cells." Breast cancer research and treatment **110**(3): 493-505.

Golub, E. E. and K. Boesze-Battaglia (2007). "The role of alkaline phosphatase in mineralization." Current opinion in Orthopaedics **18**(5): 444-448.

Grill, V., *et al*. (1991). "Parathyroid hormone-related protein: elevated levels in both humoral hypercalcemia of malignancy and hypercalcemia complicating metastatic breast cancer." The Journal of Clinical Endocrinology & Metabolism **73**(6): 1309-1315.

Grünberg, J. R., *et al*. (2014). "The novel secreted adipokine WNT1-inducible signaling pathway protein 2 (WISP2) is a mesenchymal cell activator of canonical WNT." Journal of Biological Chemistry **289**(10): 6899-6907.

Gu, X., *et al*. (2017) "Pharmacological inhibition of S6K1 impairs self-renewal and osteogenic differentiation of bone marrow stromal cells." Journal of cellular biochemistry.

Guenther, H., *et al*. (1995). "Evidence for the synthesis of parathyroid hormone-related protein (PTHrP) by nontransformed clonal rat osteoblastic cells in vitro." Bone **16**(3): 341-347.

Guise, T. A. (1997). "Parathyroid hormone-related protein and bone metastases." Cancer: Interdisciplinary International Journal of the American Cancer Society **80**(S8): 1572-1580.

Guise, T. A., *et al*. (1996). "Evidence for a causal role of parathyroid hormone-related protein in the pathogenesis of human breast cancer-mediated osteolysis." The Journal of clinical investigation **98**(7): 1544-1549.

Guise TA, *et al*. (2002). Parathyroid hormone-related protein (PTHrP)-(1-139) isoform is efficiently secreted in vitro and enhances breast can- cer metastasis to bone in vivo. Bone(30):670-676.

Guo, J., *et al*. (2012). "Fluorescent ligand-directed co-localization of the parathyroid hormone 1 receptor with the brush-border scaffold complex of the proximal tubule reveals hormone-dependent changes in ezrin immunoreactivity consistent with inactivation." Biochimica et Biophysica Acta (BBA)-Molecular Cell Research **1823**(12): 2243-2253.

Hammonds, R., *et al*. (1989). "Purification and characterization of recombinant human parathyroid hormone-related protein." Journal of Biological Chemistry **264**(25): 14806-14811.

Hanagata and Nobutaka (2016). "IFITM5 mutations and osteogenesis imperfecta." Journal of Bone & Mineral Metabolism **34**(2): 123-131.

Hanagata, N. (2016). "IFITM5 mutations and osteogenesis imperfecta." Journal of bone and mineral metabolism **34**(2): 123-131.

Hardcastle, T. J. (2012). "baySeq: Empirical Bayesian analysis of patterns of differential expression in count data." R package version **2**(0).

Hardcastle, T. J. and K. A. Kelly (2010). "baySeq: empirical Bayesian methods for identifying differential expression in sequence count data." BMC bioinformatics **11**(1): 422.

He, B., *et al*. (2001). "Tissue-specific targeting of the pthrp gene: the generation of mice with floxed alleles." Endocrinology **142**(5): 2070-2077.

Heino, T. J. and T. A. Hentunen (2008). "Differentiation of osteoblasts and osteocytes from mesenchymal stem cells." Current stem cell research & therapy **3**(2): 131-145.

Henderson, J. E., *et al*. (1995). "Nucleolar localization of parathyroid hormone-related peptide enhances survival of chondrocytes under conditions that promote apoptotic cell death." Molecular and cellular biology **15**(8): 4064-4075.

Ho, P. W., *et al*. (2015). "Knockdown of PTHR1 in osteosarcoma cells decreases invasion and growth and increases tumor differentiation in vivo." Oncogene **34**(22): 2922.

Hoare, S. R., *et al*. (2001). "Evaluating the signal transduction mechanism of the parathyroid hormone 1 receptor Effect of receptor-G-protein interaction on the ligand binding mechanism and receptor conformation." Journal of Biological Chemistry **276**(11): 7741-7753.

Holdsworth, G., *et al*. (2012). "Characterization of the interaction of sclerostin with the low density lipoprotein receptor-related protein (LRP) family of Wnt co-receptors." Journal of Biological Chemistry **287**(32): 26464-26477.

Hook, V. Y., *et al*. (2001). "Proteolysis of ProPTHrP (1–141) by “prohormone thiol protease” at multibasic residues generates PTHrP-related peptides: implications for PTHrP peptide production in lung cancer cells." Biochemical and biophysical research communications **285**(4): 932-938.

Houston, B., *et al*. (2004). "PHOSPHO1—A novel phosphatase specifically expressed at sites of mineralisation in bone and cartilage." Bone **34**(4): 0-637.

Huang, D. W., *et al*. (2009). "Systematic and integrative analysis of large gene lists using DAVID bioinformatics resources." Nature protocols **4**(1): 44.

Inada, M., *et al*. (1999). "Maturational disturbance of chondrocytes in Cbfa1-deficient mice." Developmental dynamics: an official publication of the American Association of Anatomists **214**(4): 279-290.

Inoue, Keiichi, *et al*. "A crucial role for matrix metalloproteinase 2 in osteocytic canalicular formation and bone metabolism." Journal of Biological Chemistry 281.44 (2006): 33814-33824.

Ionescu, A. M., *et al*. (2001). "PTHrP modulates chondrocyte differentiation through AP-1 and CREB signaling." Journal of Biological Chemistry **276**(15): 11639-11647.

J E Henderson, N Amizuka, H Warshawsky, *et al*. Nucleolar localization of parathyroid hormone-related peptide enhances survival of chondrocytes under conditions that promote apoptotic cell death.[J]. molecular & cellular biology, 1995, 15(8):4064.

Jimenez-Hernandez, L. E., *et al*. (2018). "NRP1-positive lung cancer cells possess tumor-initiating properties." Oncology reports **39**(1): 349-357.

Johnson R W, Brennan H J, Vrahnas C, *et al*. The primary function of gp130 signaling in osteoblasts is to maintain bone formation and strength, rather than promote osteoclast formation[J]. Journal of Bone and Mineral Research, 2014, 29(6): 1492-1505.

Johnson, R. W., *et al*. (2016). "Induction of LIFR confers a dormancy phenotype in breast cancer cells disseminated to the bone marrow." Nature cell biology **18**(10): 1078.

Jun, A. Y., *et al*. (2014) "Tetrahydrofurofuran-type lignans inhibit breast cancer-mediated bone destruction by blocking the vicious cycle between cancer cells, osteoblasts and osteoclasts." Investigational New Drugs **32**(1): 1-13.

Juppner, H., *et al*. (1991). "AG protein-linked receptor for parathyroid hormone and parathyroid hormone-related peptide." Science **254**(5034): 1024-1026.

Kahler, R. A. and J. J. Westendorf (2003). "Lymphoid enhancer factor-1 and β-catenin inhibit Runx2-dependent transcriptional activation of the osteocalcin promoter." Journal of Biological Chemistry **278**(14): 11937-11944.

Kamioka H, Honjo T, Takano-Yamamoto T. A three-dimensional distribution of osteo- cyte processes revealed by the combination of confocal laser scanning microscopy and differential interference contrast microscopy. Bone 2001;28:145–9.

Kandel, E. R. (2012). "The molecular biology of memory: cAMP, PKA, CRE, CREB-1, CREB-2, and CPEB." Molecular brain **5**(1): 14.

Kanehisa, M., *et al*. (2009). "KEGG for representation and analysis of molecular networks involving diseases and drugs." Nucleic acids research **38**(suppl_1): D355-D360.

Karaplis, A. C., *et al*. (1994). "Lethal skeletal dysplasia from targeted disruption of the parathyroid hormone-related peptide gene." Genes & development **8**(3): 277-289.

Karsenty, G. and E. N. Olson (2016). "Bone and muscle endocrine functions: unexpected paradigms of inter-organ communication." Cell **164**(6): 1248-1256.

Kartsogiannis, V., *et al*. (1997). "Temporal expression of PTHrP during endochondral bone formation in mouse and intramembranous bone formation in an in vivo rabbit model." Bone **21**(5): 385-392.

Kartsogiannis, V., *et al*. (1998). "Localization of parathyroid hormone-related protein in osteoclasts by in situ hybridization and immunohistochemistry." Bone **22**(3): 189-194.

Kato, K., *et al*. (2012). "Crystal structure of Enpp1, an extracellular glycoprotein involved in bone mineralization and insulin signaling." Proceedings of the National Academy of Sciences **109**(42): 16876-16881.

Kato, K., *et al*. (2012). "Crystal structure of Enpp1, an extracellular glycoprotein involved in bone mineralization and insulin signaling." Proceedings of the National Academy of Sciences of the United States of America **109**(42): 16876-16881.

Kawane, T., *et al*. (2003). "Parathyroid hormone (PTH) down-regulates PTH/PTH-related protein receptor gene expression in UMR-106 osteoblast-like cells via a 3', 5'-cyclic adenosine monophosphate-dependent, protein kinase A-independent pathway." Journal of endocrinology **178**(2): 247-256.

Keller H, Kneissel M. SOST is a target gene for PTH in bone[J]. Bone, 2005, 37(2): 148-158.
Kemp, B. E., *et al*. (1987). "Parathyroid hormone-related protein of malignancy: active synthetic fragments." Science **238**(4833): 1568-1570.

Kerschnitzki M, Kollmannsberger P, Burghammer M, Duda GN, Weinkamer R, Wagermaier W, *et al*. Architecture of the osteocyte network correlates with bone ma- terial quality. J Bone Miner Res 2013;28:1837–45.

Kim, J. H., *et al*. (2013). "Wnt signaling in bone formation and its therapeutic potential for bone diseases." Therapeutic advances in musculoskeletal disease **5**(1): 13-31.

Kim, R. S., *et al*. (2012). "Dormancy signatures and metastasis in estrogen receptor positive and negative breast cancer." PloS one **7**(4): e35569.

Kim, W., *et al*. (2016). "Calcium-sensing receptor promotes breast cancer by stimulating intracrine actions of parathyroid hormone–related protein." Cancer research **76**(18): 5348-5360.

Kischel, P., *et al*. (2012). "Overexpression of CD9 in human breast cancer cells promotes the development of bone metastases." Anticancer research **32**(12): 5211-5220.

Kitase, Y., *et al*. (2010). "Mechanical induction of PGE2 in osteocytes blocks glucocorticoid-induced apoptosis through both the β-catenin and PKA pathways." Journal of Bone and Mineral Research **25**(12): 2657-2668.

Kobayashi, Keiji, *et al*. "Mitochondrial superoxide in osteocytes perturbs canalicular networks in the setting of age-related osteoporosis." Scientific reports 5 (2015): 9148.

Kohl, M., *et al*. (2011). Cytoscape: software for visualization and analysis of biological networks. Data mining in proteomics, Springer**:** 291-303.

Komori, T. (2002). "Runx2, a multifunctional transcription factor in skeletal development." Journal of cellular biochemistry **87**(1): 1-8.

Komori, T., *et al*. (1997). "Branson RT, Gao YH, Inada M. Sato M, Okamoto R, Kitamura Y, Yoshiki S and Kishimoto T Targeted disruption off Cbfal results in a complete lack of bone formation owing to maturationai arrest of osteoblasts." Cell **89**: 755-764.

Kondo, H., *et al*. (2002). "Cyclic adenosine monophosphate/protein kinase A mediates parathyroid hormone/parathyroid hormone-related protein receptor regulation of osteoclastogenesis and expression of RANKL and osteoprotegerin mRNAs by marrow stromal cells." Journal of Bone and Mineral Research **17**(9): 1667-1679.

Kovacs, C. S., *et al*. (1996). "Parathyroid hormone-related peptide (PTHrP) regulates fetal–placental calcium transport through a receptor distinct from the PTH/PTHrP receptor." Proceedings of the National Academy of Sciences **93**(26): 15233-15238.

Kronenberg, H. M. (2006). "PTHrP and skeletal development." Annals of the New York Academy of Sciences **1068**(1): 1-13.

KUKREJA, S. C., *et al*. (1980). "Elevated nephrogenous cyclic AMP with normal serum parathyroid hormone levels in patients with lung cancer." The Journal of Clinical Endocrinology & Metabolism **51**(1): 167-169.

Kulkarni, N., *et al*. (2005). "Effects of parathyroid hormone on Wnt signaling pathway in bone." Journal of cellular biochemistry **95**(6): 1178-1190.

Lam, M. H., *et al*. (1999). "Importin β recognizes parathyroid hormone-related protein with high affinity and mediates its nuclear import in the absence of importin α." Journal of Biological Chemistry **274**(11): 7391-7398.

Lam, M. H., *et al*. (1999). "Phosphorylation at the cyclin-dependent kinases site (Thr85) of parathyroid hormone-related protein negatively regulates its nuclear localization." Journal of Biological Chemistry **274**(26): 18559-18566.

Lam, M. H., *et al*. (2000). "Nuclear and nucleolar localization of parathyroid hormone-related protein." Immunology and cell biology **78**(4): 395-402.

Lambert, L. J., *et al*. (2016). "Increased trabecular bone and improved biomechanics in an osteocalcin-null rat model created by CRISPR/Cas9 technology." Disease models & mechanisms **9**(10): 1169-1179.

Lee, N. K., *et al*. (2007). "Endocrine regulation of energy metabolism by the skeleton." Cell **130**(3): 456-469.

Li, J. and S. Dong (2016). "The signaling pathways involved in chondrocyte differentiation and hypertrophic differentiation." Stem cells international **2016**.

Li, S., *et al*. "Synchrotron FTIR mapping of mineralization in a microfluidic device." Lab on A Chip: 10.1039.C1036LC01393G.

Ling, Y., *et al*. (2005). "DMP1 Depletion Decreases Bone Mineralization In Vivo: An FTIR Imaging Analysis." Journal of Bone & Mineral Research **20**(12).

Linhart, R., *et al*. (2014). "Vacuolar protein sorting 35 (Vps35) rescues locomotor deficits and shortened lifespan in Drosophila expressing a Parkinson's disease mutant of Leucine-Rich Repeat Kinase 2 (LRRK2)." Molecular neurodegeneration **9**(1): 23.

Love, M. I., *et al*. (2014). "Moderated estimation of fold change and dispersion for RNA-seq data with DESeq2." Genome biology **15**(12): 550.

Lozano, D., *et al*. (2011). "The C-terminal fragment of parathyroid hormone-related peptide promotes bone formation in diabetic mice with low-turnover osteopaenia." British journal of pharmacology **162**(6): 1424-1438.

Lu, Y., *et al*. (2007). "DMP1-targeted Cre expression in odontoblasts and osteocytes." Journal of dental research **86**(4): 320-325.

Maeda, A., *et al*. (2015). "WNT1-induced secreted protein-1 (WISP1), a novel regulator of bone turnover and Wnt signaling." Journal of Biological Chemistry **290**(22): 14004-14018.

Maeda, T., *et al*. (2015). "Mineral trioxide aggregate induces osteoblastogenesis via Atf6." Bone reports **2**: 36-43.

Majumder, S., *et al*. (2004). "Identification of a novel cyclic AMP-response element (CRE-II) and the role of CREB-1 in the cAMP-induced expression of the survival motor neuron (SMN) gene." Journal of Biological Chemistry **279**(15): 14803-14811.

Malone, J., *et al*. (1982). "Recruitment of osteoclast precursors by purified bone matrix constituents." The Journal of cell biology **92**(1): 227-230.

Mamillapalli, R., *et al*. (2008). "Switching of G-protein usage by the calcium-sensing receptor reverses its effect on parathyroid hormone-related protein secretion in normal versus malignant breast cells." Journal of Biological Chemistry **283**(36): 24435-24447.

Manenti, G., *et al*. (2000). "A cancer modifier role for parathyroid hormone-related protein." Oncogene **19**(47): 5324.

Manolagas SC (2020) Osteocalcinpromotes bone mineralization but is not ahormone. PLoS Genet 16(6): e1008714.

Mangin, M., *et al*. (1990). "Structure of the mouse gene encoding parathyroid hormone-related peptide." Gene **95**(2): 195-202.

Mangin, M., *et al*. (1988). "Two distinct tumor-derived, parathyroid hormone-like peptides result from alternative ribonucleic acid splicing." Molecular Endocrinology **2**(11): 1049-1055.

Mannstadt, M., *et al*. (1999). "Receptors for PTH and PTHrP: their biological importance and functional properties." American Journal of Physiology-Renal Physiology **277**(5): F665-F675.

Manolagas, S. C. (2000). "Birth and death of bone cells: basic regulatory mechanisms and implications for the pathogenesis and treatment of osteoporosis." Endocrine reviews **21**(2): 115-137.

Martin, J., *et al*. (2010). "The role of RUNX2 in osteosarcoma oncogenesis." Sarcoma **2011**.

Martin, T., *et al*. (1980). "Calcitonin receptors in a cloned human breast cancer cell line (MCF 7)." Biochemical and biophysical research communications **96**(1): 150-156.

Martin, T., *et al*. (1976). "Parathyroid hormone-responsive adenylate cyclase in induced transplantable osteogenic rat sarcoma." Nature **260**(5550): 436.

Martin, T. J. (2005). "Osteoblast-derived PTHrP is a physiological regulator of bone formation." The Journal of clinical investigation **115**(9): 2322-2324.

Massfelder, T., *et al*. (1997). "Opposing mitogenic and anti-mitogenic actions of parathyroid hormone-related protein in vascular smooth muscle cells: a critical role for nuclear targeting." Proceedings of the National Academy of Sciences **94**(25): 13630-13635.

Meerovitch, K., *et al*. (1997). "Preproparathyroid hormone-related protein, a secreted peptide, is a substrate for the ubiquitin proteolytic system." Journal of Biological Chemistry **272**(10): 6706-6713.

Meerovitch, K., *et al*. (1998). "Proparathyroid hormone-related protein is associated with the chaperone protein BiP and undergoes proteasome-mediated degradation." Journal of Biological Chemistry **273**(33): 21025-21030.

Melnik, B. C., *et al*. (2009). "Anti-acne agents attenuate FGFR2 signal transduction in acne." Journal of Investigative Dermatology **129**(8): 1868-1877.

Menton, D., *et al*. (1984). "From bone lining cell to osteocyte—an SEM study." The Anatomical Record **209**(1): 29-39.

Meroni, G. and G. Diez-Roux (2005). "TRIM/RBCC, a novel class of 'single protein RING finger'E3 ubiquitin ligases." Bioessays **27**(11): 1147-1157.

Miao, D., *et al*. (2005). "Osteoblast-derived PTHrP is a potent endogenous bone anabolic agent that modifies the therapeutic efficacy of administered PTH 1–34." The Journal of clinical investigation **115**(9): 2402-2411.

Miao, H.-Q., *et al*. (2000). "Neuropilin-1 expression by tumor cells promotes tumor angiogenesis and progression." The FASEB journal **14**(15): 2532-2539.

Mihai, R., *et al*. (2006). "Expression of the calcium receptor in human breast cancer—a potential new marker predicting the risk of bone metastases." European Journal of Surgical Oncology (EJSO) **32**(5): 511-515.

Minagawa, M., *et al*. (2002). "Association between AAAG repeat polymorphism in the P3 promoter of the human parathyroid hormone (PTH)/PTH-related peptide receptor gene and adult height, urinary pyridinoline excretion, and promoter activity." The Journal of Clinical Endocrinology & Metabolism **87**(4): 1791-1796.

Minkin, C., *et al*. (1981). "Bone resorption and humoral hypercalcemia of malignancy: stimulation of bone resorption in vitro by tumor extracts is inhibited by prostaglandin synthesis inhibitors." The Journal of Clinical Endocrinology & Metabolism **53**(5): 941-947.

Miron, R. and Y. Zhang (2012). "Osteoinduction: a review of old concepts with new standards." Journal of dental research **91**(8): 736-744.

Moretti, J., *et al*. (2012). "The ubiquitin-specific protease 12 (USP12) is a negative regulator of notch signaling acting on notch receptor trafficking toward degradation." Journal of Biological Chemistry **287**(35): 29429-29441.

Moriishi T, Ozasa R, Ishimoto T, Nakano T, Hasegawa T, et al. (2020) Osteocalcin isnecessary for thealignment of apatite crystallites, but not glucose metabolism, testosterone synthesis, or muscle mass.PLoS Genetics. 16:e1008586.

MOSELEY, J. M., *et al*. (1991). "Immunohistochemical detection of parathyroid hormone-related protein in human fetal epithelia." The Journal of Clinical Endocrinology & Metabolism **73**(3): 478-484.

Mundy, G. R. (2002). "Metastasis to bone: causes, consequences and therapeutic opportunities." Nature Reviews Cancer **2**(8): 584-593.

Mundy, G. R. and J. W. Poser (1983). "Chemotactic activity of theγ-carboxyglutamic acid containing protein in bone." Calcified tissue international **35**(1): 164-168.

Nampei, A., *et al*. (2004). "Matrix extracellular phosphoglycoprotein (MEPE) is highly expressed in osteocytes in human bone." Journal of bone and mineral metabolism **22**(3): 176-184.

Nguyen, M. A., *et al*. (2001). "Nuclear forms of parathyroid hormone-related peptide are translated from non-AUG start sites downstream from the initiator methionine." Endocrinology **142**(2): 694-703.

Nguyen, M. A. and A. C. Karaplis (1998). "The nucleus: A target site for parathyroid hormone-related peptide (PTHrP) action." Journal of cellular biochemistry **70**(2): 193-199.

Nicolella, D. P., *et al*. (2006). "Osteocyte lacunae tissue strain in cortical bone." Journal of biomechanics **39**(9): 1735-1743.

Nijweide, P., *et al*. (1981). "Biochemical and histological studies on various bone cell preparations." Calcified tissue international **33**(1): 529-540.

Nikitovic, D., *et al*. (2016). "Parathyroid hormone/parathyroid hormone-related peptide regulate osteosarcoma cell functions: focus on the extracellular matrix." Oncology reports **36**(4): 1787-1792.

O'Brien, C. A., *et al*. (2008). "Control of bone mass and remodeling by PTH receptor signaling in osteocytes." PloS one **3**(8): e2942.

Ogawa, H., *et al*. "Mechanical motion promotes expression of Prg4 in articular cartilage."

Ogawa, H., *et al*. (2014). "Mechanical motion promotes expression of Prg4 in articular cartilage via multiple CREB-dependent, fluid flow shear stress-induced signaling pathways." Genes & development **28**(2): 127-139.

Okoumassoun, L. E., *et al*. (2007). "Parathyroid hormone-related protein (PTHrP) inhibits mitochondrial-dependent apoptosis through CK2." Journal of cellular physiology **212**(3): 591-599.

Oliveros, J. (2007). "VENNY; An interactive tool for comparing lists with Venn Diagramshttp." bioinfogp. cnb. csic. es/tools/venny/index. html.

Oliveros, J. C. (2015). VENNY. An interactive tool for comparing lists with Venn Diagrams. 2007.

Olsnes, S., *et al*. (2003). "Transport of exogenous growth factors and cytokines to the cytosol and to the nucleus." Physiological reviews **83**(1): 163-182.

Osterhoff G, Morgan E F, Shefelbine S J, et al. Bone mechanical properties and changes with osteoporosis[J]. Injury, 2016, 47: S11-S20.

Ottewell, P. D., *et al*. (2015). "Molecular alterations that drive breast cancer metastasis to bone." BoneKEy reports **4**.

Oury, F., *et al*. (2013). "Osteocalcin regulates murine and human fertility through a pancreas-bone-testis axis." The Journal of clinical investigation **123**(6): 2421-2433.

Paget, G. (1889). "Remarks on a case of alternate partial anaesthesia." British medical journal **1**(1462): 1.

Palumbo, C. (1986). "A three-dimensional ultrastructural study of osteoid-osteocytes in the tibia of chick embryos." Cell and tissue research **246**(1): 125-131.

Palumbo, C., *et al*. (1990). "Morphological study of intercellular junctions during osteocyte differentiation." Bone **11**(6): 401-406.

Partridge, N. C., *et al*. (1983). "Morphological and biochemical characterization of four clonal osteogenic sarcoma cell lines of rat origin." Cancer research **43**(9): 4308-4314.

Peacock, J. D., *et al*. (2011). "Sox9 transcriptionally represses Spp1 to prevent matrix mineralization in maturing heart valves and chondrocytes." PloS one **6**(10).

Pioszak, A. A., *et al*. (2009). "Structural basis for parathyroid hormone-related protein binding to the parathyroid hormone receptor and design of conformation-selective peptides." Journal of Biological Chemistry **284**(41): 28382-28391.

Plimpton, C. H. and A. Gellhorn (1956). "Hypercalcemia in malignant disease without evidence of bone destruction." The American journal of medicine **21**(5): 750-759.

Ploton, D., *et al*. (1986). "Improvement in the staining and in the visualization of the argyrophilic proteins of the nucleolar organizer region at the optical level." The Histochemical Journal **18**(1): 5-14.

Powell, G. J., *et al*. (1991). "Localization of parathyroid hormone-related protein in breast cancer metastases: increased incidence in bone compared with other sites." Cancer research **51**(11): 3059-3061.

Ramsey, I. S., *et al*. (2006). "An introduction to TRP channels." Annu. Rev. Physiol. **68**: 619-647.

Rey C, Collins B, Goehl T, *et al*. The carbonate environment in bone mineral: a resolution-enhanced Fourier transform infrared spectroscopy study[J]. Calcified tissue international, 1989, 45(3): 157-164.

Robinson, M. D., *et al*. (2010). "edgeR: a Bioconductor package for differential expression analysis of digital gene expression data." Bioinformatics **26**(1): 139-140.

Rowe, P., *et al*. (2004). "MEPE has the properties of an osteoblastic phosphatonin and minhibin." Bone **34**(2): 303-319.

Rowe, P. S. (2004). "The wrickkened pathways of FGF23, MEPE and PHEX." Critical Reviews in Oral Biology & Medicine **15**(5): 264-281.

Ruchon, A. F., *et al*. (2000). "Developmental expression and tissue distribution of Phex protein: effect of the Hyp mutation and relationship to bone markers." Journal of Bone and Mineral Research **15**(8): 1440-1450.

Saini, V., *et al*. (2013). "Parathyroid hormone (PTH)/PTH-related peptide type 1 receptor (PPR) signaling in osteocytes regulates anabolic and catabolic skeletal responses to PTH." Journal of Biological Chemistry **288**(28): 20122-20134.

Saito, A., *et al*. (2011). "Endoplasmic reticulum stress response mediated by the PERK-eIF2α-ATF4 pathway is involved in osteoblast differentiation induced by BMP2." Journal of Biological Chemistry **286**(6): 4809-4818.

Sardiello, M., *et al*. (2009). "A gene network regulating lysosomal biogenesis and function." Science **325**(5939): 473-477.

Schwarting, T., *et al*. (2016). "Stimulation with bone morphogenetic protein-2 (BMP-2) enhances bone–tendon integration in vitro." Connective tissue research **57**(2): 99-112.

Schwindinger, W. F., *et al*. (1998). "Coupling of the PTH/PTHrP receptor to multiple G-proteins." Endocrine **8**(2): 201-209.

Scopacasa, F., Need, A. G., *et al.* (2002). Effects of dose and timing of calcium supplementation on bone resorption in early menopausal women. Hormone and metabolic research, 34(01), 44-47.

Scully, O. J., *et al*. (2012). "Breast cancer metastasis." Cancer Genomics-Proteomics **9**(5): 311-320.

Seaman, M. N., *et al*. (1997). "Endosome to Golgi retrieval of the vacuolar protein sorting receptor, Vps10p, requires the function of the VPS29, VPS30, and VPS35 gene products." The Journal of cell biology **137**(1): 79-92.

Seki, T., *et al*. (2013). "JosD1, a membrane-targeted deubiquitinating enzyme, is activated by ubiquitination and regulates membrane dynamics, cell motility, and endocytosis." Journal of Biological Chemistry **288**(24): 17145-17155.

Shibata, S., *et al*. (2013). "Kelch-like 3 and Cullin 3 regulate electrolyte homeostasis via ubiquitination and degradation of WNK4." Proceedings of the National Academy of Sciences **110**(19): 7838-7843.

Shibue, T. and R. A. Weinberg (2011). Metastatic colonization: settlement, adaptation and propagation of tumor cells in a foreign tissue environment. Seminars in cancer biology, Elsevier.

Sims, N. A., *et al*. (2000). "Bone homeostasis in growth hormone receptor–null mice is restored by IGF-I but independent of Stat5." The Journal of clinical investigation **106**(9): 1095-1103.

Soki, F. N., *et al*. (2012). "The multifaceted actions of PTHrP in skeletal metastasis." Future Oncology **8**(7): 803-817.

Southby, J., *et al*. (1990). "Immunohistochemical localization of parathyroid hormone-related protein in human breast cancer." Cancer research **50**(23): 7710-7716.

Southby, J., *et al*. (1995). "Alternative promoter usage and mRNA splicing pathways for parathyroid hormone-related protein in normal tissues and tumours." British journal of cancer **72**(3): 702.

Southby, J., *et al*. (1995). "Alternative promoter usage and mRNA splicing pathways for parathyroid hormone-related protein in normal tissues and tumours." British journal of cancer **72**(3): 702-707.

Spatz, J. M., *et al*. (2015). "The Wnt inhibitor sclerostin is up-regulated by mechanical unloading in osteocytes in vitro." Journal of Biological Chemistry **290**(27): 16744-16758.

Spiegel, S., *et al*. (2019). "New insights into functions of the sphingosine-1-phosphate transporter SPNS2." Journal of lipid research **60**(3): 484-489.

Stein, G. S., *et al*. (2004). "Runx2 control of organization, assembly and activity of the regulatory machinery for skeletal gene expression." Oncogene **23**(24): 4315.

Steitz, Susan A., *et al.* "Osteopontin inhibits mineral deposition and promotes regression of ectopic calcification." The American journal of pathology 161.6 (2002): 2035-2046.

Stewart, A. F., *et al*. (1980). "Biochemical evaluation of patients with cancer-associated hypercalcemia: evidence for humoral and nonhumoral groups." New England Journal of Medicine **303**(24): 1377-1383.

Strehler, E. E. (2011). "Emanuel Strehler's work on calcium pumps and calcium signaling." World journal of biological chemistry **2**(4): 67.

Strewler, G. J., *et al*. (1987). "Parathyroid hormonelike protein from human renal carcinoma cells. Structural and functional homology with parathyroid hormone." The Journal of clinical investigation **80**(6): 1803-1807.

Strom, T. M., *et al*. (1997). "Pex gene deletions in Gy and Hyp mice provide mouse models for X-linked hypophosphatemia." Human molecular genetics **6**(2): 165-171.

Suda, N., *et al*. (1996). "Expression of parathyroid hormone-related protein in cells of osteoblast lineage." Journal of cellular physiology **166**(1): 94-104.

Sugawara Y, Kamioka H, Honjo T, Tezuka K, Takano-Yamamoto T. Three- dimensional reconstruction of chick calvarial osteocytes and their cell processes using confocal microscopy. Bone 2005;36:877–83.

Suva, L., *et al*. (1987). "A parathyroid hormone-related protein implicated in malignant hypercalcemia: cloning and expression." Science **237**(4817): 893-896.

Szklarczyk, D., *et al*. (2018). "STRING v11: protein–protein association networks with increased coverage, supporting functional discovery in genome-wide experimental datasets." Nucleic acids research **47**(D1): D607-D613.

Tanaka-Kamioka, K., *et al*. (1998). "Osteocyte shape is dependent on actin filaments and osteocyte processes are unique actin-rich projections." Journal of Bone and Mineral Research **13**(10): 1555-1568.

Tangseefa, P., *et al*. (2018). "Osteocalcin-dependent regulation of glucose metabolism and fertility: Skeletal implications for the development of insulin resistance." Journal of cellular physiology **233**(5): 3769-3783.

Tanno, H., *et al*. (2014). "Ubiquitin-interacting motifs confer full catalytic activity, but not ubiquitin chain substrate specificity, to deubiquitinating enzyme USP37." Journal of Biological Chemistry **289**(4): 2415-2423.

Testerink, C., *et al*. "Inactivation of a MAPK-like protein kinase and activation of a MBP kinase in germinating barley embryos." Febs Letters **484**(1): 0-59.

Thomas, R. J., *et al*. (1999). "Breast cancer cells interact with osteoblasts to support osteoclast formation." Endocrinology **140**(10): 4451-4458.

Tommasini S M, Nasser P, Hu B, *et al*. Biological co-adaptation of morphological and composition traits contributes to mechanical functionality and skeletal fragility[J]. Journal of Bone and Mineral Research, 2008, 23(2): 236-246.

Tonna, Stephen*, et al*. "EphrinB2 signaling in osteoblasts promotes bone mineralization by preventing apoptosis." The FASEB Journal 28.10 (2014): 4482-4496.

Tonna, S. and N. A. Sims (2014). "Talking among ourselves: paracrine control of bone formation within the osteoblast lineage." Calcified tissue international **94**(1): 35-45.

Tovar Sepulveda, V. A., *et al*. (2002). "Intracrine PTHrP protects against serum starvation-induced apoptosis and regulates the cell cycle in MCF-7 breast cancer cells." Endocrinology **143**(2): 596-606.

TREGEAR, G. W., *et al*. (1973). "Bovine parathyroid hormone: minimum chain length of synthetic peptide required for biological activity." Endocrinology **93**(6): 1349-1353.

Tsavaler, L., *et al*. (2001). "Trp-p8, a novel prostate-specific gene, is up-regulated in prostate cancer and other malignancies and shares high homology with transient receptor potential calcium channel proteins." Cancer research **61**(9): 3760-3769.

Tsukagoshi, H., *et al*. (1999). "Regulation by interleukin-1β of gene expression of bradykinin B1 receptor in MH-S murine alveolar macrophage cell line." Biochemical and biophysical research communications **259**(2): 476-482.

Tsukazaki, T., *et al*. (1995). "Expression of parathyroid hormone-related protein in rat articular cartilage." Calcified tissue international **57**(3): 196-200.

Uckelmann, M., *et al*. (2018). "USP48 restrains resection by site-specific cleavage of the BRCA1 ubiquitin mark from H2A." Nature communications **9**(1): 229.

Valastyan, S. and R. A. Weinberg (2011). "Tumor metastasis: molecular insights and evolving paradigms." Cell **147**(2): 275-292.

Valín, A., *et al*. (2001). "C-terminal parathyroid hormone-related protein (PTHrP)(107–139) stimulates intracellular Ca2+ through a receptor different from the type 1 PTH/PTHrP receptor in osteoblastic osteosarcoma UMR 106 cells." Endocrinology **142**(7): 2752-2759.

Van Bezooijen, R. L., *et al*. (2004). "Sclerostin is an osteocyte-expressed negative regulator of bone formation, but not a classical BMP antagonist." Journal of Experimental Medicine **199**(6): 805-814.

Vilardaga, J.-P. (2010). "Theme and variations on kinetics of GPCR activation/deactivation." Journal of Receptors and Signal Transduction **30**(5): 304-312.

Vrahnas, C., *et al*. (2018). "Increased autophagy in ephrinB2 deficient osteocytes is associated with hypermineralized, brittle bones." bioRxiv: 260711.

Vrahnas C.,*et al*. (2018). Effects of Parathyroid Hormone, Alendronate and Odanacatib on the mineralisation process in intracortical and endocortical Haversian bone of ovariectomized rabbits. bioRxiv: 255703.

Vrahnas, C., *et al*. (2016). "Anabolic action of parathyroid hormone (PTH) does not compromise bone matrix mineral composition or maturation." Bone **93**: 146-154.

Walia, M. K., *et al*. (2016). "Activation of PTHrP-cAMP-CREB1 signaling following p53 loss is essential for osteosarcoma initiation and maintenance." elife **5**: e13446.

Wassen, M. H. M., *et al*. "Collagen structure regulates fibril mineralization in osteogenesis as revealed by cross-link patterns in calcifying callus." Journal of Bone and Mineral Research 15.9 (2000): 1776-1785

Weilbaecher, K. N., *et al*. (2011). "Cancer to bone: a fatal attraction." Nature Reviews Cancer **11**(6): 411.

Wen, X.-X., *et al*. (2015). "Time related changes of mineral and collagen and their roles in cortical bone mechanics of ovariectomized rabbits." PloS one **10**(6): e0127973.

Whatling, Carl, William McPheat, and Eva Hurt-Camejo. "Matrix management: assigning different roles for MMP-2 and MMP-9 in vascular remodeling." (2004): 10-11.

White, A. D., *et al*. (2019). "Ca2+ allostery in PTH-receptor signaling." Proceedings of the National Academy of Sciences **116**(8): 3294-3299.

Wu, T. L., *et al*. (1996). "Structural and physiologic characterization of the mid-region secretory species of parathyroid hormone-related protein." Journal of Biological Chemistry **271**(40): 24371-24381.

Xiao, G., *et al*. (2000). "MAPK pathways activate and phosphorylate the osteoblast-specific transcription factor, Cbfa1." Journal of Biological Chemistry **275**(6): 4453-4459.

Xu, L., *et al*. (2000). "WISP-1 is a Wnt-1-and β-catenin-responsive oncogene." Genes & development **14**(5): 585-595.

Yavropoulou, M. P., *et al*. (2017). "PTH and PTHR1 in osteocytes. New insights into old partners." Hormones **16**(2): 150-160.

Yin, J. J., *et al*. (1999). "TGF-β signaling blockade inhibits PTHrP secretion by breast cancer cells and bone metastases development." The Journal of clinical investigation **103**(2): 197-206.

Yin, Z., *et al*. (2011). "Differential role of PKA catalytic subunits in mediating phenotypes caused by knockout of the Carney complex gene Prkar1a." Molecular endocrinology **25**(10): 1786-1793.

Yu, B., *et al*. (2012). "Parathyroid hormone induces differentiation of mesenchymal stromal/stem cells by enhancing bone morphogenetic protein signaling." Journal of Bone and Mineral Research **27**(9): 2001-2014.

Zhang, R., *et al*. (2019). Parathyroid hormone-related protein (PTHrP): an emerging target in cancer progression and metastasis. Human Cell Transformation, Springer**:** 161-178.

Zhao, Q., *et al*. (2002). "Expression of parathyroid hormone-related peptide (PTHrP) and its receptor (PTH1R) during the histogenesis of cartilage and bone in the chicken mandibular process." Journal of anatomy **201**(2): 137-151.

Zhou, F., *et al*. (2014). "Nuclear receptor NR4A1 promotes breast cancer invasion and metastasis by activating TGF-β signalling." Nature communications **5**: 3388.

Zhu, D., *et al*. (2011). "The appearance and modulation of osteocyte marker expression during calcification of vascular smooth muscle cells." PloS one **6**(5): e19595.